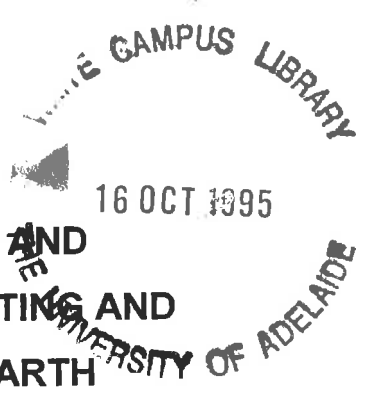


**EFFECT OF METHODS OF WETTING AND
RAINFALL CHARACTERISTICS ON CRUSTING AND
HARDSETTING OF A RED-BROWN EARTH**



Sikstus Gusli

Bachelor of Agricultural Science (Hasanuddin University)
Insinyur (Hasanuddin University)
Master of Rural Science (University of New England)

A thesis submitted for the degree of Doctor of Philosophy
of the University of Adelaide

Submitted March, 1995

Awarded 1995

58408

Abstract

Tillage practices are aimed at improving soil conditions for plant growth by altering aggregate size and pore-size distribution and to provide friable aggregate structure. However, the beneficial effects of tillage are often negated in a large group of Australian soils by poor aggregate structural stability. If irrigation or rain falls on exposed freshly tilled soil, crusting or hardsetting often develops on drying. Control of soil crusting and hardsetting can enhance crop establishment and yield and reduce soil erosion.

Factors such as rainfall intensity and kinetic energy, rate of wetting, antecedent water content and soil management history have been implicated in aggregate breakdown, which leads to the development of surface crusts or deeper hardset layers on drying. The two features differ from each other in morphology, mechanical properties and in the processes of formation. Thin surface seals precede the formation of crusts, whereas deep disrupted layers precede hardsetting.

Much evidence supports the notion that sealing, crusting, aggregate disruption and hardsetting are controlled by environmental processes in addition to properties of the soils themselves. This implies that both environmental conditions and soil properties will dictate whether a freshly tilled soil will crust, hardset, or remain friable following wetting and drying. A given soil can behave differently under varying environmental conditions. This assertion is supported by anecdotal evidence from many land managers.

While much is known about crusting, comparatively less is known about hardsetting, in particular little is known about the circumstances which determine whether a soil will set hard, as distinct from crusting. The influence of rainfall properties

and antecedent soil water condition on hardsetting, the distinctions between hardsetting and crusting, and factors which result in the development of hardsetting rather than crusting are not well understood. This study was aimed at identifying and describing these properties and factors.

A laboratory rainfall simulator was constructed by which rainfall kinetic energy could be varied from 1.6 to 19.9 J m⁻² mm⁻¹ and intensity from 40 to over 100 mm h⁻¹. Kinetic energy was controlled by changing the height of the rain modules or the size of emitters. Intensity was controlled by changing the outflow rate from a peristaltic pump. The simulator had innovative features such as automatic logging of runoff and rainfall intensity, and simulation of natural soil profile drainage.

The A-horizon (0 to 100 mm) of a Kapunda red-brown earth (fine, mixed, thermic, Calcic Rhodoxeralf), was used as the test soil (< 5 mm diameter aggregates). In the field this soil can, under different conditions, either crust or hardset or remain friable at the surface. Aggregate beds of 104 mm internal diameter, 54 mm high, retained in PVC tubing, and set on a target bed consisting of 8 aggregate beds surrounded by a splash exchange bed, covering a total area of 0.75 by 0.75 m². The aggregates were either air dry or pre-wetted at 0.30 m of water suction before being subjected to either wetting by suction or flooding or by rainfall of various kinetic energies and intensities. The structural conditions resulting from these different modes of wetting were compared.

Rainfall intensity and runoff were recorded electronically at one minute intervals. Infiltration was calculated as the difference. The proportion of soil materials at the surface (0 to 5 mm depth) smaller than 0.125 mm diameter was measured immediately

after rainfall. During draining and drying to various matric suctions, collapse of the aggregate beds (vertical strain), surface penetration resistance and needle emergence resistance were measured.

Methods of wetting determined the structural condition following wetting and drying. Suction wetting (0.30 m of water suction) preserved friable aggregate structure, and produced a maximum vertical strain of only 0.05 and emergence resistance at 5 m suction of less than 1 MPa. Flood wetting destroyed aggregate structure to a large extent, producing vertical strain of 0.11 and emergence resistance greater than 1.9 MPa at matric suction of 5 m of water if the aggregates were initially air dry; or vertical strain of 0.14 and emergence resistance greater than 3 MPa if the aggregates were pre-wetted under suction. Both suction and flood wetting produced strength profiles which were relatively uniform from the surface to the base of aggregate beds. High strength with deep, uniform aggregate disruption produced by flood wetting of aggregates showed that hardsetting behaviour was associated with rapid wetting of soil to the depth of the aggregate bed.

The extent of aggregate disruption caused by rainfall wetting depended on kinetic energy and intensity and soil antecedent water content before rainfall. Only when both kinetic energy and intensity were low ($1.6 \text{ J m}^{-2} \text{ mm}^{-1}$ and 40 mm h^{-1}) did the beds retain the friable aggregate structure of freshly tilled Kapunda red-brown earth. Low kinetic energy rainfall ($1.6 \text{ J m}^{-2} \text{ mm}^{-1}$) at an intensity of 70 mm h^{-1} did not cause sealing, maintained a high infiltration rate and severely disrupted the aggregates at depth below the surface, especially for pre-wetted aggregates, causing hardsetting similar to that from flood wetting. High kinetic energy rainfall ($19.9 \text{ J m}^{-2} \text{ mm}^{-1}$) caused severe breakdown of

air-dry aggregates and a high proportion of materials smaller than 0.125 mm was produced. A surface seal developed rapidly which reduced infiltration rate and rate of wetting into the layer below the seal. On drying, the surface seal formed a crust with penetration resistance greater than 2 MPa, but below the crust the aggregate structure remained relatively friable, similar to that of suction-wetted aggregates. High kinetic energy rainfall caused greater disruption of pre-wetted aggregates. This is attributed to matric suction of aggregates below the surface decreasing to zero or near zero during rainfall. Consequently, a crust with deeper disruption (hardsetting with surface crust) developed on drying.

Impeded soil drainage exacerbated the process of hardsetting by rainfall on pre-wetted aggregates, compared to when the aggregate beds were well drained. Poor drainage facilitated a rapid decline of matric suction to zero during rainfall causing increased aggregate disruption and packing. The resulting hardsetting condition was similar to that produced by flood wetting of pre-wetted aggregates.

In summary, the balance between a freshly tilled soil becoming crusted, hardset, or remaining friable is determined by the extent of surface (0 to 10 mm) aggregate breakdown. If breakdown is rapid and complete, a surface seal will form and entry of water into the soil will be restricted and matric suction below the surface will be high. Consequently, sub-surface aggregates will remain intact and retain friability on drying. The surface seal will dry to form a crust. If surface aggregate breakdown is incomplete, rate of water entry is high, soil matric suction is low, approaching zero, sub-surface aggregates break down extensively which causes deep aggregate disruption. On drying, a hardset layer develops. Poor sub-surface drainage causes more rapid decrease of matric

suction during rainfall, and hence exacerbates aggregate disruption and hardsetting. If surface aggregate breakdown is incomplete and water entry is low (due to low rainfall intensity), soil matric suction below the surface is maintained high, sub-surface aggregate breakdown is minimal. On drying the soil remains friable.

One limitation of the research reported in this thesis, is that only one soil was used. Nevertheless, soils similar to that used in this research are common in the cereal producing area of south-eastern Australia. With the aid of computer modelling, results reported here should be transferable to other soils.

Declaration

I declare that this thesis contains no material which has been accepted for the award of any other degree or diploma in any university or other tertiary institution. To the best of my knowledge and belief, this thesis contains no material previously published or written by another person, except where due reference is made in the text.

I give consent to this copy of my thesis, when deposited in the University Library, being available for loan and photocopying.

Signed:

Sikstus Gusli

Date : 20 Feb. 1995

Acknowledgments

I wish to thank my supervisors, Dr. A. Cass, Ass. Prof. D. A. MacLeod, Mr. C. T. Hignett, and Dr. R. Murray for their encouragement, advice, critique and help in various ways during my PhD study and stay in Australia. Dr. Cass and Ass. Prof. MacLeod gave me constructive comments on the development of ideas to define the research problems. Dr. Cass, Mr. Hignett and Mr. William Besz contributed in design and construction of the rainfall simulator. To Mr. Hignett, I am grateful for his encouragement and help, especially during the difficult time in the early part of my experiments. My thanks also to Mr. P. Willmott for technical assistance.

I wish to thank: Equity and Merit Scholarship Scheme (EMSS) of the Australian International Development of Assistance Bureau (AIDAB) for the scholarship that allowed me and my family to reside in Australia and which provided financial support for my project; CRC for Soil and Land Management which provided laboratory and office space as well as additional funding for my PhD study; CSIRO Division of Soils, Adelaide, for allowing me access to their facilities; and special thanks to the CSIRO librarians (Ms Anne Symons, Ms Michele Gaca, Mrs Fiona Cahill, and Ms Cheryl Thompson) and workshop staff (Mr Ralph J. Gilbert and Mr Graham Blows).

The welfare of my family cannot be separated from my academic life. I thank the catholic community of Kingswood Parish, especially Sr. Patricia Sexton, Jan Ruff, Dorothy Campbell, Dr. P. Henschke, the family of Anne and Rino De Fransisco, the St. Vincent De Paul and many more friends at Kingswood Parish, for their love, care and support.

To my wife, Hermin and my children, Rika, Lucky and Austin, thank you for the love, support and encouragement. Finally, I thank my mother for her continuous encouragement, carrying love and prayers. I pay respect and tribute to her.

Table of contents

Abstract	i
Declaration of originality	vi
Acknowledgments	vii
Table of Contents	ix
List of Tables	xiii
List of Figures	xiv
List of Plates	xx
List of terminology and abbreviation used	xxi
List of publications	xxiv
Introduction	1
Aims	2
References	2
1. Literature review: Soil crusting and hardsetting	4
1.1 Introduction	4
1.2 Aggregate stability	4
1.2.1 Water stability	5
1.2.2 Mechanical stability to rainfall	7
1.2.2.1 Raindrop kinetic energy	8
1.2.2.2 Rainfall intensity and kinetic energy flux density	8
1.2.2.3 Rainfall momentum, cumulative energy and duration	10
1.3 Change of soil structure by wetting	12
1.3.1 Sealing and crusting	13
1.3.1.1 Type of seals	13
1.3.1.2 Processes of sealing	14
1.3.1.3 Characteristics of sealing	15
1.3.1.4 Antecedent soil water content and sealing	15
1.3.1.5 Thickness of seal and disrupted layer	18
1.3.2 Hardsetting	21
1.3.2.1 Characteristics of hardset soil	21
1.3.2.2 Process of hardsetting	23
1.3.2.3 Factors affecting hardsetting	24
1.4 The distinction between crusting and hardsetting	26
1.5 Conclusions	27
1.6 References	28
2. An automated laboratory rainfall simulation system with controlled rainfall intensity, raindrop energy and soil drainage	35
2.1 Introduction	35
2.2 Design and description of the apparatus	38
2.2.1 Rainfall module design	38

2.2.2	Rainfall module operation	41
2.2.3	Test bed construction	42
2.2.4	Test bed operation	45
2.2.5	Data collection	46
2.2.6	Performance of the simulator	49
2.3	Discussion	52
2.4	Conclusions	53
2.5	References	54
3.	Effect of rainfall kinetic energy flux density on infiltration	56
3.1	Introduction	56
3.2	Materials and methods	58
3.2.1	Soil properties	58
3.2.2	Preparation of aggregate beds	59
3.2.3	Simulation of rainfall	60
3.2.4	Measurements	62
3.3	Results and discussion	62
3.3.1	Cumulative infiltration	62
3.3.2	Infiltration rate	68
3.3.3	Time to runoff	70
3.3.4	Infiltration associated with crusting and hardsetting	72
3.4	Conclusions	74
3.5	References	75
4.	Breakdown and packing of aggregates under rainfall	77
4.1	Introduction	77
4.2	Materials and methods	80
4.2.1	Soil properties and preparation of aggregate beds	80
4.2.2	Wetting of the aggregate beds	80
4.2.2.1	Rainfall wetting	80
4.2.2.2	Suction and flood wetting	81
4.2.3	Control of aggregate bed drainage	81
4.2.4	Measurements	82
4.2.4.1	Infiltration rate	82
4.2.4.2	Surface aggregate size	82
4.2.4.3	Matric suction	83
4.2.4.4	Vertical strain	83
4.2.4.5	Bulk density profile	84
4.3	Results and discussion	84
4.3.1	Change in vertical strain with matric suction following different wetting conditions	84
4.3.2	Effect of rainfall kinetic energy flux density on surface aggregate size and infiltration rate	87
4.3.3	Surface aggregate size and vertical strain	92

4.3.4	Effect of rainfall intensity and kinetic energy on vertical strain	100
4.3.5	Rate of wetting of soil beds and final vertical strain	104
4.3.6	Bulk density profile	107
4.4	Conclusions	108
4.5	References	110
5.	Effect of rainfall and antecedent water content on development of surface crust strength	114
5.1	Introduction	114
5.2	Materials and methods	116
5.2.1	Method of wetting and aggregate bed preparation	116
5.2.2	Measurements	116
5.3	Results and discussion	120
5.3.1	Penetration resistance characteristic	120
5.3.1.1	Suction and flood wetting	120
5.3.1.2	Rainfall wetting	123
5.3.2	Rainfall kinetic energy flux density and penetration resistance	125
5.3.3	Fine aggregates and penetration resistance	126
5.3.4	Infiltration rate and penetration resistance	128
5.4	Conclusions	131
5.5	References	132
6.	Effect of rainfall kinetic energy and antecedent water content on needle emergence resistance through the soil surface	134
6.1	Introduction	134
6.2	Materials and methods	137
6.2.1	Soil properties and preparation and wetting of aggregate beds	137
6.2.2	Measurements	137
6.2.2.1	Emergence resistance	137
6.2.2.2	Bulk density and degree of saturation	138
6.2.2.3	Visible pores	139
6.3	Results and discussion	141
6.3.1	Emergence resistance	141
6.3.2	Emergence resistance characteristic	146
6.3.3	Effect of restricted drainage	154
6.3.4	Visible pores	155
6.4	Conclusions	157
6.5	References	158

7. General Discussion: Factors that determine crusting or hardsetting in Kapunda red-brown earth	161
7.1 Introduction	161
7.2 Development of hydraulic resistance	163
7.3 Packing of disrupted aggregates	164
7.4 Strength development	169
7.5 Relationship to other soils	171
7.6 Practical implications	172
7.7 Suggestions for future research	174
7.8 References	175

List of tables

Table 2.1	Kinetic energy distribution from the rainfall simulator for drop diameters of 5.1 and 2.7 mm.	49
Table 3.1	Simulated rainfall kinetic energy (e_{rain}), intensity (i_{rain}), kinetic energy flux density (q), and cumulative kinetic energy (E_{rain}) applied on initially air-dry or pre-wetted (300 mm suction) soil beds. Rainfall duration was 30 minutes in all cases.	61
Table 4.1	Effect of methods and conditions of wetting and draining on final vertical strain of aggregate beds after wetting and drying. Antecedent water content of dry and wet in column two refer to air-dry and pre-wetted aggregates (0.30 m suction), respectively. Values in brackets are the standard errors of the means ($n = 8$).	94
Table 5.1	Relationships between maximum surface penetration resistance (P) (MPa) and matric suction (ψ_m) (m of water): $P = a + b\psi_m$, obtained from different methods of wetting and antecedent water content (θ_i) prior to wetting. a and b are regression coefficients, and R^2 are coefficient of determination. All relationships are significant at $p < 0.01$ to $p < 0.001$ ($n = 8$). Suction wetting was performed at matric suction of 0.57 m of water. Antecedent water content: dry and wet refer to air dry and pre-wetted at 0.30 m suction, respectively.	119
Table 6.1	Effect of method of wetting on the coefficients (a and b) of the regression equation $P_E = a S^{-b}$, where P_E = needle emergence resistance and S = degree of saturation. Antecedent water content of dry and wet refer to air-dry and pre-wetted aggregates (0.30 m suction), respectively. R^2 is coefficient of determination. All relationships are significant at $p < 0.05$ to $p < 0.01$ (number of observations = 8).	153
Table 6.2	Effect of method of wetting on the proportion of pores > 0.25 mm, as measured by digital image processing of the vertical cross section of aggregate beds.	157

List of figures

Figure 1.1	Effect of rainfall kinetic energy flux density on air permeability and associated penetration resistance. The variable kinetic energy flux density was derived from a constant kinetic energy ($13.9 \text{ J m}^{-2} \text{ mm}^{-1}$) and variable intensity (from 1.7 to 20.7 mm h^{-1}). The rainfall duration was varied so that cumulative rainfall energy was constant, 77.8 J m^{-2} . (Kinetic energy flux density has been calculated and figure re-drawn from Mantell and Goldberg, 1966).	12
Figure 1.2	Relationship between thickness of rain-induced disrupted layer and water dispersible clay relative to clay content from various soils (from West <i>et al.</i> , 1992).	20
Figure 2.1	Schematic diagram of laboratory rainfall simulator system: (a) the main components of the simulator; (b) an overall diagram of the simulator.	39
Figure 2.2	Plane and cross-sectional views of the rainfall aggregate bed.	42
Figure 2.3	An aggregate bed container (PVC ring) and its drainage base.	43
Figure 2.4	Configuration of the capacitance water depth sensors.	46
Figure 2.5	Calibration curves for the rainfall and the mean ($n=16$) runoff and drainage depth gauges and fitted functions (solid lines). Standard errors of the means are smaller than the triangular symbols used to show the data.	47
Figure 2.6	Block diagram of the electronic circuit used to capture and log depth of runoff, drainage and rainfall from the rainfall simulator.	48
Figure 2.7	Calibration of rainfall peristaltic pump (Masterflex 6-600 rpm): as a mean of all target sites ($n=9$) (circular symbol) and the values for the central, pluviometer position (triangle). The solid line shows the fitted calibration function for the mean data respectively. Error bars are 2 standard errors of the mean, which are generally smaller than the mean data symbols.	50
Figure 2.8	Components of the hydrological balance: rainfall (square symbols), runoff (circles), infiltration (triangles) and drainage (diamonds) during a single run using simulated rainfall on air-dry soil with high energy rainfall ($19.9 \text{ J m}^{-2} \text{ mm}^{-1}$) and intensities of 50.7 mm h^{-1} (closed symbols) and 49.2 mm h^{-1} (open symbols). Mean drop diameter of rainfall was 5.1 mm . Error bars are 2 standard errors of the mean of 8 replicated soil targets.	51

- Figure 2.9 Components of the hydrological balance: rainfall (square symbols), runoff (circles), infiltration (triangles) and drainage (diamonds) during a single run using simulated rainfall on air-dry soil with high energy rainfall ($19.9 \text{ J m}^{-2} \text{ mm}^{-1}$) and intensities of 50.7 mm h^{-1} (closed symbols) and 49.2 mm h^{-1} (open symbols). Mean drop diameter of rainfall was 5.1 mm. Error bars are 2 standard errors of the mean of 8 replicated soil targets. 51
- Figure 3.1 Cumulative infiltration of rainfall into soil aggregate beds as a function of cumulative rainfall depth at variable rainfall kinetic energy flux density (q) for: (a) air-dry aggregates and (b) aggregates pre-wetted at 0.3 m matric suction. For clarity, standard errors are not shown. 63
- Figure 3.2 Cumulative infiltration prior to runoff as a function of rainfall kinetic energy flux density for initially air-dry and pre-wetted (at 0.30 m of water suction) aggregates. Kinetic energy applied are given in the legend. $2 \times$ standard errors of the means were smaller than the symbols. 65
- Figure 3.3 Cumulative infiltration prior to runoff as a function of rainfall kinetic energy flux density redrawn from data of: (a) Mohammed and Kohl (1987) for initially air-dry aggregates (open symbols) and pre-wetted aggregates from previous rain (closed symbols); (b) Thompson and James (1985) for initially air-dry aggregates. Kinetic energy applied is given in the legend. 67
- Figure 3.4 Effect of rainfall kinetic energy flux density applied during 30 minutes of rain on infiltration rate after 30 minutes for air-dry aggregates (open symbols and broken regression line) and pre-wetted aggregates (0.3 m suction) (solid symbols and unbroken regression line). Kinetic energy applied is given in the legend. Error bars are $2 \times$ standard errors of the means. 69
- Figure 3.5 Time to runoff during rainfall as a function of rainfall intensity and kinetic energy. (a) Data obtained from experiments reported here, for initially air-dry and pre-wetted (0.30 m suction) aggregates. (b) Data from (a) above superimposed on regression relationships derived from data published by Ragab (1983) for initially dry aggregates. Kinetic energy applied, e_{rain} , is given in the legends. 71
- Figure 4.1 Aggregate bed collapse (vertical strain) on draining and drying after wetting of (a) air-dry and (b) suction wetted (0.30 m suction) aggregates by rainfall of variable kinetic energy flux density (q), and (c) wetting by flooding of air-dry or pre-wetted aggregates, or suction wetting without subsequent rainfall. Bars are 2 standard errors of the means. 85

Figure 4.2	Effect of rainfall kinetic energy flux density (q) on aggregate size distribution of (a) initially air-dry and (b) pre-wetted at 0.30 m suction, after 30 minutes of rainfall. Solid symbols represent wetting without raindrop energy by flooding and by suction wetting at 0.30 m suction was given for comparison with rainfall wetting.	89
Figure 4.3	Effect of rainfall kinetic energy flux density on the proportion of materials <0.125 mm at 0 to 5 mm depth after 30 minutes rainfall for initially dry and pre-wetted soils.	90
Figure 4.4	Effect of proportion of materials <0.125 mm (A_{125}) in the 0 to 5 mm depth on infiltration rate after 30 minutes of rain (i_{30}) of various kinetic energies (e_{rain}) applied on initially air-dry (open symbols) and pre-wetted soils (closed symbols).	92
Figure 4.5	Effect of surface aggregate disruption on packing of aggregate beds as a function of rainfall kinetic energy (e_{rain}) for initially air-dry (open symbols) or pre-wetted at 0.30 m of matric suction (closed symbols). Treatments with no rain: original air-dry soil, flood wetting of initially dry soil, and tension wetting at 0.30 m suction. Bars are 2 standard errors of the means.	98
Figure 4.6	Aggregate bed collapse (vertical strain) as a function of rainfall kinetic energy flux density (q), applied at different intensities on either air-dry pre-wetted aggregates bed. Bars are 2 standard errors of the means.	102
Figure 4.7	Relationship between infiltration rate after 30 minutes rain (i_{30}) and final aggregate bed vertical strain (ϵ_f) for different rainfall kinetic energies (e_{rain}) and antecedent water contents. Bars are 2 standard errors of the means.	105
Figure 4.8	Typical bulk density profiles of aggregate beds for: (a) suction-wetted (0.30 m of water) aggregate beds, represented by ● symbol (friable); (b) subjected to rainfall of high kinetic energy (>6.2 J m ⁻² mm ⁻¹), represented by □ symbol, or flood wetted represented by ◆ symbol (hardset); and (d) flood wetting of suction-wetted aggregate beds, represented by ■ symbol (severely hardset).	107
Figure 5.1	A brass core sampler used to measure surface bulk density at 0 to 5 mm. Left: vertical view of the sampler; right: vertical section through the sampler (not to scale).	120
Figure 5.2	Relationships between penetration resistance (P) and degree of saturation (S) of surface soil (0 to 5 mm depth) for: (a) air-dry aggregates wetted by suction (□, $P = 0.21 S^{-0.79}$), by flooding at zero suction (○, $P = 0.25 S^{-2.33}$) and first by suction then by flooding (Δ, $P = 0.48 S^{-2.28}$); (b) after rainfall of variable kinetic energy flux density (q) on pre-wetted soil (0.57 m suction); and (c)	

- after rainfall of variable q on air-dry aggregate beds. Values of q are given in the legend. Regression lines from (a) have been repeated in (b) and (c) for comparison between suction, flood and rainfall wetting. Bars are 2 standard error of the mean ($n = 3$). 121
- Figure 5.3 Effect of rainfall kinetic energy flux density (q) and antecedent water content on maximum penetration resistance at the surface 0 to 5 mm depth at matric suctions of (a) $\psi_m = 0.57$ m and (b) $\psi_m = 5$ m of water. Open triangles represent initially air-dry aggregates and closed triangles represent pre-wetted (0.30 m suction) aggregates. Error bars are $2 \times$ standard error of the means ($n = 8$). Penetration resistance at $\psi_m = 0.57$ was measured; that at $\psi_m = 5$ m was calculated using Equation (5.2). Boundaries drawn are around groups of data which are (i) crusting or (ii) friable or hardsetting. 126
- Figure 5.4 Effect of the proportion of materials less than 0.125 mm diameter (A_{125}) generated at the soil surface (0 to 5 mm) by rainfall on the surface penetration resistance (P) at matric suctions of (a) 0.57 m (P was measured), and (b) 5 m of water (P was calculated from Equation 5.2). 127
- Figure 5.5 Penetration resistance (P) of aggregate beds at matric suctions (ψ_m) of 0.57 m (squares) and 5.0 m of water (triangles) after being subjected to rainfall, as a function of infiltration rate 30 minutes after commencement of rainfall, i_{30} . Open and closed symbols represent initially dry and pre-wetted (0.30 m suction) aggregates, respectively. The dashed line corresponds to i_{30} equal to 25 mm h^{-1} (associated with kinetic energy of $\geq 6.2 \text{ J m}^{-2} \text{ mm}^{-1}$), considered to be critical infiltration rate distinguishing sealed (crusted) from disrupted (hardset) surface soil. Error bars ($2 \times$ standard error) for measurements at ψ_m of 0.57 m are too small to be shown; P values for ψ_m of 5 m were calculated from Equation 5.2. 130
- Figure 6.1 Profiles of: (a) mass water content measured at various matric suctions, and (b) the associated bulk density values. Error bars are $2 \times$ the standard error of the mean ($n = 3$). No error bars imply $2 \times$ SE was smaller than the symbol. 139
- Figure 6.2. Emergence resistance of aggregate beds at a matric suction of 0.57 m of water after subjecting the beds to different methods of wetting at various antecedent water contents: (a) Wetting, without rainfall, of air-dry aggregates by a suction of 0.30 m of water; flooding; and suction (0.30 m) then flooding; (b and c) wetting by rainfall of various kinetic energies (e_{rain}) and intensities and therefore kinetic energy flux densities (q) on (b) air-dry aggregates and (c) suction (0.30 m) wetted aggregates. Error bars are $2 \times$ pooled standard error for 10, 20 and 30 mm depths. 142
- Figure 6.3 Emergence resistance of aggregate beds at a matric suction of 0.57

m of water after subjecting the beds to different methods of wetting at various antecedent water contents: **(a)** Wetting, without rainfall, of air-dry aggregates by a suction of 0.30 m of water; flooding; and suction (0.30 m) then flooding; **(b and c)** wetting by rainfall of various kinetic energies (e_{rain}) and intensities and therefore kinetic energy flux densities (q) on **(b)** air-dry aggregates and **(c)** suction (0.30 m) wetted aggregates. Error bars are $2 \times$ pooled standard error for 10, 20 and 30 mm depths.

144

Figure 6.4 Emergence resistance characteristics for different methods of wetting at 0 to 10 mm depth. Error bars are $2 \times$ standard error of the means ($n = 8$).

147

Figure 6.5 Emergence resistance characteristics of aggregate beds following rainfall of various kinetic energies (e_{rain}) and kinetic energy flux densities (q) on **(a)** initially air-dry and **(b)** pre-wetted (0.30 m suction) aggregate beds at 0 to 10 mm depth. Emergence resistance characteristics of suction (0.30 m), flood and suction then flood wetted beds (Figure 6.4) are superimposed on the data of rain treated beds for comparison. Error bars are $2 \times$ standard error of the means ($n = 8$).

148

Figure 6.6 Emergence resistance characteristics of aggregate beds following rainfall of various kinetic energies (e_{rain}) and kinetic energy flux densities (q) on **(a)** initially air-dry and **(b)** pre-wetted (0.30 m suction) aggregate beds at 10 to 20 mm depth. Emergence resistance characteristics (10 to 20 mm) of suction (0.30 m), flood and suction then flood wetted beds are superimposed on the data of rain treated beds for comparison. Error bars are $2 \times$ standard error of the means ($n = 8$).

149

Figure 6.7 Emergence resistance characteristics of aggregate beds following rainfall of various kinetic energies (e_{rain}) and kinetic energy flux densities (q) on **(a)** initially air-dry and **(b)** pre-wetted (0.30 m suction) aggregate beds at 20 to 40 mm depth. Emergence resistance characteristics (20 to 40 mm) of suction (0.30 m), flood and suction then flood wetted beds are superimposed on the data of rain treated beds for comparison. Error bars are $2 \times$ standard error of the means ($n = 8$).

151

Figure 6.8 Effect of restricted drainage during rainfall on pre-wetted (0.30 m suction) aggregate beds on emergence resistance, measured at a matric suction of 5 m of water, after subjecting the beds to rainfall with kinetic energy of $19.9 \text{ J m}^{-2} \text{ mm}^{-1}$, and intensity of 70 mm h^{-1} . Error bars are $2 \times$ pooled standard error for 10, 20 and 30 mm depths.

154

Figure 7.1 Factors and processes which determine the surface condition of a soil after rainfall. Symbols e_{rain} , i_{rain} , and q are rainfall kinetic

energy, intensity, and kinetic energy flux density, respectively, θ_i is antecedent soil water content and ψ_i is antecedent soil matric suction.

162

Figure 7.2. Aggregate deformation by wetting of friable aggregates (State 1) to produce collapsed aggregate structure (States 2). (A) flood wetting of air-dry aggregates causing disruption due to slaking (differential swelling and the pressure of trapped air); (B) suction wetting of air dry aggregates then flood wetting of the moist aggregates causing disruption due to the release of effective stress.

167

List of plates

- Plate 6.1. Surface features of Kapunda soil produced by different methods of wetting and different antecedent soil water contents: *friable* (resulted from suction wetting air-dry aggregates at 0.30 m of water suction); *crusted* (high rainfall kinetic energy and intensity, $19.9 \text{ J m}^{-2} \text{ mm}^{-1}$ and 70 mm h^{-1} , on air-dry aggregates); and *hardset* (flood wetting of air-dry aggregates).

156

List of Terminology and Abbreviation Used

Processes:

Slaking is a process by which dry soil aggregates break down into smaller fragments as a result of shear stress due to differential swelling and the pressure of entrapped air during rapid wetting (e.g. flood wetting at zero matric suction on air-dry aggregates).

Slumping is a process by which moist soil aggregates deform as they are wetted rapidly to zero matric suction. The process is caused by the reduction of effective stress, which previously held the aggregates or particles together, to approximately zero. (e.g. flood wetting of previously suction wetted, about field capacity matric suction, aggregates).

Seal, is a surface condition, resulting from comminution of aggregates by raindrop impact of sufficiently high (above the critical value) kinetic energy, dispersion of clay, and rearrangement of fragments at the surface, < 10 mm deep. The surface seal referred in this thesis is essentially a rain induced seal.

Surface hydraulic resistance is any form of retardation of water infiltration as a result of surface aggregate breakdown. It may be a result of sealing (caused by rainfall kinetic energy) or slaking (caused by hydration energy of water, when rainfall kinetic energy is smaller than the critical value) or both (when both rainfall kinetic energy and intensity are high).

Crust is a soil surface layer, few (< 10 mm) millimetres thick, which has distinctly higher bulk density than the layer below which develops from a seal as it dries out.

Disrupted layer is a soil surface layer which develops from deep (> 10 mm) comminuted aggregates and rearrangement of comminuted fragments during wetting. The difference in the extent of comminution between the surface (< 10 mm) and the layer below is minimal.

Hardset layer is a soil surface which develops from disrupted layer as effective stress increases during draining and drying. Penetration resistance of hardset soil is high (>1.5 MPa) when it is still relatively wet (matric suction of about 5 m of water). While both crusted and hardset layers have high bulk density, the former is typically less than 10 mm, while the later is more than 10 mm thick.

Symbols and abbreviations:

a, a', a'', ... are regression coefficients that take various values, depending on the regression data.

A₁₂₅ Proportion of materials smaller than 0.125 mm at the 0 to 5 mm depth, obtained by the wet sieving method, following wetting by rainfall, or wetting under 0.30 m

suction or under flooding at zero matric suction. For convenience, A_{125} is also referred to as “fine material”.

- b, b', b'', \dots are regression coefficients that take various values, depending on the regression data.
- d Diameter (mm).
- ϵ_{rain} Raindrop kinetic energy ($J m^{-2} mm^{-1}$).
- ϵ Aggregate bed vertical strain, *i.e.* the ratio of the difference in bed's height between initial condition (before wetting) and ‘final’ condition (after wetting and drying to a certain matric suction) to the aggregate bed height at initial condition (unitless). ϵ may or may not increase with increasing matric suction.
- ϵ_f Final aggregate bed vertical strain. Further increase of matric suction no longer affects the vertical strain.
- F Penetration force (MPa).
- F_t Total emergence force (MPa).
- F_f Force due to soil - metal friction (MPa).
- F_s Emergence force, $F_t - F_f$ (MPa).
- f Output signal frequency (Hz).
- I_{rain} Cumulative rainfall (mm).
- i_{rain} Rainfall intensity ($mm h^{-1}$).
- I_{ro} Cumulative rainfall before runoff commences (mm)
- I_{soil} Cumulative infiltration (mm).
- i_{soil} Infiltration rate ($mm h^{-1}$).
- i_{30} Infiltration rate after 30 minutes of rainfall commencement ($mm h^{-1}$).
- k Air permeability ($mL sec^{-1}$).
- L_Z The vertical distance that the needle probe has travelled through an aggregate bed when the surface flake ruptures.
- P Maximum penetration resistance (MPa) of the surface soil measured by cone penetrometer.
- P_E Emergence resistance measured by a blunt probe driven from the base of the aggregate bed (MPa).
- ρ_b Soil bulk density ($kg m^{-3}$).
- ρ_p Soil particle density ($kg m^{-3}$).
- ρ_w Density of water (assumed to be $1000 kg m^{-3}$).
- q Raindrop kinetic energy flux density ($J m^{-2} h^{-1}$).
- t Time (h)
- t_{ro} Time required for the initiation of runoff (minute).

R_z	The thickness of flake which ruptures from the surface of an aggregate bed, as the needle probe is emerging.
S	Degree of saturation: volumetric water content divided by total porosity.
θ_m	Volumetric water content ($\text{kg}^1 \text{kg}^{-1}$)
θ_v	Volumetric water content ($\text{m}^3 \text{m}^{-3}$).
θ_i	Antecedent water content status (air-dry, or pre-wetted at 0.30 m of water suction).
ψ_m	Soil matric suction (m of water).
S	Degree of saturation.
m	Mass (g)
V	Velocity of raindrop falling (m s^{-1}).
ρ_b	Soil bulk density (Mg m^{-3}).
σ'	Effective stress (kPa, or MPa)

List of publications from the thesis

The following papers have arisen from the work reported in this thesis:

Journals article:

1. Hignett, C.T., S. Gusli, A. Cass, W. Besz (1995). An automated laboratory rainfall simulation system with controlled rainfall intensity, raindrop energy and soil drainage. *Soil Technology (in press)*. (extracted from Chapter 2).

Conference articles:

1. Gusli, S., A. Cass, D. A. MacLeod, C. T. Hignett (1994). Processes that distinction between hardsetting and rain induced crusting. The International Symposium on Sealing, Crusting, Hardsetting Soils: Productivity and Conservation 7-11 February 1992, University of Queensland, Brisbane, Australia. (a poster paper, will appear in the Proceeding of the symposium).
2. Gusli, S. and A. Cass (1994). Rainfall factors determining soil surface sealing and aggregate packing. "Annual meetings of American Society of Agronomy, American Society of Crop Science, and American Society of Soil Science", 13-19 Nov. 1994, Seattle, WA, USA. (a poster paper with abstract appears in *Agronomy Abstracts*).

Introduction

Crusts and hardset layers are two distinctly different soil surface structural features described in the soil science literature (Northcote, 1979; Mullins *et al.*, 1987; Mullins *et al.*, 1990). Both structural features occur in Australian soils and can impose serious limitation to soil management and crop productivity (McIntyre, 1958; Chan, 1989; Mullins *et al.*, 1987, 1990). The development of soil crusts and hydrological and management implications of crusts have been the subject of considerable research for the last 6 decades, beginning by a study by Duley (1939). The morphology and mechanisms of crust development are widely documented and relatively well understood (West *et al.*, 1992, among others).

Hardsetting, as a structural feature, as a process of aggregate breakdown, as a determinant of surface hydrology, and as a factor of soil management, has been less extensively studied. Hardsetting as a surface feature was described in the late 1970's (Northcote, 1979; Cockroft and Martin, 1981), but it has not received wide recognition outside Australia.

Mullins *et al.* (1990) reviewed the published literature on the behaviour, occurrence and management of hardsetting soils. Subsequently, the mechanisms of hardsetting have been investigated in detail by Weaich *et al.* (1992) and Gusli *et al.* (1994a and b). None of these studies, however, has investigated how the properties of rainfall influence hardsetting. In particular, the interaction between rainfall and soil structural properties in determining whether a soil crusts, sets hard or remains friable, has not been studied.

Aims

The aims of the research reported in this thesis are to:

- 1) review the literature on processes and mechanism of aggregate disruption by water and how these are related to hardsetting and crust formation;
- 2) investigate the influence of rainfall properties and mode of soil wetting on aggregate breakdown and the mechanisms that subsequently lead to the formation of crusts or hardset layers;
- 3) identify the conditions of rainfall, wetting and antecedent water content that lead to hardsetting or crusting.

Because of the detailed nature of this work, only one soil was used in the research project. This soil is representative of a very large area of Australian soils and results from the research will be transferable to much of the south eastern cereal producing area of Australia.

References

- Chan, K.Y. (1989). Friability of a hardsetting soil under different tillage and land use practices. *Soil & Tillage Research* 13: 287-298.
- Cockroft, B. and F. M. Martin (1981). Irrigation. In: J. M. Oades, D. G. Lewis and K. Norrish (eds.). Red-brown Earths of Australia. Waite Agr. Res. Inst. and CSIRO Div. of Soils, Adelaide, South Australia, p.: 133-147.
- Duley, F. L. (1939). Surface factors affecting the rate of intake of water by soils. *Soil Science Society of America Proceedings* 4: 60-64.
- Gusli, S., A. Cass, D. A. MacLeod, and P. S. Blackwell (1994a). Structural collapse and strength of some Australian soils in relation to hardsetting: I. Structural collapse on wetting and draining. *European Journal of Soil Science* 45: 15-21.

- Gusli, S., A. Cass, D. A. MacLeod, and P. S. Blackwell (1994b). Structural collapse and strength of some Australian soils in relation to hardsetting: II. Tensile strength of collapsed aggregates. *European Journal of Soil Science* 45: 23-29.
- McIntyre, D.S. (1958). Soil splash and the formation of surface crusts by raindrop impact. *Soil Science* 85: 261-266.
- Mullins, C. E., I. M. Young, A. G. Bengough, and G. J. Ley (1987). "Hard-setting soils". *Soil Use and Management* 3: 79-83.
- Mullins, C. E., D. A. MacLeod, K. H. Northcote, J. M. Tisdall, and I. M. Young (1990). Hardsetting soils: behaviour, occurrence, and management. *Advances in Soil Science* 11: 37-108.
- Northcote, K. H. (1979). A Factual Key for the Recognition of Australian Soils. 4th edition. Rellim Technical Publishers, Adelaide.
- Weaich, K., A. Cass, and K. L. Bristow (1992). Use of a penetration resistance characteristic to predict soil strength development during drying. *Soil and Tillage Research* 25: 149-166.
- West, L.T., S.C. Chiang, and L.D. Norton (1992). The morphology of surface crusts. In: M.E. Sumner and B.A. Stewart (eds.). Soil Crusting. Chemical and Physical Processes. Advances in Soil Science. Lewis Publ., Boca Raton, pp.: 73-92.

Chapter 1

Literature review: Soil crusting and hardsetting

1.1 Introduction

The broad aim of this literature review is to describe distinctions between the mechanical properties and development of processes of crusts and hardset layers. Because these features are respectively derived from surface seals and deeper disrupted layers (Bristow *et al.*, 1994), the review will also cover the process of seal formation as distinct from aggregate disruption. In particular, the review will cover:

- 1) rainfall and soil factors that determine aggregate breakdown;
- 2) mechanism of aggregate breakdown by wetting;
- 3) effect of modes of wetting and antecedent soil moisture content on development of seals or disrupted layers and subsequent development of crusts or hardset layers;
- 4) properties of crusts and hardset layers;
- 5) distinctions between crusting and hardsetting.

1.2 Aggregate stability

An aggregate is a cluster of inorganic and organic soil particles, combined in such a way that the forces which bind the particles within the aggregate exceed the external forces surrounding the aggregate (Farres, 1980). When the external forces such as those generated by water entering the aggregates or mechanical manipulation (such as root growth, tillage and raindrop impact) exceed the internal forces, aggregates will deform or

disrupt. The ability of aggregates to resist deformation is referred to as aggregate stability (Baver *et al.*, 1972, p. 182). Dexter (1988) identified two main types of structural stability: (1) stability opposing disruption by wetting with water (water stability, or stability against hydration forces), and (2) stability opposing deformation by mechanical stress (mechanical stability). In this review, the only mechanical stress to be discussed is that arising from raindrop impact.

1.2.1 Water stability

Many factors influence aggregate resistance to disruption by wetting with water. Properties of the soil, known to affect water stability include particle-size distribution, clay mineralogy, organic matter, iron and aluminium oxides and exchangeable sodium (Marshall and Holmes, 1988, p. 216-219). In addition, hydrological factors such as soil water content and matric suction, and methods of wetting, greatly influence the stability of aggregates to the stresses induced by wetting (Gusli *et al.*, 1994a).

Kemper *et al.* (1985) concluded that both antecedent water content and rate of wetting determined aggregate stability. Higher rates of wetting and lower water content prior to wetting caused greater aggregate breakdown. However, the effect of initial water content on stability decreased as the rate of wetting decreased. When slow wetted (≥ 17 minutes to wet a 2-mm diameter aggregate, equivalent to an absorption rate of ≤ 0.13 mm h^{-1}), initial water content had little or no influence on aggregate stability. But, when the rate of wetting was fast (< 1.5 minutes to wet a 2-mm diameter aggregate), initial water content had a large effect on stability. The more unstable the soil, the more

sensitive are dry aggregates were to rapid wetting (Kemper and Koch, 1966; Collis-George and Lal, 1971).

Soil water content affects aggregate stability by influencing the rate at which water is absorbed into the aggregates. This rate in turn determines the pressure of entrapped air in the aggregates, and differential swelling of clay minerals (Emerson and Grundy, 1954; Panabokke and Quirk, 1957). When wetted rapidly at zero matric suction, dry aggregates of some soils, especially the red and red-brown earths of Australia (Northcote, 1979), slake as a result of the pressure of entrapped air and differential swelling, exceeding the internal forces binding the aggregates. Panabokke and Quirk (1957) found that when aggregates were pre-wetted to a suction of 1 m of water, they remained stable when immersed in water.

Slow wetting using suctions greater than 0.20 m of water can prevent aggregate disruption (Kemper and Koch, 1966; Gusli *et al.*, 1994a). Suction wetting does not cause slaking because slow water absorption into the soil matrix allows air to escape gradually, minimises stresses resulting from uneven swelling of clay minerals and rapid release of heat of wetting (Panabokke and Quirk, 1957; Collis-George and Lal, 1971).

When matric suction is decreased from 1 m of water toward zero, aggregate stability of some soils decreases to a level close to the stability of the air-dry condition (Cernuda *et al.*, 1953; Panabokke and Quirk, 1957). Francis and Cruse (1983) observed a decline in stability as soil matric suction was decreased from 0.30 to zero m of water. Similarly, Al-Durrah and Bradford (1981) found that aggregate stability increased as matric suction was increased from 0.05 to 0.60 m of water. Soil particles are held together by effective stress under the influence of capillary retention, which is directly related to matric suction (Marshall and Holmes, 1988, p. 232). When a soil's matric

suction is between zero and the air-entry value, aggregates are mechanically weakest and are easily deformed by mechanical stress. As a soil dries and matric suction increases above the air-entry value, air enters the aggregates, creating air - water interfaces. This allows surface tension forces to operate, acting as effective stress to stabilise aggregates. Effective stress (σ') is determined by the extent of water - solid contact and the suction of the soil water (Bishop and Blight, 1963; Weaich *et al.*, 1992),

$$\sigma' = \chi \psi_m \quad (1.1)$$

where ψ_m is matric suction and χ is a factor related to the degree of saturation (Mullins and Panayiotopoulos, 1984), assuming external pressure on the aggregate is zero. As the soil dries further, ψ_m increases but χ decreases, and a point is reached where effective stress stabilisation against hydration forces declines (Towner and Childs, 1972).

1.2.2 Mechanical stability to rainfall

Wetting by rainfall imposes mechanical stresses on aggregates at the soil surface, in addition to the hydration effects described above. There are three basic properties of rainfall which affect aggregate breakdown: (1) rainfall kinetic energy ($\text{J m}^{-2} \text{mm}^{-1}$), a measure of the energy of raindrops per unit depth of rainfall impacting onto a given area of aggregates; (2) rainfall intensity (mm h^{-1}), a measure of the wetting energy of rainfall (the hydration component); and (3) duration of rainfall. Other rainfall properties are cumulative energy, kinetic energy flux density, and momentum, but they are derived from a combination of the three basic properties of rainfall.

1.2.2.1 Raindrop kinetic energy

Kinetic energy is used widely to explain the effect of rainfall on surface aggregate breakdown and water infiltration (Al-Durrah and Bradford, 1981; Agassi *et al.*, 1985; Shainberg and Singer, 1988). These workers, among others, found that aggregate breakdown increased with an increase in raindrop impact energy. Hignett (1991) applied simulated rainfall with intensity of up to 200 mm h⁻¹ to several soils, but did not record runoff, unless the raindrop energy was increased above a certain value. This indicates that there was a critical raindrop energy, below which aggregates are not broken down and therefore water infiltration was not affected by the rainfall.

1.2.2.2 Rainfall intensity and kinetic energy flux density

Measurement of rainfall intensity is simpler than kinetic energy. Probably for this reason, many workers have used rainfall intensity in preference to rainfall kinetic energy to explain surface soil aggregate breakdown, infiltration, and soil strength (Lyles *et al.*, 1969; Busch *et al.*, 1973; Agassi and Levy, 1991).

If rainfall kinetic energy is reduced to zero, such as by adding a protective mulch to the soil surface, rainfall intensity affects aggregate comminution through hydration effects only, as discussed in Section 1.1.1. However, in natural rain, raindrop energy is related to rainfall intensity (Kinnell, 1981, 1987; Rosewell, 1986). Hence, it is often difficult to conclude with certainty whether the effect measured was actually caused by varying intensity (hydration) or the combined effect of kinetic energy and intensity (frequency of mechanical impact). For example, Morin and Benyamini (1977) found that infiltration rate through a bare soil decreased as rainfall intensity was increased from 29

to 56 and finally to 130 mm h⁻¹. When they applied surface cover, the 130 mm h⁻¹ rainfall did not decrease the infiltration rate. Similar data were reported by Mohammed and Kohl (1987). Thus, high rainfall intensity did not decrease infiltration rate when kinetic energy was suppressed to approximately zero.

Both kinetic energy and intensity have been investigated to explain the effect of rainfall on aggregate breakdown or infiltration. Epstein and Grant (1973) found that both kinetic energy and intensity caused compaction of the surface soil, reducing porosity and infiltration rate. There was an interactive effect between the two rainfall factors. The product of kinetic energy (J m⁻² mm⁻¹) and intensity (mm h⁻¹) is kinetic energy flux density, with units of J m⁻² h⁻¹. Kinetic energy flux density will increase as kinetic energy or intensity, or both are increased. Ragab (1983) on the other hand found that neither intensity nor kinetic energy affected the aggregate stability of a clay soil, although the volume of pores in the surface soil decreased as kinetic energy increased.

Wischmeier and Smith (1958) used the concept of kinetic energy flux density in a factor which they called "kinetic energy times maximum 30 minute intensity" (EI₃₀) to explain soil loss from various locations in the USA. They found that soil loss was a positive linear function of EI₃₀, independent of rainfall amount and soil type. EI₃₀ has been used in the Universal Soil Loss Equation to calculate soil loss (Wischmeier, 1959).

Shvebs (1968) suggested that rainfall kinetic energy flux density characterises the effect of rainfall on aggregate breakdown better than kinetic energy, since it encapsulates both rainfall intensity and energy. Farres (1980) examined a number of rainfall variables by multivariate analysis, to find which variable(s) played the major role in the rate of aggregate breakdown. He found that the intensity of drop impact (kinetic energy flux

density) was the most important rainfall factor controlling the initiation of aggregate breakdown. This was attributed to kinetic energy flux density dictating the relaxation time that the aggregate experienced between successive impacts. The more intense the impacts within a given time, the less time was available for the aggregate to readjust the new internal system in terms of physical stresses, electro-kinetic and electro-chemical bonding. As a result, internal strength decreased more rapidly and slaking intensified as kinetic energy flux density was increased (Farres, 1980).

Thompson and James (1985) applied simulated rainfall with kinetic energies varying from 0.5 to 8.5 J m⁻² mm⁻¹ at intensities of 30 to 150 mm h⁻¹, for 5 to 240 minutes duration. Mohammed and Kohl (1987) applied rainfall of kinetic energy 0 to 24.4 J m⁻² mm⁻¹ at 44 to 155 mm h⁻¹. Both studies found that infiltration depended on both kinetic energy and intensity, but it was much more strongly correlated with kinetic energy flux density.

1.2.2.3 Rainfall momentum, cumulative energy and duration

Rose (1960) found that the rate of soil detachment under rainfall was determined by both rainfall momentum per unit area and time and by rainfall kinetic energy flux density. However, he concluded that rainfall momentum per unit area and time was a better rain factor describing soil detachment than kinetic energy flux density. Rose (1960) expressed his results as M, the rainfall momentum (kg m s⁻¹) per unit area (m²) and time (s), with units of N m⁻². Units of M (N m⁻²) may be transformed to kN m⁻² and subsequently to J m⁻² mm⁻¹, a unit of rainfall kinetic energy. Thus, Rose's quantity (M) is equivalent to kinetic energy. The result of Rose's (1960) study is, therefore, that both kinetic energy and kinetic energy flux density determine soil detachment.

The cumulative energy delivered by rainfall has been used by some researchers to assess aggregate breakdown and infiltration (Morin and Benyamini, 1977; Baumhardt *et al.*, 1990). Increasing cumulative energy resulted in larger aggregate breakdown and lower infiltration rate. However, the usefulness of cumulative energy in describing surface soil processes may be questioned, as others have found little effect of cumulative energy on aggregate breakdown. As early as 1958, Wischmeier and Smith (1958) reported that rainstorms of equal total amount falling on the same field and on comparable surface conditions can produce widely different soil loss. Eigel and Moore (1983) showed that during rainfall, seal development occurred rapidly (< 10 minutes), remaining static after this time, indicating that prolonged rainfall duration may be irrelevant to surface aggregate breakdown. Romkens *et al.* (1986) applied simulated rainfall of kinetic energy of $27.5 \text{ J m}^{-2} \text{ mm}^{-1}$ to a silty clay loam and observed that sealing only occurred as cumulative energy increased from 0 to 250 J m^{-2} , *i.e.* at cumulative rainfall of up to 9.1 mm. Subsequent rainfall did not change soil hydraulic conductivity. The time required for a seal to form decreased with increasing rainfall intensity, from 27 minutes for rainfall intensity of 20 mm h^{-1} to just 6 minutes for intensity of 90 mm h^{-1} . This suggests that generally, aggregate breakdown occurs before ponding with little change after surface ponding (Thompson and James, 1985; Geeves *et al.*, 1994). Consequently, only pre-ponding cumulative energy can be related to aggregate breakdown.

Mualem *et al.* (1990) stated that it is more appropriate to relate the dynamics of seal formation to rainfall kinetic energy rather than to cumulative rainfall. Mantell and Goldberg (1966) applied simulated rainfall of drop diameter 2.59 mm from 2 m height and intensity varying from 1.7 to 20.7 mm h^{-1} . This gave constant rainfall kinetic energy

of $13.9 \text{ J m}^{-2} \text{ mm}^{-1}$ but variable kinetic energy flux density, ranging from 23.6 to $287.7 \text{ J m}^{-2} \text{ h}^{-1}$. By varying rainfall duration, they maintained constant rainfall amount and hence cumulative rainfall energy. They found that both penetration resistance and air permeability of the soil were a function of rainfall kinetic energy flux density (Figure 1.1), even though cumulative rainfall energy was constant.

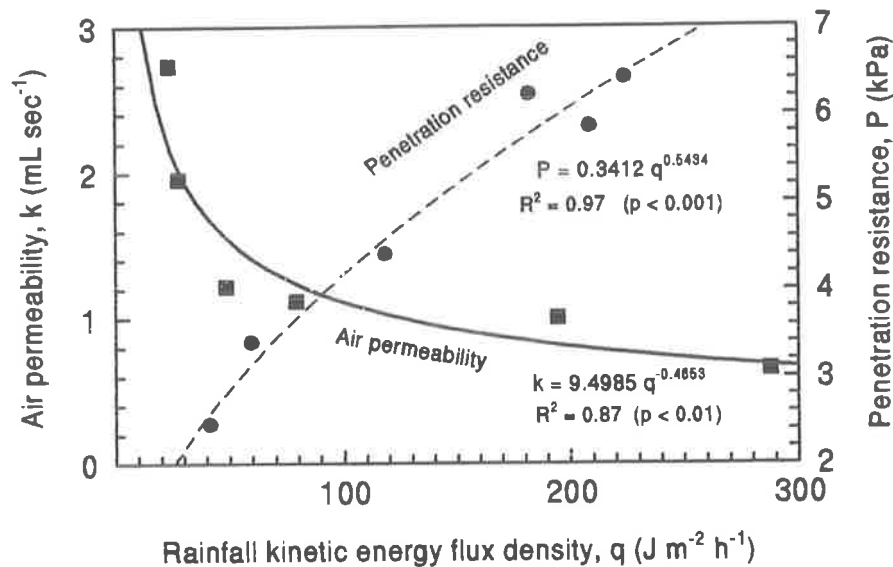


Figure 1.1. Effect of rainfall kinetic energy flux density on air permeability and associated penetration resistance. The variable kinetic energy flux density was derived from a constant kinetic energy ($13.9 \text{ J m}^{-2} \text{ mm}^{-1}$) and variable intensity (from 1.7 to 20.7 mm h^{-1}). The rainfall duration was varied so that cumulative rainfall energy was constant, 77.8 J m^{-2} . (Kinetic energy flux density has been calculated and figure re-drawn from Mantell and Goldberg, 1966).

1.3 Change of soil structure by wetting

The packing of primary particles as individuals or as clusters in domains or in aggregates determines the total amount of pore space and the distribution of pore space in various size classes. Marshall and Holmes (1988, p. 196) defined soil structure as the arrangement of soil particles and of the pore space between them. Aggregate

deformation and disruption, due to wetting or mechanical manipulation, causes changes in the structure of soil. This change may lead to sealing and crusting, or hardsetting.

1.3.1 Sealing and crusting

The terms sealing and crusting are frequently used to describe surface soil disruption caused by raindrop impact (Duley, 1939). These terms are often used interchangeably, which is incorrect. Recently the distinctions between seal and crust were clarified by Mualem *et al.* (1990) and Romkens *et al.* (1990). They proposed that the term *seal* be used to describe particular sealing conditions prevailing during formation, and hence should be used only for wet soil. The term *crust* refers to a dry seal and should be used for dry soil condition. Bristow *et al.* (1994) pointed out that, while a crust is often simply regarded as a dry seal, properties of crusts differ from those of seals. For example, crusts are likely to be denser than seals, as during draining and drying the disrupted particles that make up the seals can pack further as matric suction increases during drying, as shown by Gusli *et al.* (1994a).

1.3.1.1 Types of seals

Researchers have classified types of crusts rather than of seals. Because crusts develop from seal, classification of types of crusts should also be valid for types of seals. Chen *et al.* (1980), Boiffin (1985) and Bresson and Boiffin (1990) described two main types of crust (and therefore seals): (1) structural crusts which develop from the seal caused by direct impact of raindrops; and (2) depositional crusts, which develop from a seal formed as a result of the transport and deposition of detached soil materials carried by runoff water. Structural crusts (seals) refer to seals that form in place by processes directly

related to raindrop impact and associated rapid wetting of the soil surface (West *et al.*, 1992). Structural crusts are also termed 'rain-impact crust' (Moss, 1991). This literature review will be confined to processes that cause development of structural crusts.

1.3.1.2 Processes of sealing

Farres (1978) proposed a simple model for the development of disrupted layers by rainfall based on aggregate breakdown and filling of interstices by smaller aggregates and particles. Thus, according to Farres (1978), a rain-impacted seal develops from two stages: (1) aggregate breakdown, and (2) rearrangement and packing of the disrupted materials. He also found that sealing developed vertically and took place as soon as aggregate breakdown started. But, once the equilibrium thickness had been reached, vertical development of the disrupted layer stopped and the aggregates below the seal were wetted slowly and remained at high matric suction, and hence protected from further breakdown.

Le Bissonnais *et al.* (1989) and Moss (1991) distinguished three stages in the process of sealing under simulated rainfall:

- 1) *Water entry stage*: at this stage most of the rain water enters the soil directly with little lateral flow, surface disturbance or air-splashing of soil particles;
- 2) *Slaking and air-splashing stage*: water entry decreases, while lateral outflow discharge increases, deep craters develop and particle segregation takes place resulting in formation of a silt (10 to 50 μm) layer at the surface (smaller and large particles were preferentially removed by airsplash);

3) *Development of planar surface*: craters are flattened by water ponding, and runoff initiated. A rain-impact seal forms in the transition between stages 2 and 3.

1.3.1.3 Characteristics of sealing

Sealing is a surface structural condition prevailing during rainfall. Its characterisation, therefore, should only be based on measurements made during rainfall or immediately after rainfall ceases. Water flow indices, such as hydraulic conductivity, relative conductivity, or infiltration rate, have been used to characterise sealing (Hillel and Gardner, 1969; Romkens *et al.*, 1990; Bohl and Roth, 1993). The proportion of fine materials at the surface, such as those smaller than 0.125 mm, measured immediately after the rain ceases has also been used to characterise sealing (Glanville and Smith, 1988; Geeves *et al.*, 1994; Loch, 1994).

Sealing can also be characterised indirectly by measuring crust properties. This includes crust micromorphological features (Chen *et al.*, 1980; Onofiok and Singer, 1984; Bresson and Boiffin, 1990) and surface strength (Morrison *et al.*, 1985; Bradford *et al.*, 1986; Govers and Poesen, 1986). A limitation of these methods is that a seal can deform during drying, so that the measurements made on the crust may differ from those of a seal.

1.3.1.4 Antecedent soil water content and sealing

Antecedent soil water content influences surface sealing by rainfall through its effect on the stability of aggregates against raindrop impact. This can be explained in terms of the effect of water content on slaking caused by the disruptive forces of entrapped air, double layer swelling, and heat of wetting (Collis-George and Lal, 1971; Emerson, 1977), and the effect of water on the strength of aggregates (Truman *et al.*, 1990). Le Bissonnais *et al.*

(1989) compared crusts which developed from initially air-dry aggregates with those developed from aggregates pre-wetted under vacuum (until saturation) and found that:

- 1) Dry aggregates were more prone to disruption by raindrop impact than pre-wetted aggregates, leading to more rapid sealing of the former. A complete seal formed and ponding started on initially dry beds. On pre-wetted beds, however, pores between aggregates were only partially clogged by fine particles, mainly mobilised silt, and ponding did not occur.
- 2) There was greater surface particle mobilisation during rainfall on initially dry aggregates than in pre-wetted aggregates. Aggregates larger than 2 mm decreased, while those smaller than 0.1 mm increased rapidly within 5 minutes. In pre-wetted beds, aggregates larger than 2 mm were maintained almost unchanged. There was no difference in particle mobilisation between the seal and the layer below the seal within the 0 to 10 mm depth in pre-wetted aggregates. This resulted in more homogenous aggregate disintegration in the 0 to 10 mm depth.
- 3) There were three distinct stages of seal evolution developed from initially dry aggregates: (i) wetting of the upper layer of aggregates, development of micro-cracks and initiation of particle mobilisation and weakening of bonding between aggregates; (ii) saturation of aggregates, mobilised particles during the first stage were moved by raindrop impact and subsequently filled inter-aggregate pores; and (iii) ponding initiation. Mobilised particles sealed the soil surface, and seal hydraulic conductivity became smaller than rainfall intensity. The surface consisted of aggregates or particles of less than 1 mm with an increased proportion of those smaller than 0.1 mm.

- 4) There were no clearly distinct stages of seal evolution observed on pre-wetted beds and development of the seal was very slow. Rainfall caused little aggregate breakdown. A small proportion of particles smaller than 0.1 mm (mainly silt grains) were mobilised, bridging the aggregates just under the surface layer. The surface was not completely sealed as some aggregates remained relatively intact. The crust which developed was not as dense as that developed from initially dry aggregates, but was thicker.

Results of many studies have shown that infiltration rate (Collis-George and Lal, 1971; Helalia *et al.*, 1988; Le Bissonnais and Singer, 1992; Geeves *et al.*, 1994) and shear strength of soil, measured by fall cone penetrometer (Truman and Bradford, 1990; Truman *et al.*, 1990) were higher in pre-wetted than initially dry soils subjected to rain. Le Bissonnais and Singer (1992) found that the greater infiltration rate for pre-wetted soils was maintained even on the third rainfall event, although the difference narrowed in subsequent rainfalls.

Some researchers have reported contrary results: sealing increased with increasing water content (Cousen and Farres, 1984). Experimental technique may explain this discrepancy. Cousen and Farres (1984) pre-wetted the aggregates by adding distilled water drop-wise from a micro-syringe to produce water contents of 0, 10, 20, 30 and 40 kg kg⁻¹. They did not mention the actual rate of wetting (*i.e.* the time needed to reach each of these predetermined water contents), nor the size of the drops produced from the syringe. If the rate of wetting was different, then aggregates could have experienced different degrees of internal stresses caused by different swelling and relaxation time, which might have weakened the aggregates. It would be expected that the weakening

effect would increase with the final water content, which determined the number of drops added.

In the field, water content varies seasonally and, because water content is a key factor in the process of sealing and crusting, susceptibility of surface aggregates to crusting and degree of crusting in the field changes with seasons (Bullock *et al.*, 1988; Le Bissonnais and Bruand, 1993). Therefore, there is no universal crust morphology for all soil conditions, or specific morphology for each soil. While some soils may be more prone to crusting due to their inherent properties, the degree of crusting largely depends on rainfall characteristics, and climatic conditions and soil management affecting soil water content.

1.3.1.5 Thickness of seal and disrupted layer

The thickness of the seal and disrupted layer observed in the field varies, from a few millimetres to a few tens of millimetres, depending on soil antecedent water content, aggregate stability and rainfall characteristics. Indeed, even in the same soil, thickness of the disrupted layer can vary considerably if antecedent soil conditions such as soil matric suction and aggregate size are different. Le Bissonnais *et al.* (1989) found that thin crusts (about 5 mm) were associated with initially dry aggregates compared with thicker crusts (10 mm or more) which were associated with pre-wetted aggregates of the same soil. Timm *et al.* (1971) observed a 'crust' as thick as 75 mm on the ridge of a furrow irrigated sandy loam soil following intense rainfall. The crust in the furrow was only several millimetres thick. Timm *et al.* (1971) did not explain the conditions of the soil on the ridge which lead to a deep disrupted layer after rainfall. However, it is likely that the soil on the ridge was less compact than in the furrow. The porous structure on the ridge favoured

rapid water entry and promoted extensive and deep aggregate breakdown. On drying, this disrupted layer would develop features more consistent with hardsetting rather than crusting.

Farres (1978) found that the thickness of the crust that developed following simulated rainfall depended on initial aggregate size and the volume of water applied (a function of rainfall intensity, area of soil target, and rainfall duration). Crust thickness was a linear function of the volume of water applied and the slope of the relationship increased with antecedent aggregate size. Vertical development of the disrupted layer took place as soon as aggregate breakdown commenced, but once the 'equilibrium' thickness of the seal had been reached, aggregates below the seal were protected from raindrop impact. Thus, only when water can penetrate into the deeper layers in the aggregate bed, will the aggregates below the surface layer comminute, allowing a thicker disrupted layer to develop. Therefore, it is the depth of water that penetrates the soil before sealing that influences the vertical development of the seal or disrupted layer. As soil hydraulic conductivity before sealing is much higher than after sealing (Geeves *et al.*, 1994), most disruption and subsequent packing occurs before seal formation, and not after.

Collis-George and Lal (1971) reported that the degraded structure of the surface layers prevented fast entry of water into lower layers. Therefore, if a complete seal forms rapidly during rainfall, a thin crust will form on drying. West *et al.* (1992) proposed a model which related the thickness of a structural crust to the rate that surface aggregates broke down during rainfall. According to this model, crust thickness is governed by the rate and degree of sealing. Soils with more stable aggregates (*i.e.* which do not seal readily) would form thicker disrupted layers as they allow more water to infiltrate. Soils with unstable aggregates (*i.e.* which form a seal readily) would form thinner crusts. Figure

1.2 shows that the thickness of the disrupted layer is negatively related to the amount of water dispersible clay.

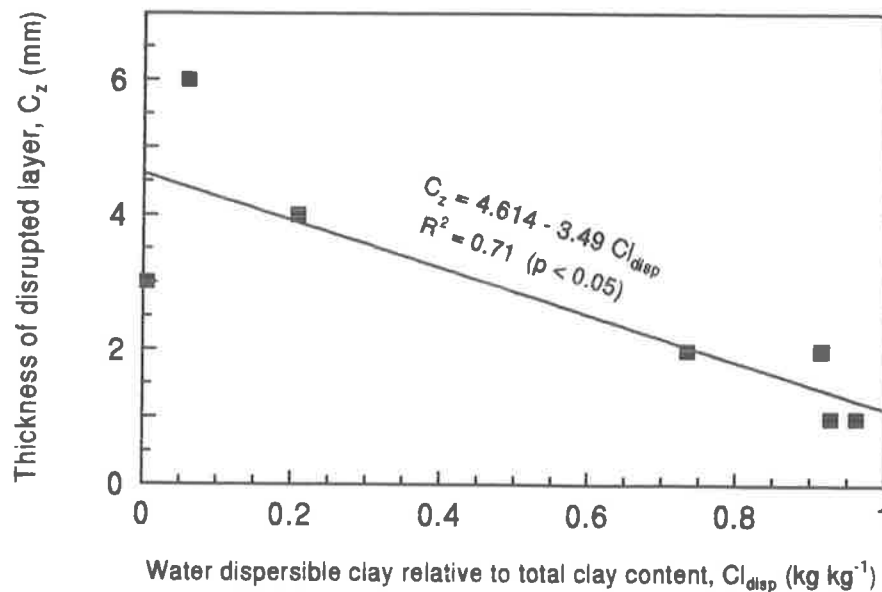


Figure 1.2. Relationship between thickness of rain-induced disrupted layer and water dispersible clay relative to clay content from various soils (from West *et al.*, 1992).

Most of the published data is confined to discussion of the thickness of the disrupted layer as affected by soil conditions such as water content and aggregate stability. However, aggregate breakdown is also a function of rainfall characteristics. Yet, studies on how rainfall characteristics, in combination with soil conditions, affect the thickness of the disrupted layer have been given little attention. The development of sealing, crusting and the associated disrupted layer as a function of rainfall characteristics deserves more study.

1.3.2 Hardsetting

1.3.2.1 Characteristics of hardset soil

Hardsetting soils were first given recognition in Australia and the state of hardsetting was described as “a compact, hard, apparently apedal condition forms on drying. Surface not disturbed or indented by pressure of forefinger” (Northcote, 1979). As more information about hardsetting has become available, it is apparent that this definition does not give an adequate description of the condition or the processes of hardsetting. A new definition is required to describe hardsetting adequately, and perhaps more quantitatively. Ley *et al.* (1989) characterised hardsetting on the basis of the extent to which structural degradation caused a rapid increase in compressive and tensile strength within a narrow range of decrease in water content. Hardsetting is closely associated with aggregate slaking, but not necessarily with dispersion (Mullins *et al.*, 1990). On draining, following rapid wetting, the slaked aggregates collapse extensively. On drying, soil strength increases rapidly over a small decrease of water content, leading to high soil strength when the soil is still relatively wet (Ley *et al.*, 1989; Mullins *et al.*, 1990; Gusli *et al.*, 1994a, b).

Gusli (1989) attempted to describe hardsetting more quantitatively using properties such as bulk density, volume strain on drying, tensile strength, air-entry suction, air-filled porosity, particle-size distribution and clay mineralogy. The characteristics of his hardsetting soils were: 1) when subjected to flood wetting, the soil suffered a volume reduction of 25 % or more from a minimum air-dry bulk density and on subsequent drying developed a tensile strength of more than 20 kPa at an air-dry water content; 2) after forming a hardset layer, the air-entry suction of the soil was greater than 0.4 m of water and air-filled porosity at a matric suction of 0.5 m was less than 0.1 m⁻³; 3) at a depth

of 0 to 100 μm , particle-size distribution was such that more than 0.80 kg kg^{-1} was less than 200 μm in diameter, and more than 0.15 kg kg^{-1} was 2 to 20 μm ; 4) the ratio of illite to kaolinite was greater than 0.5; 5) organic carbon content was less than 0.01 kg kg^{-1} ; and 6) the ESP of hardsetting soils were not necessarily high, *i.e.* soils with ESP values as low as 1.5 set hard quite readily under appropriate circumstances.

Mullins *et al.* (1990) listed types of soil over a wide range of texture classes that are potentially hardsetting, in terms of their shrink/swell potential: sandy loam, sandy clay loam, sandy loam and loamy sand soils. Clay soils are not potentially hardsetting, because they contain sufficient clay to shrink and swell in all directions (not uniaxial), which regenerates structure. Sandy soils are also not hardsetting because of their low shear and tensile strength. Kaolinitic and illitic soils have greater potential to become hardsetting than smectitic soils. Clearly, there is a wide range of soils that can hardset, but in reality, many soils in the texture classes identified by Mullins *et al.* (1990) do not set hard. The question of what exactly are the factors that induce hardsetting arises.

Mullins *et al.* (1990) stated that, given an appropriate particle-size distribution and clay mineralogy, low organic matter content is conducive hardsetting. Soil organic matter is sensitive to soil management. Ley *et al.* (1989) concluded that clearing vegetation in the tropics followed by tillage led to a decrease in soil organic matter and wet aggregate stability and increased bulk density, leading to an increase in soil strength. The increase of soil strength with decreased water content was much more marked for tilled soils than for the less disturbed soils associated with native forests or no-till cropping. Similarly, Chan (1989) found that the friability of Australian red-brown earths was affected by land use and tillage practices. Soils under permanent pasture for 25 years were friable and did not

exhibit hardsetting. However, grazing and cropping by conventional cultivation reduced friability of the soil and exacerbated the tendency for hardsetting.

1.3.2.2 Process of hardsetting

The process of hardsetting involves collapse of aggregates during wetting and draining (Cockroft and Martin, 1981; Gusli *et al.*, 1994a) and the rapid development of high strength during drying (Gusli *et al.*, 1994b). Mullins *et al.* (1990) identified three distinct sequential physical processes in hardsetting: (1) *slumping* associated with slaking or comminution which occurs during and after wetting; (2) *uniaxial shrinkage* which takes place mainly during drainage from 0 to 0.5 m matric suction; and (3) *rapid hardening* caused by a rapid increase of strength over a small decrease in water content. The greater the collapse (slumping and uniaxial shrinkage) during wetting and draining, the greater the tendency for the soil to set hard on drying (Aylmore and Sills, 1982; Gusli *et al.*, 1994a, b).

Flooding unstable, air-dry aggregates caused hardsetting (Gusli, 1989; Weaich, *et al.*, 1992; Gusli *et al.*, 1994a). However, deformation did not occur while aggregates remained saturated, *i.e.* zero effective stress (Equation 1.1). Deformation took place only after draining and drying, and was associated with increased effective stress. This suggests that development of effective stress during draining and drying is an essential part of the process of hardsetting (Gusli *et al.*, 1994a).

1.3.2.3 Factors affecting hardsetting

The method of wetting plays an important role in hardsetting process, as it determines whether unstable aggregates slake on wetting or not. Gusli *et al.* (1994a) found that soils that set hard in the field remained friable if wetted under 0.20 m matric suction with distilled water. When wetted by flooding, however, the soils set hard on drying.

Published data on the hardsetting behaviour in relation to method of wetting has been limited to flood or suction wetting (Mullins *et al.*, 1992; Weaich *et al.*, 1992; Gusli *et al.*, 1994a). No studies have related hardsetting to rainfall characteristics and the question of how rainfall influences hardsetting deserves more attention.

Arndt (1985) has indicated that surface crusting processes can extend deeper, depending on aggregate-size distribution and rainfall 'disjunctivity' (a complex parameter, which is proportional to rainfall kinetic energy, intensity and duration). Fine (0 to 3 mm) aggregates showed greatest collapse and developed a thicker crust and higher strength on drying compared to 3 to 40 mm aggregates. However, his data also show that increasing aggregate size range from 3 - 6 mm, to 6 - 13 and finally 23 - 41 mm resulted in development of thicker crusts, especially under highly disjunctive rain. Effect of initial aggregate size on strength of dry crust followed the same trend.

Arndt (1985) suggested that rapid development of a seal under certain initial conditions of aggregate size and rainfall disjunctivity prevented aggregates below the seal from being saturated. He claimed that "evidence from northern Australia suggests that a thin seal produced on fine clods by heavy rain before ponding occurs should reduce infiltration rates and hence slaking due to saturation below the seal". Unlike rainfall wetting, flooding did not produce a seal, but all aggregates (3 to 6 mm diameter) in the

bed of 20 mm thick were disrupted by the wetting process and on drying the bed set hard.

Arndt's (1985) data relate quite well to the model proposed by Farres (1978) for vertical crust development. The larger the aggregates and the more water applied to the beds, the deeper is the disrupted layer. Nevertheless, we still do not understand the actual mechanisms of how and what rainfall factors and soil conditions determine the thickness of the disrupted layer, and the development of strength on drying.

Soil water content and matric suction prior to and during wetting also play an important role in the extent of aggregate disruption imposed by wetting energy (hydration or mechanical energy). Fast wetting (such as by flooding or intense rain) of air-dry aggregates induces slaking which produces smaller fragments of aggregates (Panabokke and Quirk, 1957; Chan and Mullins, 1994). Pre-wetting under suction to about field capacity can stabilise aggregates against wetting energy (Panabokke and Quirk, 1957; Le Bissonnais *et al.*, 1989; Truman *et al.*, 1990) as it prevents or minimises slaking. However, further decreasing matric suction to zero weakens aggregates due to decreased aggregate strength (Al-Durrah and Bradford, 1981; Francis and Cruse, 1983).

At zero matric suction, aggregate strength is weakest due to zero effective stress (Equation 1.1), making it susceptible to external stresses such as those imposed by wetting and subsequent draining. When saturated, the confined aggregates may be incompressible as the majority of pores are filled with water, but individual aggregates may slump due to the overburden mass of water and soil resulting in particle rearrangement and packing. As matric suction decreases during irrigation, from about 0.4 m to zero, Keller (1970) and Ghavami *et al.* (1974) observed increased soil settlement. Deep aggregate disruption may well be attributable to deformation of

aggregates because of low (near zero) matric suction during wetting, as well as slaking. At present we do not fully understand the role of matric suction in aggregate disruption, especially when related to wetting energy.

Soil drainage rate influences the change of matric suction during flood wetting and rainfall, as it controls the balance between the inflow and outflow of water. Therefore, the soil's drainage status can be expected to influence aggregate slumping during wetting. Information on the extent of drainage and interaction between drainage and matric suction affecting aggregate disruption and hardsetting is lacking in the literature.

1.4 The distinction between crusting and hardsetting

Hardsetting differs from crusting, even though they both reflect surface aggregate breakdown and packing of disrupted materials. Mullins *et al.* (1987) illustrated hardsetting behaviour as an extreme type of soil structural degradation that can develop from friable soil. They proposed that friable, crusting and hardsetting soil behaviour was a continuum with crusting lying between hardsetting and friable behaviour. The position of a soil on the continuum depended on the soil properties and management. Subsequently, Mullins *et al.* (1990) distinguished crusting from hardsetting in terms of the depth of disrupted layer: hardsetting disrupts the whole A₁ horizon, while crusting is only few millimetres thick. Bristow *et al.* (1994) stated that a crust is typically less than 10 mm thick, while a hardset layer can extend deeper than 50 mm.

It appears, therefore, that crusting develops from a thin surface seal, while hardsetting develops from a thicker disrupted layer. However, as crusting and

hardsetting depend on soil management, especially in relation to soil water condition and aggregate stability (Mullins *et al.*, 1987), the tendency to form a crust or hardset layer should depend on wetting conditions. Flooding unstable air-dry aggregates caused hardsetting (thick disrupted layer), while suction wetted soil (0.20 m of water) remained friable (Gusli *et al.*, 1994a). On the other hand, rainfall of sufficiently high kinetic energy, caused sealing (Agassi, *et al.*, 1985; Hignett, 1991). Mechanical impact of raindrops and surface aggregate breakdown are conditions promoting crusting, but not necessarily hardsetting (Mullins *et al.*, 1990). Field observations indicate that hardsetting does develop in tilled soil after rainfall. However, it is not clear from the literature, to what extent rainfall influences hardsetting. When does rainfall cause deep aggregate disruption rather than form a thin surface seal? Are there conditions when a soil will behave as a crusting soil under certain circumstances, but exhibit hardsetting under different circumstances? Is hardsetting caused by rainfall similar to that caused by flooding?

1.5 Conclusions

1. Aggregate breakdown by wetting is controlled by modes of wetting (associated with hydration and mechanical energy) and antecedent soil matric suction. Faster rates of wetting and/or greater mechanical energy cause greater aggregate breakdown. Antecedent matric suction determines the extent of the effect of hydration or mechanical energy on aggregate breakdown imposed by wetting. Aggregates pre-wetted to about field capacity water content are more stable than air-dry aggregates. However, saturated aggregates are weakest and most susceptible to stresses during wetting.

2. Drainage, through its indirect effect on soil matric suction during wetting, also influences aggregate stability on wetting.
3. The potential effect of rainfall on aggregate breakdown has been assessed from a number of rainfall parameters: kinetic energy, intensity, kinetic energy flux density, momentum, cumulative energy, and duration. Kinetic energy and kinetic energy flux density (kinetic energy multiplied by intensity) are considered to be better parameters for describing the effects of rainfall on surface aggregate disruption than others, especially for unstable soil aggregates.
4. Crusting is different to hardsetting. A crust develops from a seal, typically less than 10 mm thick, whereas a hardset surface layer develops from a disrupted layer, thicker than 50 mm.
5. There is much literature available on the process of sealing (crusting) by rainfall. A surface seal is formed by rainfall of sufficiently high kinetic energy. There is much information in the literature on processes of hardsetting by flood wetting and conditions favouring it, but little is known about how rainfall affects hardsetting. We do not understand how rainfall can cause deep aggregate disruption to form hardsetting, as observed in the field. We also do not know why an unstable soil can behave as a crusting soil under certain rainfall and soil conditions, but exhibit hardsetting under different circumstances.

1.6 References

- Agassi, M. and G. J. Levy (1991). Stone-cover and rain intensity: Effects on infiltration, erosion and water splash. *Australian Journal of Soil Research* 29: 565-575.
- Agassi, M., J. Morin, and I. Shainberg (1985). Effect of raindrop impact energy and water salinity on infiltration rates of sodic soils. *Soil Science Society of America Journal* 49: 186-190.

- Al-Durrah, M. M. and J. M. Bradford (1981). New methods of studying soil detachment due to waterdrop impact. *Soil Science Society of America Journal* 45: 949-953.
- Arndt, W. (1985). Factors Affecting the Nature and Impedance of Soil Surface Seal at Katherine, N.T. CSIRO Austr. Div. Soils Rep. No. 79.
- Aylmore, L. A. G. and I. D. Sills (1982). Characterization of soil structure and stability using modulus of rupture-exchangeable sodium percentage relationship. *Australian Journal of Soil Research* 20: 213-224.
- Baumhardt, R. L., Romkens, M. J. M., F. D. Whisler, and J.-Y. Parlange (1990). Modeling infiltration into a sealing soil. *Water Resources Research* 26: 2497-2505.
- Baver, L. D., W. H. Gardner, and W. R. Gardner (1972). Soil Physics. John Wiley, New York.
- Bishop, A. W. and G. E. Blight (1963). Some aspect of effective stress in saturated and partly saturated soils. *Geotechnique* 13: 177-197.
- Bohl, H. and Ch. H. Roth (1993). A simple method to assess the susceptibility of soils to form surface seals under field conditions. *Catena* 20: 247-256.
- Boiffin, J. (1985). Stages and time-dependency of soil crusting *in-situ*. In: Callebaut *et al.* (eds.). Assessment of Soil Surface Sealing and Crusting. Proceedings of the Symposium, Department of Soil Physics, State University of Ghent, Ghent, Belgium, p. 91-98.
- Bradford, J. M., P. A. Remley, J. E. Ferris, and J. B. Santini (1986). Effect of surface sealing on splash from a single waterdrop. *Soil Science Society of America Journal* 50: 1547-1552.
- Bresson, L. M. and J. Boiffin (1990). Morphological characterization of soil crust development stages on an experimental field. *Geoderma* 47: 301-325.
- Bristow, K. L., A. Cass, K. R. J. Smettem, and P. J. Ross (1994). Modelling effects of surface sealing on water entry and re-distribution. Proceedings of the International Symposium on 'Sealing, Crusting, Hardsetting Soils: Productivity and Conservation' 7-11 February 1992, University of Queensland, Brisbane, Australia. (*in press*).
- Bullock, M. S., W. D. Kemper, and S. D. Nelson (1988). Soil cohesion as affected by freezing, water content, time and tillage. *Soil Science Society of America Journal* 52: 770-776.
- Busch, C. D., E. W. Rochester, C. L. Jernigan (1973). Soil crusting related to sprinkler intensity. *Transactions of American Society of Agricultural Engineers* 16: 808-809.
- Cernuda, C. F., R. M. Smith, and J. Vicente-Chandler (1953). Influence of initial soil moisture condition on resistance of macroaggregates to slaking and to water-drop impact. *Soil Science* 77: 19-27.
- Chan, K.Y. (1989). Friability of a hardsetting soil under different tillage and land use practices. *Soil & Tillage Research* 13: 287-298.

- Chan, K. Y. and C. E. Mullins (1994). Slaking characteristics of some Australian and British soils. *European Journal of Soil Science* 45: 273-283.
- Chen, Y., J. Tarchitzky, J. Brouwer, J. Morin, and A. Banin (1980). Scanning electron microscope observations on soil crusts and their formation. *Soil Science* 130: 49-55.
- Cockroft, B. and F. M. Martin (1981). Irrigation. *In: J. M. Oades, D. G. Lewis and K. Norrish (eds.). Red-brown Earths of Australia.* Waite Agr. Res. Inst. and CSIRO Div. of Soils, Adelaide, South Australia.
- Collis-George, N. and R. Lal (1971). Infiltration and structural changes as influenced by initial moisture content. *Australian Journal of Soil Research* 9: 107-116.
- Cousen, S. M. and P. J. Farres (1984). The role of moisture content in the stability of soil aggregates from a temperate silty soil to raindrop impact. *Catena* 11: 313-320.
- Dexter, A. R. (1988). Advances in characterization of soil structure. *Soil and Tillage Research* 11: 199-238.
- Duley, F. L. (1939). Surface factors affecting the rate of intake of water by soils. *Soil Science Society of America Proceedings* 4: 60-64.
- Eigel, J. D. and I. D. Moore (1983). Effect of rainfall energy on infiltration into bare soil. Proc. of the National Conf. on Advances in Infiltration, Dec. 12-13, 1983, Chicago, Illinois, ASAE, p. 188-200.
- Emerson, W. W. (1977). Physical properties and structure. *In: J. S. Russell and E. L. Greacen (eds.). Soil Factors in Crop Production in a Semi-arid Environment.* Queensland University Press, Brisbane, p. 78-104.
- Emerson, W. W. and G. M. F. Grundy (1954). The effect of rate of wetting on water uptake and cohesion of soil crumbs. *Journal of Agricultural Science* 44: 249-253.
- Epstein, E. and W.J. Grant (1973). Soil crust formation as affected by raindrop impact. *In: Hadas et al. (eds.). Physical Aspects of Soil Water and Salts in Ecosystems.* Springer-Verlag, New York, pp.: 195-201.
- Farres, P. (1978). The role of time and aggregate size in the crusting process. *Earth Surface Processes* 3: 243-254.
- Farres, P. J. (1980). Some observations on the stability of soil aggregates to raindrop impact. *Catena* 7: 223-231.
- Francis, P. B. and R. M. Cruse (1983). Soil water matric potential effects on aggregate stability. *Soil Science Society of America Journal* 47: 578-581.
- Geeves, G. W., P. B. Hairsine, and I. D. Moore (1994). Rainfall induced aggregate breakdown and surface sealing on a light textured soil. Proceedings of the International Symposium on 'Sealing, Crusting, Hardsetting Soils: Productivity and Conservation' 7-11 February 1992, University of Queensland, Brisbane, Australia. (*in press*).

- Ghavami, M., J. Keller, and I. S. Dunn (1974). Predicting soil density following irrigation. *Transactions of the American Society of Agricultural Engineers* 17: 166-171.
- Glanville, S. F and G. D. Smith (1988). Aggregate breakdown in clay soils under simulated rain and effects on infiltration. *Australian Journal of Soil Research* 26: 111-120.
- Govers, G. and J. Poesen (1986). A field-scale study of surface sealing and compaction of loam and sandy loam soils. Part I. Spatial variability of surface sealing and crusting. In: F. Callebaut *et al.* (eds.). Assessment of soil surface sealing and crusting. State University of Ghent, Belgium, p. 171-182.
- Gusli, S. (1989). Structural collapse and strength of some Australian soils in relation to hardsetting behaviour. M. Rur. Sc. Thesis. University of New England, Australia.
- Gusli, S., A. Cass, D. A. MacLeod, and P. S. Blackwell (1994a). Structural collapse and strength of some Australian soils in relation to hardsetting: I. Structural collapse on wetting and draining. *European Journal of Soil Science* 45: 15-21.
- Gusli, S., A. Cass, D. A. MacLeod, and P. S. Blackwell (1994b). Structural collapse and strength of some Australian soils in relation to hardsetting: II. Tensile strength of collapsed aggregates. *European Journal of Soil Science* 45: 23-29.
- Helalia, A. M., J. Letey and R. C. Graham (1988). Crust formation and clay migration effects on infiltration rate. *Soil Science Society of America Journal* 52: 251-255.
- Hignett, C. T. (1991). Relating soil structure to runoff quality and quantity. International Hydrology & Water Resources Symposium, Perth 2-4 October 1991, Inst. of Engineers Australia, Publication 91/22, p. 301-305.
- Hillel, D. and W. R. Gardner (1969). Steady infiltration into crust topped profiles. *Soil Science* 108: 137-142.
- Keller, J. (1970). Sprinkler intensity and soil tilth. *Transactions of the American Society of Agricultural Engineers* 13: 118-125.
- Kemper, W. D. and E. J. Koch (1966). Aggregate stability of soils from western United States and Canada, US Dept. Agr. Tech. Bull. No. 1355.
- Kemper, W. D., T. J. Trout, M. J. Brown, and R. C. Rosenau (1985). Furrow erosion and water and soil management. *Transactions of the American Society of Agricultural Engineers* 28: 1564-1572.
- Kinnell, P.I. (1981). Rainfall intensity - kinetic energy relationships for soil loss prediction. *Soil Science Society of America Journal* 45: 153-155.
- Kinnell, P.I. (1987). Rainfall energy in Eastern Australia: Intensity - kinetic energy relationships for Canberra, ACT. *Australian Journal of Soil Research* 25: 547-553.
- Le Bissonnais, Y. and A. Bruand (1993). Crust micromorphology and runoff generation on silty soil materials during different seasons. *Catena Supplement* 24: 1-16.
- Le Bissonnais, Y., A. Bruand, and M. Jamagne (1989). Laboratory experimental study of soil crusting: relation between aggregate breakdown mechanisms and crust structure. *Catena* 16: 377-392.

- Le Bissonnais, Y. and M. J. Singer (1992). Crusting, runoff, and erosion response to soil water content and successive rainfalls. *Soil Science Society of America Journal* 56: 1898-1903.
- Ley, G. J., C. E. Mullins, and R. Lal (1989). Hard-setting behaviour of some structurally weak tropical soils. *Soil and Tillage Research* 13: 365-381.
- Loch, R. J. (1994). A method for measuring aggregate water stability of dryland soils with relevance to surface seal development. *Australian Journal of Soil Research* 32: 687-700.
- Lyles, L., L. A. Disrud, and N. P. Woodruff (1969). Effects of soil physical properties, rainfall characteristics, and wind velocity on clod disintegration by simulated rainfall. *Soil Science Society of America Proceedings* 33: 302-306.
- Mantell, A. and D. Goldberg (1966). Effect of water application rate on soil structure. *Journal of Agricultural Engineering Research* 11: 76-79.
- Marshall, T. J. and J. W. Holmes (1988). Soil Physics. Cambridge Univ. Press. London.
- Mohammed, D. and R. A. Kohl (1987). Infiltration response to kinetic energy. *Transactions of American Society of Agricultural Engineers* 30: 108-111.
- Morin, J. and Y. Benyamini (1977). Rainfall infiltration into bare soils. *Water Resources Research* 13: 813-817.
- Morrison, M. W., L. Prunty, and J. F. Giles (1985). Characterizing strength of soil crusts formed by simulated rainfall. *Soil Science Society of America Journal* 49: 427-431.
- Moss, A.J. (1991). Rain impact soil crust: I. Formation on a granite-derived soil. *Australian Journal of Soil Research* 29: 271-289.
- Mualem, Y., S. Assouline, and H. Rohdenburg (1990). Rainfall induced soil seal. (A) A critical review of observations and models. *Catena* 17: 185-203.
- Mullins, C. E., A. Cass, D. A. MacLeod, D. J. M. Hall and P. S. Blackwell (1992). Strength development during drying of cultivated, flood-irrigated hardsetting soil. II. Trangie soil, and comparison with theoretical predictions. *Soil and Tillage Research* 25: 129-147.
- Mullins, C. E., D. A. MacLeod, K. H. Northcote, J. M. Tisdall, and I. M. Young (1990). Hardsetting soils: behaviour, occurrence, and management. *Advances in Soil Science* 11: 37-108.
- Mullins, C. E., I. M. Young, A. G. Bengough, and G. L. Ley (1987). Hard-setting soils. *Soil Use and Management* 3: 79-83.
- Mullins, C. E. and K. P. Panayiotopoulos (1984). The strength of unsaturated mixtures of sand and kaolin and the concept of effective stress. *Journal of Soil Science* 35: 459-468.
- Northcote, K.H. (1979). A Factual Key for the Recognition of Australian Soils. Rellim, Adelaide.
- Onofiok, O. and M. Singer (1984). Scanning electron microscope studies of surface crusts formed by simulated rainfall. *Soil Science Society of America Journal* 48: 1137-1143.

- Panabokke, C. R. and J. P. Quirk (1957). Effect of initial water content on stability of soil aggregates in water. *Soil Science* 83: 185-195.
- Ragab, R. A. (1983). The effect of sprinkler intensity and energy of falling drops on soil surface sealing. *Soil Science* 136: 117-123.
- Romkens, M. J. M., R. L. Baumhardt, M. B. Parlange, F. D. Whisler, J.-Y. Parlange, and S. N. Prasad (1986). Rain-induced surface seals: their effect on ponding and infiltration. *Annales Geophysicae* 4, B, 4, 417-424.
- Romkens, M. J. M., S. N. Prasad, and J.-Y. Parlange (1990). Surface seal development in relation to rainstorm intensity. In: R. B. Bryan (ed.) Soil Erosion. Experiments and Models. *Catena Supplement* 17: 1-11.
- Rose, C. W. (1960). Soil detachment caused by rainfall. *Soil Science* 89: 28-35.
- Rosewell, C. J. (1986). Rainfall kinetic energy in Eastern Australia. *Journal of Climate and Applied Meteorology* 25: 1695-1701.
- Shainberg, I. and M. Singer (1988). Drop impact energy - soil exchangeable sodium percentage interactions in seal formation. *Soil Science Society of America Journal* 52: 1449-1452.
- Shvebs, G.I. (1968). Data on the erosive action of water drops. *Soviet Soil Science* No.2: 262-269.
- Thompson, A.L. and L.G. James (1985). Water droplet impact and its effect on infiltration. *Transactions of American Society of Agricultural Engineers* 28: 1506-1510, 1520.
- Timm, H., J. C. Bishop, J. W. Perdue, D. W. Grimes, R. E. Voss, and D. N. Wright (1971). Soil crusting effects on potato plant emergence and growth. *California Agriculture* 25 (8): 5-7.
- Towner, G. D. and E. C. Childs (1972). The mechanical strength of unsaturated porous granular material. *Journal of Soil Science* 23: 481-498.
- Truman, C. C. and J. M. Bradford (1990). Effect of antecedent soil moisture on splash detachment under simulated rainfall. *Soil Science* 150: 787-798.
- Truman, C. C., J. M. Bradford, and J. E. Ferris (1990). Antecedent water content and rainfall energy influence on soil aggregate breakdown. *Soil Science Society of America Journal* 54: 1385-1392.
- Weaich, K., A. Cass, and K. L. Bristow (1992). Use of penetration resistance characteristic to predict soil strength development during drying. *Soil and Tillage Research* 25: 149-166.
- West, L. T., S. C. Chiang, and L. D. Norton (1992). The morphology of surface crusts. In: *M.E. Sumner and B.A. Stewart (eds.). Soil Crusting. Chemical and Physical Processes*. Advances in Soil Science. Lewis Publ., Boca Raton, pp.: 73-92.
- Wischmeier, W. H. (1959). A rainfall erosion index for a Universal Soil-Loss Equation. *Soil Science Society of America Proceedings* 23: 246-249.
- Wischmeier, W. H. and D. D. Smith (1958). Rainfall energy and its relationship to soil loss. *Transactions American Geophysical Union* 39: 285-291.

Young, R. A. and J. L. Wiersma (1973). The role of rainfall impact in soil detachment and transport. *Water Resources Research* 9: 1629-1636.

Chapter 2

An automated laboratory rainfall simulation system with controlled rainfall intensity, raindrop energy and soil drainage

2.1 Introduction

Change of soil structure after tillage is primarily induced by water, through rainfall or irrigation. Many researchers have used rainfall simulators to study change of soil structure induced by rain. Aggregate breakdown by rainfall is determined by rainfall properties (kinetic energy and intensity) and soil factors, *i.e.* the resistance of aggregates to breakdown by external forces induced by rainfall.

Raindrop energy influences aggregate breakdown through its effect on mechanical stresses impacted by raindrops, while rainfall intensity influences aggregate stability through its effect on hydration processes. In natural rainfall the two rainfall factors are loosely correlated (Rosewell, 1986; Kinnell, 1987). However, different combinations of these properties can yield different degrees of aggregate breakdown (Ragab, 1983; Thompson and James, 1985; Mohammed and Kohl, 1987). Particular combinations of kinetic energy and intensity determine whether hydration (rainfall intensity) or mechanical forces (impact energy) is the dominant factor causing aggregate breakdown, or both.

Equally important, antecedent soil water content and matric suction determine the stability of aggregates against the mechanical stress and hydration effect imposed by rainfall (Al-Durrah and Bradford, 1981; Francis and Cruse, 1983; Le-Bissonnais *et al.*, 1989; Truman and Bradford, 1993). Drainage condition, which influences soil matric

suction during rainfall, therefore also determines aggregate breakdown by raindrop impact. Furthermore, the saturated and undrained condition of a confined aggregate bed may prevent aggregate deformation by rainfall, as the soil pores which are fully filled by water become incompressible.

Qualitative relationships between rainfall energy and soil damage have been established for some time. However, the effect of drop size and kinetic energy of rain on soil surfaces have not been studied in quantitative detail, in part because of the difficulty of measuring rapid changes in water balance at the soil surface. Rainfall simulators used to measure effects of rain on soil structure have been one of two types: (1) simulators designed to produce large drops at near terminal velocity, usually delivered from modules with arrays of hypodermic needles and falling 5 m or more (*e.g.* Walker *et al.*, 1977); (2) simulators of the spinning disk type (Morin *et al.*, 1967) which produce rain dominated by large drops falling at very high instantaneous intensity but pulsed to give lower overall intensity. These rainfall simulators are appropriate to erosion studies which have been the concern of most workers in this field.

Flexibility in choice of raindrop energy offers greater scope for determining structural changes that would not be observed if only high energy rainfall is used. A number of important measures of soil structural behaviour could be found if low energy or variable energy rain was used (Ragab, 1983; Thompson and James, 1985; Mohammed and Kohl, 1987; Hignett, 1991). Among them, a minimum rainfall energy was identified, below which many soils do not break down, irrespective of rain depth even at very high rainfall intensity (Hignett, 1991). Low energy rainfall applied to beds of air-dry aggregates induced different degrees of surface breakdown and rainfall runoff that could be effectively correlated with different soil and land management systems. These

hydrological responses also had direct relevance to behaviour of the soil in the field. Work reported by Gusli *et al.* (1994) with hardsetting soils has found a range of quite unexpected interactions between rainfall energy flux density and the disruption of soil aggregates of different antecedent water contents due to rainfall and wetting rate.

Rainfall simulators used in field erosion studies need to have uniform distribution of drops over a large area ($\sim 1 \text{ m}^2$). Spinning disk and spray nozzle types achieve this requirement but suffer from the disadvantage that raindrop energy is constant and high ($\sim 30 \text{ J m}^{-2} \text{ mm}^{-1}$) irrespective of the rate of application. In such sprays, the nozzle flow and drop size distribution remain constant and variation in intensity is achieved by intercepting the stream before it reaches the soil. A consequence of this combination of factors is that while higher intensity produces more runoff in a given time, the rate of change of infiltration rate of water into the soil surface is a function of accumulated rain depth and is independent of the intensity of applied rain (Morin and Benjamini, 1977). This contradicts numerous field and laboratory observations which show that low intensity natural rainfall does less damage to surface soil structure, per unit depth of rain, than higher intensity rain (Wischmeier and Smith, 1958; Mantell and Goldberg, 1966; Lyles *et al.*, 1969).

Gusli *et al.* (1994) showed that crusting and hardsetting under rainfall are a result of complex processes involving variable rainfall kinetic energy and intensity and antecedent soil conditions. Clearly, to obtain meaningful data from experiments dealing with processes that lead to change of soil structure such as hardsetting and crusting using rainfall simulators, both rainfall components (raindrop kinetic energy and intensity) and aggregate bed conditions (matric suction and drainage) must be controlled.

This chapter describes a laboratory rainfall simulator which could simulate rainfall at one or two drop sizes, a range of fall heights and with controlled intensity so that soil aggregate breakdown and disruption associated with sealing, crusting and hardsetting could be studied in relation to a wide range of rainfall factors under laboratory conditions. Of particular importance was the control of rainfall energy flux density which could be varied by independently varying raindrop energy and rainfall intensity. The matric suction and drainage condition of aggregate beds were also controlled. Incorporation of electronic sensors in various parts of the simulator allowed detailed measurements of rainfall intensity, runoff and drainage, producing new insights into the effects of rain on surface sealing and aggregate disruption.

2.2 Design and description of the apparatus

2.2.1 Rainfall module design

A diagram of the rainfall simulator is presented in Figure 2.1a (the overall schematic diagram of the rainfall simulator is shown in Figure 2.1b). The housing was a 1140 mm x 1400 mm enclosure 3800 mm high constructed on a box frame of 50 mm square galvanised section (16 gauge). Windows on opposite sides allowed access to the sample area while the rest of the sides were covered with thin galvanised sheeting or transparent PVC sheeting to allow light access. A waterproof tray of heavier gauge galvanised sheeting just above the floor provided a solid base and extended outside the frame to intercept any water escaping through the windows.

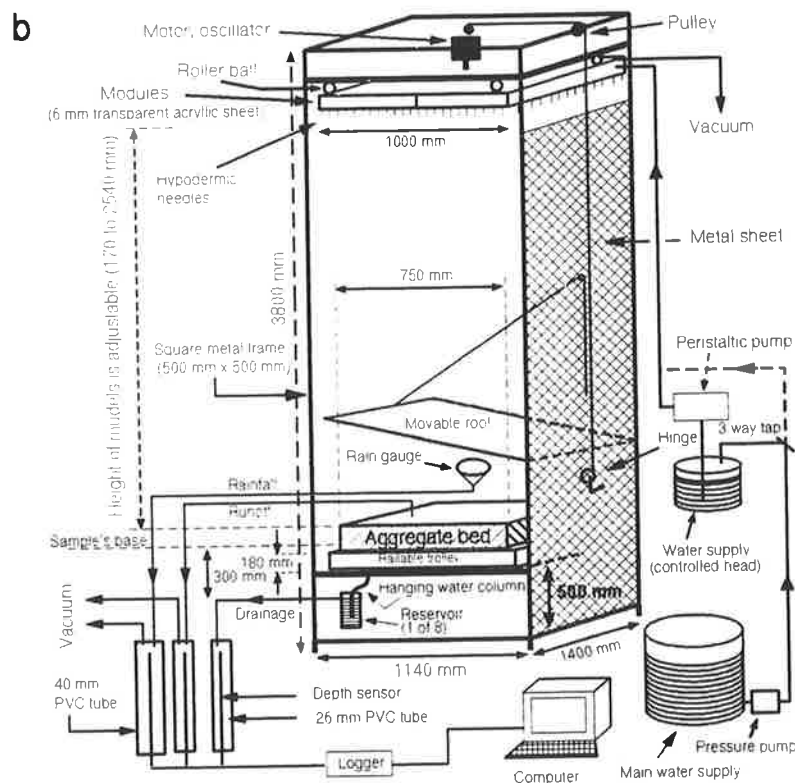
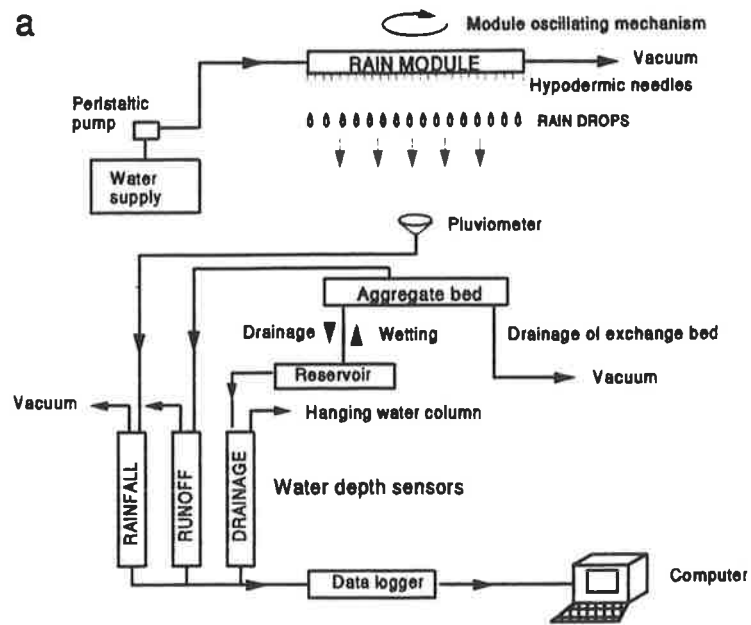


Figure 2.1: Schematic diagram of laboratory rainfall simulator system: (a) the main components of the simulator; (b) an overall diagram of the simulator.

The rain module (Figure 2.1a) was constructed from two rectangular transparent acrylic containers 500 mm x 1000 mm x 70 mm high disposed side by side to cover an area of 1 m². The total capacity of the module was 0.047 m³. The acrylic sheets, of 6 mm thickness, were glued and screwed together and the upper sheet was attached via removable bolts and a rubber gasket to allow access to the interior. Emitters were formed from hypodermic needles (23 gauge, 31.75 mm long) inserted into an array of holes, of 25 mm spacing, drilled into the lower surface of the modules (total of 1600 emitters m⁻²). These emitters produced raindrops of 2.7 mm diameter. An emitter with a different drop size (5.1 mm diameter) was made by placing the hypodermic needle sheath, after sectioning the tip to create an aperture, over the needle. Raindrops of a range of sizes can be created by varying the type of needles and their receptacles. The modules were originally designed to operate in the rainfall simulator described by Walker et al. (1977).

The rectangular tanks were mounted within a steel frame to form a module that could deliver rainfall of a given drop size, over an area of 1 m². The module was mounted on four rollers and an electric motor and eccentric drive were used to oscillate the module at a frequency of 0.23 s⁻¹ with a horizontal circular motion over a path of 100 mm diameter (Figure 2.1b). This facility ensured that raindrops from individual needles were distributed evenly over the soil target area. The height of the rain module was adjustable from 0.17 to 2.54 m from the surface of the target soil bed. At 2.54 m high, 5.1 mm drops has a velocity at impact of 6.31 m s⁻¹ or 69 % of the terminal velocity (Gunn and Kinzer, 1949). This range of height could produce rainfall kinetic energy from 1.6 to 16.6 J m⁻² mm⁻¹ for 2.7 mm diameter drops and from 1.6 to 19.9 J m⁻² mm⁻¹ for 5.1 mm diameter drops (see Table 2.1).

2.2.2 Rainfall module operation

While the modules were being filled and adjusted, soil samples in the simulator were covered to prevent water reaching the soil. Deionised water was pumped from a constant head reservoir while a small vacuum (0.1 m of water) was applied to the modules, counteracting pressure due to filling, minimising air entrapment and preventing water flow from the needles during filling. When full, the vacuum was released and water was briefly (about 4 minutes) pumped at high rate through the needles to clear them of obstructions such as air bubbles or algal growth. During this time needles were checked for delivery of water and any remaining obstructions were cleared by applying a vacuum on the needle with a hypodermic syringe.

A peristaltic pump (Masterflex, 6 to 600 rpm) was used to deliver water from a constant head tank to the module in order to achieve a constant, controllable, delivery rate (rainfall intensity) from the needles. A pluviometer, placed on the soil cover, recorded rainfall intensity electronically and the output was used to manually adjust the delivery rate of the peristaltic pump to the desired rainfall intensity. Rainfall intensity was monitored throughout the test using a pluviometer in the test bed. Intensity was relatively constant during all tests especially if in excess of 40 mm h⁻¹, but required some adjustment during the test at lower intensities.

When the desired rainfall intensity has been set and checked, the test bed cover was removed, and the experiment commenced.

2.2.3 Test bed construction

The aggregate test bed (Figure 2.2) was mounted on a railed platform, 680 mm above the floor such that the entire sample holder could be slid out of the simulator for sample preparation and post rainfall measurements (Figure 2.1b). The platform was 180 mm high mounted on a metal frame 500 mm above the drip tray on the base of the simulator. Figure 2.2 is a diagram of the soil test bed in its most commonly used configuration, while Figure 2.3 is a diagram detailing a soil sample holder.

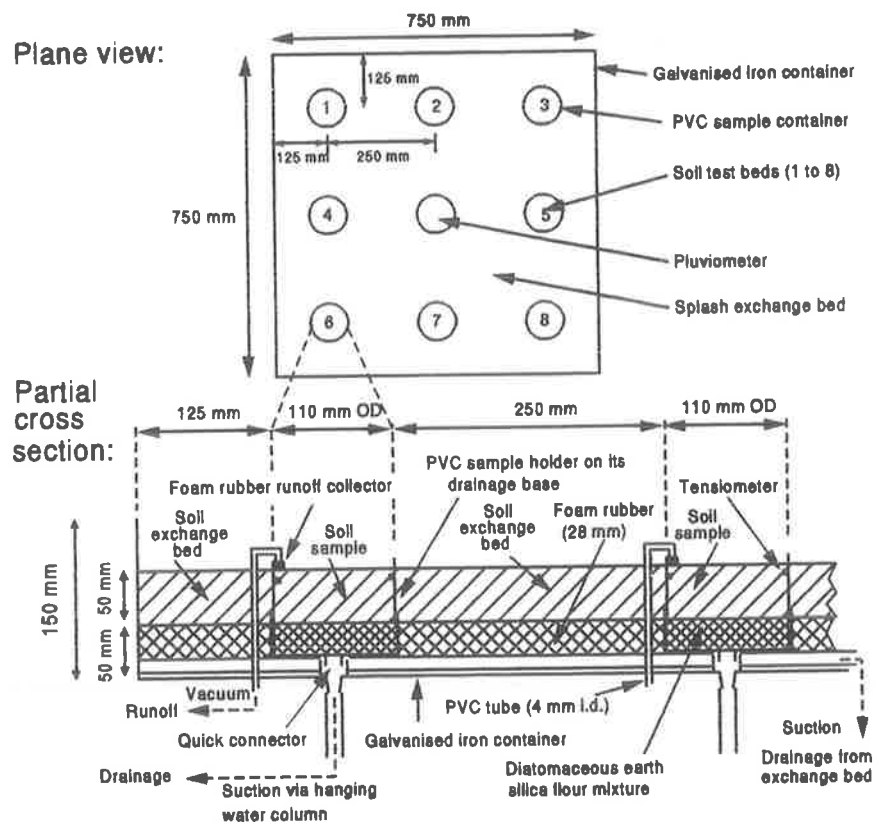


Figure 2.2. Plane and cross-sectional views of the rainfall aggregate bed.

The importance of the exchange bed for splash export and import with the soil samples has been shown, among others, by Moss and Watson (1991). Accordingly, the

soil sample beds were surrounded by a large splash exchange bed (Figure 2.2). The splash exchange bed was made from 50 mm thick foam plastic, supporting a thin layer of soil, laid on top of a network of perforated PVC tubes under vacuum of 300 mm of water, to provide drainage. The foam plastic reduced the quantity of exchange bed soil required and filtered coarse particles from the drainage system. Soil similar to that under test was used in the exchange bed. The exchange bed and test soil samples were set at a slope of 3 % to facilitate runoff collection.

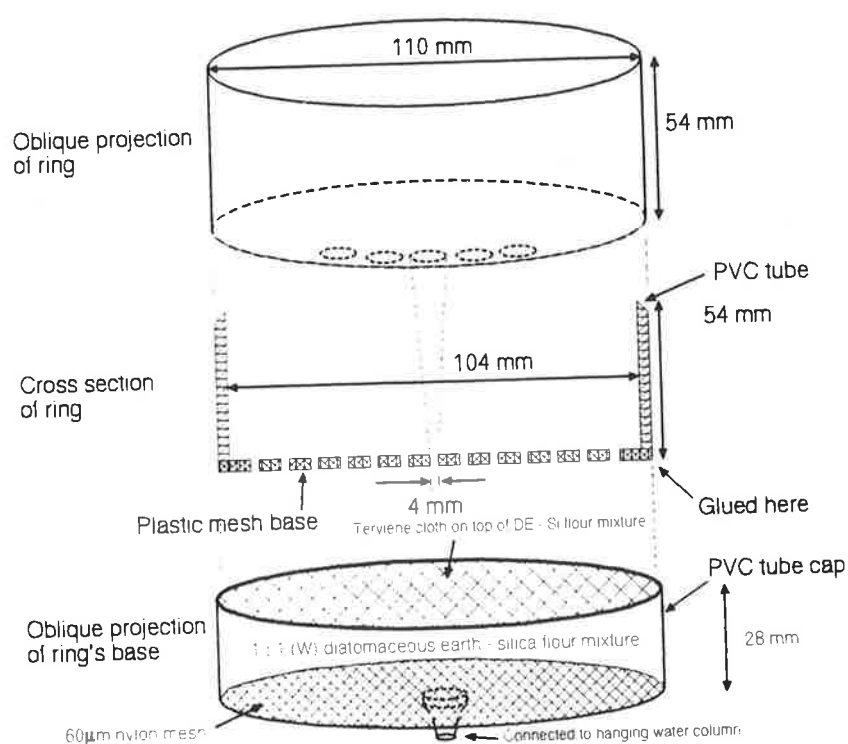


Figure 2.3 An aggregate bed container (PVC ring) and its drainage base.

Figure 2.3 shows details of a sample holder and its drainage base. The sample holders were constructed from PVC tubing (54 mm high, 110 mm outside diameter, 3 mm wall) with an outside facing knife edge (30 degree angle) machined on the upper rim

and a disk of PVC mesh (4 mm openings) was glued to the base of the cylinder. A standard PVC pipe end cap fitting (inside diameter 110 mm, height 28 mm) was used as a drained base for the sampler holder. A plastic spigot was inserted into a hole (10 mm diameter) in the centre of the end cap. The end cap was filled with a slurry of equal proportions, by mass, of diatomaceous earth and silica flour (400G). The drainage bed could hold a suction up to 1.18 m of water without air entry and had a reasonably high saturated hydraulic conductivity (17 mm h^{-1}). This mixture was used in preference to ceramic plates because it was inexpensive, discardable when contaminated with silt and clay from the sample and provided means to vary the sub-sample drainage rate by varying the proportions of the mixture. Two layers of open weave synthetic cloth were placed on top of the drainage bed to filter some silt and clay emanating from soil sample, so prolonging the useful life of the drainage bed.

The sample holder was placed on the cloth covering the drainage bed and held in firm contact with a broad rubber band. The assembly of drainage base and sample holder was inserted into an aperture in the test bed via the drainage spigot. This provided a connection between the drainage base and a hanging water column below the simulator which was designed to drain the soil sample being tested. A thin layer of diatomaceous earth was spread over the mesh on the bottom of the sample holder to provide better hydraulic contact between the soil sample and the top of the drainage base. Hydraulic contact was established by filling the drainage system from the sample holder. A suction of 0.30 m of water was established on the base of the sample and maintained throughout the test.

2.2.4 Test bed operation

Soil samples were prepared by air drying, gently crushing large aggregates and passing the soil through a 5 mm sieve. The soil sample was rapidly dumped into the sample holder to minimise particle segregation. The surface aggregates were lightly stirred to redistribute aggregates and reduce any extreme surface irregularities. In the case of tests on dry soil, rainfall was applied immediately after this. However, rainfall could also be delayed until the soil surface was wetted by upward flux of water from the hanging water column attached to the base of each test sample. Suctions of up to 0.50 m of water were possible.

Soil samples and test bed were covered until rainfall intensity was correctly adjusted and data logging equipment was operating satisfactorily, at which time the cover was removed and the test commenced. During the test, changes in cumulative rainfall, runoff and drainage were measured automatically once per minute. Water accumulating on the surface of the sample (runoff) was removed by vacuum through a small (10 mm square) plastic foam element (Wace and Hignett, 1991) and delivered to a tube equipped with a capacitance water depth sensor (Ross, 1983). Air-entry suction of the plastic foam was about 5 mm of water, so that minimum suction was transferred to the soil surface, but any free water touching the foam element was extracted. Rainwater collected from the pluviometer was delivered under vacuum to a capacitance water depth sensor. Water draining through the bottom of the test sample was collected and delivered by gravity to capacitance water depth sensors via a hanging water column of 300 mm.

2.2.5 Data collection

Water depth sensors (Figure 2.4) were constructed using the electronic circuitry and the teflon coated brass rod (500 mm length, 1 mm diameter) obtained from commercial borehole water depth sensors (Dataflow Systems). The electronics and rod were inserted into the base of a transparent acrylic tube (26 mm internal diameter for runoff and drainage, 40 mm for the pluviometer) (Figure 2.4). Fine wire was wound loosely around the outside of the tube and covered with aluminium foil. This assembly enabled reliable measurement of water depths with a sensitivity better than 0.5 mm over the lower half of the capacity of the acrylic tube. Sensor output was a frequency signal which was calibrated against water depth in the cylinder (Figure 2.5). Below 40 Hz the sensitivity of the sensor was lower than 0.8 mm Hz⁻¹, increasing rapidly above this frequency. Accordingly, the latter condition was always avoided during tests.

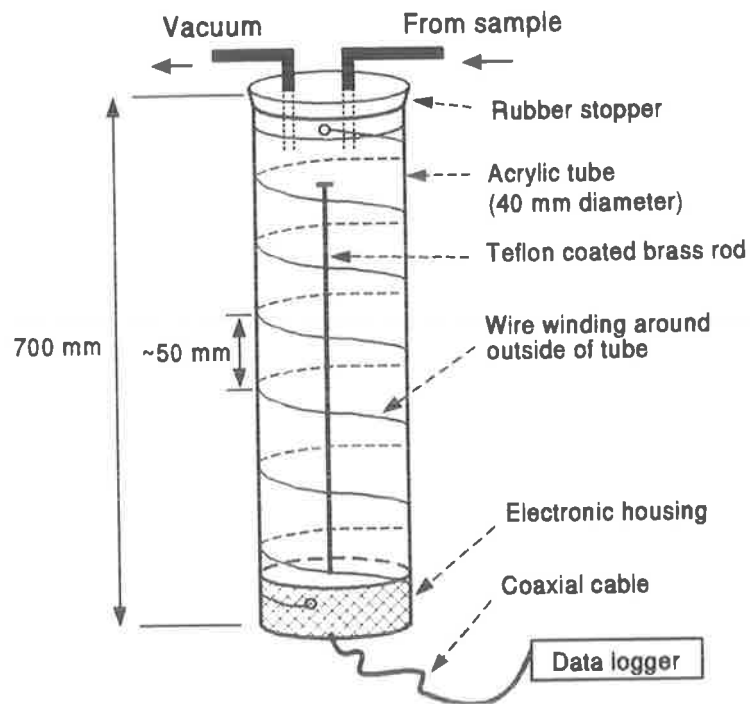


Figure 2.4. Configuration of the capacitance water depth sensors.

A personal computer and custom software were used to interrogate and log the output from the sensors measuring rainfall intensity, runoff and drainage from the test samples. A commercially available PC timer/counter card (PCL830) was configured as a 3 channel frequency counter (Figure 2.6). A solid state multiplexer was built to select a further 6 channels for each of the 3 frequency inputs to the PCL830 card, thus enabling 18 channels of measurement.

The modified capacitance water depth sensors were connected to each of the channels as shown in Figure 2.6. Sixteen channels were dedicated to each of runoff and drainage from the 8 soil sample holders and two to rainfall intensity via the pluviometer. The two channels devoted to logging rain intensity were used alternatively in order to remain within the range of maximum sensitivity of the water depth sensors, the operator draining whichever one was not in use at any given time.

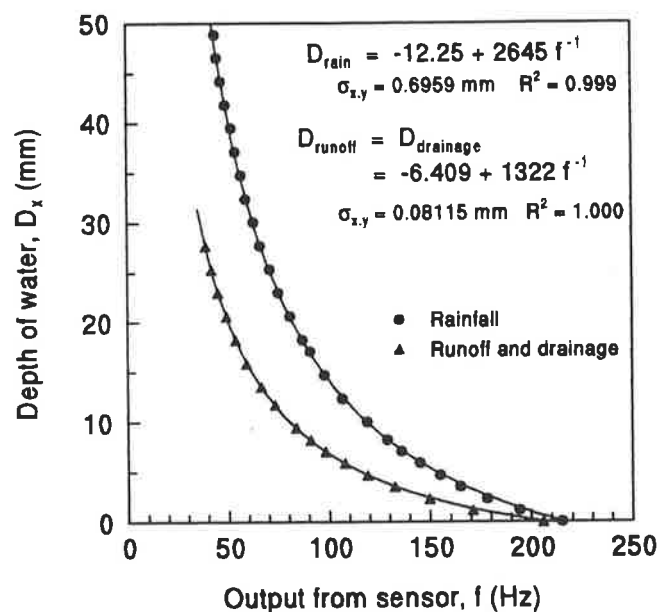


Figure 2.5. Calibration curves for the rainfall and the mean (n=16) runoff and drainage depth gauges and fitted functions (solid lines). Standard errors of the means are smaller than the triangular symbols used to show the data.

Depth of water in each sensor was read every minute, the data stored in RAM and displayed on the screen. Rainfall intensity was calculated each minute, stored in RAM and displayed on the screen together with an updated average of the previous ten readings. At the conclusion of each test, all data were written from RAM to the computer disk.

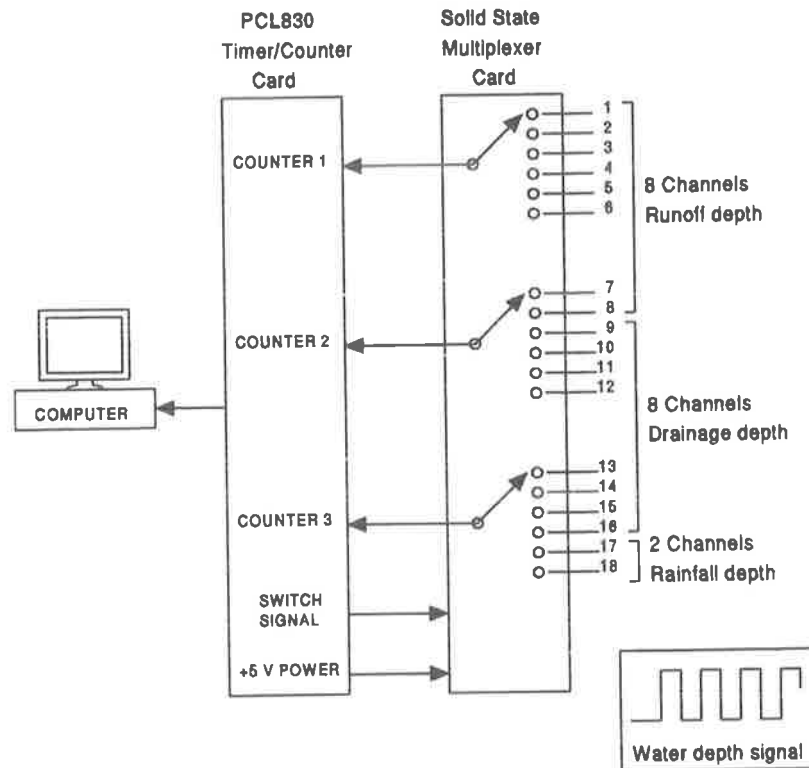


Figure 2.6. Block diagram of the electronic circuit used to capture and log depth of runoff, drainage and rainfall from the rainfall simulator.

Prior calibration of the water depth sensors enabled measurements to be normalised to standard units of depth (mm) and rate (mm h^{-1}). As each depth sensor filled during a test, the sensitivity of the sensor decreased because of the shape of the calibration curve (Figure 2.5). In order to optimise sensitivity (<0.8 mm) and capacity

(~50 %), the software was programmed to activate an alarm at 40 Hz, alerting the operator to the need to change or drain the sensor.

2.2.6 Performance of the simulator

The simulator delivered rain drops with energy varying from 1.6 to 19.9 J m⁻² mm⁻¹ (Table 2.1). Energy at the soil surface was calculated from the theory of Wang and Pruppacher (1977) using computer code that required drop size and fall height input data (Dr P. Kinnell, pers. comm., 1993). Kinetic energy was varied by changing the height of modules as well as excluding or including the plastic hypodermic needle cover.

Table 2.1. Kinetic energy distribution from the rainfall simulator for drop diameters of 5.1 and 2.7 mm

Fall height (m)	Drop size = 5.1 mm		Drop size = 2.7 mm	
	Velocity (mm h ⁻¹)	Kinetic energy (J m ⁻² mm ⁻¹)	Velocity (mm h ⁻¹)	Kinetic energy (J m ⁻² mm ⁻¹)
0.17	1.811	1.64	1.792	1.61
0.67	3.519	6.19	3.407	5.80
1.17	4.556	10.38	4.328	9.36
1.67	5.324	14.18	4.977	12.38
2.17	5.937	17.62	5.472	14.97
2.54	6.313	19.93	5.765	16.62

Rainfall intensity was varied linearly, from below 40 to over 100 mm h⁻¹, by changing the rotation rate of the peristaltic pump (Figure 2.7). Spatial variation in intensity across the test bed was very small, with coefficient of variation < 5 % at low rainfall intensities (< 40 mm h⁻¹) and < 3 % at higher intensities. Figure 2.7 shows that

rainfall intensity at the centre of the bed (pluviometer position) was not significantly different to the mean rainfall intensity across the entire bed. Reproducibility in rainfall intensity from one test to another was also high (Figure 2.8). Variation in intensity was within 2 mm h^{-1} for intensities of 50 mm h^{-1} , and approaching zero variation at high intensity ($\sim 70 \text{ mm h}^{-1}$).

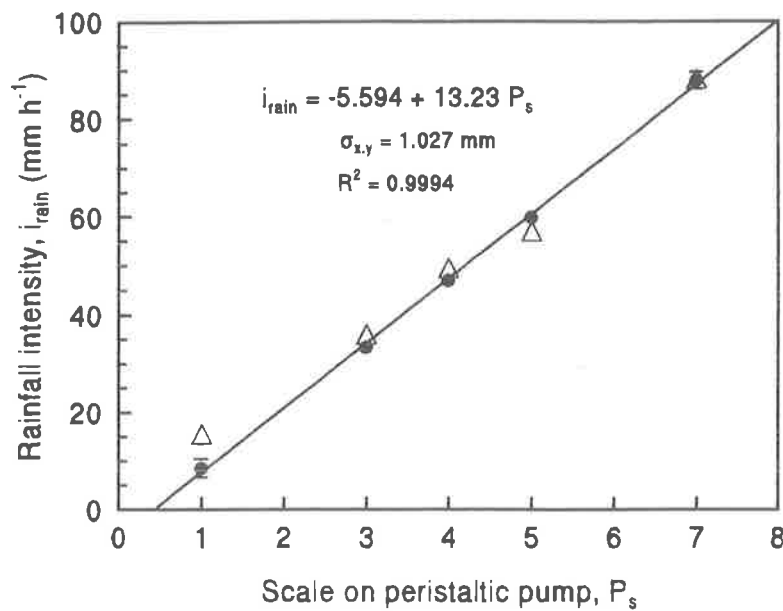


Figure 2.7. Calibration of rainfall peristaltic pump (Masterflex 6-600 rpm): as a mean of all target sites ($n=9$) (circular symbol) and the values for the central, pluviometer position (triangle). The solid line shows the fitted calibration function for the mean data respectively. Error bars are 2 standard errors of the mean, which are generally smaller than the mean data symbols.

Figures 2.8 and 2.9 show examples of overall performance and reproducibility of the rainfall simulator and the aggregate bed at high ($19.9 \text{ J m}^{-2} \text{ mm}^{-1}$) and low ($1.6 \text{ J m}^{-2} \text{ mm}^{-1}$) kinetic energy, respectively. Low variation in rainfall permitted high

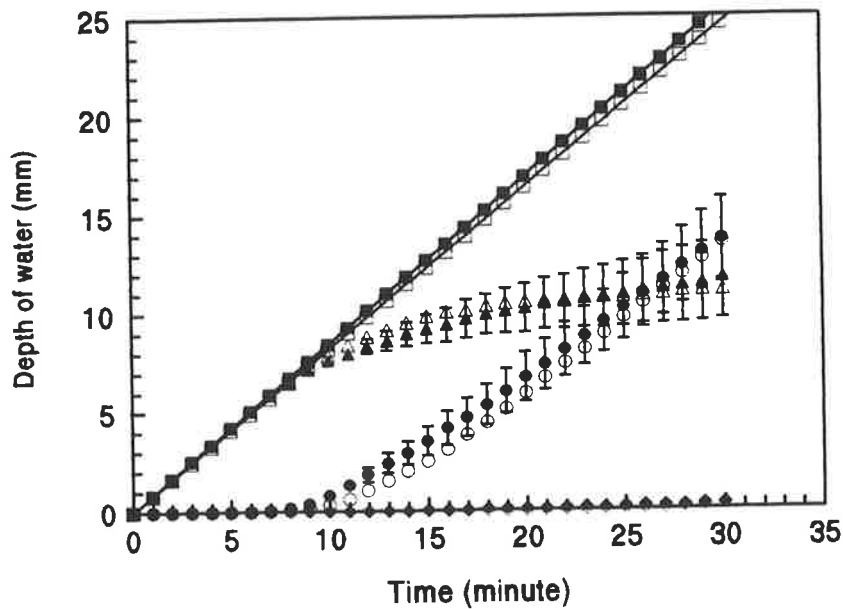


Figure 2.8. Components of the hydrological balance: rainfall (square symbols), runoff (circles), infiltration (triangles) and drainage (diamonds) during a single run using simulated rainfall on air-dry soil with high energy rainfall ($19.9 \text{ J m}^{-2} \text{ mm}^{-1}$) and intensities of 50.7 mm h^{-1} (closed symbols) and 49.2 mm h^{-1} (open symbols). Mean drop diameter of rainfall was 5.1 mm . Error bars are 2 standard errors of the mean of 8 replicated soil targets.

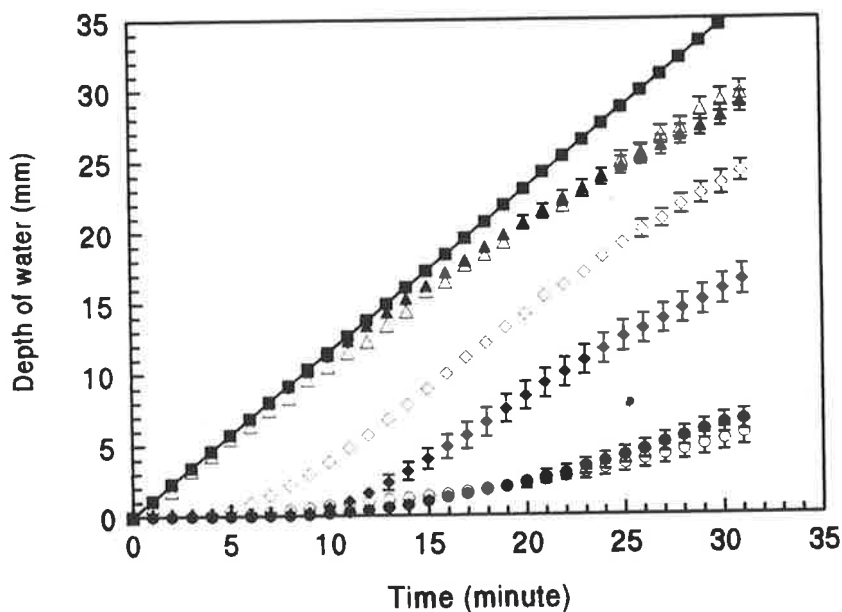


Figure 2.9 Components of the hydrological balance: rainfall (square symbols), runoff (circles), infiltration (triangles) and drainage (diamonds) during a single run using simulated rainfall on air-dry (closed symbols) and pre-moistened soil (suction of 300 mm water) (open symbols). Rainfall energy was $1.64 \text{ J m}^{-2} \text{ mm}^{-1}$, intensity 70 mm h^{-1} and mean drop diameter was 5.1 mm . Error bars are 2 standard errors of the mean.

levels of reproducibility in measurement of infiltration and runoff between both samples within a test and between tests. Visual observation of surface ponding, seal condition, surface roughness and time to ponding and runoff indicated that the exchange bed behaved in a manner similar to that of the samples although no comparative measurements were made.

2.3 Discussion

The chronological detail made available by this simulator system allowed infiltration (the water passing through the soil surface) to be distinguished from drainage (the water draining from the base of the soil sample) over time. Provision of under sample drainage simulated field soil behaviour more realistically than undrained samples. The formulation of the under bed drainage base (1:1 diatomaceous earth and silica flour) allowed variation of drainage rate. Removal of ponded water on the surface allowed fuller development of rainfall-surface soil interactions than would be observed if ponding had been allowed to occur. Test samples were surrounded by an exchange bed, preventing the net export of particles from the test sample. The height of the rain module above the test bed and the drop size of the simulated rainfall allowed control of raindrop energy. Finally the control of delivery of water to the modules with a peristaltic pump allowed control of rainfall intensity. These features permitted the investigation of the behaviour of different soils exposed to a range of rainfall conditions without the limitations of rapid shielding of the soil surface by ponded water and the rapid saturation of the soil associated with small samples. Specifically, the rainfall simulator system permitted the study of processes that lead to different surface features as a result of different extent and

deep of disrupted layer, a key to understanding process of crusting and hardsetting (Bristow *et al.*, 1994).

Some difficulty was experienced with lack of control of rainfall delivery at low intensity when the modules leaked air, particularly at low intensities when the modules were under suction. This proved to be a problem with the seal between the acrylic sheets failing due to the considerable stresses caused by water pressure and applied suction over the large surface area (0.5 m²) of the module. Use of acrylic sheet for construction of the modules was not entirely satisfactory. Acrylic is known to swell when in contact with water and shrink on drying. This alternate expansion and contraction contributed to the deterioration of the rubber gasket and failure of glued joints. Some difficulties were also experienced with algae growth encouraged by the transparency of the module material. Some of these problems might be solved by using smaller modules (500 mm x 500 mm x 40 mm) constructed from opaque PVC sheeting.

2.4 Conclusions

A laboratory rainfall simulator was designed and constructed to deliver simulated rain to small soil samples under conditions where rainfall energy and intensity were controlled and runoff and drainage collected under conditions where no net loss of soil occurred from the test samples. Features of the simulator included hypodermic needle emitters, moving rainfall modules, small soil test samples surrounded by an exchange bed area, a regulated suction on the base of the soil under test and rapid (1 minute intervals), precise (<0.5 mm) and fully automated acquisition of accumulated rainfall, surface runoff and drainage.

The use of small samples with sub-drainage conditions enabled the measurement of surface aggregate breakdown without the complex effects of raindrop cushioning by ponded water and the multitude of interactions caused by flowing water on the sample surface. Use of electronic measuring cylinders of high sensitivity, with computer monitoring has provided a level of chronological detail not previously possible in this type of work. The properties of rain that are most important in understanding soil structural stability and hardsetting processes, kinetic energy, intensity, total energy, and energy flux density, could be controlled in this rainfall simulator.

2.5 References

- Al-Durrah, M. M. and J. M. Bradford (1981). New methods of studying soil detachment due to waterdrop impact. *Soil Science Society of America Journal* 45: 949-953.
- Bristow, K. L., A. Cass, K. R. J. Smettem, and P. J. Ross (1994). Modelling effects of surface sealing on water entry and re-distribution. Proceedings of the International Symposium on 'Sealing, Crusting, Hardsetting Soils: Productivity and Conservation' 7-11 February 1992, University of Queensland, Brisbane, Australia. (*in press*).
- Francis, P. B. and R. M. Cruse (1983). Soil water matric potential effects on aggregate stability. *Soil Science Society of America Journal* 47: 578-581.
- Gunn, R. and G. D. Kinzer (1949). The terminal velocity of fall for water droplets in stagnant air. *Journal of Meteorology* 6: 243-248.
- Gusli, S., A. Cass, D. A. MacLeod, and C. T. Hignett (1994). Processes that distinguish hard setting from rain induced crusting. Proceedings of the International Symposium on 'Sealing, Crusting, Hardsetting Soils: Productivity and Conservation' 7-11 February 1992, University of Queensland, Brisbane, Australia. (*in press*).
- Hignett, C. T. (1991). Relating soil structure to runoff quality and quantity. International Hydrology and Water Resources Symposium. Institute of Engineers Australia, Publication 91/22, pp. 301- 305.
- Le Bissonnais, Y., A. Bruand and M. Jamagne (1989). Laboratory experimental study of soil crusting: relation between aggregate breakdown mechanisms and crust structure. *Catena* 16: 377-392.
- Lyles L., L. A. Disrud, and N. P. Woodruff (1969). Effects of soil physical properties, rainfall characteristics, and wind velocity on clod disintegration by simulated rainfall. *Soil Science Society of America Proceedings* 33: 302-306.

- Kinnell, P. (1987). Rainfall energy in eastern Australia: intensity-kinetic energy relationships for Canberra, A.C.T. *Australian Journal of Soil Research* 25: 547-553.
- Mantell, A. and D. Goldberg (1966). Effect of water application rate on soil structure. *Journal of Agricultural Engineering Research* 11: 76-79.
- Mohammed, D. and R. A. Kohl (1987). Infiltration response to kinetic energy. *Transactions of American Society of Agricultural Engineers* 30: 108-111.
- Morin, J., and Y. Benyamini (1977). Rainfall infiltration into bare soils. *Water Resources Research* 13: 813-817.
- Morin, J., D. Goldberg, and I. Seginer (1967). A rainfall simulator with a rotating disk. *Transactions of the American Society of Agricultural Engineers* 10: 74.
- Moss, A. J. and C. L. Watson (1991). Rain impact soil crust. III. Effect of continuous and flawed crusts on infiltration, and the ability of plant covers to maintain crustal flaws. *Australian Journal of Soil Research* 29: 311-330.
- Ragab, R. A. (1983). The effect of sprinkler intensity and energy of falling drops on soil surface sealing. *Soil Science* 136: 117-123.
- Rosewell, C. J. (1986). Rainfall kinetic energy in eastern Australia. *Journal of Climate and Applied Meteorology* 25, 1965-1968.
- Ross, P. J. (1983). A water level sensor using a capacitance to frequency converter. *Journal of Physics* E16: 827-828.
- Thompson, A. L. and L. G. James (1985). Water droplet impact and its effect on infiltration. *Transactions of American Society of Agricultural Engineers* 28: 1506-1510, 1520.
- Truman, C. C. and J. M. Bradford (1993). Relationships between rainfall intensity and the interrill soil loss-slope steepness ratio as affected by antecedent water content. *Soil Science* 156: 405-413.
- Wace S. J. and C. T. Hignett (1991). The effect of rainfall energy on tilled soils of different dispersion characteristics. *Soil & Tillage Research* 20: 57-67.
- Walker, P.H., J. Hutka, A. J. Moss, and P. A. Kinnell (1977). Use of a versatile experimental system for soil erosion studies. *Soil Science Society of America Journal* 41: 610-612.
- Wang, P. K. and H. R. Pruppacher (1977). Acceleration to terminal velocity of cloud and raindrops. *Journal of Applied Meteorology* 16: 275-280.
- Wischmeier, W. H. and D. D. Smith (1958). Rainfall energy and its relationship to soil loss. *Transactions American Geophysical Union* 39: 285-291.

Chapter 3

Effect of rainfall kinetic energy flux density on infiltration

3.1 Introduction

Raindrop kinetic energy and rainfall intensity are important rainfall properties that influence aggregate breakdown at the soil surface and infiltration of water into the soil (Ragab, 1983; Arndt, 1985; Thompson and James, 1985). Raindrop kinetic energy, expressed as $\text{J m}^{-2} \text{mm}^{-1}$, determines the magnitude of the mechanical forces on aggregates at the soil surface, and therefore influences surface sealing and ultimately infiltration rate. Rainfall intensity refers to the amount of rainfall per unit time (mm h^{-1}) which determines, to some extent, the rate of wetting and hence the magnitude of the hydration forces on the aggregates. Rainfall intensity affects infiltration through aggregate slaking and collapse (Keller, 1970; Farres, 1980).

Sealing and crusting are associated with structural damage which is limited to a few millimetres below the surface, while hardsetting develops from a deep disrupted layer (Bristow *et al.*, 1994). As kinetic energy causes surface aggregate detachment, increasing kinetic energy should increase the propensity for sealing. Rainfall intensity, on the other hand, influences aggregate breakdown through its effect on hydration (slaking), which can cause aggregate disruption to depth, not limited only to the surface layer (Chapter 6). This implies that high kinetic energy rainfall favours development of a seal, and ultimately a crust, more than high intensity rainfall. Thus, an appreciation of

the different effects of rainfall kinetic energy and intensity, particularly as they affect infiltration, are crucial to understanding how hardsetting and crusting develop.

Morin and Benyamini (1977) applied simulated rainfall with constant kinetic energy of $22 \text{ J m}^{-2} \text{ mm}^{-1}$ over a range of intensities. They found that when rain was applied to mulched soil (which presumably reduced raindrop energy to zero) infiltration rate was equal to rainfall intensity, even at a rate of 130 mm h^{-1} . That is, zero or negligible drop energy did not decrease infiltration. This is consistent with findings of Glanville and Smith (1988) who concluded that aggregate breakdown without involvement of rainfall kinetic energy may not reduce infiltration. It appears that there are circumstances when rainfall intensity alone has no effect on infiltration rate. When kinetic energy is below a certain threshold value (Wace and Hignett, 1991) or is largely eliminated (Glanville and Smith, 1988), high intensity rainfall may not cause a seal to form and reduce infiltration rate.

Clearly, both rainfall kinetic energy and intensity determine aggregate breakdown, rate of seal development and infiltration. Several studies have demonstrated that increasing rainfall kinetic energy or intensity or both, results in lower infiltration rate (Thompson and James, 1985; Mohammed and Kohl, 1987).

The product of raindrop energy ($\text{J m}^{-2} \text{ mm}^{-1}$) and intensity (mm h^{-1}) yields rainfall kinetic energy flux density ($\text{J m}^{-2} \text{ h}^{-1}$) (Rose, 1960; Thompson and James, 1985). As it takes into account both energy and intensity, it is particularly useful for relating rainfall to aggregate breakdown. The higher kinetic energy flux density, the greater is aggregate breakdown or seal development (Thompson and James, 1985). Shvebs (1968) and Farres (1980) concluded that kinetic energy flux density, was the most sensitive

rainfall parameter affecting surface aggregate breakdown. Farres (1980) pointed out that as kinetic energy flux density is a measure of the speed at which rainfall is applied, it determines the relaxation time for the aggregates to readjust to an equilibrium condition between successive drop impacts.

In addition to rainfall properties, aggregate breakdown and subsequent packing of disrupted material during rainfall are influenced by the soil water content prior to rainfall. Air-dry aggregates are more unstable to raindrop impact and form a seal more rapidly than pre-wetted aggregates (Le Bissonnais *et al.*, 1989; Truman *et al.*, 1990). However, Le Bissonnais *et al.* (1989) also found that the disrupted layer was thicker when the aggregates were pre-wetted than if they were dry before rainfall. Clearly, interaction between antecedent water content and rainfall kinetic energy and intensity should determine whether a surface seal or disrupted layer will form during rainfall, and ultimately whether a surface crust or hardset layer develops on drying.

The aims of the experiments described in this chapter are to examine:

- 1) how rainfall kinetic energy and intensity and antecedent soil water content influence infiltration of rain into Kapunda red-brown earth; and
- 2) the role of infiltration rate in determining whether Kapunda red-brown earth forms a crust, hardset layer or remains friable.

3.2 Materials and methods

3.2.1 Soil properties

A red-brown earth, classified as a fine, mixed, thermic, Calcic Rhodoxeralf (Soil Survey Staff, 1988) from Kapunda, South Australia was sampled at the depth of 0 to 100 mm.

At the time of sampling, soil water content was 0.21 kg kg^{-1} , corresponding to a matric suction of about 5 m of water. The soil was air-dried and large clods were gently crushed before sieving through a 5-mm sieve. The soil was then stored in sealed 200 L drums.

The soil had been under a wheat - fallow crop rotation since 1983, prior to which it had been mostly under permanent pasture. Wheat was grown during the winter, when the highest amount of rain falls (Smettem *et al.*, 1992). During the remaining period of the year, the soil was left fallow under naturally regenerated pasture, consisting mainly of barley grass, annual ryegrass, silvergrass and brome grass (Smettem *et al.*, 1992).

The soil is a sandy loam, which over the depth of 0 to 100 mm contained 110 g kg^{-1} clay ($<2 \mu\text{m}$), comprising mainly kaolin and illite (R. Fitzpatrick, 1992, personal communication), 280 g kg^{-1} silt (2 to $20 \mu\text{m}$), 510 g kg^{-1} fine sand ($20 \mu\text{m}$ to 0.2 mm) and 50 g kg^{-1} coarse sand (0.2 to 2 mm). The organic carbon content was 18 g kg^{-1} , cation exchangeable capacity of $83 \text{ mmol}_c \text{ kg}^{-1}$ with exchangeable sodium percentage of 1.0. The aggregates of this soil slaked completely within less than 2 minutes when immersed in distilled water, but did not disperse at all, unless remoulded. In the field, freshly tilled soil developed a crust readily after rainfall and drying, especially if the surface soil was not covered by crops or stubble mulch. However, the soil also sets hard when covered by mulch. Bulk densities of 1.45 and 1.70 Mg m^{-3} were reported at the depths of $<100 \text{ mm}$ and 100 to 400 mm , respectively (Hignett, 1989).

3.2.2 Preparation of aggregate beds

Preparation of the aggregate test beds was fully described in Section 2.2.3. The beds consisted of eight replicated samples contained in PVC tubing (54 mm high, 110 mm

outside diameter), surrounded by a splash exchange bed covering a total area of 0.75 by 0.75 m². Aggregate beds were formed by rapidly dumping air-dry aggregates of a known mass into the sample holders through a large plastic funnel to minimise aggregate segregation (Gusli et al., 1994). This procedure simulated freshly tilled soil with no vegetative cover at the surface. After transferring the aggregates to the sample holder, the surface was levelled carefully to provide a relatively flat surface with uniform distribution of all aggregate sizes on the surface. The air-dry aggregates were subjected to simulated rainfall, or pre-wetted at 300 mm suction prior to rainfall, as described in Section 2.2.3.

3.2.3 Simulation of rainfall

A rainfall drop size of 5.1 mm diameter was used in all experiments described in this thesis, but a range of rainfall energies and intensities was obtained by varying fall height and delivery rate. Variation of raindrop energy was achieved by using three fall heights of 0.17, 0.67, and 2.54 m to give kinetic energies of 1.6, 6.2 and 19.9 J m⁻² mm⁻¹, respectively (Table 2.1, Section 2.2.6).

The intensity of the rainfall applied was controlled by changing the pumping rate of the peristaltic pump that delivered water to the rainfall modules of the simulator (Section 2.2.2). Two intensities, 40 and 70 mm h⁻¹, were applied in most of the runs, but some treatments received 49, 54 and 100 mm h⁻¹ to produce a wider range of kinetic energy flux density. Rainfall was characterised as kinetic energy flux density, q (J m⁻² h⁻¹), and calculated as

$$q = e_{\text{rain}} \times i_{\text{rain}} \quad (3.1)$$

where e_{rain} is rainfall kinetic energy ($J m^{-2} mm^{-1}$), and i_{rain} is rainfall intensity ($mm h^{-1}$). The rainfall kinetic energies, intensities and the respective kinetic energy flux densities applied in the experiments are shown in Table 3.1.

Table 3.1. Simulated rainfall kinetic energy (e_{rain}), intensity (i_{rain}), kinetic energy flux density (q), and cumulative kinetic energy (E_{rain}) applied on initially air-dry or pre-wetted (300 mm suction) soil beds. Rainfall duration was 30 minutes in all cases.

Soil water content	e_{rain} ($J m^{-2} mm^{-1}$)	i_{rain} ($mm h^{-1}$)	q ($J m^{-2} h^{-1}$) ($e_{rain} \times i_{rain}$)	E_{rain} ($J m^{-2}$)
Air-dry	1.6	40	64	32
Air-dry	1.6	70	112	56
Air-dry	1.6	100	160	80
Air-dry	6.2	40	248	124
Air-dry	6.2	70	434	217
Air-dry	19.9	40	796	398
Air-dry	19.9	49	975	488
Air-dry	19.9	70	1393	697
Air-dry	19.9	102	2030	1015
Pre-wetted	1.6	40	64	32
Pre-wetted	1.6	70	112	56
Pre-wetted	1.6	100	160	80
Pre-wetted	6.2	40	248	124
Pre-wetted	6.2	70	434	217
Pre-wetted	19.9	40	796	398
Pre-wetted	19.9	54	1075	538
Pre-wetted	19.9	70	1393	697

Rainfall was applied for 30 minutes. No effort was made to vary rainfall duration in order to distinguish effects of kinetic energy from cumulative energy as Mantell and Goldberg (1966), Farres (1980), and Hignett (1991) have shown that cumulative rainfall is less important compared to kinetic energy flux density in terms of surface sealing and infiltration.

3.2.4 Measurements

Rainfall rate and runoff data were recorded electronically at one minute intervals during tests (Chapter 2). Cumulative infiltration (I_{soil} , mm) was calculated as the difference between rainfall and runoff. Infiltration rate (i_{soil} , mm h⁻¹) was calculated by fitting cumulative infiltration and corresponding time (t) data to Philip's (1957) model

$$I_{\text{soil}} = S t^{1/2} + A t \quad (3.2)$$

to obtain regression coefficients S and A, and then using

$$i_{\text{soil}} = 0.5 S t^{-1/2} + A \quad (3.3)$$

to calculate infiltration rate. In all cases R² values were always >0.98, significant at p <0.001. Infiltration rate after 30 minutes of rain (i_{30}) was taken to be near steady infiltration rate. Examination of numerous infiltration rate curves obtained during these experiments, for both initially air-dry and pre-wetted aggregates, confirmed that differences between infiltration measured at 30, 60 and 120 minutes were smaller than the standard error of i_{30} .

Runoff was collected through a vacuum system (Chapter 2) and recorded at one minute intervals. Runoff was considered to have commenced when the mean of runoff from eight sample beds was >0.5 mm. Time to commencement of runoff was noted.

3.3 Results and discussion

3.3.1 Cumulative infiltration

Figures 3.1a and b show that infiltration declined as kinetic energy flux density increased for both initially air-dry and pre-wetted aggregate beds. Runoff commenced earlier for

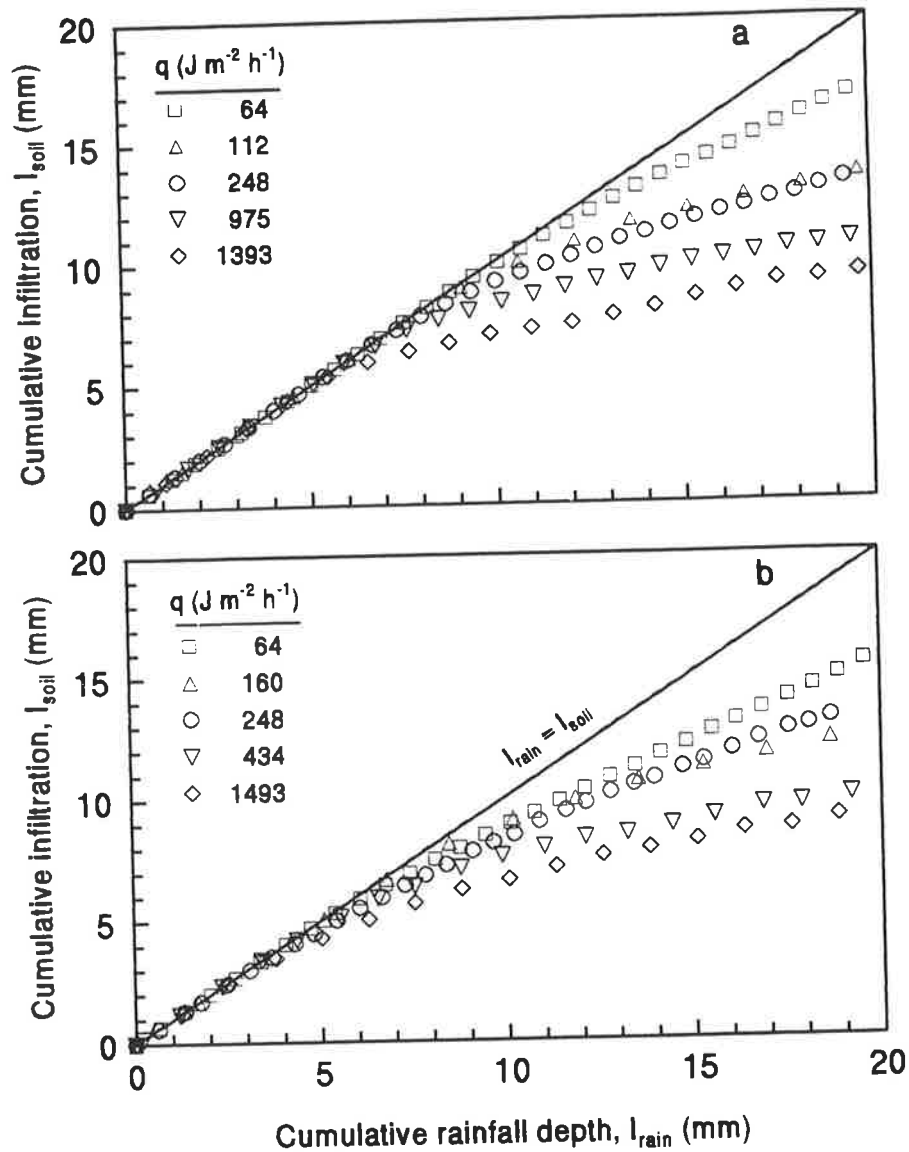


Figure 3.1. Cumulative infiltration of rainfall into soil aggregate beds as a function of cumulative rainfall depth at variable rainfall kinetic energy flux density (q) for: (a) air-dry aggregates and (b) aggregates pre-wetted at 0.3 m matric suction. For clarity, standard errors are not shown.

the pre-wetted beds. As pre-wetted (300 mm suction) aggregates did not slake when immersed into distilled water, presumably due to lower entrapped air and swelling compared to initially dry aggregates, this more rapid decrease of infiltration capacity for

the pre-wetted soil may not be attributable to slaking. A more rapid decline in hydraulic conductivity for pre-wetted soil was also observed by Geeves *et al.* (1994). The most likely explanation for the difference is the higher degree of saturation (0.51, at 300 mm suction) for the pre-wetted soil compared with 0.02 for the initially air-dry aggregates prior to rainfall.

Deformation and packing of aggregates below the surface 0 to 5 mm may also have influenced infiltration. The surface (0 to 5 mm depth) of pre-wetted aggregates contained much less fine material than initially air-dry aggregates (Figures 4.2 and 4.3, Section 4.3.2). However, aggregate breakdown, as measured by surface deflation of the aggregate beds (“collapse”), was greater in pre-wetted beds than the initially air-dry beds (Section 4.3.3).

Cumulative infiltration prior to runoff (I_{ro}) first increased then decreased as kinetic energy flux density increased (Figure 3.2). The decrease agrees with the findings of Thompson and James (1985) and Mohammed and Kohl (1987) that the influence of kinetic energy flux density on infiltration prior to runoff overshadowed the influence of rainfall kinetic energy, application rate and duration. The initial increase in cumulative infiltration indicates that the lower rainfall intensities used (40 and 70 mm h⁻¹) were lower than the infiltration rates of water into aggregate beds at the low rainfall energy (1.6 J m⁻² mm⁻¹).

Thompson and James applied rainfall kinetic energies of 0.5, 4.5 and 8.5 J m⁻² mm⁻¹ and but higher intensities of 30, 50, 100 and 150 mm h⁻¹. Mohammed and Kohl applied rainfall with kinetic energies of 0, 7.2, 8.2, 12.4, 19.4 to 24.4 J m⁻² mm⁻¹ with constant intensity of 155 mm h⁻¹. The relationship between cumulative infiltration prior to runoff and kinetic energy flux density for these two studies is shown in Figure 3.3.

Values of cumulative infiltration were much higher than those found in the present study. This may be due to greater structural stability as suggested by the higher organic carbon content, 31 g kg^{-1} , compared to 18 g kg^{-1} for the Kapunda soil. Nevertheless, the relationship between cumulative infiltration prior to runoff and kinetic energy flux density is similar to that shown in Figure 3.3. All these data fitted a power function

$$I_{ro} = a q^{-b} \quad (3.4)$$

where a and b are coefficients of regression, I_{ro} is cumulative infiltration prior to runoff (mm), and q is rainfall kinetic energy flux density ($\text{J m}^{-2} \text{ h}^{-1}$).

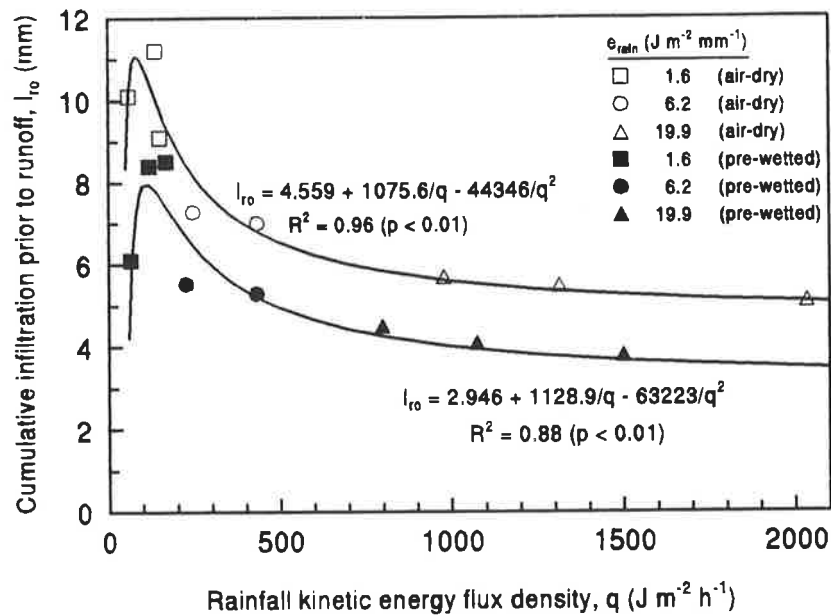


Figure 3.2. Cumulative infiltration prior to runoff as a function of rainfall kinetic energy flux density for initially air-dry and pre-wetted (at 0.30 m of water suction) aggregates. Kinetic energy applied are given in the legend. $2 \times$ standard errors of the means were smaller than the symbols.

Soil water content prior to rainfall influenced the effect of kinetic energy flux density on infiltration, particularly at low ($1.6 \text{ J m}^{-2} \text{ mm}^{-1}$) kinetic energy (Figure 3.2).

Greater kinetic energy flux density (obtained by increasing the rainfall intensity from 40 to 70 then 100 mm h⁻¹) at low rainfall kinetic energy on pre-wetted beds did not reduce but instead increased I_{r0} . It appears that for pre-wetted Kapunda aggregates, kinetic energy higher than 1.6 J m⁻² mm⁻¹ is required for the development of a surface seal. On these pre-wetted beds, when the rainfall kinetic energy was 1.6 J m⁻² mm⁻¹, the proportion of fine material at the surface, an indicator of surface soil hydraulic resistance (Loch and Foley, 1994), remained low and virtually unchanged at about 0.240 kg kg⁻¹ (Figure 4.3, Chapter 4). Consequently, increasing rainfall intensity (from 40 to 70 mm h⁻¹) resulted in greater cumulative infiltration of rain into aggregate beds. However, a further increase in rainfall intensity to 100 mm h⁻¹ did not change I_{r0} , because runoff occurred at an earlier time than when rainfall intensity was 70 mm h⁻¹. This suggests that hydraulic resistance (sealing) increased as the rainfall kinetic energy flux density was increased by increasing the rainfall intensity from 70 to 100 mm h⁻¹. However, the proportion of fine material at the bed surface (< 0.125 mm) did not increase in response to this intensity increase (Section 4.3.2). The higher rainfall kinetic energy flux density probably caused soil matric suction to decrease close to zero (saturated condition). Effective stress that previously held the aggregates together was released, allowing rearrangement and packing of particles or aggregates at the soil surface during rainfall, which consequently decreased the time and cumulative infiltration prior to runoff.

I_{r0} for air-dry aggregates increased when rainfall intensity was increased from 40 to 70 mm h⁻¹, but declined rapidly as the intensity was further increased from 70 to 100 mm h⁻¹ (Figure 3.2). The greater hydraulic resistance at 100 mm h⁻¹ was associated with an increase of fine material at the surface, from 0.395 to 0.430 kg kg⁻¹ (Section 4.3.2).

Slaking was thus the likely cause of the increased hydraulic resistance. Air-dry aggregates slaked readily when immersed in distilled water.

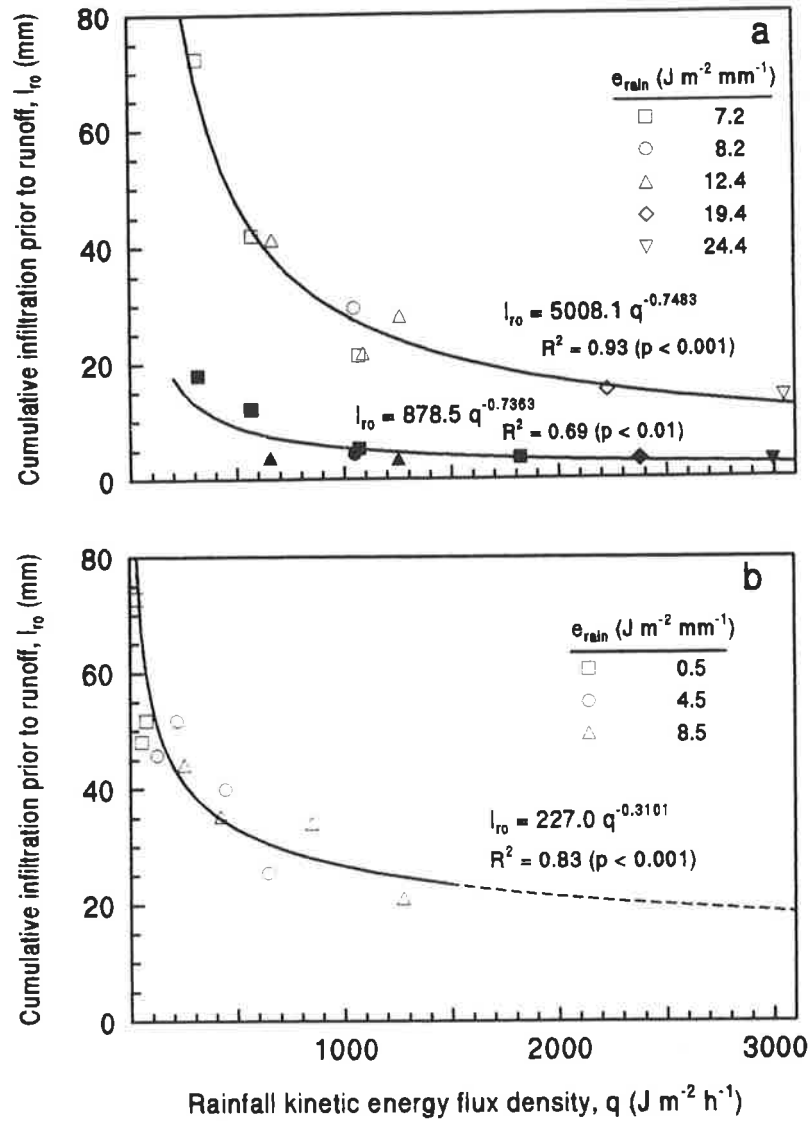


Figure 3.3. Cumulative infiltration prior to runoff as a function of rainfall kinetic energy flux density redrawn from data of: (a) Mohammed and Kohl (1987) for initially air-dry aggregates (open symbols) and pre-wetted aggregates from previous rain (closed symbols); (b) Thompson and James (1985) for initially air-dry aggregates. Kinetic energy applied is given in the legend.

Differences in hydraulic resistance and infiltration behaviour associated with different antecedent water contents reflect the contrast in resistance of aggregates to raindrop impact and the degree of packing of particles or fragments (Sections 4.3.2 and 4.3.3). It seems that for initially air-dry aggregates, about 0.4 kg kg^{-1} of fine materials ($< 0.125 \text{ mm}$) is needed before a seal formed. In pre-wetted aggregates, however, smaller amounts of fine material were needed to effectively retard water infiltration, as probably because pre-wetting caused more efficient packing of aggregates during rainfall (Figures 4.4 and 4.5).

Interaction between rainfall kinetic energy flux density and antecedent water content was also demonstrated by Mohammed and Kohl (1987). In their case, pre-wetting was done by subjecting the aggregates to an initial simulated rainfall, then draining the beds for 17 to 24 hours, followed by a second rainfall. Their results would, therefore, reflect the effect of successive rainfall. Although the method of wetting differs from that used in the present study, a similar type of relationship was found between I_{r0} and q for both dry and pre-wetted soil beds, with higher values of I_{r0} for initially dry aggregates (Figure 3.3a, b).

3.3.2 Infiltration rate

Infiltration rate after 30 minutes of rain (i_{30}) first increased as kinetic energy flux density increased up to about $112 \text{ J m}^{-2} \text{ h}^{-1}$ (Figure 3.4). Thereafter, i_{30} decreased rapidly up to kinetic energy flux density of $500 \text{ J m}^{-2} \text{ h}^{-1}$, then declined gradually at higher values of kinetic energy flux density. The range of q from 0 to $112 \text{ J m}^{-2} \text{ h}^{-1}$ was achieved using raindrop kinetic energies of $1.6 \text{ J m}^{-2} \text{ mm}^{-1}$ with rainfall intensities ranging from 40 to 70

mm h⁻¹. At low intensity (40 mm h⁻¹), low kinetic energy (hence low q) produced less fine materials (<0.125 mm) at the surface (Section 4.3.2). At 70 mm h⁻¹ the aggregates were wetted more rapidly and the speed of the rainfall mechanical energy impacting the aggregates was higher. For air-dry aggregates slaking was more rapid and more than 0.40 kg kg⁻¹ fine material was generated at the surface (Section 4.3.2).

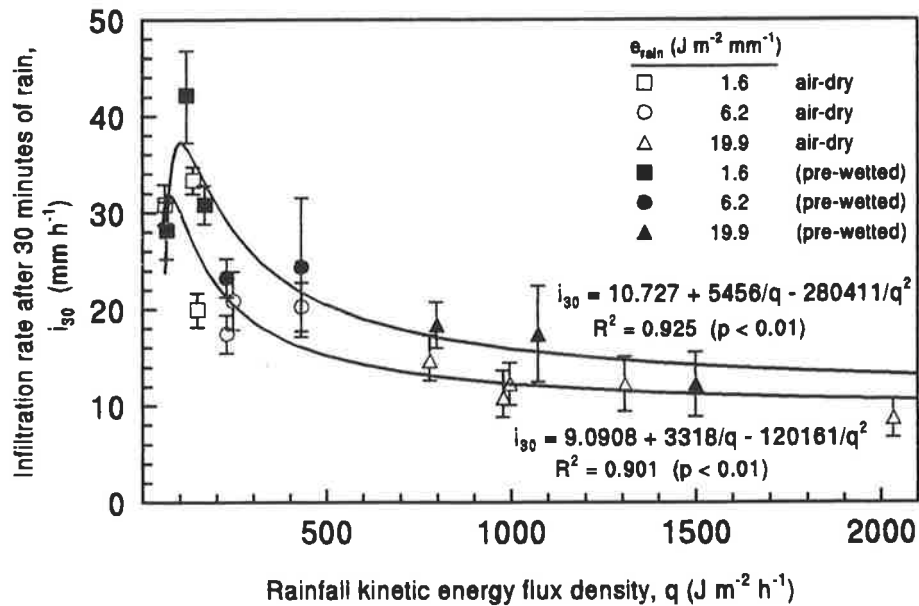


Figure 3.4. Effect of rainfall kinetic energy flux density applied during 30 minutes of rain on infiltration rate after 30 minutes for air-dry aggregates (open symbols and broken regression line) and pre-wetted aggregates (0.3 m suction) (solid symbols and unbroken regression line). Kinetic energy applied is given in the legend. Error bars are 2 × standard errors of the means.

For pre-wetted aggregates, however, slaking was retarded and practically no additional fine material was generated at the surface as the rainfall intensity was increased at this low raindrop energy. Consequently, increasing rainfall intensity from 40 to 70 mm h⁻¹ at kinetic energy of 1.6 J m⁻² mm⁻¹ (associated with an increase of kinetic

energy flux density from 64 to 112 J m⁻² h⁻¹) caused an increase of infiltration rate from 28 to 42 mm h⁻¹. As the intensity was increased further to 100 mm h⁻¹ (q increased to 160 J m⁻² h⁻¹) infiltration rate declined to 31 mm h⁻¹ (Figure 3.4). As explained earlier (Section 3.3.1), this initial rise in infiltration rate with rainfall intensity occurs through surface aggregates remaining stable until a critical kinetic energy flux density was reached. The decline in infiltration rate at 100 mm h⁻¹ was probably the result of surface aggregate packing or particle rearrangement, rather than aggregate breakdown. At a given kinetic energy flux density, infiltration rate of initially air-dry aggregates was consistently lower than that of pre-wetted aggregates (Figure 3.4), indicating that air-dry aggregates sealed more readily than pre-wetted aggregates (Le Bissonnais *et al.*, 1989).

3.3.3 Time to runoff

The time required for a seal to develop (increase of hydraulic resistance of the surface) may be inferred from the relationship between the time for a rainfall event to produce runoff and the intensity of the rain, provided the steady state infiltration rate declines to a value lower than the intensity. Figure 3.5 shows such a relationship as a function of rainfall kinetic energy. Figure 3.5a shows data from the present experiments, while Figure 3.5b shows the same data superimposed on regression lines calculated from data provided by Ragab (1983). These two sets of data are complementary, covering a wide range of kinetic energy flux density and kinetic energy values, and providing a more complete picture of the effect of rain on runoff.

For a given kinetic energy, all the relationships between time to runoff (t_{ro}) and q shown in Figure 3.5a and b were fitted to a power function of the type

$$t_{ro} = a' q^{-b'} \quad (3.5)$$

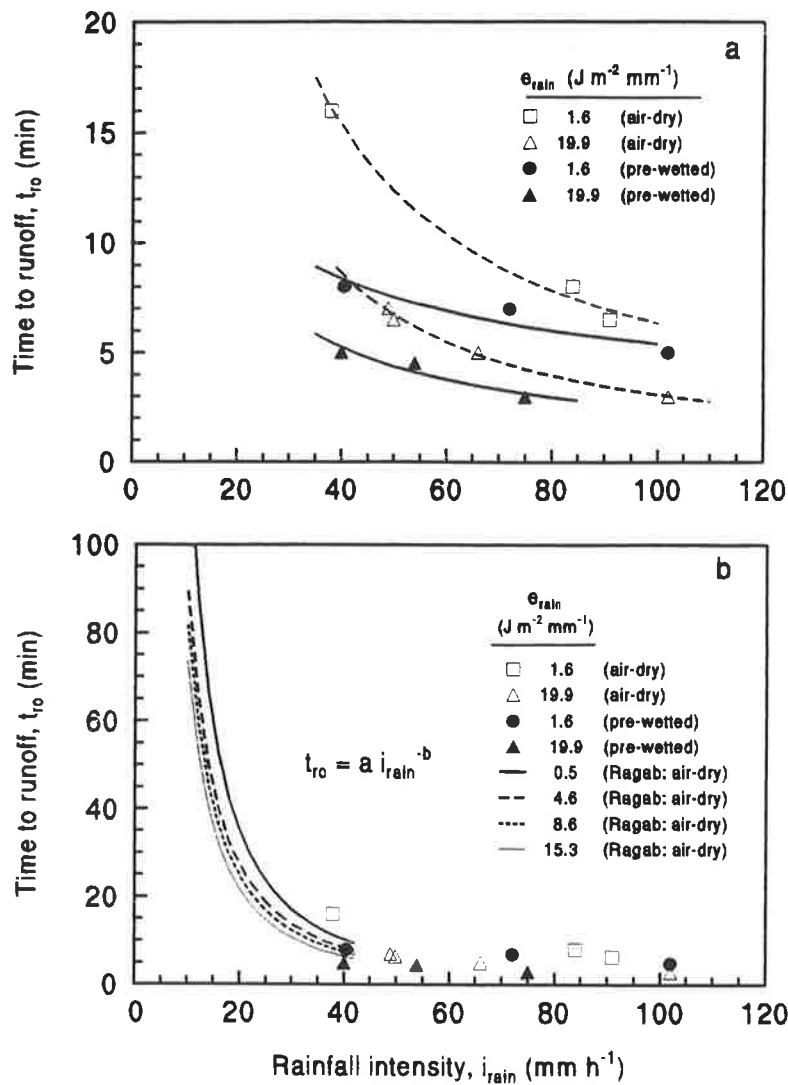


Figure 3.5. Time to runoff during rainfall as a function of rainfall intensity and kinetic energy. (a) Data obtained from experiments reported here, for initially air-dry and pre-wetted (0.30 m suction) aggregates. (b) Data from (a) above superimposed on regression relationships derived from data published by Ragab (1983) for initially dry aggregates. Kinetic energy applied, e_{rain} , is given in the legends.

where a' and b' are regression constants. Ragab's (1983) data (Figure 3.5b) had $R^2 > 0.96$, significant at $p < 0.0001$. The present data were less adequate for fitting

Equation 3.5 because of insufficient data points and lack of low intensity data. However, the two data sets are entirely complimentary and together allow more general conclusions to be drawn.

If time to runoff is interpreted as the rate of seal formation, then Figure 3.5a shows that for Kapunda soil a seal formed more rapidly if the aggregates were pre-wetted rather than air-dry aggregates and if rainfall intensity was high. Air dry aggregates were more sensitive to an increase in rainfall intensity than pre-wetted aggregates in terms of rate of seal formation.

Both data sets indicate that within the range of kinetic energy applied, time to runoff declined sharply as intensity increased from zero to about 25 mm h⁻¹. Above 25 mm h⁻¹, time to runoff changed little with increasing q . These data show that rate of sealing, as indicated by time to runoff, is relatively independent of rainfall intensity beyond about 25 mm h⁻¹. This suggests that slaking (hydration forces) is more important than packing (caused by raindrop impact) in formation of a hydraulic resistance.

3.3.4 Infiltration associated with crusting and hardsetting

Mullins *et al.* (1990) and Bristow *et al.* (1994) distinguished crusted (dry seal) from hardset surfaces on the basis of the depth of the disrupted layer: crusts are typically less than 10 mm, while hardset layers are usually more than 50 mm deep. As crusting is limited to the top few millimetres of the surface, disruption of aggregates by water must be restricted to the surface. This implies that water entry (infiltration) into the soil is retarded. In contrast, for hardsetting water must penetrate deeper into the soil to disrupt the sub-surface aggregates. Bedaiwy and Rolston (1993) proposed that densification of a

deep 'crust' (in reality a hardset layer), associated with particle reorganisation and close packing, was only possible if the aggregates below the surface were saturated or near saturated. Farres (1978) showed that thickness of the disrupted layer was a function of the volume of water applied.

Clearly, water infiltration is a key factor determining the processes of hardsetting or crusting by rainfall. Infiltration of rain water into the soil has been shown earlier in this chapter to be dependent on rainfall kinetic energy, intensity and rainfall kinetic energy flux density, and on antecedent water content before rainfall. Higher kinetic energy rainfall favours rapid development of sealing, as opposed to lower kinetic energy (Figures 3.2, 3.4 and 3.5). Therefore, under high kinetic energy rainfall, a crust should form rather than a hardset surface soil.

Hardsetting by rainfall should only develop from low kinetic energy rainfall, especially on pre-wetted aggregates, to allow water entry into the sub-surface soil to cause aggregate disruption. Pre-wetting should also enhance the process of hardsetting as it facilitates higher infiltration rates (Figure 3.4), and so promote saturation with matric suction decreasing to zero or near zero during rainfall. This weakens the aggregates (Al-Durrah and Bradford, 1981; Francis and Cruse, 1983), making them susceptible to deformation during rainfall and subsequent draining. Le Bissonnais *et al.* (1989) found that pre-wetting caused deeper and homogenous aggregate disruption in the beds, whereas disruption was shallower for air-dry aggregates, occurring mostly at the surface and decreasing gradually with depth.

From the results obtained in this experiment it is postulated that high kinetic energy rainfall ($19.9 \text{ J m}^{-2} \text{ mm}^{-1}$) should result in the formation of a surface seal and a crust on drying. Low kinetic energy rainfall ($1.6 \text{ J m}^{-2} \text{ mm}^{-1}$) with high intensity (70 mm

h^{-1}), especially on pre-wetted aggregates, should cause deep disruption and develop hardsetting on drying of the soil; but if the intensity is low ($40 \text{ mm} \cdot \text{h}^{-1}$), the soil would remain friable. The effects of rainfall properties and soil antecedent water content on crusting and hardsetting are further discussed in Chapters 4, 5 and 6.

3.4 Conclusions

1. Rainfall kinetic energy flux density is a more meaningful rainfall factor affecting sealing and infiltration compared with cumulative kinetic energy, especially for weakly structured soils. This was because a seal developed rapidly on unstable aggregates, and most surface structural changes occurred before sealing.
2. The rate of seal formation did depend on rainfall intensity and rainfall kinetic energy, but beyond a certain critical value of intensity (about $25 \text{ mm} \cdot \text{h}^{-1}$) this dependence was subdued. This suggests that slaking of aggregates is more important than packing in seal formation.
3. Although a seal formed rapidly on pre-wetted aggregates compared to air dry aggregates, the latter were more sensitive to changes in rainfall intensity because air-dry aggregates of the Kapunda soil slaked readily on wetting, which produced large amounts of fine materials at the soil surface.
4. Infiltration plays an important role in the process of hardsetting. High kinetic energy rainfall, especially on initially dry aggregates, favours the development of seals with high hydraulic resistance and reduced penetration of water to deep aggregates. Low kinetic energy rainfall, especially on pre-wetted aggregates, leads to surface soil with

low hydraulic resistance and hence deeper aggregate disruption during rainfall and hence hardsetting on drying

3.5 References

- Al-Durrah, M.M. and J.M. Bradford (1981). New methods of studying soil detachment due to waterdrop impact. *Soil Science Society of America Journal* 45: 949-953.
- Arndt, W. (1985). Factors affecting the nature and impedance of soil surface seal at Katherine, N.T. CSIRO Div. of Soils. Div. Rep. 79.
- Bedaiwy, M. N. and D. E. Rolston (1993). Soil surface densification under simulated high intensity rainfall. *Soil Technology* 6: 365-376.
- Bristow, K. L., A. Cass, K. R. J. Smettem, and P. J. Ross (1994). Modelling effects of surface sealing on water entry and re-distribution. Proceedings of the International Symposium on 'Sealing, Crusting, Hardsetting Soils: Productivity and Conservation' 7-11 February 1992, University of Queensland, Brisbane, Australia. (*in press*).
- Farres, P. (1978). The role of time and aggregate size in the crusting process. *Earth Surface Processes* 3: 243-254.
- Farres, P.J. (1980). Some observations on the stability of soil aggregates to raindrop impact. *Catena* 7: 223-231.
- Francis, P. B. and R. M. Cruse (1983). Soil water matric potential effects on aggregate stability. *Soil Science Society of America Journal* 47: 578-581.
- Geeves, G. W., P. B. Hairsine, and I. D. Moore (1994). Rainfall induced aggregate breakdown and surface sealing on a light textured soil. Proceedings of the International Symposium on 'Sealing, Crusting, Hardsetting Soils: Productivity and Conservation' 7-11 February 1992, University of Queensland, Brisbane, Australia. (*in press*).
- Glanville, S. F and G. D. Smith (1988). Aggregate breakdown in clay soils under simulated rain and effects on infiltration. *Australian Journal of Soil Research* 26: 111-120.
- Gusli, S., A. Cass, D. A. MacLeod, P. S. Blackwell (1994). Structural collapse and strength of some Australian soils in relation to hardsetting: I. Structural collapse on wetting and draining. *European Journal of Soil Science* 45: 15-21.
- Hignett, C. T. (1989). Physical measurements on a red-brown earth at Kapunda. CSIRO Div. of Soils, Divisional Report No. 107.
- Hignett, C. T. (1991). Relating soil structure to runoff quality and quantity. *International Hydrology & Water Resources Symposium*, Perth 2-4 October 1991, Inst. of Engineers Australia, Publication 91/22, p. 301-305.
- Keller, J. (1970). Sprinkler intensity and soil tilth. *Transactions of the American Society of Agricultural Engineers* 13: 118-125.

- Le Bissonnais, Y., A. Bruand and M. Jamagne (1989). Laboratory experimental study of soil crusting: relation between aggregate breakdown mechanisms and crust structure. *Catena* 16: 377-392.
- Loch, R. L. and J. L. Foley (1994). Measurement of aggregate breakdown under rain: Comparison with tests of water stability and relationships with field measurements of infiltration. *Australian Journal of Soil Research* 32: 701-720.
- Mantell, A. and D. Goldberg (1966). Effect of water application rate on soil structure. *Journal of Agricultural Engineering Research* 11: 76-79.
- Mohammed, D. and R. A. Kohl (1987). Infiltration response to kinetic energy. *Transactions of American Society of Agricultural Engineers* 30: 108-111.
- Morin, J. and Y. Benyamini (1977). Rainfall infiltration into bare soils. *Water Resources Research* 13: 813-817.
- Mullins, C. E., D. A. MacLeod, K. H. Northcote, J. M. Tisdall, and I. M. Young (1990). Hardsetting soils: behaviour, occurrence, and management. *Advances in Soil Science* 11: 37-108.
- Philip, J. R. (1957). The theory of infiltration: 4. Sorptivity and algebraic infiltration equations. *Soil Science* 83: 257-264.
- Ragab, R. A. (1983). The effect of sprinkler intensity and energy of falling drops on soil surface sealing. *Soil Science* 136: 117-123.
- Rose, C. W. (1960). Soil detachment caused by rainfall. *Soil Science* 89: 28-35.
- Shvebs, G.I. (1968). Data on the erosive action of water drops. *Soviet Soil Science* No.2: 262-269.
- Smettem, K. R. J., A. D. Rovira, S. A. Wace, B. R. Wilson, and A. Simon (1992). Effect of tillage and crop rotation on the surface stability and chemical properties of a red-brown earth (Alfisol) under wheat. *Soil & Tillage Research* 22: 27-40.
- Thompson, A.L. and L.G. James (1985). Water droplet impact and its effect on infiltration. *Transactions of American Society of Agricultural Engineers* 28: 1506-1510, 1520.
- Truman, C. C., J. M. Bradford, and J. E. Ferris (1990). Antecedent water content and rainfall energy influence on soil aggregate breakdown. *Soil Science Society of America Journal* 54: 1385-1392.
- Wace, S. A. and C. T. Hignett (1991). The effect of rainfall energy on tilled soils of different dispersion characteristics. *Soil & Tillage Research* 20: 57-67.

Chapter 4

Breakdown and packing of aggregates under rainfall

4.1 Introduction

The disruptive effect of rainfall kinetic energy on aggregates is confined largely to surface soil and diminishes rapidly with depth (Sor and Bertrand, 1962; Eigel and Moore, 1983). The main exception to this generalisation is the effect of pressure waves on aggregate deformation (Moss, 1991). By contrast, the disruptive effect of rapid wetting of aggregates is dependent on depth of wetting at low matric suction (Mullins *et al.*, 1990; Gusli *et al.*, 1994a). From this, it follows that depth of water penetration is likely to be influenced by the speed and completeness of seal formation at the surface.

The development of a surface seal by raindrop impact involves two processes: (1) breakdown of aggregates into finer fragments or primary particles, which may fill voids; and (2) compaction of the fragments and particles by raindrops (Epstein and Grant, 1973). The degree of sealing has been correlated with the production of fine materials at the surface during rainfall (Glanville and Smith, 1988; Le Bissonnais *et al.*, 1989; Loch and Foley, 1994). Production of fine material at the soil surface depends on both wetting energy (rate of wetting) which is related to rainfall intensity (Sor and Bertrand, 1962; Lyles *et al.*, 1969; Agassi and Levy, 1991). Agassi *et al.* (1985) attributed decreased infiltration rate with increased kinetic energy of raindrops to the disintegration of surface aggregates and their compaction to form a thin seal. Consequently, both rainfall intensity and kinetic energy affect seal development and compaction of aggregates (Epstein and Grant, 1973; Ragab, 1983). The

thickness of the seal (crust) formed during this process is typically less than 10 mm (Moss, 1991; Bristow *et al.*, 1994).

The second major disruptive process during rainfall is deep penetration of water at low matric suction. Depth of water penetration and therefore depth of aggregate disruption has been reported to vary with aggregate size prior to rainfall (Farres, 1978; Arndt, 1985), aggregate stability (West *et al.*, 1992), and rainfall characteristics (Arndt, 1985). Bristow *et al.* (1994) in reviewing the literature reported that if crusts are thicker than 10 mm, the process of deep aggregate disruption and hardsetting is probably involved rather than seal formation and crusting. Although causes for the variation in the depth of aggregate breakdown have been proposed, the mechanism that determines the thickness of the disrupted layer is not well understood.

Soil water content influences the stability of aggregates to raindrop impact (Cernuda *et al.*, 1953; Bruce-Okine and Lal 1975; Cousen and Farres, 1984; Le Bissonnais *et al.*, 1989; Truman *et al.*, 1990). Thus, antecedent water content, as well as rainfall kinetic energy flux density, should affect surface sealing and hence the collapse of aggregates below the seal. The greater the depth of water penetration, the greater the collapse of aggregates below the surface, and the thicker is the disrupted layer. Le Bissonnais and Bruand (1993) proposed that seasonal variation in soil moisture content in the field governs the extent (degree and depth) of structural change at the soil surface caused by rainfall.

From the above considerations, it is postulated that different combinations of rainfall kinetic energy, rainfall intensity and antecedent soil water content would result in different degrees of breakdown of surface aggregates, production of fine materials and

sealing. These factors will determine collapse of underlying aggregates. In this respect several possible hypotheses can be proposed:

- 1) First, rainfall of high kinetic energy and medium to high intensity (*i.e.* medium to high kinetic energy flux density) on a dry surface produces a high proportion of fine materials (<0.125 mm) and hence a seal of low hydraulic conductivity. Aggregates beneath the seal remain dry or are wetted slowly under suction, so that breakdown is likely to be minimal. The disrupted surface layer will be thin and on drying a thin crust will form.
- 2) Rainfall with the same properties falling on moist soil at a lower matric suction produces less breakdown of surface aggregates and less sealing. The infiltration rate of the rain will be greater, causing more aggregate breakdown. On drying a hardsetting surface layer will form.
- 3) Rainfall of low kinetic energy and intensity (*i.e.* low kinetic energy flux density) falling on soil with stable surface structure, either moist or dry, will produce no appreciable breakdown of surface or underlying aggregates. In this case no surface crust or hardset layer is formed, and the soil remains friable.

Drainage status of the aggregate bed is likely to play an important role in the disruption of the bed by wetting, as drainage rate will influence the soil matric suction during rainfall by controlling the outflow, as opposed to inflow, of rain water. Restricted drainage should cause a more rapid decrease of matric suction. When drainage rate is smaller than rain infiltration rate, aggregates in the bed should be saturated during rainfall, creating condition for extensive aggregate breakdown.

To test these hypotheses, experiments with the following aims were set up:

- 1) to investigate the effect of rainfall kinetic energy flux density on surface aggregate disruption and subsequent aggregate bed packing on draining and drying at two antecedent water contents;
- 2) to compare aggregate breakdown and packing resulting from wetting (i) by rainfall, (ii) under suction, and (iii) by flooding; and
- 3) to examine the effect of soil drainage status on aggregate packing for rainfall wetting.

4.2 Materials and methods

4.2.1 Soil properties and preparation of aggregate beds

A red-brown earth (fine, mixed, thermic, Calcic Rhodoxeralf) (Soil Survey Staff, 1988) from Kapunda, South Australia was used for all experimental work reported in this thesis. The properties and behaviour of the soil in the field and management history are given in Section 3.2.1. Aggregate beds were prepared as described in Section 3.2.2, and either wetted by rainfall, or by flooding or suction without rainfall.

4.2.2 Wetting of the aggregate beds

4.2.2.1 Rainfall wetting

A rainfall simulator (Section 2.2.1) was used to deliver simulated rainfall (drop diameter of 5.1 mm) to aggregate beds as described in Section 3.2.3.

4.2.2.2 Suction and flood wetting

Sample beds were wetted without rainfall using high flow rate ceramic plates (air-entry suction = 10 m of water). A thin layer, about 3 mm thick, of diatomaceous earth was spread evenly over the plate to provide good hydraulic contact between aggregates and the plate.

Samples were wetted at a suction of 0.30 m of water (the base of the bed as a reference). The same suction as was applied to the pre-wetted bed for rainfall wetting (Section 2.2.3). Wetting at this matric suction should not cause marked structural change (Gusli *et al.*, 1994a). Aggregates were fully wetted in less than 10 hours, but the soil was retained on the plates for a further 14 hours to give to total wetting time of 24 hours.

Flood wetting of air-dry and pre-wetted aggregates (0.30 m suction) was done by flooding the soil under zero suction (the upper surface of the bed was used as reference level) in a constant temperature room, as described by Gusli *et al.* (1994a). This water level was maintained until the beds were fully saturated. After 24 hours of flooding, the sample beds were drained to 0.57 m water suction for 24 hours. After this, the aggregate beds were transferred to a glasshouse and dried to various matric suctions (Section 5.2.2). Eight replicate beds were prepared for each of the treatments.

4.2.3 Control of aggregate bed drainage

For rainfall wetting treatments, the rate of drainage of aggregate beds was controlled by imposing a suction of 0.3 m of water through a layer of mixture of diatomaceous earth and silica flour at the base of the aggregate bed. Two contrasting drainage rates were applied: a “non-limiting” rate, in which the drainage rate was greater than rainfall

application rate; and completely restricted drainage rate. Drainage flux density at the imposed matric suction of 0.30 m was 230 mm h⁻¹, greater than the maximum rainfall intensity applied of 100 mm h⁻¹.

4.2.4 Measurements

4.2.4.1 Infiltration rate

Rainfall and runoff were recorded electronically at 1 minute intervals (Section 2.2.5). Infiltration was calculated as the difference between rainfall and runoff. Infiltration rate after 30 minutes of rainfall was calculated by fitting Philip's (1957) model (Section 3.2.3, Equations 3.2 and 3.3) to cumulative infiltration data. This value was assumed to be the steady state infiltration rate (see Section 3.2.3).

4.2.4.2 Surface aggregate size

The aggregate size distribution of the surface soil from 0 to 5 mm was measured immediately after rainfall using a modification of the wet sieving method recommended by Cleary *et al.*, (1987) and Loch (1994) (Section 3). Samples of surface material (0 to 5 mm depth) from five beds were removed using a scalpel blade (Loch, 1994). The sieve sizes used were 2.0, 1.0, 0.5, 0.25 and 0.125 mm. The objective of this measurement was to relate the degree of sealing and rate of water entry to surface aggregate disruption. If meaningful data were to be obtained, it was necessary to prevent further aggregate breakdown during wet sieving. For this reason, the sieving time was reduced to one minute, during which samples went through 35 oscillations. No problems due to inadequate time for the aggregates (about 2.5 g equivalent air-dry weight) to

pass through the sieves after 1 minute sieving, and no difference in aggregate-size distribution between using 2 and 4 grams of dry aggregates were observed. Aggregates of air-dry soil did not disperse when immersed in distilled water, but did so if remoulded. Consequently, samples were sieved in $10 \text{ mol}_c \text{ m}^{-3} \text{ CaCl}_2$ rather than water to avoid dispersion during sieving (Smettem *et al.*, 1992). After wet sieving, the soil plus sieves were oven dried at $105 \text{ }^\circ\text{C}$ for 24 hours. Aggregate-size distribution was calculated as mean weight diameter (MWD) (van Bavel, 1949), and the proportion of materials (aggregates and particles) less than 0.125 mm was calculated.

4.2.4.3 Matric suction

Matric suction was controlled by means of hanging water columns (for suctions of 0.3 and 0.57 m), and measured by mercury manometers at higher matric suctions, from about 1 to 6 m of water during drying in the glass house.

4.2.4.4 Vertical strain

Vertical strain, as a measure of collapse of aggregates, was determined using a dial gauge (sensitivity 0.01 mm), similar to the method used by Gusli *et al.* (1994a). The dial gauge was screwed onto a square metal bar which during measurement was placed on the surface rim of the PVC sample tubing (reference level). Ten height measurements, spaced approximately at equal distance from each other (based on a scale on the bar) across the surface of the aggregate beds were made before wetting, after draining at 0.30 and 0.57 m suctions following wetting, and at various matric suctions during drying (Section 4.2.4.3). Vertical strain (ϵ_ψ) at matric suction ψ , was calculated as:

$$\epsilon_\psi = (H_0 - H_\psi) / H_0 \quad (4.1)$$

where H_0 is the mean initial height of the soil bed and H_ψ is the height at the soil bed at matric suction of ψ .

4.2.4.5 Bulk density profile

After drying the bulk density of the soil bed was measured at 2.5 mm increments for the first 5 mm depth, and then at 5 mm increments below this. The aggregate bed was sectioned horizontally, after removal of the base mesh using a device in which the aggregate bed was pushed up by means of a piston to a known height above the upper rim of the retaining cylinder. The exposed part of the bed was then carefully and gradually sliced away with a sharp blade. The diameter of the bed was measured with a calliper, and the volume of the slice was calculated. To minimise compression and rupture of beds during handling and piston movement, beds were sampled at a moisture content corresponding approximately to the plastic limit.

4.3 Results and discussion

4.3.1 Change in vertical strain with matric suction following different wetting conditions

The effect of the various treatments on vertical strain are shown in Figure 4.1. On draining to between 1 to 2 m of suction, vertical strain increased regardless of type and energy of wetting. However, rain of low kinetic energy flux density ($\leq 115 \text{ J m}^{-2} \text{ h}^{-1}$, associated with kinetic energy of $\leq 1.6 \text{ J m}^{-2} \text{ mm}^{-1}$) caused less subsequent collapse on draining and drying than rain of higher kinetic energy flux density. Vertical strain ceased

to change when matric suction in the beds reached about 1-2 m. Despite a similar pattern of vertical strain change with increasing matric suction, pre-wetted (0.30 m suction)

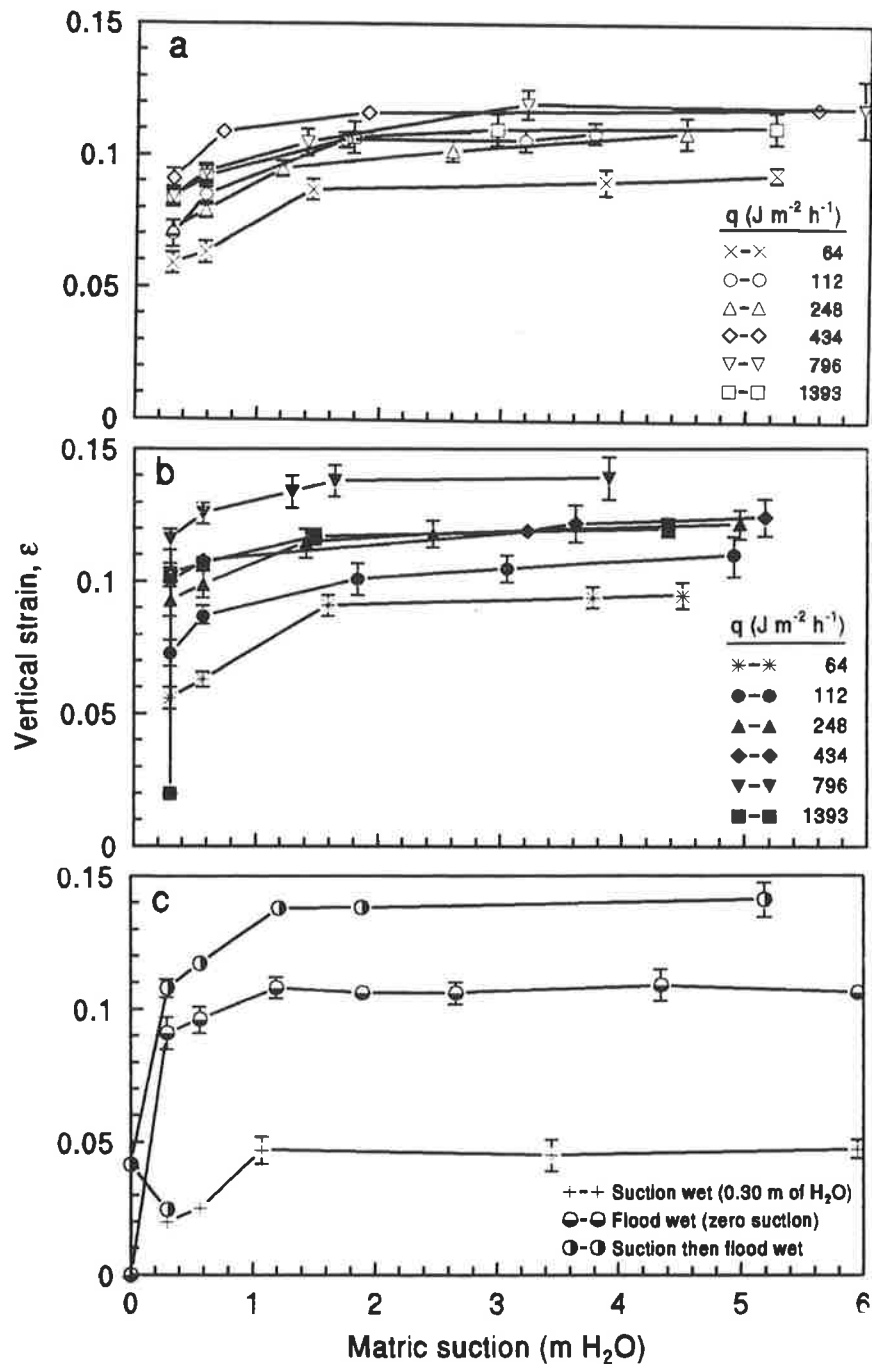


Figure 4.1. Aggregate bed collapse (vertical strain) on draining and drying after wetting of (a) air-dry and (b) suction wetted (0.30 m suction) aggregates by rainfall of variable kinetic energy flux density (q), and (c) wetting by flooding of air-dry or pre-wetted aggregates, or suction wetting without subsequent rainfall. Bars are 2 standard errors of the means.

aggregates were more sensitive than initially air-dry beds to variation in kinetic energy flux density (Figures 4.1a and b). However, when kinetic energy flux density was $\leq 115 \text{ J m}^{-2} \text{ h}^{-1}$, pre-wetting did not have a different effect on vertical strain compared to air-dry beds.

Generally, values of vertical strain resulting from flood wetting of dry beds were similar to aggregate beds (air-dry or pre-wetted) that had been subjected to rainfall of $>115 \text{ J m}^{-2} \text{ h}^{-1}$ (Figures 4.1a, b and c). An exception, however, was for rainfall of $797 \text{ J m}^{-2} \text{ h}^{-1}$ on pre-wetted soil which caused greater vertical strain. This energy flux density was derived from rain of $19.9 \text{ J m}^{-2} \text{ mm}^{-1}$ kinetic energy falling at 40 mm h^{-1} intensity. Possibly, the higher energy flux density of $1395 \text{ J m}^{-2} \text{ h}^{-1}$, achieved by applying rain at $19.9 \text{ J m}^{-2} \text{ mm}^{-1}$ at 70 mm h^{-1} , caused a marked decline in surface soil conductance even on pre-wetted beds compared to the $19.9 \text{ J m}^{-2} \text{ mm}^{-1}$ falling at 40 mm h^{-1} (energy flux density of $797 \text{ J m}^{-2} \text{ h}^{-1}$). As a result, the former had a lower infiltration rate (high matric suction below the seal during rain) and hence lower final vertical strain than the latter. Flood wetting dry beds resulted in higher vertical strain than rainfall of kinetic energy flux density $64 \text{ J m}^{-2} \text{ h}^{-1}$ on both pre-wetted and air-dry beds (Figures 4.1a, b and c).

Suction wetted beds without subsequent rainfall showed the least vertical strain change on draining and drying (Figure 4.1c). However, when suction wetted aggregate beds were subsequently flooded, vertical strain was large and similar to that produced when pre-wetted beds were subjected to rainfall with kinetic energy flux density of $797 \text{ J m}^{-2} \text{ h}^{-1}$ (Figure 4.1a).

4.3.2 Effect of rainfall kinetic energy flux density on surface aggregate size and infiltration rate

Fine aggregates were generated at the expense of coarser aggregates by increased rainfall kinetic energy flux density on both initially dry and pre-wetted aggregates (Figure 4.2). However, pre-wetted aggregates broke down to a lesser extent than initially dry aggregates, with pre-wetted aggregates producing fewer fine fragments at all levels of rainfall kinetic energy flux density than dry soil. The greater resistance of pre-wetted aggregates to the disruptive effect of rainfall energy is well recognised (Cernuda *et al.*, 1953; Bruce-Okine and Lal 1975; Cousen and Farres, 1984; Le Bissonnais *et al.*, 1989; Truman and Bradford, 1993). Dry aggregates of the Kapunda soil slaked readily, within less than two minute, when immersed in distilled water. In contrast, the pre-wetted aggregates did not slake at all, unless remoulded. Due to the greater susceptibility to slaking of the initially dry aggregates, there was less variation in surface aggregate size produced by rainfall at different kinetic energy flux densities.

Flood wetting of air-dry soil generated less fine material than rainfall on dry soil. Suction wetting of air-dry soil generated the least amount of aggregate fragmentation. High energy flux rainfall on pre-wetted soil generated about the same amount of fine materials as flood wetting of air-dry soil.

Flood wetting of suction wetted aggregates caused more fragmentation (greater proportion of aggregates less than 2 mm diameter) than flood wetting of air-dry aggregates (Figure 4.2). This contradicts the fact that when immersed into distilled water, air-dry aggregates of Kapunda soil slaked extensively, but pre-wetted (0.30 m suction) aggregates did not, consistent with what many workers expect (Panabokke and Quirk, 1957; Le Bissonnais *et al.*, 1989; Chan and Mullins, 1994). The mechanisms by

which the aggregates are fragmented by flooding of air-dry and of pre-moistened aggregates should be different. For initially dry aggregates, comminution would be due to stresses arising from swelling and trapped air. Aggregate fragmentation resulting from these stresses should produce fragments of generally greater than 0.5 mm (Chan and Mullins, 1994). This is because forces induced by swelling and trapped air are likely to be exerted mainly at the weak planes of aggregates, *i.e.* between the coarse fragments of the aggregates. As the aggregates comminute, the stresses are released, and further breakdown to finer fragments does not take place.

The large aggregate breakdown observed in suction then flood wetted treatments cannot be attributable to stresses due to swelling and trapped air. This is because: (1) at a matric suction of 0.30 m of water most clay layers should have reached maximum swelling, and (2) wetting slowly under suction does not cause build up of pressure due to trapped air. During wetting by suction aggregates and fragments that constitute them are held by small effective stress, equivalent to the wetting suction. However, micro-cracks within the aggregates and the fragments of aggregates also develop during suction wetting, creating weak planes (Quirk and Panabokke, 1962). As the aggregates were subsequently flooded, effective stress which held the aggregates and fragments was reduced to zero, and mechanical force of flowing water during flooding can dislocate the coarser and finer fragments. Collapse of beds during flooding of suction wetted aggregates was visually observed. This produced finer fragments than flooding of air-dry aggregates (Figure 4.2). Similar results were observed in four other soils of different aggregate stability (data not shown).

The proportion of materials <0.125 mm increased with rainfall kinetic energy flux density as a power function (Figure 4.3). Antecedent water content did not change the

type of relationship (power function), but initially dry aggregates fragmented more extensively than pre-wetted aggregates at a given kinetic energy flux density. Increased stability resulting from pre-wetting aggregates to a matric suction of about 0.50 m is well documented (Quirk, 1950; Emerson and Grundy, 1954; Cernuda *et al.*, 1953; Panabokke and Quirk, 1957).

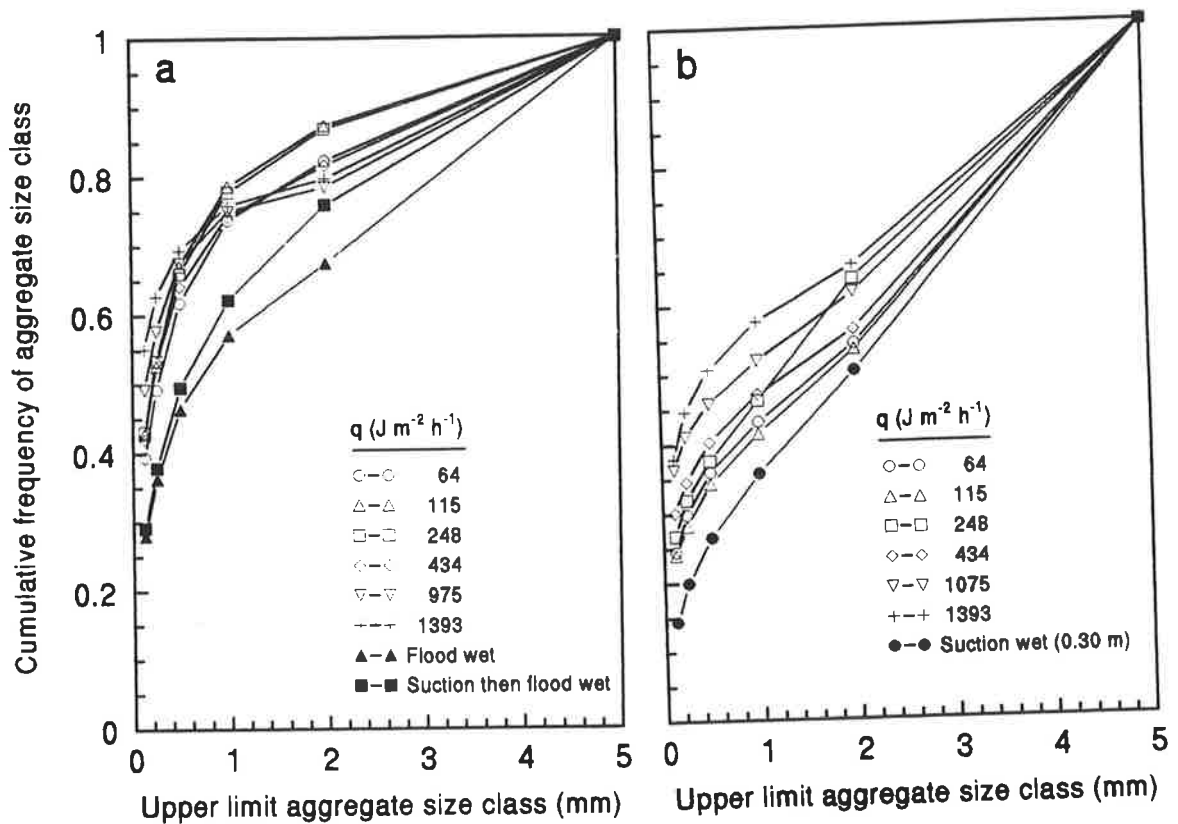


Figure 4.2. Effect of rainfall kinetic energy flux density (q) on aggregate size distribution of (a) initially air-dry and (b) pre-wetted at 0.30 m suction, after 30 minutes of rainfall. Solid symbols represent wetting without raindrop energy by flooding and by suction wetting at 0.30 m suction was given for comparison with rainfall wetting.

The rate of aggregate breakdown with increasing kinetic energy flux density, q , was greatest at q values of less than $200 \text{ J m}^{-2} \text{ h}^{-1}$ for both pre-wetted and dry soil.

Aggregates continued to break down at q values from 200 to 1500 $\text{J m}^{-2} \text{h}^{-1}$, but at a lower rate.

Figure 4.4 shows that infiltration rate after 30 minutes of rainfall (i_{30}) was a negative power function of the proportion of materials <0.125 mm in the 0 to 5 mm depth (A_{125}). The kinetic energy of rainfall controlled the proportion of fine materials generated during rainfall. High kinetic energy rainfall produced a greater proportion of fine materials and hence lower infiltration rate than lower kinetic energy for both antecedent water contents. The effect of kinetic energy on the relationship between i_{30} and A_{125} was such that values of i_{30} and A_{125} produced by different kinetic energies (from 1.64 to 19.9 $\text{J m}^{-2} \text{mm}^{-1}$) formed one regression line for the same antecedent water content.

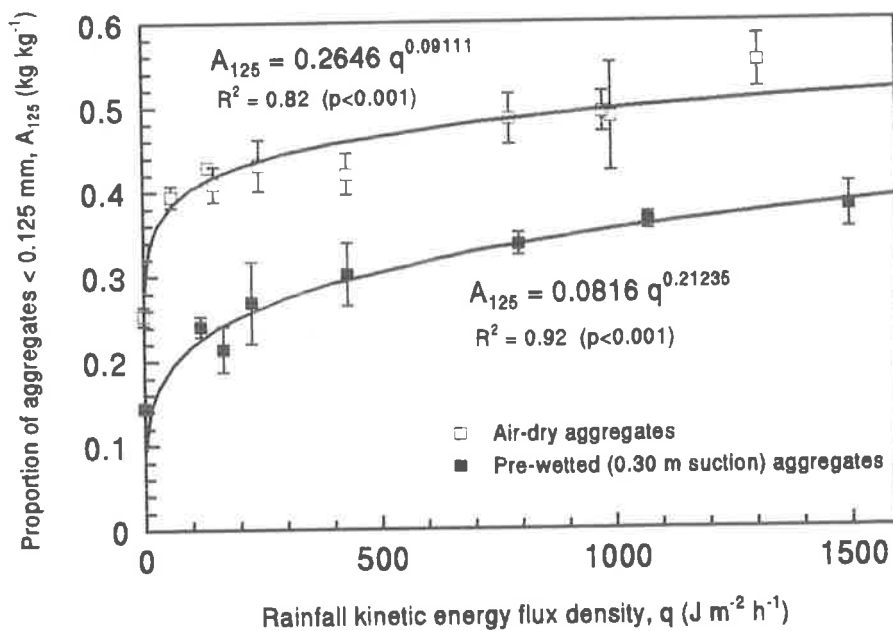


Figure 4.3. Effect of rainfall kinetic energy flux density on the proportion of materials <0.125 mm at 0 to 5 mm depth after 30 minutes rainfall for initially dry and pre-wetted soils.

Loch and Foley (1994) found a similar relationship to that shown in Figure 4.4, although it was expressed as an exponential function. However, they found rainfall with an energy of $29 \text{ J m}^{-2} \text{ mm}^{-1}$ on various soils produced a different regression line to that from 'near zero' kinetic energy. They did not study the effect of antecedent water content. Different regression lines for low and high kinetic energy rainfall reported by Loch and Foley should have reflected different stabilities of the soils they tested (Al-Durah and Bradford, 1982). Such relationships may be expected when constant kinetic energy throughout the rainfall event is applied on different soils. Applying rainfall of a single kinetic energy should be more appropriate for testing aggregate stability than for studying processes of aggregate breakdown, crusting or hardsetting. This is because high kinetic energy rainfall tends to cause extensive aggregate breakdown in a very short time. In addition, aggregates of many Australian soils disintegrate at kinetic energies $>12 \text{ J m}^{-2} \text{ mm}^{-1}$ (Hignett, 1991). At higher kinetic energy ($29 \text{ J m}^{-2} \text{ mm}^{-1}$), aggregates of these soils would be broken down to primary particles, so that the surface seal conductivity, which determines infiltration rate of rain water, would be governed by packing of the soil primary particles rather than fine aggregates.

Antecedent water content prior to rainfall strongly influenced the production of fine materials that are likely to affect infiltration rate. For a given proportion of fine materials ($<0.125 \text{ mm}$), infiltration rate of initially air-dry aggregates was higher than for pre-wetted aggregates. This suggests that although A_{125} is a good predictor of infiltration rate, other factors associated with initial water content, such as arrangement of disrupted materials at the surface, were affecting infiltration (Farres, 1978; Le Bissonnais *et al.*, 1989; Moss, 1991).

Most researchers agree that it is the hydraulic conductivity of the surface seal that dictates the infiltration rate of the soil profile (Thompson and James, 1985; Loch and Foley, 1994). Following rainfall, pre-wetted soil consistently showed greater vertical strain than initially dry soil, as discussed in Table 4.1. Greater vertical strain indicates closer packing of disrupted materials and lower porosity, which would be expected to result in lower water infiltration.

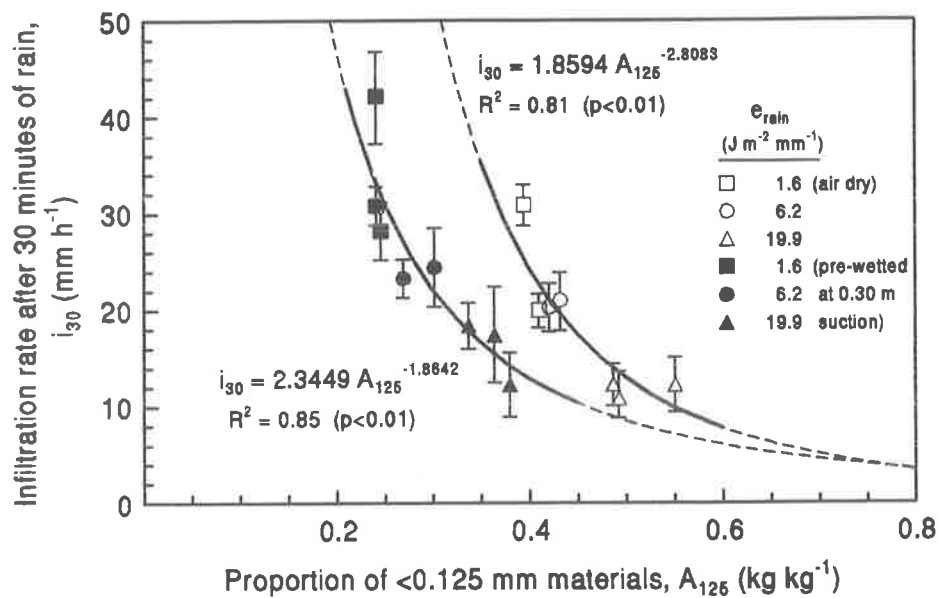


Figure 4.4. Effect of proportion of materials <0.125 mm (A_{125}) in the 0 to 5 mm depth on infiltration rate after 30 minutes of rain (i_{30}) of various kinetic energies (e_{rain}) applied on initially air-dry (open symbols) and pre-wetted soils (closed symbols).

4.3.3 Surface aggregate size and vertical strain

The higher the rainfall kinetic energy or the more rapidly aggregate beds were wetted (flood compared to slower tension wetting), the greater was the final vertical strain (Table 4.1). Without rainfall, suction wetted aggregate beds had the lowest final vertical

strain (0.045), whereas flood wetted aggregate beds had a final vertical strain of 0.106. Where wetting was by rainfall, kinetic energies of 1.6, 6.2 and 19.9 J m⁻² mm⁻¹ produced final vertical strains of 0.093, 0.109 and 0.118 respectively for initially dry aggregate beds, and 0.094, 0.127 and 0.139 for pre-wetted aggregate beds. When the rainfall kinetic energy was greater than 6.2 J m⁻² mm⁻¹, the final vertical strain of pre-wetted beds was greater than that of flood wetted beds without rainfall (0.127 as opposed to 0.106). On initially dry beds, rainfall of 6.2 J m⁻² mm⁻¹ resulted in similar final vertical strain (ϵ_f) to flood wetted beds. These results are re-examined in Chapter 7.

Antecedent water content also determined the extent of aggregate breakdown by flooding. Table 4.1 shows that suction wetted beds (0.30 m suction) that were subsequently flood wetted showed greater aggregate bed collapse ($\epsilon_f = 0.141$) than when dry aggregates were flood wetted ($\epsilon_f = 0.106$). This shows the importance of matric suction and hence effective stress and strength of aggregates (Al-Durrah and Bradford, 1981; Gusli *et al.*, 1994b) in stabilising aggregates during rainfall. Flooding of suction wetted beds caused matric suction and effective stress to decline to approximately zero, releasing the soil - water tension which formerly stabilised the aggregates (Mohammed and Kohl, 1987), causing fragmentation (Figure 4.2). Subsequently, as effective stress increased on draining and drying, final vertical strain increased from 0.106 (flooding of air-dry beds) to 0.141 (flooding of initially suction wetted beds).

Table 4.1 also shows that free drainage during rainfall, provided by a drainage suction of 300 mm on the base of the aggregate bed, reduced aggregate disruption and packing. It is assumed that during rain, the matric suction never reached zero because water was never allowed to pond on the soil surface. Excess water on the surface ("runoff") was immediately removed by vacuum. In addition, the base of the test bed

(mixture of diatomaceous earth and silica flour) had a high water flux density (230 mm h⁻¹) compared to rainfall intensity which was always less than 100 mm h⁻¹. Under these conditions, a small effective stress was maintained in the soil matrix during rainfall. Thus, aggregate breakdown and packing resulted only from raindrop mechanical energy and the rate of wetting allowed by the infiltration rate.

Table 4.1. Effect of methods and conditions of wetting and draining on final vertical strain of aggregate beds after wetting and drying. Antecedent water content of dry and wet in column two refer to air-dry and pre-wetted aggregates (0.30 m suction), respectively. Values in brackets are the standard errors of the means (n = 8).

Wetting method	Antecedent water content	Drainage status	Rainfall intensity (mm ⁻² h ⁻¹)	Rainfall kinetic energy (J m ⁻² mm ⁻¹)	Final vertical strain
<u>Without rainfall</u> a) Suction b) Flood c) Flood	Dry	-	-	-	0.045 (0.006)
	Dry	-	-	-	0.106 (0.003)
	Wet	-	-	-	0.141 (0.006)
<u>By rainfall</u>	Dry	Free	40	1.6	0.093 (0.003)
			40	6.2	0.109 (0.006)
			40	19.9	0.118 (0.010)
	Wet	Free	40	1.6	0.094 (0.004)
			40	6.2	0.127 (0.005)
			40	19.9	0.139 (0.011)
			70	1.6	0.110 (0.008)
			70	6.2	0.126 (0.004)
			70	19.9	0.120 (0.004)
	Wet	Restricted	70	1.6	0.137 (0.006)
			70	19.9	0.206 (0.011)

When the drainage rate was reduced to zero during rainfall by restricting drainage from the base of the aggregate beds, pre-wetted soil beds collapsed extensively during rainfall (Table 4.1). The final vertical strains were 0.137 at low ($1.6 \text{ J m}^{-2} \text{ mm}^{-1}$) and 0.206 at high ($19.9 \text{ J m}^{-2} \text{ mm}^{-1}$) rainfall kinetic energies falling at 70 mm h^{-1} . These values are significantly higher than those obtained under drained conditions for the same kinetic energies and intensity (0.110 and 0.120). Without drainage, aggregate breakdown and packing are a result of the effects of raindrop mechanical energy plus slumping of aggregates caused by decrease of matric suction to or near zero. The results show that, regardless of whether aggregates are wetted by flooding or by rainfall, matric suction in the aggregate bed during wetting determines the extent of aggregate disruption on wetting and subsequent draining and drying.

Figure 4.5 shows final vertical strain as a function of the amount of materials $<0.125 \text{ mm}$ at the surface for various wetting conditions and rainfall kinetic energies. Solid symbols trace a pathway from pre-wetted soil subjected to no rain, then rain of increasing kinetic energy. Open symbols show a similar path, but for initially dry soil. Data from flood wetting of air-dry aggregates (open diamond) are included for comparison. A number of deductions can be drawn from these data:

1. Increasing rainfall kinetic energy caused greater surface (0 to 5 mm) aggregate breakdown, regardless of antecedent water content. However, for the same kinetic energy, initially dry aggregate beds had a higher proportion of materials $<0.125 \text{ mm}$ at the surface than pre-wetted (300 mm suction) aggregate beds. Yet, for the same proportion of materials $<0.125 \text{ mm}$, pre-wetted beds had greater vertical strain. It may be postulated that in initially dry beds a seal readily formed at the surface, which reduced the disruption and packing of underlying aggregates.

2. An increase in the proportion of material <0.125 mm for both pre-wetted and initially dry beds did not produce increased vertical strain when rainfall kinetic energy was >6.2 J m⁻² mm⁻¹, despite the fact that greater kinetic energy caused more surface aggregate breakdown (Figure 4.3). A difference in final vertical strain between pre-wetted and initially dry beds had developed at kinetic energy of 6.2 J m⁻² mm⁻¹, and this remained unchanged at higher kinetic energy (Figure 4.5). Increasing rainfall kinetic energy resulted in greater aggregate disruption and packing only at the surface, and the bed as a whole did not collapse. Evidence of this is shown in the penetration resistance profile (Section 6.3.1). Therefore, disruption of aggregates beneath the seal was controlled by the rate of wetting (infiltration rate through the seal) which influenced soil matric suction and hence aggregate breakdown during rainfall. For a rainfall kinetic energy of 6.2 J m⁻² mm⁻¹, above which no change in vertical strain was observed, the corresponding infiltration rate was about 25 mm h⁻¹ (Figure 3.4, Section 3.3.2). It is proposed that at high kinetic energy, infiltration rate was not sufficiently high to cause further sub-surface aggregate disruption.
3. Increasing kinetic energy from 1.6 to 6.2 J m⁻² mm⁻¹ caused both an increased proportion of materials smaller than 0.125 mm at the surface and larger final vertical strain. However, at a rainfall kinetic energy of 1.6 J m⁻² mm⁻¹, there was no difference in final vertical strain between pre-wetted and initially dry aggregate beds, despite the difference in the proportion of materials <0.125 mm at the surface. At this kinetic energy the infiltration rate for both pre-wetted and dry aggregate beds was >25 mm h⁻¹ (Figure 3.4, Section 3.3.2), which apparently was high enough to reduce the soil matric suction sufficiently (approaching zero) to

generate similar aggregate disruption below the surface layer. Greater aggregate disruption by raindrop mechanical energy at the surface for initially dry beds (Figure 4.3) might have been counteracted by a faster rate of wetting under the surface in pre-wetted beds due to the greater infiltration rate.

4. Rainfall of low ($1.6 \text{ J m}^{-2} \text{ mm}^{-1}$) kinetic energy generated a relatively small proportion of materials $<0.125 \text{ mm}$ at the surface of the bed. Consequently, collapse of soil aggregates would have been mainly controlled by hydration associated with rate of wetting, *i.e.* rainfall intensity. Final vertical strain was equal to or less than that of flood wetted dry beds, depending on rainfall intensity. It was observed that rainfall at low kinetic energy ($1.6 \text{ J m}^{-2} \text{ mm}^{-1}$) falling at high intensity ($\geq 70 \text{ mm h}^{-1}$) did not cause a surface seal to form, but aggregates were disrupted to well below ($>10 \text{ mm}$) the normal thickness of seal. On drying the vertical strain was similar to that for flood wetting dry beds, known to form a hardset layer. Rainfall of 40 mm h^{-1} intensity on pre-wetted beds formed a more friable soil bed on drying than rainfall of higher intensity. Rainfall on air-dry beds generated a higher proportion of fine materials at the surface compared to pre-wetted beds (Figure 4.5), but did not cause much aggregate disruption either. However, rainfall of $1.6 \text{ J m}^{-2} \text{ mm}^{-1}$ on both pre-wetted and dry soil beds resulted in greater vertical strain than suction wetting (0.30 m) of dry soil.
5. Rainfall at kinetic energy $\geq 6.2 \text{ J m}^{-2} \text{ mm}^{-1}$ produced a higher proportion of materials $<0.125 \text{ mm}$ at the surface compared to flood wetting of air-dry soil (>0.43 compared to 0.28 kg kg^{-1}). However, both methods of wetting had similar final vertical strains (0.11 to 0.13) after draining and drying (Figure 4.5). This implies that rainfall with $>6.2 \text{ J m}^{-2} \text{ mm}^{-1}$ on initially air-dry beds caused aggregate

breakdown mainly at the surface soil, while aggregates below 5 mm depth suffered relatively little disruption. It was observed, however, that aggregate beds subjected to flood wetting had less breakdown at the surface, but disruption occurred throughout the depth of the beds. Penetration resistance data support this observation (Section 6.3.1).

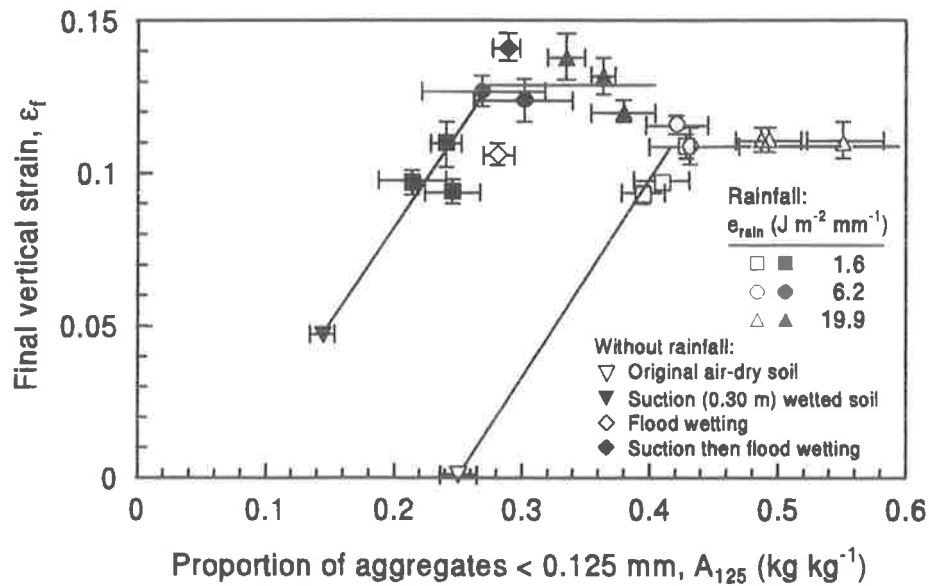


Figure 4.5. Effect of surface aggregate disruption on packing of aggregate beds as a function of rainfall kinetic energy (e_{rain}) for initially air-dry (open symbols) or pre-wetted at 0.30 m of matric suction (closed symbols). Treatments with no rain: original air-dry soil, flood wetting of initially dry soil, and tension wetting at 0.30 m suction. Bars are 2 standard errors of the means.

Le Bissonnais *et al.* (1989) reported that initially air-dry aggregates were more unstable against raindrop impact than pre-wetted aggregates, leading to more rapid crust development for the former. In the pre-wetted soil, pores between aggregates were only partially clogged by fine particles, but the surface crust was twice as thick as the crust

which had developed from initially dry aggregates. Collis-George and Lal (1971) found that initial water content affected slaking, swelling behaviour and infiltration rate of soil. The wetter the soil initially, the greater was the infiltration rate and the smaller the slaking and swelling. In unstable soils, the heat of wetting is correlated with amount of aggregate collapse (Collis-George and Lal, 1971). Heat of wetting decreases with increasing antecedent water content, suggesting that a more energetic reaction occurs between water and soil when the soil is drier (Marshall and Holmes, 1988, p. 20-21). The disruption of aggregates of the surface layers prevents fast entry of water into the lower layers. Farres (1978) found that the thickness of 'equilibrium' crust (a term used by Farres) was shown to be related to initial aggregate size. The larger the antecedent aggregate size, the thicker the final disrupted layer.

Seals and disrupted layers in soils are formed by two related but different processes: aggregate breakdown and particle rearrangement (Moss, 1991, West *et al.*, 1992). Surface aggregates are broken down by forces associated with wetting and the mechanical energy of rainfall. This disruption causes an increase in the proportion of fine material (<0.125 mm diameter) at the soil surface (Glanville and Smith, 1988; Loch and Foley, 1994). During rain, the disrupted aggregates and particles are rearranged and repacked at the surface to form a surface seal, if sufficient fine materials are present (Moss, 1991). The conductivity of the seal during rainfall dictates the extent of aggregate disruption beneath the seal (West *et al.*, 1992). The higher the conductivity, the lower the matric suction of in-flowing water and the greater the degree of aggregate disruption beneath the seal. The greater the aggregate disruption, the larger the vertical strain on draining and drying.

4.3.4 Effect of rainfall intensity and kinetic energy on vertical strain

Higher rainfall intensity at a given kinetic energy increased kinetic energy flux density, which in turn influenced aggregate disruption and packing. On pre-wetted beds, rainfall of $19.9 \text{ J m}^{-2} \text{ mm}^{-1}$ at 70 mm h^{-1} (energy flux density of $1393 \text{ J m}^{-2} \text{ h}^{-1}$) (rightmost solid upright triangle in Figure 4.5) generated 0.38 kg kg^{-1} materials of $<0.125 \text{ mm}$ at the soil surface. In comparison, rainfall of the same energy at 40 mm h^{-1} (energy flux density of $797 \text{ J m}^{-2} \text{ h}^{-1}$) (leftmost solid upright triangle in Figure 4.5) generated 0.34 kg kg^{-1} materials of this size class at the surface. Thus, under rainfall of $19.9 \text{ J m}^{-2} \text{ mm}^{-1}$ kinetic energy on pre-wetted beds, an increase from 0.34 to 0.38 kg kg^{-1} of this fine material reduced final vertical strain from 0.139 to 0.120 (Figure 4.5). This was associated with a decrease in rate of water entry from 18 to 12 mm h^{-1} (Figure 4.4, top and bottom solid triangles). Collis-George and Lal (1971) reported that breakdown of surface structure prevents fast entry of water into the underlying soil layers. In contrast, for the initially dry beds, at kinetic energy $>6.2 \text{ J m}^{-2} \text{ mm}^{-1}$, no significant effect of kinetic energy flux density on aggregate packing was observed (Figure 4.5). This rainfall produced $>0.42 \text{ kg kg}^{-1}$ materials of $<0.125 \text{ mm}$ at surface. This amount of fine material apparently was sufficient to reduce the rate of water penetrating through the surface to $<20 \text{ mm h}^{-1}$, so that aggregates below the surface were unaffected by increasing rainfall kinetic energy or intensity (Figure 4.5).

At any rainfall intensity, increasing kinetic energy flux density resulting from increased kinetic energy caused an increase of vertical strain, regardless of antecedent water content (Figure 4.6). The relationship between final vertical strain (ϵ_f) and rainfall kinetic energy flux density (q) was a hyperbolic function:

$$\varepsilon_f = q / (a q + b)$$

where a and b are regression coefficients. Fitting this function to either air-dry or pre-wetted aggregate data gave values of a = 7.601 and b = 212.127 for pre-wetted soil ($R^2 = 0.69$, significant at $p < 0.05$) and a = 8.865 and b = 110.495 for initially dry soil ($R^2 = 0.59$, significant at $p < 0.01$). This hyperbolic relationship implies that for Kapunda soil, regardless of antecedent water content, disruption and packing of aggregates progressed rapidly as rainfall kinetic energy was increased from zero (no rain) to $6 \text{ J m}^{-2} \text{ mm}^{-1}$, corresponding to an increase in kinetic energy flux density of 0 to $420 \text{ J m}^{-2} \text{ h}^{-1}$ (Figure 4.6). As the rainfall was applied for 0.5 hour, this kinetic energy flux density value is equivalent to cumulative kinetic energy of 0 to about 210 J m^{-2} . Maximum final vertical strain occurred when a rainfall kinetic energy flux density ranging from 200 to $420 \text{ J m}^{-2} \text{ h}^{-1}$ was reached. Higher energy flux density did not increase final vertical strain significantly.

Epstein and Grant (1967) and Romkens *et al.* (1986) reported that seal development and soil densification occurred extensively and very rapidly during the first few minutes of rainfall. These processes had virtually reached completion when the cumulative rainfall energy reached 250 J m^{-2} , equivalent to 9.1 mm cumulative rainfall (Romkens *et al.*, 1986). The data obtained in this study also indicates that the collapse of aggregate beds occurs mainly during the early stage of rainfall, before the soil surface seals, at a q value of $420 \text{ J m}^{-2} \text{ h}^{-1}$ equivalent to cumulative kinetic energy of $< 220 \text{ J m}^{-2}$ (Figure 4.6), which agrees fairly well with data of Romkens *et al.* (1986). This implies that aggregate collapse, particularly in unstable soils such as those which are prone to hardsetting or crusting processes, is mainly controlled by the early stage of rainfall.

Prolonged rainfall with cumulative kinetic energy $>250 \text{ J m}^{-2}$ has little consequence on processes of hardsetting and crusting.

For rainfall with kinetic energy of $25 \text{ J m}^{-2} \text{ mm}^{-1}$, commonly measured in the field (Kinnell, 1981; Rosewell, 1986; and Kinnell, 1987), kinetic energy flux density of 200 to $420 \text{ J m}^{-2} \text{ h}^{-1}$ is achieved at rainfall intensities ranging from 8 to 17 mm h^{-1} . At Kapunda, for a two year average recurrence interval, rainfall of about 15 mm h^{-1} falls for 1 hour (Canterford, 1987). Thus, rainfall with intensities of 8 to 17 mm h^{-1} , sufficient to cause maximum aggregate packing of this soil, as indicated by Figure 4.5, are common at Kapunda.

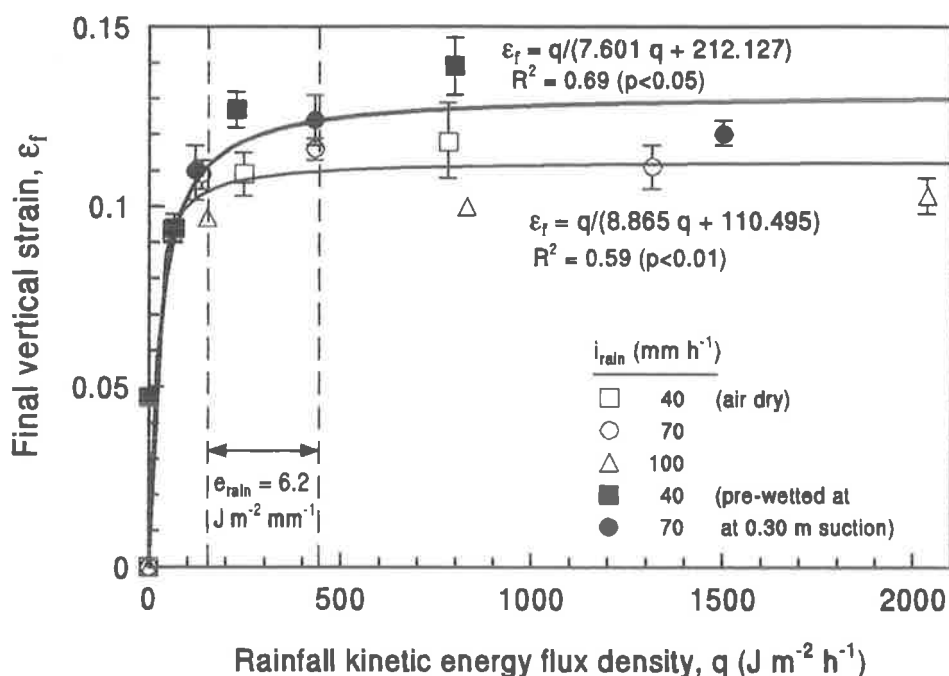


Figure 4.6. Aggregate bed collapse (vertical strain) as a function of rainfall kinetic energy flux density (q), applied at different intensities on either air-dry pre-wetted aggregates bed. Bars are 2 standard errors of the means.

Many researchers (e.g. Sor and Bertrand, 1962; Morin and Benyamini, 1977; Bedaiwy and Rolston, 1993) have related cumulative energy of rainfall to surface sealing or crusting. However, Mualem *et al.* (1990) considered that it was more appropriate to relate the dynamics of seal formation to the rainfall kinetic energy rather than to the cumulative energy. Young and Wiersma (1973) reported that decreasing rainfall energy while the rainfall intensity remained constant led to a significant decrease of fine particles released from destruction of aggregates. On the other hand, Agassi and Levy (1991) found that at constant kinetic energy, increasing rainfall intensity resulted in lower infiltration rate. Whether kinetic energy or intensity or both were increased, kinetic energy flux density increased. Therefore, kinetic energy flux density which reflects both droplet kinetic energy and intensity influenced surface sealing and infiltration rate (Shvebs, 1968; Epstein and Grant, 1973; Ragab, 1983; Mohammed and Kohl, 1987). This agrees with the result reported here.

Clearly, vertical strain cannot just be related to cumulative kinetic energy without regard to rainfall kinetic energy and intensity. Equally, antecedent water content has to be taken into account, as all these factors interact to determine to what extent rainfall affects collapse of the soil bed. Without knowing rainfall intensity and kinetic energy, relating aggregate packing to cumulative rainfall energy *per se* can be misleading since for the same cumulative kinetic energy, different vertical strains may be obtained under different rainfall intensities (Figure 4.6). Morin *et al.* (1981) observed that matric suction just below the seal increased more rapidly under higher intensity than under lower intensity rainfall for the same amount of rainfall. Mantell and Goldberg (1966) concluded that at constant cumulative rainfall energy, both penetration resistance and air permeability changed as a result of a change in energy flux resulting from increased

rainfall intensity. Therefore, kinetic energy flux density (which combines both rainfall intensity and kinetic energy) is a better rainfall parameter to describe the effect of rainfall on aggregate packing.

Rainfall intensity preceding drainage of aggregate beds influenced vertical strain (packing) during draining and drying, especially for high kinetic energy rain ($19.9 \text{ J m}^{-2} \text{ mm}^{-1}$) on pre-wetted beds (Figure 4.1b). High rainfall intensity (70 mm h^{-1}) caused less vertical strain than low intensity (40 mm h^{-1}) ($\epsilon_f = 0.120$ as opposed to 0.139), despite the fact that the former had higher cumulative rainfall energy than the latter. Cumulative rainfall energy is not the only rainfall factor affecting aggregate disruption and packing. The flux of water with low matric suction into soil is certainly also a major factor influencing aggregate disruption (Figure 4.6).

4.3.5 Rate of wetting of soil beds and final vertical strain

Aggregate packing, expressed as final vertical strain, increased with the rate of water penetration into aggregate beds, expressed as infiltration rate after 30 minutes of rain (Figure 4.7). The relationship may be expressed as

$$\epsilon_f = a' i_{30}^{1/2} + b' i_{30} \quad (4.3)$$

where ϵ_f is final vertical strain, i_{30} is infiltration rate at 30 minutes rain, a' and b' are regression coefficients.

The type of relationship shown in Equation 4.3 implies that aggregate packing (vertical strain) was larger for greater infiltration rates. The more rapid water entry into the beds, the greater the vertical strain, especially at high rainfall energy. At low rainfall energy, vertical strain was less sensitive to rate of water entry (Figure 4.7).

This relationship also suggests that both rate of wetting and mechanical energy of rainfall determine aggregate packing. Rate of wetting is related to rainfall intensity (i_{rain}), especially at low kinetic energy, while mechanical energy is associated with raindrop energy (e_{rain}). Rainfall kinetic energy flux density (the combined effect of e_{rain} and i_{rain}) has been shown to be well correlated with vertical strain (Figure 4.6) and rate of transmission of water into aggregate beds (Figure 3.4, Section 3.3.2). Higher kinetic energy flux density resulted in greater aggregate breakdown (Figure 4.3), producing surface sealing, lower infiltration rate and hence less aggregate disruption at depth and lower final vertical strain. Lower final vertical strain for initially dry compared to pre-wetted beds is attributed to more extensive surface aggregate breakdown, seal formation and hence slower transmission of water into deeper layers of the aggregate beds.

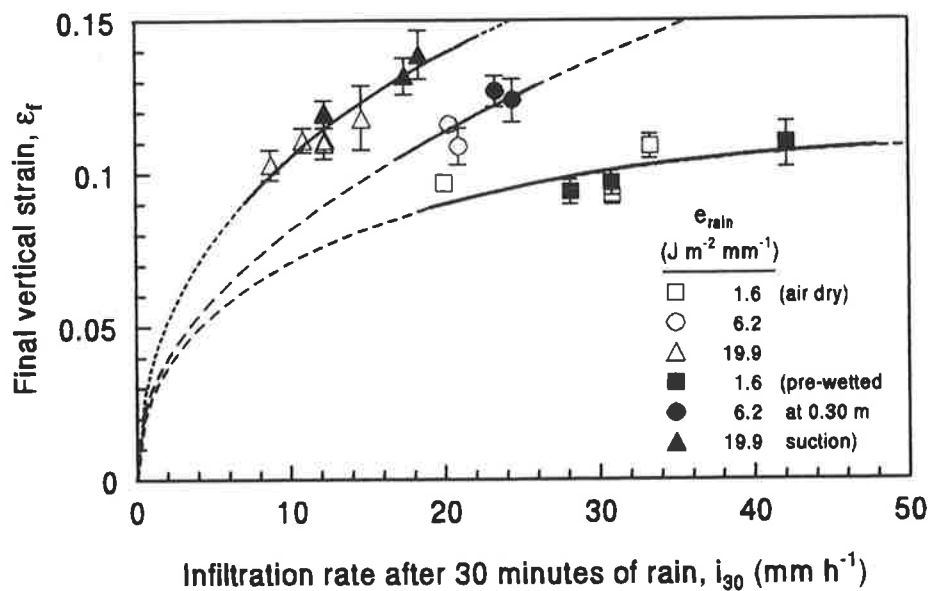


Figure 4.7. Relationship between infiltration rate after 30 minutes rain (i_{30}) and final aggregate bed vertical strain (ϵ_f) for different rainfall kinetic energies (e_{rain}) and antecedent water contents. Bars are 2 standard errors of the means.

For the Kapunda soil, the maximum final vertical strain under rainfall with free soil drainage condition was about 0.14 for pre-wetted beds and 0.12 for initially dry beds (Table 4.1). Most of this collapse (final vertical strains of 0.125 and 0.11 for the respective antecedent water contents) occurred at kinetic energy flux density below $420 \text{ J m}^{-2} \text{ h}^{-1}$ (Figure 4.6). Vertical strain development was greatest over the energy flux range from 0 and $220 \text{ J m}^{-2} \text{ h}^{-1}$. At kinetic energy flux in excess of $420 \text{ J m}^{-2} \text{ h}^{-1}$, vertical strain virtually did not change as flux increased (Figure 4.6). Similarly, infiltration rate decreased most substantially at kinetic energy flux density less than $200 \text{ J m}^{-2} \text{ h}^{-1}$, while values in excess of $420 \text{ J m}^{-2} \text{ h}^{-1}$ did not cause much change to infiltration rate (Figure 3.4, Section 3.3.2). Thompson and James (1985) reported that water infiltration prior to ponding decreased sharply as kinetic energy flux density increased from 0 to about $100 \text{ J m}^{-2} \text{ h}^{-1}$.

Relationships between final vertical strain and kinetic energy flux density (Figure 4.6) fitted a hyperbolic function, whereas infiltration rate and kinetic energy (Figure 3.4, Chapter 3) fitted a second order hyperbolic function. Except for the slight difference in the small values of kinetic energy flux densities ($<115 \text{ J m}^{-2} \text{ h}^{-1}$), these two functions are a mirror image of each other. However, it was noticed that while virtually no change in vertical strain occurred at kinetic energy flux densities greater than about $420 \text{ J m}^{-2} \text{ h}^{-1}$, infiltration rate still continued to decrease slightly. It is suggested that for aggregate disruption to occur, infiltration rate should be greater than a certain limiting value. For the Kapunda soil, the data shown in Figure 3.4 indicates that this limiting value was approximately 25 mm h^{-1} . It is speculated that the further decrease of infiltration rate at kinetic energy flux density greater than $420 \text{ J m}^{-2} \text{ h}^{-1}$ was primarily due to surface particle

rearrangement which caused surface pore sealing by fine particles but did not result in change of volume strain.

4.3.6 Bulk density profile

Conclusive evidence of packing as a function of wetting treatment is to be found in the distribution of bulk density down the aggregate beds. Data obtained from these measurements were variable because of limitations in the method used. However, a typical data set as a function of wetting treatment is shown in Figure 4.8.

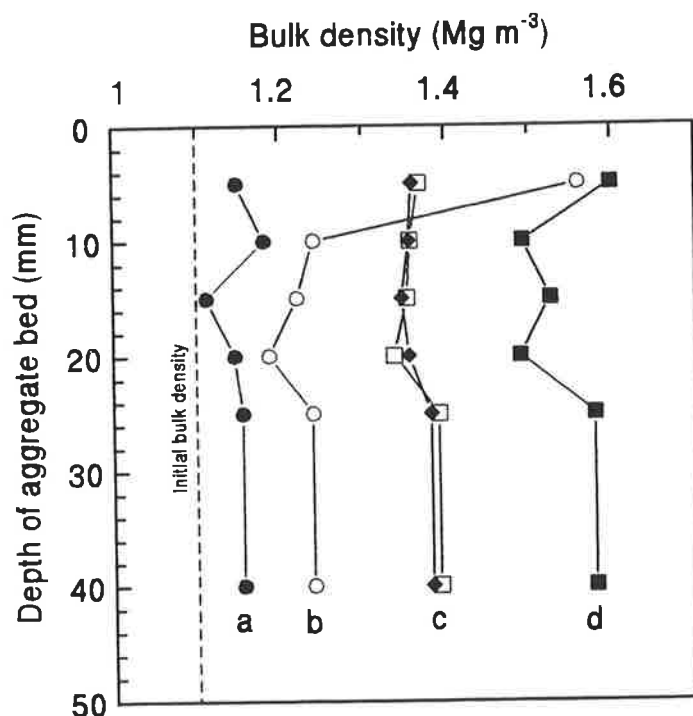


Figure 4.8. Typical bulk density profiles of aggregate beds for: (a) suction-wetted (0.30 m of water) aggregate beds, represented by ● (friable); (b) subjected to rainfall of high kinetic energy ($>6.2 \text{ J m}^{-2} \text{ mm}^{-1}$), represented by ○ (crusted); (c) subjected to rain of low kinetic energy ($<6.2 \text{ J m}^{-2} \text{ mm}^{-1}$), represented by □ (hardset) or flood wetted represented by ◆ (hardset); and (d) flooding of suction-wetted aggregate beds, represented by ■ (severely hardset).

Method of wetting, rainfall intensity and kinetic energy, and antecedent soil water content strongly influenced packing of aggregate beds. Beds with initial bulk density of 1.1 Mg m^{-3} remained friable with a low bulk density throughout the depth of the bed ($<1.2 \text{ Mg m}^{-3}$) if wetted by suction of 0.30 m of water (Figure 4.8: a). Rainfall of high kinetic energy ($>6.2 \text{ J m}^{-2} \text{ mm}^{-1}$) produced a crust with bulk density ($>1.5 \text{ Mg m}^{-3}$) and lower bulk density (approximately 1.2 Mg m^{-3}) below the crust (Figure 4.8: b). Rainfall of low kinetic energy ($<2 \text{ J m}^{-2} \text{ mm}^{-1}$) on pre-wetted (0.30 m suction) aggregate beds or flood wetting of air-dry aggregates resulted in high bulk density (approximately 1.4 Mg m^{-3}) uniformly distributed down the aggregate beds (Figure 4.8: c). This condition is typical of hardsetting (Mullins *et al.*, 1990; Weaich *et al.*, 1992; Gusli *et al.*, 1994a). When pre-wetted aggregate beds were flooded, the highest bulk density was observed (approximately 1.6 Mg m^{-3}), again uniformly distributed down the bed (Figure 4.8: d). These bulk density data conform to the results of vertical strain reported in this chapter and the strength measurements reported in Chapters 5 and 6.

4.4 Conclusions

1. The extent of aggregate disruption and packing (expressed as vertical strain) of the Kapunda soil following wetting, draining and drying was found to be dependent on (1) the type of wetting (rainfall, wetting under suction, or flood wetting); (2) kinetic energy flux density (for rainfall wetting) which is a function of kinetic energy and intensity; (3) water content prior to wetting; and (4) drainage during rainfall.
2. Under rainfall wetting, vertical strain of aggregate beds increased as a hyperbolic function of the increase in kinetic energy flux density. Infiltration rate decreased with

increasing kinetic energy flux density. This relationship was independent of antecedent water content. Kinetic energy flux density dictated breakdown and packing of aggregates by controlling the magnitude of surface soil disruption, as measured by the proportion of materials <0.125 mm produced during rain. Low rainfall kinetic energy flux density generated a lower proportion of this material at the surface, allowing a higher infiltration rate through the surface layer and therefore resulted in greater aggregate packing than high rainfall kinetic energy flux density.

3. Beds pre-wetted at 0.30 m suction stabilised aggregates against raindrop impact energy, producing a smaller proportion of aggregates <0.125 mm at the soil surface and hence greater infiltration rate. Consequently, aggregate packing was more extensive in pre-wetted beds than in initially dry beds.
4. Under constant rainfall intensity, aggregate disruption and packing increased with rainfall kinetic energy. For the Kapunda soil, the critical rainfall kinetic energy above which no significant increase in aggregate packing occurred, was about $6.2 \text{ J m}^{-2} \text{ mm}^{-1}$. Rainfall intensity and antecedent water content did not change the critical kinetic energy, but determined the extent of aggregate disruption and packing. Vertical strain was higher under lower rainfall intensity on pre-wetted beds.
5. For bed heights of 50 mm, flood wetting at zero matric suction of air-dry beds gave similar vertical strain values to wetting dry beds by rainfall with kinetic energy of 6.2 to $19.9 \text{ J m}^{-2} \text{ mm}^{-1}$, but gave smaller vertical strain than wetting by rainfall at the same energy on pre-wetted beds. Flood wetted beds had higher vertical strain than rainfall at $1.6 \text{ J m}^{-2} \text{ mm}^{-1}$ kinetic energy and intensity of 40 mm h^{-1} for both air-dry and pre-wetted beds. At rainfall intensity $>70 \text{ mm h}^{-1}$ on pre-wetted beds, the vertical strain was similar to that of flood wetted air-dry soil beds. Flooding generated a lower

proportion of material <0.125 mm at the soil surface but greater aggregate disruption at depth below the surface than rainfall treatments.

6. Suction wetting without subsequent flooding or rainfall caused the lowest aggregate disruption and maintained friable soil structure on drying. However, suction wetting followed by flooding caused more aggregate disruption and packing than flood wetting dry aggregates.
7. Restricting drainage during rainfall increased vertical strain.

4.5 References

- Agassi, M. and G. J. Levy (1991). Stone-cover and rain intensity: Effects on infiltration, erosion and water splash. *Australian Journal of Soil Research* 29: 565-575.
- Agassi, M., J. Morin, and I. Shainberg (1985). Effect of raindrop impact energy and water salinity on infiltration rates of sodic soils. *Soil Science Society of America Journal* 49: 186-190.
- Al-Durrah, M.M. and J.M. Bradford (1981). New methods of studying soil detachment due to waterdrop impact. *Soil Science Society of America Journal* 45: 949-953.
- Al-Durah, M.M. and J.M. Bradford (1982). Parameters for describing soil detachment due to single waterdrop impact. *Soil Science Society of America Journal* 46: 836-840.
- Arndt, W. (1985). Factors affecting the nature and impedance of soil surface seal at Katherine, N.T. CSIRO Div. of Soils. Div. Rep. 79.
- Bedaiwy, M. N. and D. E. Rolston (1993). Soil surface densification under simulated high intensity rainfall. *Soil Technology* 6: 365-376.
- Bristow, K. L., A. Cass, K. R. J. Smettem, and P. J. Ross (1994). Modelling effects of surface sealing on water entry and re-distribution. Proceedings of the International Symposium on 'Sealing, Crusting, Hardsetting Soils: Productivity and Conservation' 7-11 February 1992, University of Queensland, Brisbane, Australia. (*in press*).
- Bruce-Okine, E. and R. Lal (1975). Soil erodibility as determined by raindrop technique. *Soil Science* 119: 149-157.
- Canterford, R. P. (1987). Australian Rainfall and Runoff. A guide to flood estimation. Volume 2. The Institution of Engineers, Australia, p. 57-62.

- Cernuda, C. F., R. M. Smith, and J. Vicente-Chandler (1953). Influence of initial soil moisture condition on resistance of macroaggregates to slaking and to water-drop impact. *Soil Science* 77: 19-27.
- Chan, K. Y. and C. E. Mullins (1994). Slaking characteristics of some Australian and British soils. *European Journal of Soil Science* 45: 273-283.
- Cleary, J. L., R. J. Loch and E. C. Thomas (1987). Effects of time under rain, sampling technique and transport of samples on size distributions of water stable aggregates. *Earth Surface Processes and Landforms* 12: 311-318.
- Collis-George, N. and R. Lal (1971). Infiltration and structural changes as influenced by initial moisture content. *Australian Journal of Soil Research* 9: 107-116.
- Cousen, S. M. and P. J. Farres (1984). The role of moisture content in the stability of soil aggregates from a temperate silty soil to raindrop impact. *Catena* 11: 313-320.
- Eigel, J. D. and I. D. Moore (1983). Effect of rainfall energy on infiltration into bare soil. Proceedings of the National Conf. on Advances in Infiltration, Dec. 12-13, 1983, Chicago, Illinois, ASAE, p. 188-200.
- Emerson, W. W. and G. M. F. Grundy (1954). The effect of rate of wetting on water uptake and cohesion of soil crumbs. *Journal of Agricultural Science* 44: 249-253.
- Epstein, E. and W. J. Grant (1967). Soil losses and crust formation as related to some soil physical properties. *Soil Science Society of America Proceedings* 31: 547-550.
- Epstein, E. and W. J. Grant (1973). Soil crust formation as affected by raindrop impact. In: Hadas *et al.* (eds.). Physical Aspects of Soil Water and Salts in Ecosystems. Springer-Verlag, New York, pp.: 195-201.
- Farres, P. (1978). The role of time and aggregate size in the crusting process. *Earth Surface Processes* 3: 243-254.
- Glanville, S. F. and G. D. Smith (1988). Aggregate breakdown in clay soils under simulated rain and effects on infiltration. *Australian Journal of Soil Research* 26: 111-120.
- Gusli, S., A. Cass, D. A. MacLeod, P. S. Blackwell (1994a). Structural collapse and strength of some Australian soils in relation to hardsetting: I. Structural collapse on wetting and draining. *European Journal of Soil Science* 45: 15-21.
- Gusli, S., A. Cass, D. A. MacLeod, and P. S. Blackwell (1994b). Structural collapse and strength of some Australian soils in relation to hardsetting: II. Tensile strength of collapsed aggregates. *European Journal of Soil Science* 45: 23-29.
- Hignett, C. T. (1991). Relating soil structure to runoff quality and quantity. International Hydrology & Water Resources Symposium, Perth 2-4 October 1991, Inst. of Engineers Australia, Publication 91/22, p. 301-305.
- Kinnell, P.I. (1981). Rainfall intensity - kinetic energy relationships for soil loss prediction. *Soil Science Society of America Journal* 45: 153-155.

- Kinnell, P.I. (1987). Rainfall energy in Eastern Australia: Intensity - kinetic energy relationships for Canberra, ACT. *Australian Journal of Soil Research* 25: 547-553.
- Le Bissonnais, Y. and A. Bruand (1993). Crust micromorphology and runoff generation on silty soil materials during different seasons. *Catena Supplement* 24: 1-16.
- Le Bissonnais, Y., A. Bruand and M. Jamagne (1989). Laboratory experimental study of soil crusting: relation between aggregate breakdown mechanisms and crust structure. *Catena* 16: 377-392.
- Loch, R. J. (1994). A method for measuring aggregate water stability of dryland soils with relevance to surface seal development. *Australian Journal of Soil Research* 32: 687-700.
- Loch, R. L. and J. L. Foley (1994). Measurement of aggregate breakdown under rain: Comparison with tests of water stability and relationships with field measurements of infiltration. *Australian Journal of Soil Research* 32: 701-720.
- Lyles, L., L. A. Disrud, and N. P. Woodruff (1969). Effects of soil physical properties, rainfall characteristics, and wind velocity on clod disintegration by simulated rainfall. *Soil Science Society of America Proceedings* 33: 302-306.
- Mantell, A. and D. Goldberg (1966). Effect of water application rate on soil structure. *Journal of Agricultural Engineering Research* 11: 76-79.
- Marshall, T. J. and J. W. Holmes (1988). *Soil Physics*. Cambridge University Press, Cambridge, p. 20-21.
- Mohammed, D. and R. A. Kohl (1987). Infiltration response to kinetic energy. *Transactions of American Society of Agricultural Engineers* 30: 108-111.
- Morin, J. and Y. Benyamini (1977). Rainfall infiltration into bare soils. *Water Resources Research* 13: 813-817.
- Morin, J., Y. Benyamini and A. Michaeli (1981). The effect of raindrop impact on the dynamics of soil surface crusting and water movement in the profile. *Journal of Hydrology* 52: 321-335.
- Moss, A. J. (1991). Rain impact soil crust: I. Formation on a granite-derived soil. *Australian Journal of Soil Research* 29: 271-289.
- Mualem, Y., S. Assouline, and H. Rohdenburg (1990). Rainfall induced soil seal. (A) A critical review of observations and models. *Catena* 17: 185-203.
- Mullins, C. E., D. A. MacLeod, K. H. Northcote, J. M. Tisdall, and I. M. Young (1990). Hardsetting soils: behaviour, occurrence, and management. *Advances in Soil Science* 11: 37-108.
- Panabokke, C. R. and J. P. Quirk (1957). Effect of initial water content on stability of soil aggregates in water. *Soil Science* 83: 185-195.
- Philip, J. R. (1957). The theory of infiltration: 4. Sorptivity and algebraic infiltration equations. *Soil Science* 83: 257-264.
- Quirk, J. P. (1950). The water stability of soil aggregates in relation to the water content at the time of wetting. CSIRO Div. of Soils, Rep. 12/50. CSIRO, Canberra, Australia.

- Quirk, J. P. and C. R. Panabokke(1962). Incipient failure of soil aggregates. *Journal of Soil Science* 13: 60-70.
- Ragab, R. A. (1983). The effect of sprinkler intensity and energy of falling drops on soil surface sealing. *Soil Science* 136: 117-123.
- Romkens, M. J. M., R. L. Baumhardt, M. B. Parlange, F. D. Whisler, J.-Y. Parlange, and S. N. Prasad (1986). Rain-induced surface seals: their effect on ponding and infiltration. *Annales Geophysicae* 4, B, 4, 417-424.
- Rosewell, C. J. (1986). Rainfall kinetic energy in Eastern Australia. *Journal of Climate and Applied Meteorology* 25: 1695-1701.
- Shvebs, G.I. (1968). Data on the erosive action of water drops. *Soviet Soil Science* No.2: 262-269.
- Smettem, K. R. J., A. D. Rovira, S. A. Wace, B. R. Wilson, and A. Simon (1992). Effect of tillage and crop rotation on the surface stability and chemical properties of a red-brown earth (Alfisol) under wheat. *Soil and Tillage Research* 22: 27-40.
- Sor, K. and A. R. Bertrand (1962). Effect of rainfall energy on the permeability of soils. *Soil Science Society of America Proceedings* 26: 293-297.
- Thompson, A.L. and L.G. James (1985). Water droplet impact and its effect on infiltration. *Transactions of American Society of Agricultural Engineers* 28: 1506-1510, 1520.
- Truman, C. C. and J. M. Bradford (1993). Relationships between rainfall intensity and the interrill soil loss-slope steepness ratio as affected by antecedent water content. *Soil Science* 156: 405-413.
- Truman, C. C., J. M. Bradford, and J. E. Ferris (1990). Antecedent water content and rainfall energy influence on soil aggregate breakdown. *Soil Science Society of America Journal* 54: 1385-1392.
- van Bavel, C. H. M. (1949). Mean weight-diameter of soil aggregates as a statistical index of aggregation. *Soil Science Society of America Proceedings* 13: 20-23.
- Weaich, K., A. Cass, and K. L. Bristow (1992). Use of a penetration resistance characteristic to predict soil strength development during drying. *Soil and Tillage Research* 25: 149-166.
- West, L.T., S.C. Chiang, and L.D. Norton (1992). The morphology of surface crusts. In: *M.E. Sumner and B.A. Stewart (eds.). Soil Crusting. Chemical and Physical Processes*. Advances in Soil Science. Lewis Publ., Boca Raton, pp.: 73-92.
- Young, R. A. and J. L. Wiersma (1973). The role of rainfall impact in soil detachment and transport. *Water Resources Research* 9: 1629-1636.

Chapter 5

Effect of rainfall kinetic energy flux density and antecedent water content on surface soil strength

5.1 Introduction

Hydraulic properties of the soil surface, such as infiltration rate and hydraulic conductivity, have been used to characterise the development of surface seals (Hillel and Gardner, 1969; Romkens *et al.*, 1990; Bohl and Roth, 1993). Results presented in Chapter 3 demonstrate that surface sealing, as characterised by infiltration rate, is influenced by rainfall kinetic energy flux density (kinetic energy \times intensity) and antecedent water content. Rainfall kinetic energy and intensity determine the magnitude of surface aggregate breakdown during rainfall, that is, whether the surface seals or not.

The surface seal which forms during rainfall is transformed into a crust on drying (Mualem *et al.*, 1990; Bristow *et al.*, 1994). Bristow *et al.* (1994) pointed out that, because some consolidation may take place during drying of the seal, properties of surface crusts can be different from those of surface seals. The extent of consolidation during drying depends on the magnitude of aggregate breakdown during wetting (Chapter 4).

Method of wetting and soil matric suction during wetting influence aggregate breakdown and the structural condition of the surface soil on drying. Gusli *et al.* (1994a) found that capillary wetting of unstable air-dry aggregates at a matric suction of >0.20 m caused little structural change and produced friable soil structure, but flooding caused marked structural change which produced hardsetting. Imposition of rainfall has

additional effects on structure and seal formation (Duley, 1939; Al-Durrah and Bradford, 1981; Agassi *et al.*, 1985; Shainberg and Singer, 1988), producing aggregate beds which are more compact at the immediate surface than in deeper layers and which dry to form a surface crust.

The magnitude of the effect of rainfall on surface aggregate breakdown, and whether a surface crust or hardset layer forms on drying, depend on rainfall kinetic energy flux density, a combination of kinetic energy (mechanical energy) and intensity (hydration), as described in Chapter 4. Questions arise as to how the strength of the soil surface is influenced by (1) variation in properties of rain (intensity and kinetic energy); (2) different methods of wetting, *i.e.* suction, flood and rainfall wetting; and (3) antecedent water content.

To address these questions, experiments were performed with the following aims:

- 1) to relate rainfall kinetic energy flux density and antecedent water content to strength of surface soil on drying;
- 2) to determine the strength characteristics that distinguished crusted from hardset surface soil;
- 3) to investigate whether the soil penetration resistance characteristic is related to infiltration rate and the size of surface aggregates broken down by rainfall.

This chapter is concerned only with the soil surface, 0 to 5 mm depth. Strength below this layer is dealt with in Chapter 6.

5.2 Materials and methods

5.2.1 Method of wetting and aggregate bed preparation

A red-brown earth (fine, mixed, thermic, Calcic Rhodoxeralf) (Soil Survey Staff, 1988) from Kapunda, South Australia was used (Section 3.2.1). Artificial rainfall of variable kinetic energy and intensity was applied to small (104 mm diameter) aggregate beds for 30 minutes, after which the aggregate beds were drained to a matric suction of 0.30 and 0.57 m of water then allowed to dry in a glasshouse for several days. During drying, strength of the beds was measured periodically. Description of the rainfall simulator used, soil antecedent water content, rainfall properties, and the preparation of the aggregate beds are given in Section 3.2.1.2.

In addition to rainfall wetting, some aggregate beds were suction (0.30 m of water) or flood wetted using high flow rate ceramic plates, as described in Section 4.2.2.2. Flood wetting was done on both air-dry and pre-wetted aggregates.

5.2.2 Measurements

Immediately after rainfall application ceased, surface aggregates were sampled using a spatula for aggregate size determination, as described in Section 4.2.4.2. The aggregate beds were then allowed to drain to a matric suction of 0.30, then 0.57 m of water for 24 hours at each suction. The beds were transferred to a glasshouse to dry to a range of matric suctions, from 0.57 to about 6 m of water. Matric suction was monitored by means of water and mercury manometers, connected to two high flow rate tensiometer cups (Coors ceramic tubes, 4.5 mm out-side diameter, 1 mm wall thickness, 15 mm long)

in the beds, 10 mm below the surface (Section 2.2.3). Manometers were read to the nearest 1 mm. Change of matric suction was monitored hourly during the early period of drying and every 15 to 30 minutes as suction approached the tensiometer limit. Five beds were periodically removed for strength measurement during this phase of drying to give a range of suctions from 0.57 to 6 m of water. Three samples were left to dry to give larger matric suctions to near air-dryness. At these low water contents, only soil water content was measured, not matric suction. When the desired suction or dryness had been achieved, the aggregate beds were placed in a sealed, thermally insulated box overnight before matric suction and penetration resistance were measured next day. Trial experiments had shown that for the size of samples used, overnight equilibration was adequate for water redistribution to achieve uniform suction throughout the bed.

Penetration resistance was measured using a J.J. Lloyd M5K universal testing machine, fitted with a cone of 2 mm basal diameter and 30° included angle. The penetrometer was driven at 10 mm min⁻¹ from the surface through to just above the base of the aggregate bed. Penetration resistance of the surface was taken as the maximum reading, generally recorded at 4 to 5 mm depth. Penetration resistance, P (Pa) was calculated as

$$P = F / [\pi (d/2)^2] \quad (5.1)$$

where F is penetration Force (N), and d is the cone basal diameter (m). P was measured at matric suctions ranging from 0.57 m of water to near air-dry water content. Three to four replicate measurements were made for each aggregate bed at a given suction or water content.

Control of matric suction during drying beyond 0.57 m was not possible, but it was necessary to compare different treatments at some arbitrary, higher suction. To achieve this, a relationship between penetration resistance and matric suction (up to just below the tensiometer limit) was established by linear regression. Penetration resistance at an arbitrary matric suction (ψ) of 5 m of water was estimated using

$$P = a + b\psi_m \quad (5.2)$$

where a and b are regression coefficients with $0.57 < \psi_m < 6$ m of water. This method of estimating P was considered to be reliable as the coefficients of correlation were high (>0.9) and significant at p of at least <0.01 (Table 5.1).

Cores of 17 mm diameter \times 5 mm deep were removed from aggregate beds for surface bulk density and water content determinations, immediately after strength measurement. A core sampler (Figure 5.1) was carefully pushed to a depth of 5 mm from the surface. An external flat brim, soldered around the core sampler, 5 mm from the cutting edge, was used to control the penetration depth. If the surface soil was not level because of roughness induced by raindrop impact, the protrusions were removed with a sharp scalpel blade, before sampling.

Core samples for bulk density were oven dried at 105 °C for 24 hours to determine the surface soil mass water content. Volumetric water content, θ_v ($\text{m}^3 \text{m}^{-3}$) was calculated as

$$\theta_v = \theta_m (\rho_b/\rho_w) \quad (5.3)$$

Table 5.1. Relationships between maximum surface penetration resistance (P) (MPa) and matric suction (ψ_m) (m of water): $P = a + b\psi_m$, obtained from different methods of wetting and antecedent water content (θ_i) prior to wetting. a and b are regression coefficients, and R^2 is coefficient of determination. All relationships are significant at $p < 0.01$ to $p < 0.001$ ($n = 8$). Suction wetting was performed at a matric suction of 0.57 m of water. Antecedent water status (dry and wet) refers to air dry and pre-wetted at 0.30 m suction, respectively.

Methods of wetting	Antecedent water status	Rainfall kinetic energy ($J m^{-2} mm^{-1}$)	Rainfall intensity ($mm h^{-1}$)	a	b	R^2
Suction	Dry	-	-	0.1007	0.1001	0.984
Flooding	Dry	-	-	0.1639	0.2255	0.976
Flooding	Wet	-	-	0.3154	0.3131	0.894
Rainfall	Dry	1.6	40	0.1109	0.2508	0.943
	Dry	1.6	70	0.0928	0.2746	0.980
	Dry	1.6	100	0.0488	0.2943	0.977
	Dry	6.2	40	0.0959	0.2462	0.978
	Dry	6.2	70	0.0928	0.2746	0.980
	Dry	19.9	40	0.1903	0.2728	0.952
	Dry	19.9	70	0.0000	0.3857	0.963
	Dry	19.9	100	0.0467	0.4473	0.995
Rainfall	Wet	1.6	40	0.0498	0.2925	0.975
	Wet	1.6	70	0.0560	0.2799	0.990
	Wet	1.6	100	0.0169	0.2460	0.937
	Wet	6.2	40	0.1576	0.2557	0.989
	Wet	6.2	70	0.0437	0.3078	0.999
	Wet	19.9	40	0.1998	0.3368	0.932
	Wet	19.9	54	0.1960	0.3406	0.946
	Wet	19.9	70	0.1484	0.3675	0.957

where θ_m is mass water content ($kg kg^{-1}$), ρ_b is bulk density of the soil ($kg m^{-3}$) and ρ_w is the density of water ($1000 kg m^{-3}$). Degree of saturation, S, was calculated as

$$S = \theta_v / [1 - \rho_b / \rho_p] \quad (5.4)$$

where ρ_p is particle density, assumed to be 2650 kg m^{-3} .

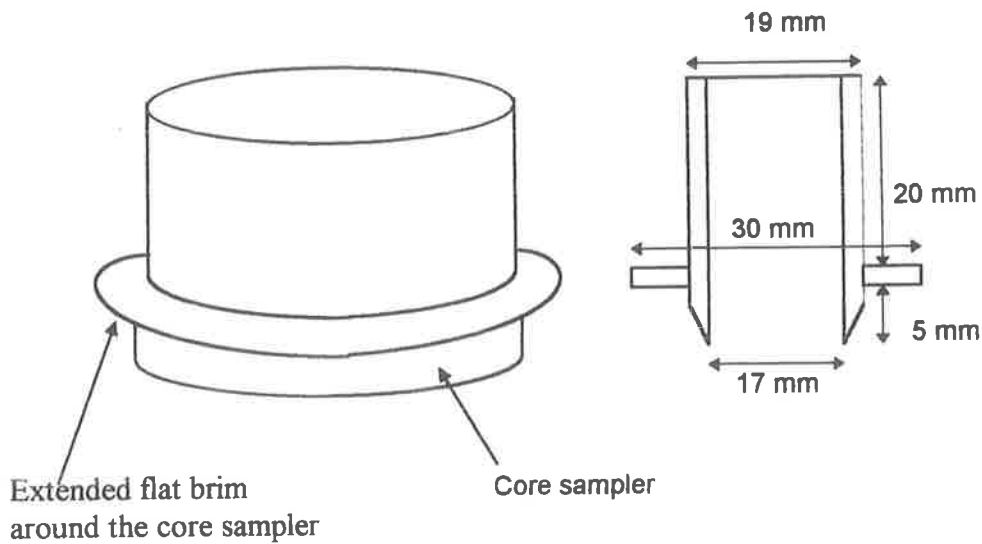


Figure 5.1. A brass core sampler used to measure surface bulk density at 0 to 5 mm. Left: vertical view of the sampler; right: vertical section through the sampler (not to scale).

5.3 Results and discussion

5.3.1 Penetration resistance characteristic

5.3.1.1 Suction and flood wetting

The relationship between penetration resistance and degree of saturation of the aggregate beds is shown in Figure 5.2 for two antecedent water contents and various modes of wetting. Following Mullins *et al.* (1992) and Weaich *et al.* (1992), this relationship is called “penetration resistance characteristic”, expressed as:

$$P = P_0 S^{-c} \quad (5.5)$$

where P is penetration resistance, S is degree of saturation, and P_0 and c are coefficients of regression.

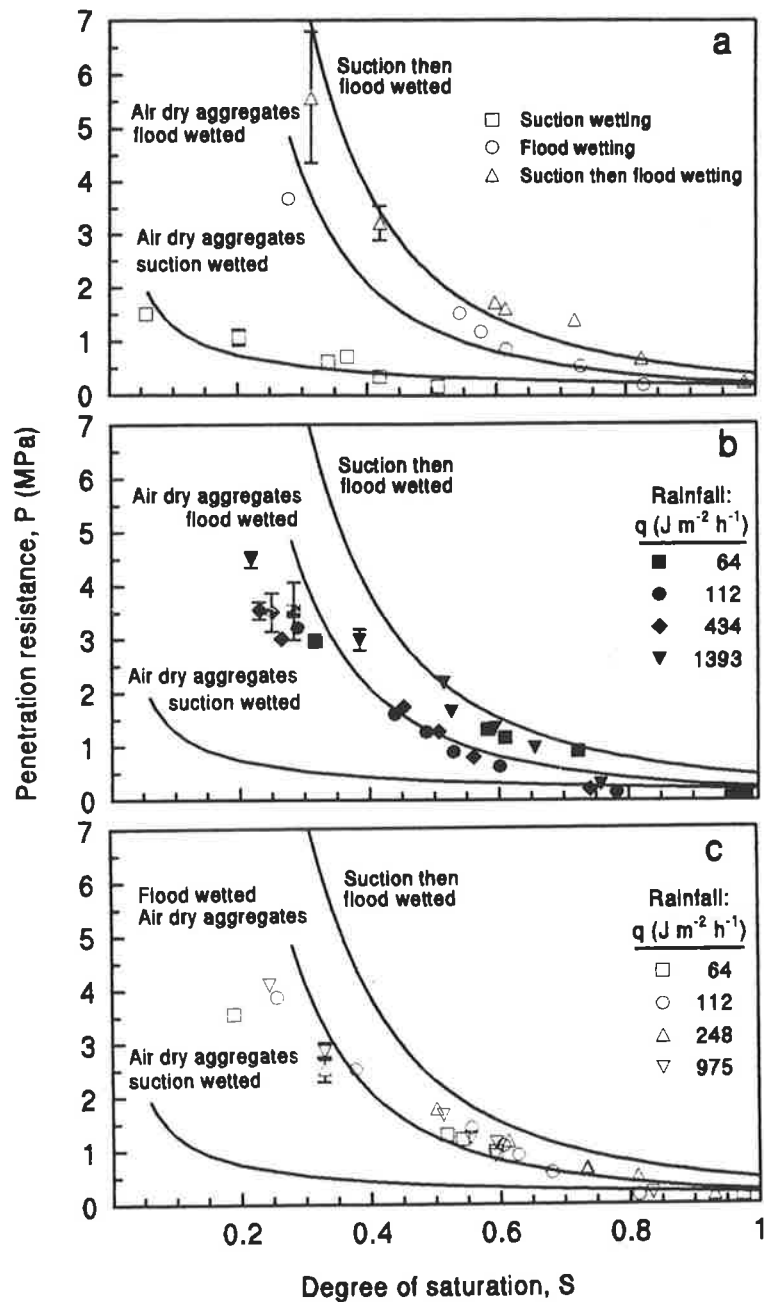


Figure 5.2. Relationships between penetration resistance (P) and degree of saturation (S) of surface soil (0 to 5 mm depth) for: (a) air-dry aggregates wetted by suction (\square , $P = 0.21 S^{-0.79}$), by flooding at zero suction (\circ , $P = 0.25 S^{-2.33}$) and first by suction then by flooding (Δ , $P = 0.48 S^{-2.28}$); (b) after rainfall of variable kinetic energy flux density (q) on pre-wetted soil (0.57 m suction); and (c) after rainfall of variable q on air-dry aggregate beds. Values of q are given in the legend. Regression lines from (a) have been repeated in (b) and (c) for comparison between suction, flood and rainfall wetting. Bars are 2 standard error of the mean ($n = 3$).

Suction wetting of air-dry soil aggregates produced the least strength development on drying (flattest penetration resistance characteristics) with values of $c = -0.79$ and $P_0 = 0.21$ MPa. At a degree of saturation of 0.05, penetration resistance was just below 2 MPa (the degree of saturation of air-dry soil was 0.02). The strength of the entire bed was low (Section 6.3.1). Clearly, the original friability of the air-dry aggregates was preserved by suction wetting.

Flood wetting of air-dry aggregates resulted in greater surface strength development on drying, giving a sharply curved penetration resistance characteristic (Figure 5.2a). Values of the regression coefficients (Equation 5.5) for flood wetted air-dry aggregates were $c = -2.33$ and $P_0 = 0.25$ MPa. Penetration resistance was as high as 2 MPa when the degree of saturation was 0.41, equivalent to a matric suction of 8.1 m of water (calculated from water retention curves, data not shown). These data show that the original friability of the air-dry aggregates was lost after flood wetting and drying, aggregates in the entire bed collapsed homogeneously from the surface to the base, and on drying the entire bed set hard (see values of b in Table 6.1, Section 6.3.2).

Suction wetting of air-dry aggregates followed by flood wetting resulted in the greatest strength development on drying giving a sharply curved penetration resistance characteristic (Figure 5.2a), with the values of $c = -2.41$ and $P_0 = 0.42$ MPa. Strength was high and uniform within the bed (see values of b in Table 6.1, Section 6.3.2). Penetration resistance reached 2 MPa at a degree of saturation of 0.53 (matric suction of 5.2 m of water). The aggregate bed formed was hardset, more than flood wetting of air-dry aggregates, *i.e.* greater vertical strain (Section 4.3.3) and smaller values of b (Table 6.1).

5.3.1.2 Rainfall wetting

Figures 5.2b and c show that rainfall wetting of air-dry or pre-wetted soil disrupted surface aggregates as severely as flood wetting of air-dry aggregates, but not as severely as suction wetting followed by flood wetting. The penetration resistance characteristics of beds that were subjected to rainfall lay midway between the penetration resistance characteristics of flood wetted and pre-wetted flooded beds without rainfall.

Increasing rainfall kinetic energy flux density (q) from 60 to 1500 J m⁻² h⁻¹ did not appear to have a significant effect on the penetration resistance characteristics of pre-wetted (0.30 m suction) beds (Figure 5.2b). No difference in penetration resistance characteristics between hardset (square and circular symbols with $q = 64$ and 112 J m⁻² h⁻¹ respectively, see Section 6.3.2) and crusted (diamond and triangular symbols with $q = >434$ J m⁻² h⁻¹) was observed. There are two possible explanations for this. Firstly, decreasing the matric suction from 0.30 m, before rainfall, to approximately zero during rainfall, caused slumping and deformation of surface aggregate beds to a similar degree, regardless of rainfall kinetic energy flux density. Secondly, variability in data was too large (Figure 5.2b) to identify the effect of rainfall kinetic energy flux density. Later (Figure 5.3), rainfall kinetic energy flux density will be shown to have an effect on penetration resistance, but this is concealed by variation in the data in Figures 5.2b and c.

The penetration resistance characteristic of the surface 0 to 5 mm produced by rainfall on initially air-dry aggregate beds was similar to that of flood wetting air-dry aggregates (Figure 5.2c). Variation in the data from different rainfall kinetic energy flux densities was less compared to that of pre-wetted beds subjected to rainfall beds (Figure 5.2b). Air-dry aggregates of the Kapunda soil slaked readily, and variation in rainfall

kinetic energy flux density made no difference to the surface structure. Thus, no difference in surface structure, as measured by penetration resistance at about 4 to 5 mm depth was observed, between crusted and hardset beds. The difference between crusted and hardset surface soils was observed only below 10 mm from the surface (Chapter 6).

At the surface (0 to 5 mm), there was virtually no difference in the penetration resistance characteristic of flood wetted air-dry aggregates (hardset) and rain-induced aggregate disruption (crusted: diamond and triangular symbols, or hardset: square and circular symbols), especially when degree of saturation exceeded 0.35 (Figures 5.2b and c). Therefore, it appears that for the Kapunda soil, whether the surface was sealed by high kinetic energy rainfall, or disrupted by flooding or low kinetic energy rainfall, the surface (0 to 5 mm) aggregates pack to a similar extent after drying to give similar penetration resistance characteristics. Only when the soil was wetted under suction (0.30 m of water), followed by no rainfall, did the aggregates maintain their integrity and remain friable (Figure 5.2a).

The apparent weaker surface when the degree of saturation is <0.35 for beds that were rainfall wetted (Figures 5.2b and c) compared to flood wetted beds was likely to be the result of a crack network which developed during penetration. The tendency for dry beds which were rainfall wetted to crack during needle penetration, before maximum penetration resistance was recorded, was observed visually. Probably, the presence of more loosely packed aggregates below the surface for rainfall wetted beds caused the beds to crack easily as the compressed zone in front of the penetrometer cone was advancing during penetration.

5.3.2 Rainfall kinetic energy flux density and penetration resistance

Both kinetic energy of rainfall (Al-Durrah and Bradford, 1981; Bradford and Huang, 1991) and intensity (Holder and Brown, 1974; Morrison *et al.*, 1985) influence the surface crust strength of soil. Combining these two properties of rain to give rainfall kinetic energy flux density (the product of kinetic energy and intensity) provided a clearer representation of the effect of rainfall on subsequent surface strength development.

Surface penetration resistance increased linearly with increasing q . The linear regression accounted for 80 % of the variance in penetration resistance of aggregate beds equilibrated at a matric suction of 0.57 m, and 91 % in the case of soils equilibrated at 5 m (Figures 5.3a and b). When the aggregate bed was at 5.0 m matric suction (Figure 5.3b), wetting without rainfall energy led to a surface soil penetration resistance of 1.38 MPa. For every $\text{J m}^{-2} \text{h}^{-1}$ of rainfall kinetic energy flux density that the soil was exposed to, penetration resistance increased by 0.46 kPa. At a lower suction, 0.57 m (Figure 5.3a), crust penetration resistance was lower, and the effect of kinetic energy flux density was more muted ($0.08 \text{ kPa m}^2 \text{h}^{-1} \text{J}^{-1}$).

Antecedent water content of beds subjected to rain did not significantly influence the slope of the relationship between penetration resistance and rainfall kinetic energy flux density. This is consistent with the similarity of the penetration resistance characteristics for air-dry and pre-wetted aggregates after rainfall (Figures 5.2b and c).

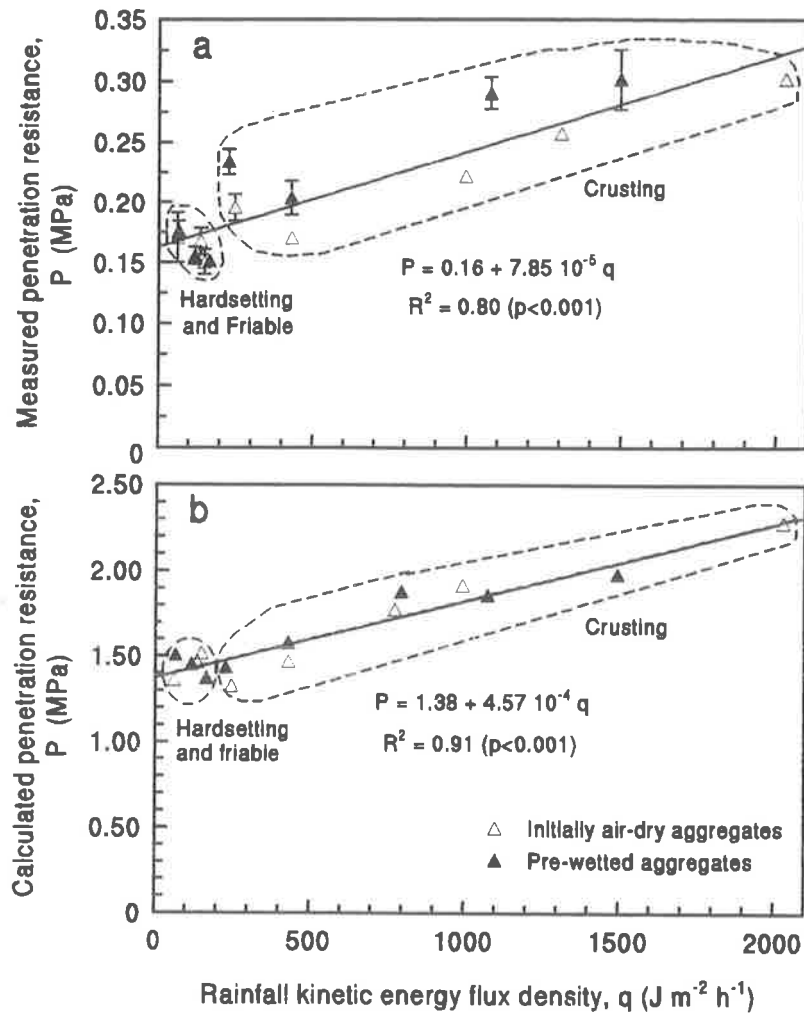


Figure 5.3. Effect of rainfall kinetic energy flux density (q) and antecedent water content on maximum penetration resistance at the surface 0 to 5 mm depth at matric suctions of (a) $\psi_m = 0.57$ m and (b) $\psi_m = 5$ m of water. Open triangles represent initially air-dry aggregates and closed triangles represent pre-wetted (0.30 m suction) aggregates. Error bars are $2 \times$ standard error of the means ($n = 8$). Penetration resistance at $\psi_m = 0.57$ was measured; that at $\psi_m = 5$ m was calculated using Equation (5.2). Boundaries drawn are around groups of data which are (i) crusting or (ii) friable or hardsetting.

5.3.3 Fine aggregates and penetration resistance

One way to assess the effect of rainfall kinetic energy flux density on aggregate structure is to measure how rainfall affects the production of fine aggregates at the soil surface

(Glanville and Smith, 1988; Loch, 1994). The present data showed that the strength of the surface soil on drying increased linearly with the amount of fine materials, less than 0.125 mm diameter (A_{125}), generated at the surface by rainfall (Figures 5.4a and b).

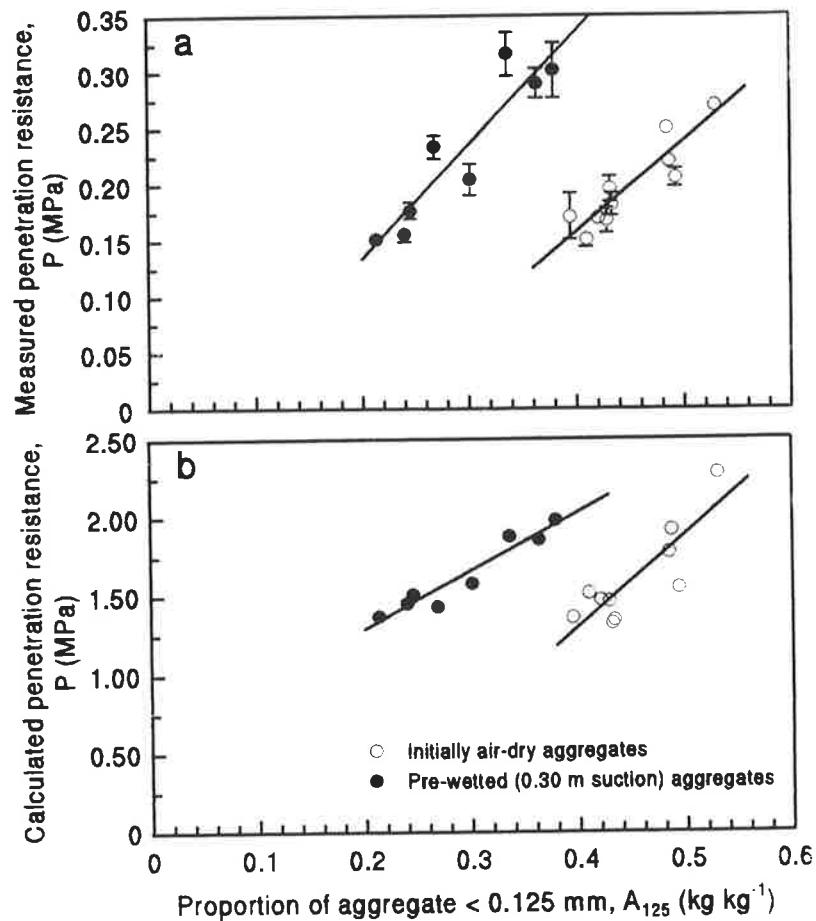


Figure 5.4. Effect of the proportion of materials less than 0.125 mm diameter (A_{125}) generated at the soil surface (0 to 5 mm) by rainfall on the surface penetration resistance (P) at matric suctions of (a) 0.57 m (P was measured), and (b) 5 m of water (P was calculated from Equation 5.2).

It is noticeable that pre-wetted aggregate beds required a smaller proportion of fine materials to give the same surface strength as initially air-dry aggregate beds. The differences between the two antecedent water contents was maintained on drying from

0.57 to 5 m of water matric suction. The proportion of materials less than 0.125 mm at the surface of the bed was shown to be a function of kinetic energy flux density (Figure 4.3.2). However, the extent of q affecting A_{125} was dependent on antecedent water content. At a given value of q , higher values of A_{125} were obtained in initially air-dry than in pre-wetted aggregate beds.

On the other hand, penetration resistance of surface soil (P) was also a linear function of q , independent of antecedent water content (Figure 5.3). This suggests that A_{125} only partially explains P , and that the influence of A_{125} on P should only be assessed at similar antecedent water contents. Pre-wetted aggregate beds appeared to pack more efficiently under rainfall than did initially air-dry beds (Section 4.3.3), as it allowed soil matric suction during wetting to decline to around zero which caused slumping (Figure 7.2, Chapter 7). Because rainfall caused larger collapse of pre-wetted than air-dry beds, despite the fact that in the latter a greater proportion of fine materials was generated at the surface, rearrangement and packing of disrupted aggregates are an important part of the collapse of aggregates which induces hardsetting. Packing of disintegrated aggregates, which influenced the strength of the surface crust, is explained only partially by A_{125} . The other major factor is the mode of packing of the disrupted materials, which determines pore-size distribution. This factor is not accounted for in measurement of A_{125} .

5.3.4 Infiltration rate and penetration resistance

Figure 5.5 shows that surface penetration resistance decreased as infiltration rate at 30 minutes (i_{30}) increased. Lower infiltration rate implies greater packing and hence higher

surface soil penetration resistance developed on drying. The relationship between penetration resistance (P) and infiltration rate after 30 minutes of rainfall (i_{30}) fitted an inverse function:

$$P = a' + b'/i_{30} \quad (5.6)$$

where a' and b' are regression coefficients, and i_{30} is always >0 . Values of a' and b' were 0.14 and 1.57 for a matric suction of 0.57 m, and 1.16 and 8.64 for a matric suction of 5.0 m of water. A relationship between infiltration rate and surface soil penetration resistance may be expected, because both are influenced by pore-size distribution. Carter (1990) and Gusli *et al.* (1994b) found that soil shear strength and penetration resistance were negatively related to the volume of pores greater than 50 μm diameter. Pores with diameters of 50 to 100 μm are classified as transmission pores (Greenland, 1977), which influence infiltration rate.

Figure 5.5 shows that antecedent water content did not influence the relationship between P and i_{30} , as was the case when P was related to A_{125} (Figure 5.4). Antecedent water content influences the proportion of pores in the aggregate beds which are able to resist the disruptive force of raindrop impact and therefore determine the value of i_{30} and P. Infiltration rate reflects pore-size distribution better than A_{125} and thus the relationship between i_{30} and P is not affected by antecedent water content. Pore-size distribution is fundamentally related to strength development (Carter, 1990; Gusli *et al.*, 1994b).

Figure 5.5, however, shows that the relationship between soil strength and infiltration rate was better at a matric suction of 5 m of water than at 0.57 m. The coefficients of determination for these two matric suctions were 0.64 ($p < 0.001$) compared to 0.22 ($p < 0.05$), respectively. The reason for this is that at a low matric

suction (0.57 m), differences in pore-size distribution are not readily detectable by strength measurements. This is consistent with vertical strain data shown in Figures 6.2 and 6.3 (Section 6.3.1).

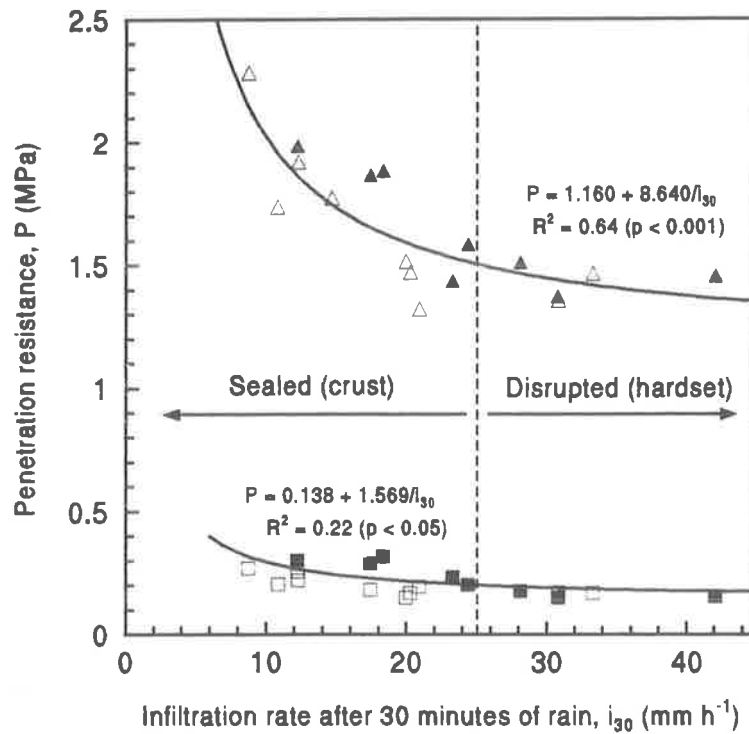


Figure 5.5. Penetration resistance (P) of aggregate beds at matric suctions (ψ_m) of 0.57 m (squares) and 5.0 m of water (triangles) after being subjected to rainfall, as a function of infiltration rate 30 minutes after commencement of rainfall, i_{30} . Open and closed symbols represent initially dry and pre-wetted (0.30 m suction) aggregates, respectively. The dashed line corresponds to i_{30} equal to 25 mm h⁻¹ (associated with kinetic energy of ≥ 6.2 J m⁻² mm⁻¹), considered to be critical infiltration rate distinguishing sealed (crusted) from disrupted (hardset) surface soil. Error bars ($2 \times$ standard error) for measurements at ψ_m of 0.57 m are too small to be shown; P values for ψ_m of 5 m were calculated from Equation 5.2.

The different surface soil conditions (crusted or hardset) generated by rainfall did not alter the relationship between P and i_{30} . The hardset surface soil did not seal during rainfall and had high i_{30} (>25 mm h⁻¹) and hence low P (<1.5 MPa). In contrast, the

crusted surface soil, which developed from rainfall with kinetic energy greater than $6.2 \text{ J m}^{-2} \text{ mm}^{-1}$ (Chapter 6), had low i_{30} ($<25 \text{ mm h}^{-1}$) and high P ($>1.5 \text{ MPa}$). Therefore, the data for a crusted surface lay in the upper region of the regression line, while the data for hardset surface lay in the lower region.

5.4 Conclusions

- 1) Rapid flood wetting of aggregate beds, without rainfall, caused extensive surface aggregate disruption, and the rapid development of high strength on drying. Flood wetting of pre-wetted aggregates was particularly disruptive, causing severe hardsetting with surface soil strength developing even more rapidly than in the case of flood wetting of air-dry aggregates. Suction wetting, however, preserved the friability at the surface of the aggregate bed.
- 2) Penetration resistance characteristics of the surface soil obtained from flood wetting and rainfall wetting were similar, but were steeper than those from suction wetting. Penetration resistance for flood or rainfall wetted beds increased rapidly with drying, but not for suction wetted beds.
- 3) Rainfall formed a crust or caused the entire bed to set hard, depending on rainfall kinetic energy and intensity, and antecedent water content. However, whether the bed was crusted, hardset, or friable, the strength of the surface following rainfall and drying can be explained in terms of rainfall kinetic energy flux density. Penetration resistance of the surface (recorded at 4 to 5 mm depth) was a linear function of kinetic energy flux density (over a range of 0 to $2000 \text{ J m}^{-2} \text{ h}^{-1}$), independent of antecedent water content or whether the soil crusted or set hard. Penetration

resistance increased by about 0.46 kPa for each $\text{J m}^{-2} \text{h}^{-1}$ increase in kinetic energy flux density.

- 4) Strength of the surface soil on drying for a specific antecedent water content was a linear function of the proportion of materials smaller than 0.125 mm at the surface.
- 5) There was a significant relationship between infiltration rate after 30 minutes of rainfall (approximately equal to steady state infiltration rate) and surface penetration resistance. The relationship was independent of antecedent water content and surface soil condition (crusted, hardset or friable) on drying.

5.5 References

- Agassi, M., J. Morin, and I. Shainberg (1985). Effect of raindrop impact energy and water salinity on infiltration rates of sodic soils. *Soil Science Society of America Journal* 49: 186-190.
- Al-Durrah, M. M. and J. M. Bradford (1981). New methods of studying soil detachment due to waterdrop impact. *Soil Science Society of America Journal* 45: 949-953.
- Bohl, H. and Ch. H. Roth (1993). A simple method to assess the susceptibility of soils to form surface seals under field conditions. *Catena* 20: 247-256.
- Bradford, J. M. and C. Huang (1991). The morphology of surface crusts. In: *M.E. Sumner and B.A. Stewart (eds.). Soil Crusting. Chemical and Physical Processes*. Advances in Soil Science. Lewis Publ., Boca Raton, pp.: 55-71.
- Bristow, K. L., A. Cass, K. R. J. Smettem, and P. J. Ross (1994). Modelling effects of surface sealing on water entry and re-distribution. Proceedings of the International Symposium on 'Sealing, Crusting, Hardsetting Soils: Productivity and Conservation' 7-11 February 1992, University of Queensland, Brisbane, Australia. (*in press*).
- Carter (1990). Relationship of strength properties to bulk density and macroporosity in cultivated loamy sand to loam soils. *Soil & Tillage Research* 15: 257-268.
- Duley, F. L. (1939). Surface factors affecting the rate of intake of water by soils. *Soil Science Society of America Proceedings* 4: 60-64.
- Glanville, S. F and G. D. Smith (1988). Aggregate breakdown in clay soils under simulated rain and effects on infiltration. *Australian Journal of Soil Research* 26: 111-120.
- Greenland, D. J. (1977). Soil damage by intensive arable cultivation: temporary or permanent? *Phil. Trans. R. Soc. Lond. B.* 281: 193.

- Gusli, S., A. Cass, D. A. MacLeod, and P. S. Blackwell (1994a). Structural collapse and strength of some Australian soils in relation to hardsetting: I. Structural collapse on wetting and draining. *European Journal of Soil Science* 45: 15-21.
- Gusli, S., A. Cass, D. A. MacLeod, and P. S. Blackwell (1994b). Structural collapse and strength of some Australian soils in relation to hardsetting: II. Tensile strength of collapsed aggregates. *European Journal of Soil Science* 45: 23-29.
- Hillel, D. and W. R. Gardner (1969). Steady infiltration into crust topped profiles. *Soil Science* 108: 137-142.
- Holder, C. B. and K. W. Brown (1974). Evaluation of simulated seedling emergence through rainfall induced soil crusts. *Soil Science Society of America Proceedings* 38: 705-710.
- Loch, R. J. (1994). A method for measuring aggregate water stability of dryland soils with relevance to surface seal development. *Australian Journal of Soil Research* 32: 687-700.
- Morrison, M. W., L. Prunty, and J. F. Giles (1985). Characterizing strength of soil crusts formed by simulated rainfall. *Soil Science Society of America Journal* 49: 427-431.
- Mualem, Y., S. Assouline, and H. Rohdenburg (1990). Rainfall induced soil seal. (A) A critical review of observations and models. *Catena* 17: 185-203.
- Mullins, C. E., A. Cass, D. A. MacLeod, D. J. M. Hall and P. S. Blackwell (1992). Strength development during drying of cultivated, flood-irrigated hardsetting soil. II. Trangie soil, and comparison with theoretical predictions. *Soil and Tillage Research* 25: 129-147.
- Romkens, M. J. M., S. N. Prasad, and J.-Y. Parlange (1990). Surface seal development in relation to rainstorm intensity. In: R. B. Bryan (ed.) *Soil Erosion. Experiments and Models. Catena Supplement* 17: 1-11.
- Shainberg, I. and M. Singer (1988). Drop impact energy - soil exchangeable sodium percentage interactions in seal formation. *Soil Science Society of America Journal* 52: 1449-1452.
- Weaich, K., A. Cass, and K. L. Bristow (1992). Use of a penetration resistance characteristic to predict soil strength development during drying. *Soil and Tillage Research* 25: 149-166.

Chapter 6

Effect of rainfall kinetic energy and antecedent water content on emergence resistance through the soil surface

6.1 Introduction

Hardsetting is distinguished from crusting in that hardsetting develops from a deep (> 50 mm) layer of disrupted aggregates, while crusting develops from a thin (<10 mm) surface seal (Bristow *et al.*, 1994). Hardsetting has been shown to develop from friable, unstable aggregates wetted by flooding (Mullins *et al.*, 1992; Weaich *et al.*, 1992; Gusli *et al.*, 1994a, b). Crusts develop on soil subjected to raindrop impact (Agassi *et al.*, 1985; Shainberg and Singer, 1988). However, numerous casual field observations suggest that either hardsetting or crusting may develop on the same soil under rainfall, depending on soil conditions and management.

The literature on crusting clearly points to the presence of a thin disrupted layer at the soil surface, which becomes hard on drying. Below the crust, at a depth below 10 mm, aggregates are softer and more friable (Duley, 1939; Tackett and Pearson, 1965; Eigel and Moore, 1983). Hardsetting, in contrast, is associated with much deeper disruption of aggregates (Mullins *et al.*, 1992; Weaich, *et al.*, 1992). Crusting and hardsetting should, therefore, have a contrasting depth distribution of aggregate breakdown (Bristow *et al.*, 1994). How the depth of aggregate disruption by rainfall varies with antecedent water content (Le Bessonnais *et al.*, 1989) and the extent to which aggregates below the surface are wetted (Farres, 1978; Bedaiwy and Rolston,

1993) are known. However, quantitative knowledge concerning the mechanisms by which these factors determine the depth distribution of aggregate breakdown and subsequent strength development, in relation to crusting and hardsetting is lacking.

Soil matric suction during wetting has a strong influence on aggregate stability. In comparison to air-dry soil, pre-wetting aggregates to about field capacity matric suction (around 0.5 to 1 m of water) increased aggregate resistance to the disruptive force of wetting (Panabokke and Quirk, 1957). However, as matric suction was decreased further to zero or near zero, the stability of aggregates declined (Al-Durrah and Bradford, 1981; Francis and Cruse, 1983). Soil matric suction during wetting is influenced by the initial water content, rate of water influx (a function of water application rate and surface sealing), and soil drainage rate relative to water influx. Soil matric suction during wetting should therefore influence the thickness of a disrupted layer, and thus whether hardsetting or crusting develops.

Le Bissonnais *et al.* (1989) found that pre-moistening aggregates before rainfall slowed seal formation, but caused development of a thicker disrupted layer than if the aggregates were initially dry. Timm *et al.* (1971) observed a 'crust' as thick as 75 mm in the field, developed on the ridge of a furrow irrigated tilled soil following intense rainfall and drying. Aggregates on the ridge would have been wetted under suction. Consequently, it is likely that these suction-wetted aggregates could have been disrupted to 75 mm when subjected to rainfall. The 'crust' Timm observed was probably a hardset layer which developed from a deeply disrupted layer.

However, the distinctions between the mechanisms of hardsetting (developed from deeply disrupted layers) and crusting (developed from thin seals) in relation to methods of wetting, rainfall factors and soil antecedent water content is not clear. In

particular, how the above factors influence strength distribution down the soil profile is not known.

Arndt (1965), Holder and Brown (1974) and Morrison *et al.* (1985) made soil beds and measured “emergence resistance” (see List of terminology and abbreviation) by upward penetration of a rigid probe. The beds they made were thick, *i.e.* 153 mm (Holder and Brown, 1974). However, the emergence resistance was measured only at 25 mm from the surface, too shallow to allow expression of differences relating to crusting or hardsetting. If the measurements are made on deeper layers, this method can be effective in differentiating strength profiles of crusted and hardset soils. Measurement of penetration resistance from below mimics resistance to seedling emergence more closely than downward penetration from the surface.

The aims of the experiments described in this chapter are:

- 1) to measure the development of soil strength and its depth distribution in aggregate beds in response to different modes of wetting, rainfall kinetic energy and intensity, and antecedent soil water content;
- 2) to relate strength and its depth distribution to known strength characteristics of friable, hardset and crusted soils;
- 3) to investigate the effect of soil drainage condition on the development of soil strength resulting from rainfall wetting and drying;

6.2 Materials and methods

6.2.1 Soil properties and preparation and wetting of aggregate beds

A red-brown earth (fine, mixed, thermic, Calcic Rhodoxeralf) (Soil Survey Staff, 1988) from Kapunda, South Australia was used. The properties and behaviour of the soil in the field and management history are given in Section 3.2.1. Aggregate beds were prepared as described in Section 3.2.2, and either wetted by rainfall, or by flooding or suction without rainfall.

6.2.2 Measurements

6.2.2.1 Emergence resistance

Emergence resistance was measured using a blunt needle (1.6 mm tip diameter), driven vertically upwards by an electric motor at a speed of 1.4 mm s^{-1} , from the base until the surface soil ruptured, indicated by the sharp decline in emergence resistance (Holder and Brown, 1974). The force on the tip of the needle was recorded electronically every 0.5 mm of upward travel. Aggregate beds were clamped firmly above the needle and 3 to 4 penetrations were made vertically upwards through the base of each bed. The penetrations were about 20 mm apart, satisfying the spatial separation recommended by Dexter (1987) and Becher (1994b). The mean and standard error of emergence resistance were calculated at each depth.

Because the needle used was blunt (flat tip), the total emergence force (F_t) recorded during the upward movement consisted of the force required to penetrate the

soil (F_s) and the force due to soil - metal friction (F_f), measured during the withdrawal of the needle (Groenevelt *et al.*, 1985; Fritton, 1990; Becher, 1994a):

$$F_t = F_s + F_f \quad (6.1)$$

The emergence resistance (P_E) at any given depth (z) was calculated as

$$P_{E(z)} = F_{s(z)} / [\pi (d/2)^2] \quad (6.2)$$

where d is the needle diameter. Substituting F_s from Equation (6.1), Equation (6.2) becomes

$$P_{E(z)} = [F_{t(z)} - F_{f(z)}] / [\pi (d/2)^2]. \quad (6.3)$$

An emergence resistance characteristic (Mullins *et al.*, 1992; Weaich *et al.*, 1992) was established by relating emergence resistance (P_E) data to degree of saturation (S) by regression analysis. The relationship is best described by a power function

$$P_E = a S^{-b} \quad (6.4)$$

where a and b are coefficients of regression. The regression was performed for each method of wetting and antecedent water content for 0 to 10, 10 to 20, and 20 to 30 mm depths.

6.2.2.2 Bulk density and degree of saturation

After drying the bulk density of the soil bed was measured at different depths, as described in Section 4.2.4.5. The degree of saturation of each depth segment was calculated from mass water content measured at the surface (0 to 5 mm depth) and bulk density of individual depth segments (Equation 5.3). Sub-surface depths were assumed to have the same mass water content as the surface depth after overnight equilibration in a sealed, temperature-insulated container, despite gradients in bulk density. Keller

(1970a) found that soil mass water content did not change with increasing bulk density from 0.98 to 1.30 Mg m⁻³. To verify this assumption, several aggregate beds which had distinct bulk density gradients were sectioned and mass water content measured. Mass water content did not change within the range of bulk densities of up to 1.7 Mg m⁻³, and only slightly within the range of 1.7 to 2.0 Mg m⁻³ (Figure 6.1).

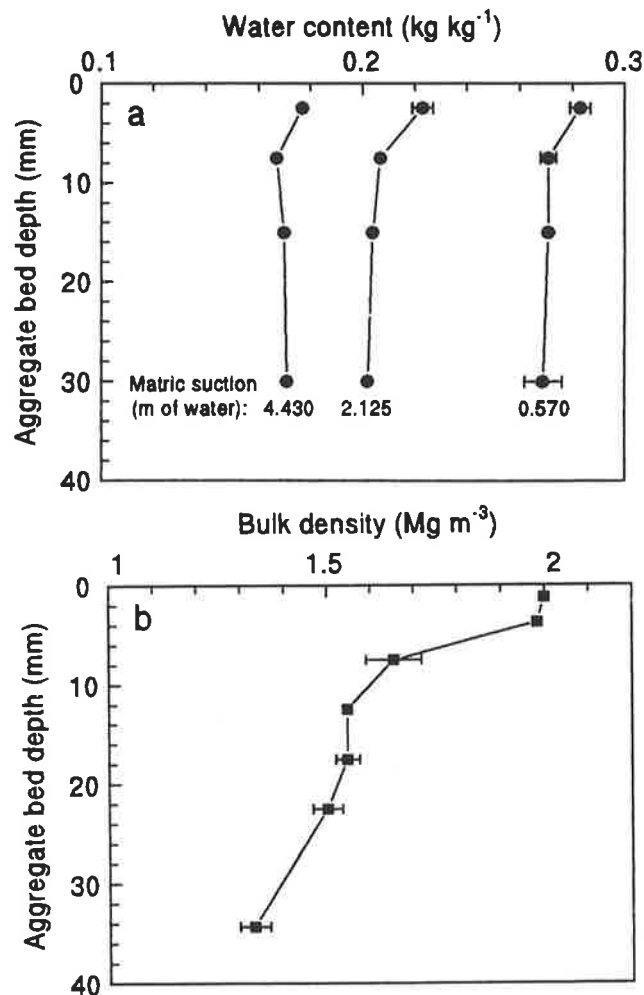


Figure 6.1. Profiles of: (a) mass water content measured at various matric suctions, and (b) the associated bulk density values. Error bars are $2 \times$ the standard error of the mean ($n = 3$). No error bars imply $2 \times$ SE was smaller than the symbol.

6.2.2.3 Visible pores

Change of surface roughness (microrelief) has been used as a measure of aggregate breakdown induced by rainfall after tillage (Burwell and Larson, 1969; Freebairn and

Gupta, 1990). Video imaging was used to estimate surface roughness (an estimate of porosity) of vertical sections of beds following different methods of wetting. Vertical sections of aggregate beds were obtained by carefully breaking the aggregate beds across their diameter. When the surface of the vertical section was lightly lit from all sides, pores showed up as shadowed areas. A video image comprising a regular grid of 256×512 points was obtained from a soil surface of about $40 \text{ mm} \times 50 \text{ mm}$. For crusted beds, observations were made only on the crusted layer, while for hardset and friable beds observation were made on the whole depth. The darkness of the image points were sampled as a 16 level grey scale (0 = black, 15 = white) and were classified into those above or below an empirically determined threshold level. The threshold was set to the level which displayed the best contrast between all the treatments. From calibration data (using a set visible soil pores of known diameter) the threshold level set was able to detect pores with approximate diameter greater than 0.25 mm. The fraction of points darker than that level was taken to be a measure of exposed pore area on the surface, and was assumed to be inversely related to aggregate disruption within the area of vertical section exposed. The lower the ratio of the pore area to the total area, the greater was aggregate disruption assumed to be. The data obtained were well correlated ($R^2 > 0.93$, significant at $p < 0.05$) with total porosity and air-filled porosity at a matric suction of 0.57 m of water.

6.3 Results and discussion

6.3.1 Emergence resistance

Figure 6.2 shows the effect of the treatments on the emergence resistance of aggregate beds at a matric suction of 0.57 m of water. In this relatively wet state, the emergence resistance each wetting method was fairly uniform throughout the depth of the bed (Figure 6.2a). This condition is typical of hardset soil strength profile.

Figure 6.2a shows that at a matric suction of 0.57 m of water, there was little consistently significant difference between the emergence resistance of initially air-dry aggregate beds that were wetted by flooding, by suction (0.30 m), or by suction then flooding. It should be noted that the aggregate packing (as indicated by vertical strain after rainfall) produced by these methods of wetting was different (Section 4.3.1). This indicates that at low matric suction (0.57 m), different degrees of packing arising from different wetting treatments, as indicated by values of vertical strain, did not translate into differences in emergence resistance.

Wetting of air-dry and suction-wetted aggregates by high energy rainfall of $19.9 \text{ J m}^{-2} \text{ mm}^{-1}$ resulted in higher emergence resistance at the surface (0 to 10 mm) than in the soil below (Figure 6.2b and c). A similar, though less pronounced, pattern was observed in suction wetted aggregate beds at rainfall kinetic energy of $6.2 \text{ J m}^{-2} \text{ mm}^{-1}$ (Figure 6.2c). However, below 10 mm, emergence resistance of the flood wetted beds as well as those that were first suction wetted then flooded was significantly higher than for beds subjected to rainfall. The lowest emergence resistance below 10 mm is shown by rainfall wetting of air-dry aggregates (Figure 6.2b).

It is seen that flooding of air-dry or previously suction-wetted aggregate beds, and low energy rainfall on suction-wetted beds tended to produce hardsetting, with

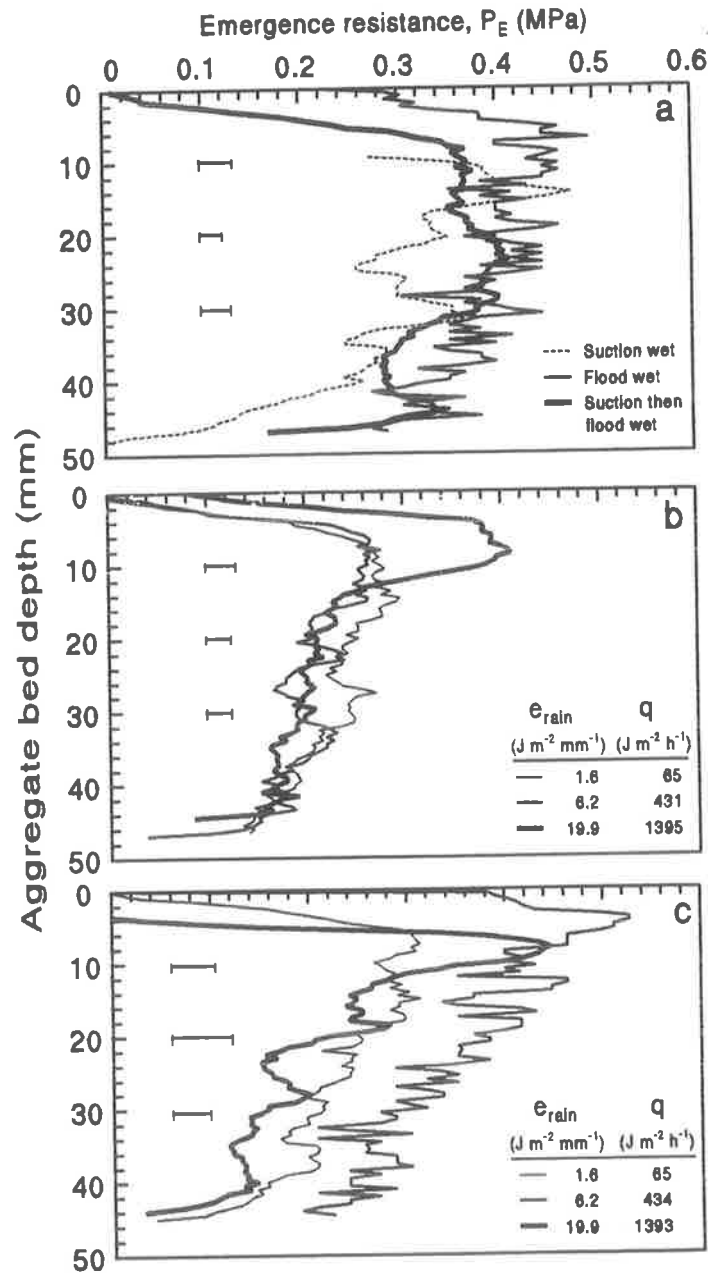


Figure 6.2. Emergence resistance of aggregate beds at a matric suction of 0.57 m of water after subjecting the beds to different methods of wetting at various antecedent water contents: (a) Wetting, without rainfall, of air-dry aggregates by a suction of 0.30 m of water; flooding; and suction (0.30 m) then flooding; (b and c) wetting by rainfall of various kinetic energies (e_{rain}) and intensities and therefore kinetic energy flux densities (q) on (b) air-dry aggregates and (c) suction (0.30 m) wetted aggregates. Error bars are $2 \times$ pooled standard error for 10, 20 and 30 mm depths.

uniform, high emergence resistance throughout the depth of the bed (Figures 6.2a and b). High energy rainfall ($19.9 \text{ J m}^{-2} \text{ mm}^{-1}$) on pre-wetted and air-dry aggregate beds produced strength profiles that conform to crusted conditions (Figure 6.2b and c). When applied to suction wetted beds, rainfall of $6.2 \text{ J m}^{-2} \text{ mm}^{-1}$ resulted in strength profiles that suggested both crusting and hardsetting. Rainfall of $1.6 \text{ J m}^{-2} \text{ mm}^{-1}$ produced hardsetting only (Figure 6.2c). On air-dry beds, rainfall of 1.6 and $6.2 \text{ J m}^{-2} \text{ mm}^{-1}$ produced a homogenous strength profile, but slightly weaker than that produced by rainfall of the same energies on pre-wetted beds.

At a matric suction of 0.57 m of water, the profile of emergence resistance for the suction-wetted aggregates was at some depths lower but generally similar to the profiles for the flood wetted beds (Figure 6.2a). Despite this similarity, the suction-wetted beds were friable, with aggregates not closely packed, whereas the flooded beds were hardset. However, as the soil dried to a matric suction of 5 m, the strength profiles of the friable and hardset beds were distinctly different (Figure 6.3a). Emergence resistance values increased in the order: suction wetting of air-dry aggregates < flood wetting of air-dry aggregates < flood wetting of pre-wetted aggregates.

The order of strength values matches the order of vertical strain (Section 4.3.3). The friable, suction wetted beds had vertical strains of less than 0.05 and emergence resistance less than 1 MPa at a matric suction of 5 m of water throughout the depth of the beds. In contrast, the hardsetting, flood-wetted aggregate beds were closely packed (vertical strain >0.11) through the entire bed profile, strong (emergence resistance >1.9 MPa at a matric suction of 5 m).

The strength profile of air-dry aggregate beds wetted by rainfall lay between that of suction and flood wetted aggregate beds, except for beds wetted by high energy

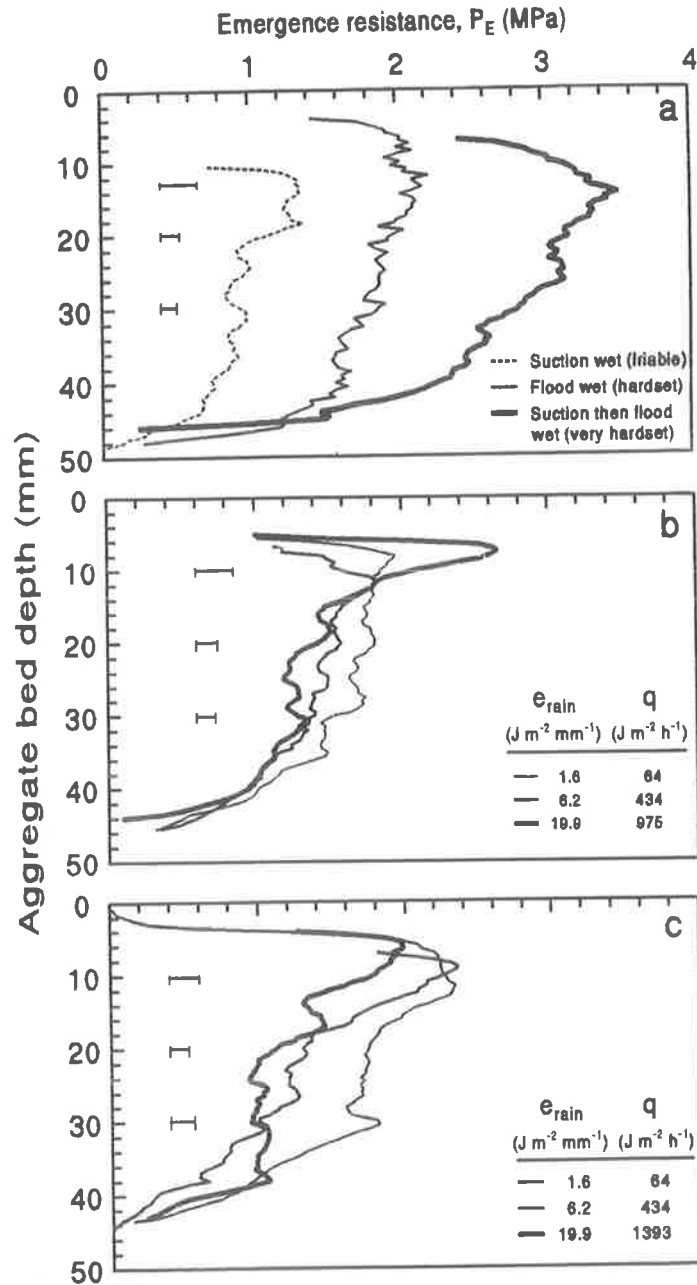


Figure 6.3. Emergence resistance of aggregate beds, at a matric suction of 5 m of water, after subjecting the beds to different methods of wetting at various antecedent water contents: (a) Wetting, without rainfall, of air-dry aggregates by a suction of 0.30 m of water; flooding; and suction (0.30 m) then flooding; (b and c) wetting by rainfall of various kinetic energies (e_{rain}) and intensities and therefore kinetic energy flux densities (q) on (b) air-dry aggregates and (c) suction (0.30 m) wetted aggregates. Error bars are $2 \times$ pooled standard error for 10, 20 and 30 mm depths.

rainfall (Figures 6.3a and b). Air-dry aggregate beds subjected to rainfall of high kinetic energy ($19.9 \text{ J m}^{-2} \text{ mm}^{-1}$) and high kinetic energy flux density ($975 \text{ J m}^{-2} \text{ h}^{-1}$) caused extensive aggregate disruption in the top 10 mm, producing a surface crust with a high emergence resistance. Rain with low kinetic energy ($1.6 \text{ J m}^{-2} \text{ mm}^{-1}$) and kinetic energy flux density ($64 \text{ J m}^{-2} \text{ h}^{-1}$) caused less aggregate disruption at the surface and emergence resistance values that were fairly uniform down the bed. The strength profile was similar to that obtained from flood wetting of air-dry aggregates (compare Figures 6.3a and b).

Similar results were observed for rainfall on pre-wetted aggregate beds (Figure 6.3c). However, high kinetic energy and kinetic energy flux density rainfall did not produce a surface crust as strong as that resulting from similar rainfall on air-dry aggregates; the strength profile was, nevertheless, typical of crusted soil. The weaker surface crust formed from rainfall on pre-wetted aggregates compared to rainfall on air-dry aggregates was consistent with the greater amount of materials smaller than 0.125 mm produced at 0 to 5 mm depth (Chapter 4).

Figures 6.2 and 6.3 show that pre-wetting of the Kapunda soil at 0.30 m of water suction preserved the friable aggregate structure of the original beds, which on drying had an emergence resistance less than 1 MPa at a matric suction of 5 m of water. Flood wetting of air-dry or pre-wetted aggregates caused severe aggregate disruption resulting in the development of typically hardset conditions with mean emergence resistance greater than 1.9 MPa at 5 m suction. Strength was fairly uniform down the profile (Figure 6.3a).

High energy rainfall ($19.9 \text{ J m}^{-2} \text{ mm}^{-1}$) on air-dry or pre-moistened aggregates produced a crust on drying with emergence resistance greater than 2 MPa at 0 to 10 mm

depth. Below the crust the soil remained friable with emergence resistance decreasing towards 1 MPa (Figures 6.3b and c). The large proportion of fine materials produced by high kinetic energy rainfall (Figure 4.5) caused infiltration rate to decrease during rainfall (Figures 3.4 and 4.4). This means that aggregates below the seal were wetted slowly, producing strength profiles which resembled those obtained from suction-wetted aggregates.

In the case of low energy rainfall ($1.6 \text{ J m}^{-2} \text{ mm}^{-1}$), a seal did not develop, water infiltrated more rapidly and aggregates below the surface were severely disrupted. The strength profile that developed on drying was similar to that for flood-wetted aggregates, with the soil being hardset rather than friable. Emergence resistance was generally higher for the pre-wetted than air-dry aggregates, which corresponds to the greater rate of infiltration for the former.

6.3.2 Emergence resistance characteristic

The relationship between degree of saturation of aggregate beds and emergence resistance (the emergence resistance characteristic) for various wetting treatments is shown in Figures 6.4 to 6.7. The strength of aggregate beds, arising from different methods of wetting, was depth dependent (Figures 6.2 to 6.7). Therefore, the emergence resistance characteristics of the beds were developed for depths of 0 to 10, 10 to 20 and 20 to 40 mm. The strength of suction wetted, flooded and suction wetted then flooded beds was uniform down the bed at all water contents. Consequently, only data for the 0 to 10 mm depths is shown in Figure 6.4. Data for other depths are shown as a contrast to rainfall data in Figures 6.6 and 6.7.

Figure 6.4 shows the emergence resistance characteristic for suction and flood wetting for the 0 to 10 mm depth. Similar characteristics were obtained for all depths. Suction wetted aggregate beds were weakest at all water contents. Drying the beds caused only a small increase in emergence resistance, from about 0.4 MPa at $S = 0.5$ to 2 MPa at $S = 0.06$. Flood wetting of air-dry aggregates caused greater aggregate disruption and a large increase of emergence resistance on drying. Flood wetting of pre-wetted aggregates caused the greatest amount of aggregate disruption and the strongest matrix on drying at all depths. Flood wetting of both air-dry and pre-wetted aggregate beds showed strength characteristics typical of hardsetting soil (Mullins *et al.*, 1990) throughout the depth of the aggregate beds.

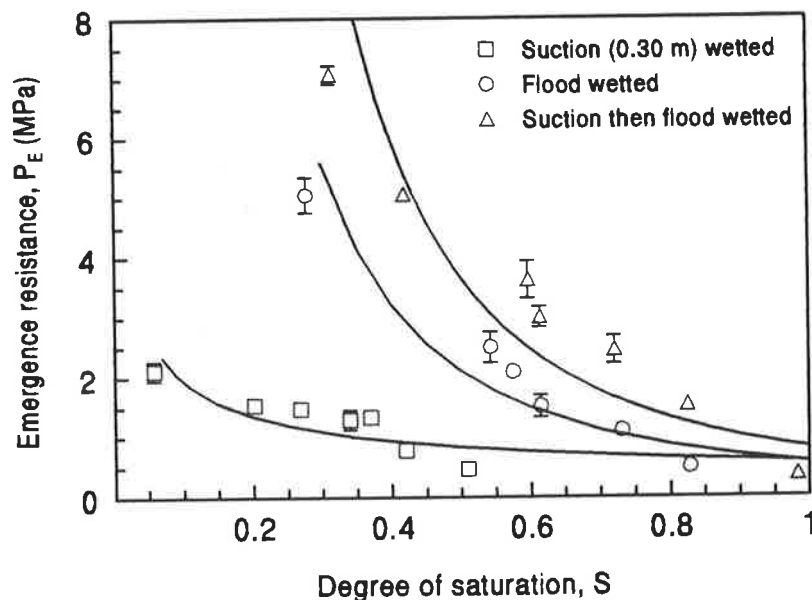


Figure 6.4. Emergence resistance characteristics for different methods of wetting at 0 to 10 mm depth. Error bars are $2 \times$ standard error of the means ($n = 8$).

Aggregate beds wetted by rainfall had a surface (0 to 10 mm) emergence characteristic which was similar to that resulting from flood wetting of air-dry aggregate beds (Figure 6.5). Neither antecedent water content of the beds, nor raindrop energy

appeared to have a marked effect on the emergence characteristic. However, when Equation 6.5 was fitted to these data, significant differences in the b values (Equation 6.4) were obtained for different rainfall kinetic energy flux density values (Table 6.1). The lower emergence resistance for rainfall wetting compared to flooding when the degree of saturation is less than 0.35 was due to a greater tendency for rainfall wetted aggregate beds to crack during the passage of the needle than flood wetted beds. (See also the results on emergence resistance, Section 5.3.1.2).

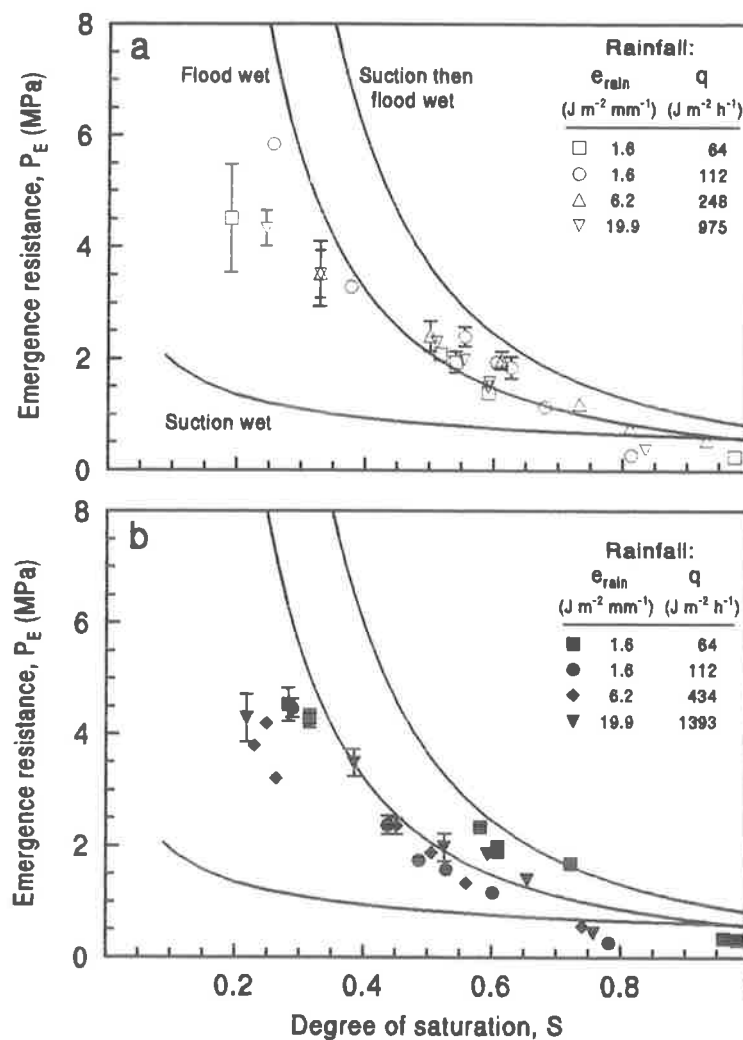


Figure 6.5. Emergence resistance characteristics of aggregate beds following rainfall of various kinetic energies (e_{rain}) and kinetic energy flux densities (q) on (a) initially air-dry and (b) pre-wetted (0.30 m suction) aggregate beds at 0 to 10 mm depth. Emergence resistance characteristics of suction (0.30 m), flood and suction then flood wetted beds (Figure 6.4) are superimposed on the data of rain treated beds for comparison. Error bars are $2 \times$ standard error of the means ($n = 8$).

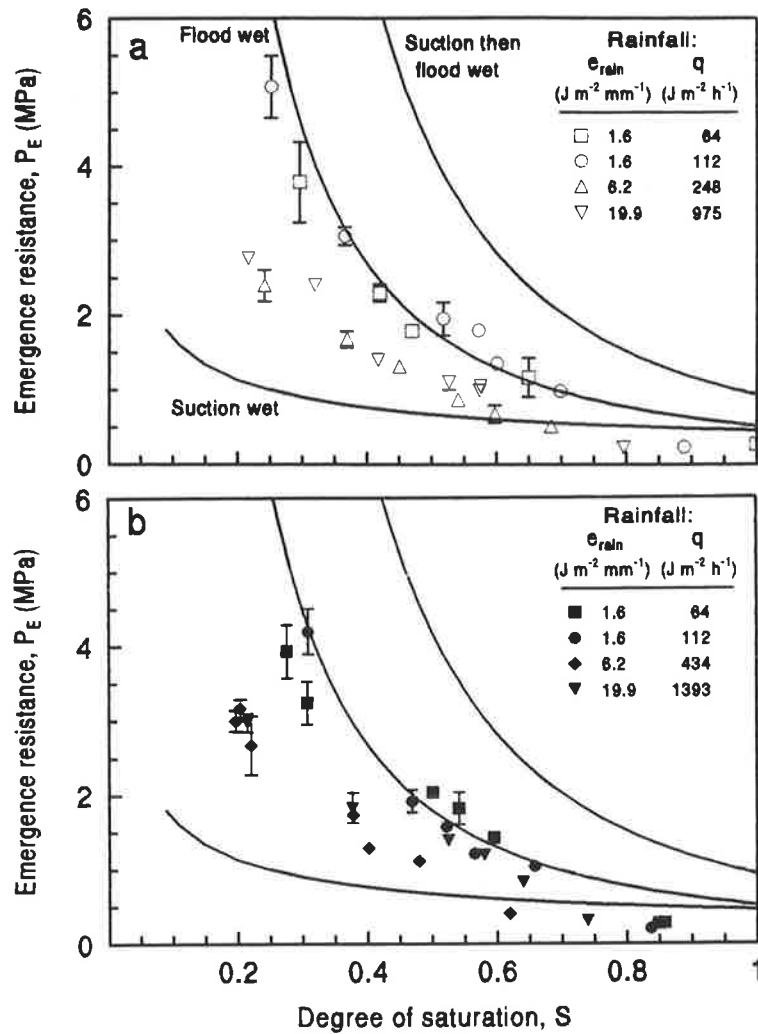


Figure 6.6. Emergence resistance characteristics of aggregate beds following rainfall of various kinetic energies (e_{rain}) and kinetic energy flux densities (q) on (a) initially air-dry and (b) pre-wetted (0.30 m suction) aggregate beds at 10 to 20 mm depth. Emergence resistance characteristics (10 to 20 mm) of suction (0.30 m), flood and suction then flood wetted beds are superimposed on the data of rain treated beds for comparison. Error bars are $2 \times$ standard error of the means ($n = 8$).

At the 10 to 20 mm depth, rainfall with kinetic energy of $1.6 J m^{-2} mm^{-1}$ and kinetic energy flux density of 64 to $112 J m^{-2} h^{-1}$ on air-dry aggregates gave emergence resistance characteristics similar to that for flood wetting of air-dry (Figure 6.6a), *i.e.* the

beds were hardset. At a rainfall kinetic energy of $6.2 \text{ J m}^{-2} \text{ mm}^{-1}$ or greater (kinetic energy flux density $> 248 \text{ J m}^{-2} \text{ h}^{-1}$), the aggregate beds at this depth were weaker, with the emergence resistance characteristic tending to approach that of the suction wetted aggregates, *i.e.* friable beds. Similar strength characteristics were observed for aggregate beds pre-wetted at 0.30 m suction prior to rainfall (Figure 6.6b).

At the 20 to 40 mm depth, the emergence resistance characteristics of pre-wetted aggregate beds and air-dry beds were similar for high kinetic energy ($>6.2 \text{ J m}^{-2} \text{ mm}^{-1}$) rainfall (Figures 6.7a and b). Low kinetic energy rainfall ($1.6 \text{ J m}^{-2} \text{ mm}^{-1}$) resulted in a stronger matrix at 20 to 40 mm, especially when the low kinetic energy rainfall was applied to pre-wetted beds. The shape of this characteristic resembled that of flood wetted beds (Figure 6.7b). These results indicate that low kinetic energy rainfall tended to produce hardsetting, while high kinetic energy rainfall produced crusting.

The effect of method of wetting and antecedent water content on the emergence resistance characteristic may be evaluated by the difference in value of the *b* exponent of Equation 6.4 as shown in Table 6.1. The smaller the *b* values (more negative), the more rapidly did emergence resistance develop on drying. Comparison of values of *b* for the surface (0 to 10 mm) with the layers below (10 to 20 and 20 to 40 mm) reflects differences in strength at these depths. Hardset beds had relatively constant and small *b* values throughout the entire depth of the bed. Crusted beds had smaller *b* values at the surface and larger at the deeper depths.

Data in Table 6.1 shows that both method of wetting and antecedent water content influenced the emergence resistance characteristic. Without rainfall, suction (0.30 m of water) wetting produced the largest (less negative) *b* values, *i.e.* weakest matrix structure. The *b* values were relatively constant (-0.526 to -0.576) at different depths in

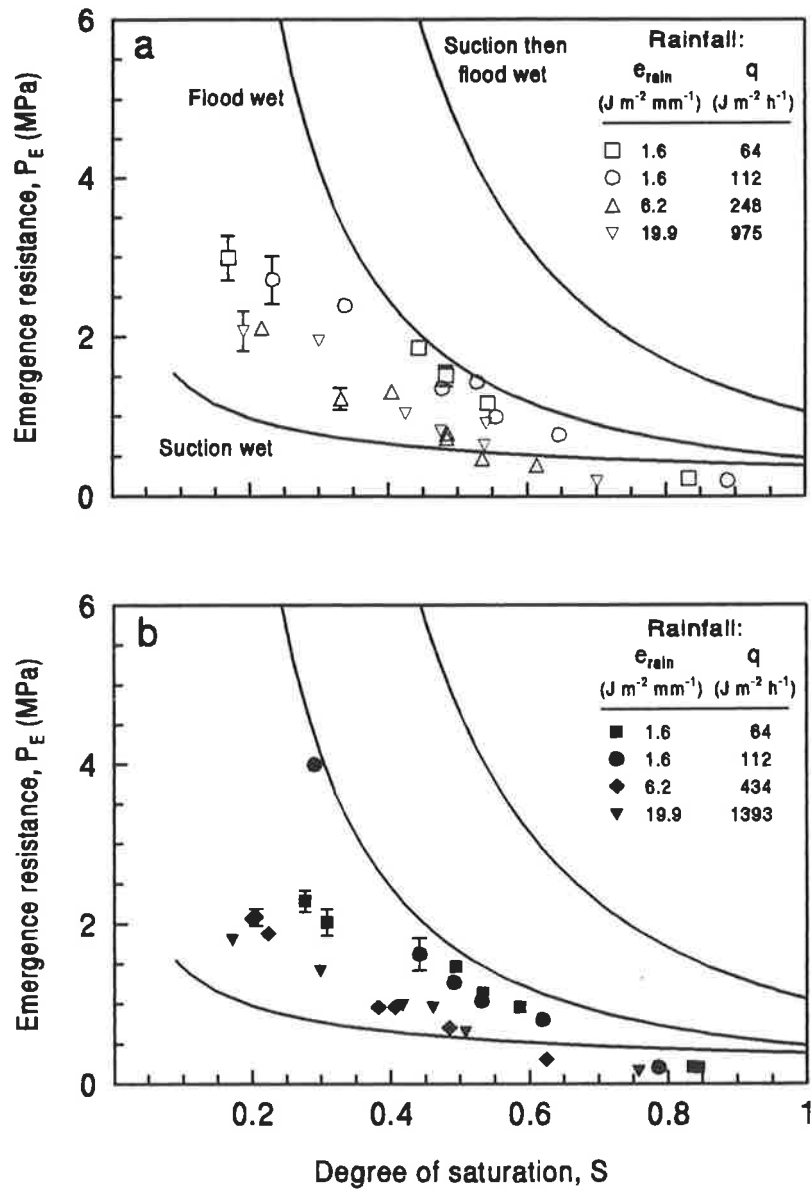


Figure 6.7. Emergence resistance characteristics of aggregate beds following rainfall of various kinetic energies (e_{rain}) and kinetic energy flux densities (q) on (a) initially air-dry and (b) pre-wetted (0.30 m suction) aggregate beds at 20 to 40 mm depth. Emergence resistance characteristics (20 to 40 mm) of suction (0.30 m), flood and suction then flood wetted beds are superimposed on the data of rain treated beds for comparison. Error bars are $2 \times$ standard error of the means ($n = 8$).

the soil bed. For flood wetting of air-dry aggregate beds, b values were lower (-1.788 to -1.905), and tended to increase slightly with depth. Flood wetting of pre-wetted (0.30 m suction) aggregate beds gave yet lower b values (-2.137 to -2.185), and again increased slightly with depth. The data indicate that, without rainfall, flood wetting of pre-wetted aggregate beds caused more rapid strength development than flood wetting of air-dry aggregate beds. Suction wetting caused little increase of emergence resistance on drying. Thus, without rainfall, flood wetting of pre-wetted aggregates caused the greatest aggregate disruption, followed by flood wetting, and suction wetting of air-dry aggregates (see data of vertical strain in Section 4.3.1).

Table 6.1 shows that wetting by rainfall at low kinetic energy ($1.6 \text{ J m}^{-2} \text{ mm}^{-1}$) gave more negative b values, reflecting a stronger matrix as the soil dried, than high kinetic energy rainfall ($>6 \text{ J m}^{-2} \text{ mm}^{-1}$). This difference between the two kinetic energies existed at all depths in the aggregate beds, but was more pronounced at depth than at the surface. Increasing rainfall kinetic energy flux density from 64 to $112 \text{ J m}^{-2} \text{ h}^{-1}$ at low raindrop energy ($1.6 \text{ J m}^{-2} \text{ mm}^{-1}$) led to a decreased value of b (stronger matrix), which was similar to the b value for flood wetting without rain.

Table 6.1. Effect of method of wetting on the coefficients (a and b) of the regression equation $P_E = a S^{-b}$, where P_E = emergence resistance and S = degree of saturation. Antecedent water content of dry and wet refer to air-dry and pre-wetted aggregates (0.30 m suction), respectively. R^2 is coefficient of determination. All relationships are significant at $p < 0.05$ to $p < 0.01$ (number of observations = 8).

Depth (mm)	Antecedent water content	Wetting method		a (MPa)	b	R^2	
		Without rainfall	With rainfall:				
			$\frac{e_{rain}}{(J m^{-2} mm^{-1})}$				$\frac{q}{(J m^{-2} h^{-1})}$
0 - 10	Dry	Suction		0.582	-0.526	0.596	
		Flood		0.565	-1.905	0.844	
		Flood		0.811	-2.185	0.782	
	Dry		1.6	64	0.493	-1.568	0.745
			1.6	112	0.471	-2.069	0.730
			6.2	248	0.611	-1.780	0.899
			19.9	975	0.544	-1.697	0.799
	Wet		1.6	64	0.493	-2.022	0.827
			1.6	112	0.235	-2.630	0.887
			6.2	434	0.546	-1.436	0.868
			19.9	1393	0.614	-1.492	0.710
	10 - 20	Dry	Suction		0.452	-0.575	0.601
Flood				0.518	-1.798	0.881	
Flood				0.938	-2.168	0.723	
Dry			1.6	64	0.344	-2.121	0.953
			1.6	112	0.375	-2.124	0.844
			6.2	248	0.338	-1.485	0.944
			19.9	975	0.307	-1.671	0.798
Wet			1.6	64	0.286	-2.272	0.861
			1.6	112	0.213	-2.804	0.878
			6.2	434	0.293	-1.517	0.896
			19.9	1393	0.382	-1.494	0.755
20 - 40		Dry	Suction		0.387	-0.576	0.567
	Flood			0.480	-1.788	0.879	
	Flood			1.061	-2.137	0.650	
	Dry		1.6	64	0.373	-1.390	0.686
			1.6	112	0.296	-1.813	0.815
			6.2	248	0.215	-1.599	0.880
			19.9	975	0.225	-1.582	0.743
	Wet		1.6	64	0.210	-2.102	0.851
			1.6	112	0.154	-2.810	0.935
			6.2	434	0.203	-1.502	0.943
			19.9	1393	0.198	-1.488	0.752

6.3.3 Effect of restricted drainage

High kinetic energy ($19 \text{ J m}^{-2} \text{ mm}^{-1}$) and intensity (70 mm h^{-1}) rainfall on pre-wetted aggregates, under conditions where drainage from the aggregate bed was restricted (Section 4.2.3), resulted in greater strength development of the aggregate bed on drying compared to well drained conditions (Figure 6.8). In poorly drained beds, a surface (0 to 10 mm) crust, with emergence resistance $>3 \text{ MPa}$ at matric suction of 5 m of water, was present and below this depth the bed was hardset (emergence resistance $>2 \text{ MPa}$ at 5 m suction). These strength values were appreciably greater than those obtained from well drained beds, where emergence resistance was 2 MPa at the surface and 1 MPa below 20 mm.

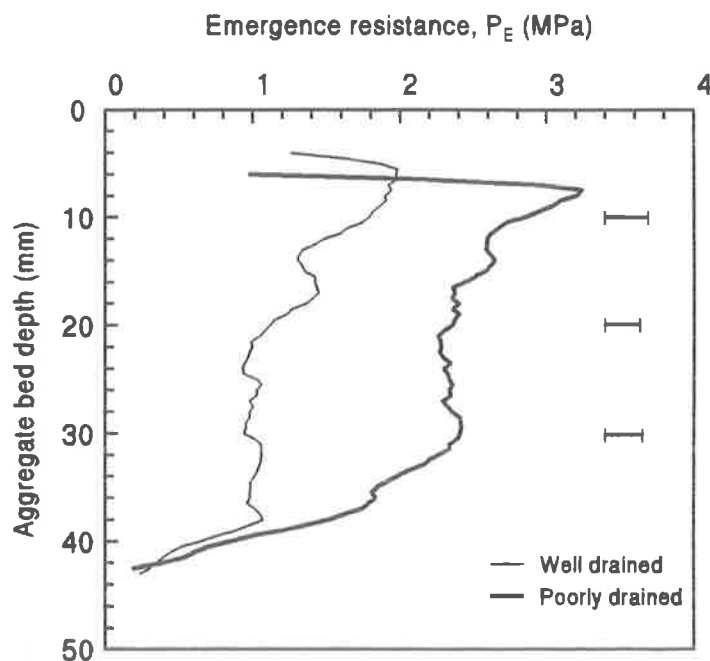


Figure 6.8. Effect of restricted drainage during rainfall on pre-wetted (0.30 m suction) aggregate beds on emergence resistance, measured at a matric suction of 5 m of water, after subjecting the beds to rainfall with kinetic energy of $19.9 \text{ J m}^{-2} \text{ mm}^{-1}$, and intensity of 70 mm h^{-1} . Error bars are $2 \times$ pooled standard error for 10, 20 and 30 mm depths.

Table 6.2. Effect of method of wetting on the proportion of pores > 0.25 mm, as measured by digital image processing of the vertical cross section of aggregate beds.*

Method of wetting	Structural condition	Relative pores > 0.25 mm	
		Mean	Standard error
Suction wetting	Friable	0.042	0.0034
Rainfall of 19.9 J m ⁻² mm ⁻¹ , 70 mm h ⁻¹ on air-dry aggregates	Crusted (0 to 10 mm)	0.014	0.0020
Flood wetting of air-dry aggregates	Hardset	0.020	0.0009
Flood wetting of suction (0.30 m) wetted aggregates	Hardset	0.011	0.0012

* Computer code for the digital image analysis was written by C. T. Hignett, CSIRO Div. of Soils, Adelaide, S.A., Australia

6.4 Conclusions

1. Suction wetting of friable air-dry aggregates, either by capillary rise or as a result of the development of a sealed layer above the aggregate bed, maintained the integrity of aggregates, reducing aggregate disruption and producing weak (friable) beds on drying (emergence resistance < 1 MPa at a matric suction of 5 m of water).

2. Wetting of air-dry or pre-wetted aggregates by flooding or by low kinetic energy rainfall but with high enough intensity so that water influx was high, tended to cause disruption throughout the aggregate bed, producing typically hardset profiles. Emergence resistance was > 1.9 MPa throughout the bed at a matric suction of 5 m of water. However, disruption by rainfall was deeper for the pre-wetted than for the air-dry aggregates.
3. High kinetic energy rainfall on air-dry or pre-moistened aggregates caused aggregate disruption at the surface, forming a surface seal which reduced influx of water, maintaining a higher soil water suction and reduced aggregate disruption below the seal. On drying, this produced a strong surface crust (emergence resistance > 2 MPa at a matric suction of 5 m), with weaker aggregates below the crust (≤ 1 MPa at matric suction of 5 m).
4. Rainfall on pre-moistened aggregates tended to form surface crusts at rainfall kinetic energies much lower ($6.2 \text{ J m}^{-2} \text{ mm}^{-1}$) than the kinetic energy that caused crusting on air-dry aggregates ($19.9 \text{ J m}^{-2} \text{ mm}^{-1}$).
5. Rainfall on aggregate beds with poor drainage produced a stronger matrix than similar rainfall on well drained beds. Poor drainage exacerbated hardsetting by rainfall.

6.5 References

- Agassi, M., J. Morin, and I. Shainberg (1985). Effect of raindrop impact energy and water salinity on infiltration rates of sodic soils. *Soil Science Society of America Journal* 49: 186-190.
- Al-Durrah, M. M. and J. M. Bradford (1981). New methods of studying soil detachment due to waterdrop impact. *Soil Science Society of America Journal* 45: 949-953.

- Arndt, W. (1965). The nature of the mechanical impedance to seedlings by soil surface seals. *Australian Journal of Soil Research* 3: 45-54.
- Becher, H. H. (1994a). Evaluating the resistance to penetration within the surface layer of soil aggregates. *Soil Technology* 7: 105-111.
- Becher, H. H. (1994b). Soil compaction around a small penetrating cylindrical body and its consequences. *Soil Technology* 7: 83-91.
- Bedaiwy, M. N. and D. E. Rolston (1993). Soil surface densification under simulated high intensity rainfall. *Soil Technology* 6: 365-376.
- Bristow, K. L., A. Cass, K. R. J. Smettem, and P. J. Ross (1994). Modelling effects of surface sealing on water entry and re-distribution. Proceedings of the International Symposium on 'Sealing, Crusting, Hardsetting Soils: Productivity and Conservation' 7-11 February 1994, University of Queensland, Brisbane, Australia (*in press*).
- Burwell, R. E. and W. E. Larson (1969). Infiltration as influenced by tillage-induced random roughness and pore space. *Soil Science Society of America Proceedings* 33: 449-452.
- Dexter, A. R. (1987). Compression of soil around roots. *Plant and Soil* 97: 401-406.
- Duley, F. L. (1939). Surface factors affecting the rate of intake of water by soils. *Soil Science Society of America Proceedings* 4: 60-64.
- Eigel, J. D. and I. D. Moore (1983). Effect of rainfall energy on infiltration into bare soil. Proc. of the National Conf. on Advances in Infiltration, Dec. 12-13, 1983, Chicago, Illinois, ASAE, p. 188-200.
- Farres, P. (1978). The role of time and aggregate size in the crusting process. *Earth Surface Processes* 3: 243-254.
- Francis, P. B. and R. M. Cruse (1983). Soil water matric potential effects on aggregate stability. *Soil Science Society of America Journal* 47: 578-581.
- Freebairn, D. M. and S. C. Gupta (1990). Microrelief, rainfall and cover effects on infiltration. *Soil and Tillage Research* 16: 307-327.
- Fritton, D. D. (1990). A standard for interpreting soil penetrometer measurements. *Soil Science* 150: 542-551.
- Ghavami, M., J. Keller, and I. S. Dunn (1974). Predicting soil density following irrigation. *Transactions of the American Society of Agricultural Engineers* 17: 166-171.
- Groenevelt, P. H., B. D. Kay, and C. D. Grant (1984). Physical assessment of a soil with respect to rooting potential. *Geoderma* 34: 101-114.
- Gusli, S., A. Cass, D. A. MacLeod, and P. S. Blackwell (1994a). Structural collapse and strength of some Australian soils in relation to hardsetting: I. Structural collapse on wetting and draining. *European Journal of Soil Science* 45: 15-21.
- Gusli, S., A. Cass, D. A. MacLeod, and P. S. Blackwell (1994b). Structural collapse and strength of some Australian soils in relation to hardsetting: II. Tensile strength of collapsed aggregates. *European Journal of Soil Science* 45: 23-29.

- Holder, C. B. and K. W. Brown (1974). Evaluation of simulated seedling emergence through rainfall induced soil crusts. *Soil Science Society of America Proceedings* 38: 705-710.
- Keller, J. (1970a). Control of soil moisture during sprinkler irrigation. *Transaction of the American Society of Agricultural Engineers* 13: 885-890.
- Keller, J. (1970b). Sprinkler intensity and soil tilth. *Transactions of the American Society of Agricultural Engineers* 13: 118-125.
- Le Bissonnais, Y., A. Bruand and M. Jamagne (1989). Laboratory experimental study of soil crusting: relation between aggregate breakdown mechanisms and crust structure. *Catena* 16: 377-392.
- Morrison, M. W., L. Prunty, and J. F. Giles (1985). Characterizing strength of soil crusts formed by simulated rainfall. *Soil Science Society of America Journal* 49: 427-431.
- Mullins, C. E., D. A. MacLeod, K. H. Northcote, J. M. Tisdall, and I. M. Young (1990). Hardsetting soils: behaviour, occurrence, and management. *Advances in Soil Science* 11: 37-108.
- Mullins, C. E., A. Cass, D. A. MacLeod, D. J. M. Hall and P. S. Blackwell (1992). Strength development during drying of cultivated, flood-irrigated hardsetting soil. II. Trangie soil, and comparison with theoretical predictions. *Soil and Tillage Research* 25: 129-147.
- Panabokke, C. R. and J. P. Quirk (1957). Effect of initial water content on stability of soil aggregates in water. *Soil Science* 83: 185-195.
- Shainberg, I. and M. Singer (1988). Drop impact energy - soil exchangeable sodium percentage interactions in seal formation. *Soil Science Society of America Journal* 52: 1449-1452.
- Tackett, J. L. and R. W. Pearson (1965). Some characteristics of soil crusts formed by simulated rainfall. *Soil Science* 99: 407-413.
- Timm, H., J. C. Bishop, J. W. Perdue, D. W. Grimes, R. E. Voss, and D. N. Wright (1971). Soil crusting effects on potato plant emergence and growth. *California Agriculture* 25 (8): 5-7.
- Weaich, K., A. Cass, and K. L. Bristow (1992). Use of a penetration resistance characteristic to predict soil strength development during drying. *Soil and Tillage Research* 25: 149-166.

Chapter 7

General discussion: Factors that determine crusting or hardsetting in Kapunda red-brown earth

7.1 Introduction

Figure 7.1 summarises the soil and rainfall factors and the sequence of processes that are thought to determine the surface condition of a soil after rainfall or irrigation. The extent of aggregate disruption during rainfall and the subsequent formation of a crust or hardset layer was found to be dependent on kinetic energy flux density of rainfall (a function of rainfall kinetic energy and intensity), soil antecedent water content, and internal drainage rate of the soil during rainfall.

The changes in surface soil structure induced by rainfall involved a number of stages (Figure 7.1), beginning with aggregate breakdown. The finer fragments generated by aggregate disruption increased the hydraulic resistance at the surface, restricting the rate of water entry into soil. In turn, reduced influx of water through the surface modified the matric suction of water in deeper layers of the soil. Disruption, packing and vertical straining of aggregates below the surface was decreased if the matric suction is high and *vice versa*. The structural condition of the aggregates then influenced the development of strength during drying. Because the changes were sequential, the extent of structural change in the first stage (aggregate breakdown and development of hydraulic resistance) determined the successive stages which ultimately determined whether an aggregate bed developed a friable, hardset or crusted surface condition.

RAIN FACTORS

SOIL PROCESSES

SOIL FACTORS

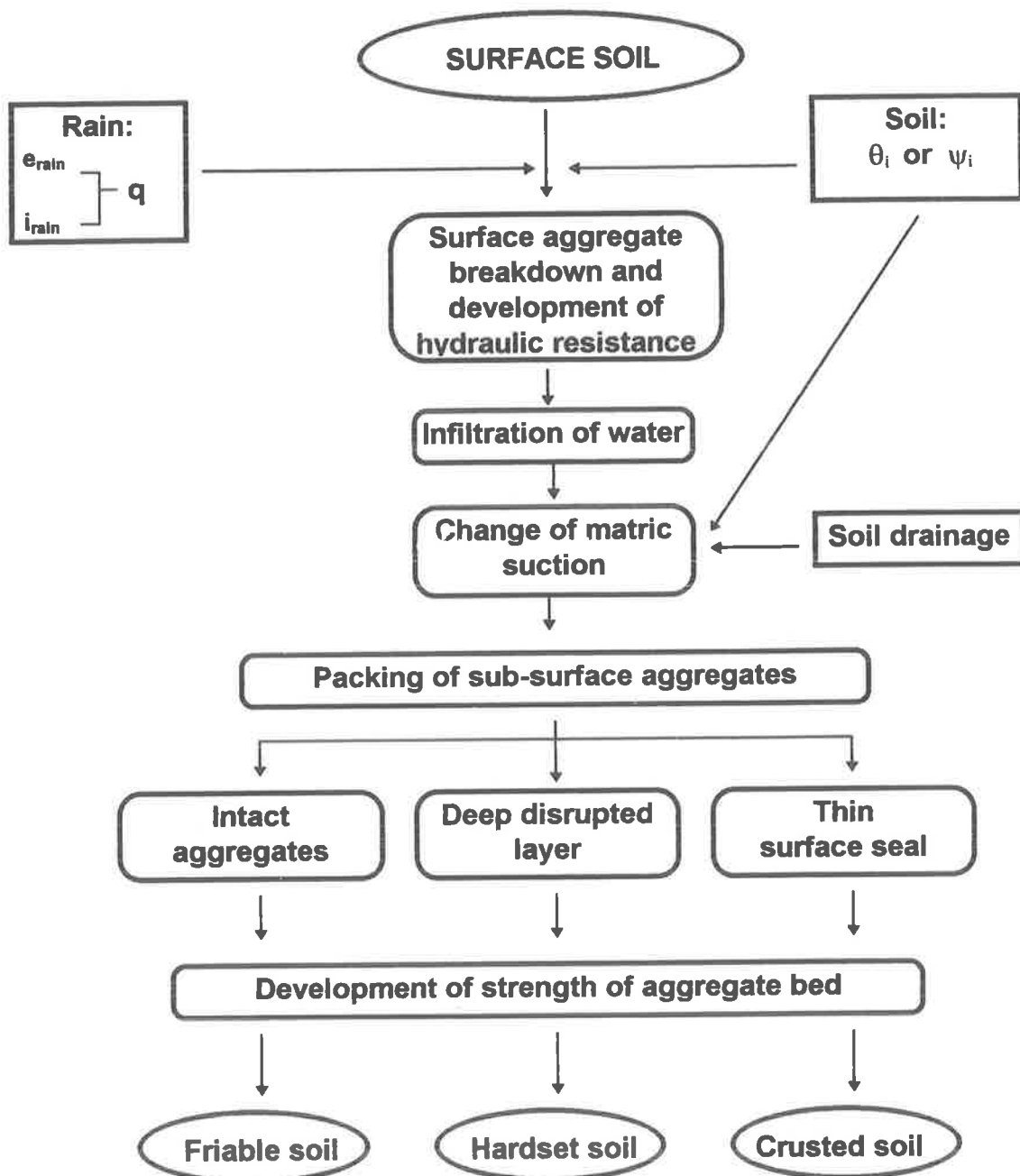


Figure 7.1. Factors and processes which determined the surface condition of Kapunda red-brown earth after rainfall. Symbols e_{rain} , i_{rain} , and q are rainfall kinetic energy, intensity, and kinetic energy flux density, respectively, θ_i is antecedent soil water content and ψ_i is antecedent soil matric suction.

The present results show that there were three distinct stages in the process of hardsetting due to rain falling on a bed of Kapunda friable aggregates: (1) some disruption and rearrangement of aggregates at the surface which lead to some reduction in surface hydraulic conductivity, yet allowed water to enter the soil at a relatively fast rate at a low matric suction; (2) disruption and packing of aggregates at depth below the surface; and (3) development of strength on drying that was more deeply distributed in the soil than a typical crust. Surface sealing occurred when aggregate disruption at the surface was more extensive and a large hydraulic resistance developed so that water entry was slow and occurred at a high matric suction.. Disruption and packing of aggregates below the seal was minimal and on drying a thin surface crust formed but aggregates below the crust remained friable .

7.2 Development of hydraulic resistance

The kinetic energy and intensity of rainfall and antecedent water content of the soil determine the extent of aggregate disruption and the magnitude of hydraulic resistance of the surface, *i.e.* whether a seal is formed or not (Figure 7.1). The development of hydraulic resistance during rainfall may be gauged by the progressive increase in the proportion of materials (aggregates or particles) smaller than 0.125 mm at the surface (Chapter 4). The higher the proportion of fine materials, the greater the hydraulic resistance and hence the smaller the infiltration rate and the higher the matric suction of the inflowing water. Soil matric suction during wetting is an important factor governing aggregate breakdown and packing (Panabokke and Quirk, 1957; Al-Durrah and Bradford, 1981; Francis and Cruse, 1983; Gusli *et al.*, 1994a).

Soil internal drainage rate also influenced matric suction during wetting, as it controlled the balance between inflow and outflow of water, and therefore the net rate of wetting and change of matric suction during rainfall. If rain water influx was higher than internal drainage rate, the soil become saturated, aggregates were weakened and easily deformed by the overburden weight, by pressure waves of raindrop impact (Alder, 1979; Moss, 1991), or possibly by the mechanical action of flowing water (Collis-George and Green, 1979) during rainfall. A fast rate of water influx combined with slow internal drainage rate produced optimum conditions for sub-surface aggregate disruption (Chapter 4).

7.3 Packing of disrupted aggregates

During rainfall, aggregate breakdown and packing of the fragments occurred at the surface as a result of wetting and the direct impact of raindrops. The extent of breakdown and size of fragments produced determined the magnitude of hydraulic resistance which controlled the rate of water entry through the soil surface (Figure 7.1). Disruption of aggregates below the surface (> 10 mm depth) is only possible if a surface seal does not form (Farres, 1978; West, *et al.*, 1992; Bedaiwy and Rolston, 1993). Rainfall intensity indirectly influenced packing of sub-surface (deeper than 10 mm) aggregates and, in the absence of a surface seal, dictated whether Kapunda soil developed a thin or deep disrupted layer or remained friable.

The higher the kinetic energy or kinetic energy flux density, the greater was the proportion of fine materials that were produced at the expense of large aggregates, and the greater the hydraulic resistance or degree of sealing. Extensive surface aggregate

breakdown during rainfall with high kinetic energy ($>6.2 \text{ J m}^{-2} \text{ mm}^{-1}$), resulted in a high proportion of fine material ($< 0.125 \text{ mm}$) at the surface, which allowed rapid development of a surface seal, which subsequently reduced wetting of aggregates below the surface. The disrupted layer was, therefore, thin and was limited to the immediate surface only. However, if kinetic energy was low ($1.6 \text{ J m}^{-2} \text{ mm}^{-1}$), less fine material was generated by aggregate breakdown, hydraulic resistance remained low and the possibility of rapid water penetration to depth existed. Consequently, if rainfall intensity was high ($> 40 \text{ mm h}^{-1}$) aggregate disruption below the surface occurred and the entire aggregate bed set hard on drying. If rainfall intensity was low, aggregate disruption was less and the aggregate bed remained friable.

One way to assess packing of disrupted aggregates is to measure vertical strain (Gusli *et al.*, 1994a). Vertical strain expresses the change of aggregate bed height after wetting and drying relative to the height before wetting. It is, therefore, a reflection of the overall change of structural condition within a given reference thickness of aggregate bed. Because the aggregate beds (50 mm deep) extended beyond the depth of the surface layer directly affected by raindrop energy ($<10 \text{ mm}$), the change of vertical strain as a result of rainfall gave a measure of the disruption of aggregates below the surface.

Vertical strain of aggregate beds following rainfall and drying was found to be directly related to water infiltration rate (Chapter 4). The higher the infiltration rate, the greater was the vertical strain. The relationship between vertical strain and infiltration rate varied, however, according to kinetic energy. The higher the kinetic energy, the greater the aggregate packing and the greater the vertical strain. This indicates that there was an interaction between effects of rate of wetting and the mechanical effects of raindrop energy.

Antecedent water content did not change the relationship between vertical strain and infiltration rate for Kapunda red-brown earth, but it controlled the extent of aggregate packing resulting from a given kinetic energy through its effect on infiltration rate. Pre-wetting of aggregates reduced the generation of fine materials by raindrop impact and hence increased infiltration rate and packing of aggregates below the surface (Chapter 4).

The higher infiltration rate for pre-wetted aggregates caused consistently greater vertical strain for any given rainfall kinetic energy. As explained in Section 7.2, the drop in matric suction during rainfall was associated with the greater packing observed in pre-wetted beds. A similar result was obtained for flood wetting treatments: flood wetting of pre-wetted beds caused greater collapse than flood wetting of air-dry beds (Chapter 4).

Figure 7.2 postulates a mechanism explaining why flood wetting of pre-wetted aggregates showed greater packing than flood wetting air-dry aggregates. Wetting air-dry aggregates to about zero matric suction (by flooding or by a high infiltration rate of rain water) caused slaking of aggregates (Figure 7.2 A). The precursors for slaking are differential stresses due to swelling and the pressure of entrapped air during rapid wetting (Emerson and Grundy, 1954; Emerson, 1977). Because of these stresses, the aggregates will tend to break down along any planes of weakness that exist in the aggregates. The size of slaked fragments is variable, but generally greater than 0.5 mm (Chan and Mullins, 1994). This indicates that forces induced by swelling and entrapped air are exerted at a high hierarchical level, between the coarser fragments that constitute the aggregates. Once the stresses are released by aggregate comminution, further aggregate breakdown to produce finer fragments or release primary particles does not seem to occur.

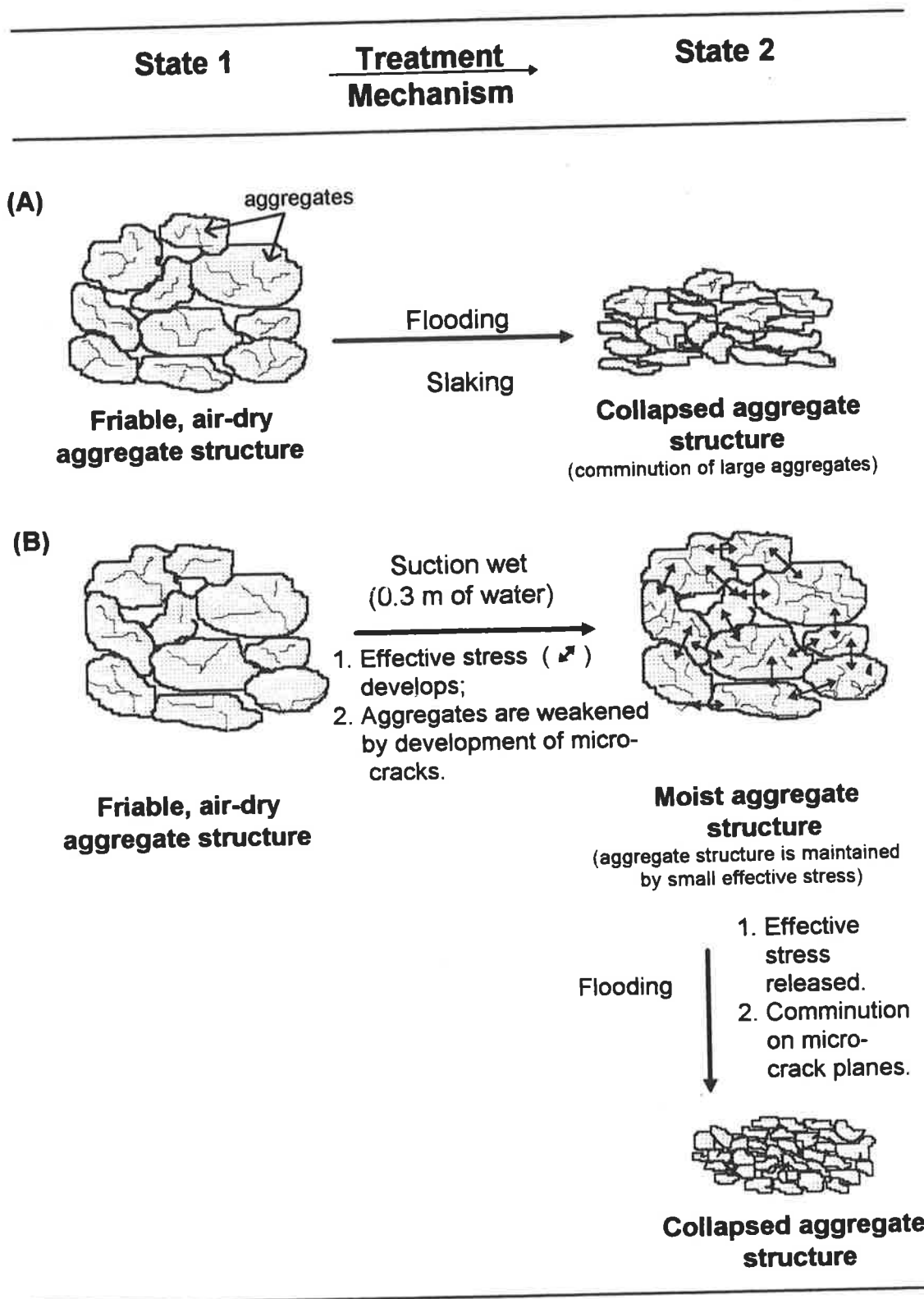


Figure 7.2. Aggregate deformation by wetting of friable aggregates (State 1) to produce collapsed aggregate structure (States 2). (A) flood wetting of air-dry aggregates causing disruption due to slaking (differential swelling and the pressure of trapped air); (B) suction wetting of air dry aggregates then flood wetting of the moist aggregates causing disruption due to the release of effective stress.

Pre-wetted aggregates of Kapunda soil did not slake, as expected from the work of Panabokke and Quirk (1957), Le Bissonnais *et al.* (1989) and Chan and Mullins (1994). Wetting air dry aggregates under a matric suction avoids the build up of stresses due to differential swelling and the pressure of entrapped air associated with flood wetting. The matric suction creates an effective stress which acts to hold aggregates and fragments of aggregates together during the wetting process (Figure 7.2 B). However, suction wetted aggregates are weakened due to the development of an extensive system of micro-cracks (Quirk and Panabokke, 1962). When wetted further by flooding at zero matric suction, the suction wetted Kapunda aggregates were disrupted by loss of effective stress. Because of the system of fine micro-cracks created by suction wetting, the fragments released were probably finer than those measured from flooding of air-dry aggregates (Section 4.3.2) and deformation and packing was more extensive than flood wetting of air-dry aggregates.

Depending on rainfall kinetic energy and intensity and antecedent soil water content, three different aggregate structures were produced at the surface of Kapunda soil (Figure 7.1). Low rainfall kinetic energy and intensity ($1.6 \text{ J m}^{-2} \text{ mm}^{-1}$ and 40 mm h^{-1} , respectively) did not disrupt aggregates, packing was minimal and the beds remained friable on drying. When rainfall kinetic energy was high ($>6.2 \text{ J m}^{-2} \text{ mm}^{-1}$), a surface seal formed, infiltration rate was reduced to less than 25 mm h^{-1} and deep aggregate disruption was prevented. The thickness of the surface seal tended to decrease with increasing intensity. A seal was readily formed on air-dry aggregates, but the seal was deeper for pre-wetted beds.

Rainfall of low kinetic energy ($1.6 \text{ J m}^{-2} \text{ mm}^{-1}$) but high intensity (70 mm h^{-1}) caused a deep ($\sim 50 \text{ mm}$) homogenous, disrupted layer to form. The depth of the

disrupted layer was greater for pre-wetted beds than for air-dry beds. The resulting aggregate packing was similar to that observed from flood wetting of air-dry aggregates (Chapter 4). The overall effect of wetting by rainfall of low kinetic energy and high (70 mm h^{-1}) intensity, especially on pre-wetted beds, was hardsetting on drying. Increasing intensity to 100 mm h^{-1} , for any kinetic energy level, tended to produce a thinner disrupted layer which formed a crust on drying.

7.4 Strength development

The primary difference between friable, on the one hand, and crusted or hardset soil on the other hand, is the magnitude of strength development on drying (*i.e.* the shape of the strength characteristic). The strength of a soil with friable structure does not increase markedly on drying while that of crusts and hardset layers does. The primary difference between crusted and hardset soil is the way strength is distributed with depth at any water content. Crusted soil has a high strength at the surface, which decreases with depths beyond about 10 mm. Hardset soil has uniformly high strength to greater depths which correspond to the depth to which water penetrated during wetting. Each of these strength features have been produced in Kapunda soil by varying antecedent soil water content, method of wetting and the energy and intensity of rain falling on the surface.

Strength development of soil during drying is determined by the extent of disruption and packing (vertical strain) during wetting and subsequently during drying (Gusli et al., 1994b). The greater the disruption and packing, the higher the strength. This study confirmed this finding and extended it to rainfall wetting. In the case of flood and suction wetting, soil strength remained fairly constant throughout the depth of the

aggregate bed because these modes of wetting produced fairly uniform aggregate wetting and consequently aggregate disruption. In the case of suction wetting, beds did not develop marked strength on drying because aggregates were not disrupted by the suction wetting. Flood wetted beds, on the other hand, did develop strength rapidly on drying because aggregate disruption was more extensive.

In the case of wetting by rainfall, distribution of strength with depth varied according to rainfall conditions and antecedent water content. This was because rainfall did not necessarily produce uniform wetting down the depth of the aggregate beds. Beds subjected to high energy rainfall ($>6.2 \text{ J m}^{-2} \text{ mm}^{-1}$) suffered rapid and extensive aggregate breakdown at the surface, forming a surface seal which moderated aggregate disruption below the surface. On drying they developed a thin crust ($< 10 \text{ mm}$), which had a high strength ($>2 \text{ MPa}$ at a matric suction of 5 m). Below the surface, aggregates remained friable and had low strength ($<1 \text{ MPa}$ at 5 m of water). Aggregate beds subjected to low energy ($<6.2 \text{ J m}^{-2} \text{ mm}^{-1}$) and high intensity ($>40 \text{ mm h}^{-1}$) rainfall had a high rate of water entry during rainfall and aggregate disruption at depth was more extensive and homogenous throughout a greater depth. These beds set hard on drying (strength was greater than 1.9 MPa at a matric suction of 5 m), resembling flood wetted beds in all respects.

The antecedent water content of the soil was an important factor in determining surface structural condition during wetting. Flood wetting of pre-wetted aggregate beds caused the most aggregate disruption and development of the highest strength. Rainfall on pre-wetted aggregate beds tended to form strong surface crusts at rainfall kinetic energies much lower ($6.2 \text{ J m}^{-2} \text{ mm}^{-1}$) than the kinetic energy that caused strong crusts to develop on air-dry aggregates ($19.9 \text{ J m}^{-2} \text{ mm}^{-1}$).

Rainfall on aggregate beds with restricted basal drainage caused more aggregate disruption than on well drained beds and this resulted in development of much greater strength on drying. Generally, poor drainage tended to exacerbate hardsetting by rainfall.

7.5 Relationship to other soils

Only one soil was used in this study, the Kapunda red-brown earth, although the original intention had been to investigate a range of soils. However, restrictions of time and the need to investigate fully the response of at least one soil to a range of rainfall conditions, wetting, initial water content and drainage precluded much work on the other soils.

Kapunda soil was chosen for this purpose because of field observations showing that the soil fluctuated between hardsetting, crusting or a friable condition, depending on management and environmental conditions. It therefore provided an ideal opportunity for establishing the methodology and basic principles of the study.

A red-brown earth from Trangie in New South Wales was one of the other soils sampled for inclusion in the research project reported in this thesis. Several experiments were done involving air-dry and pre-wetted aggregates wetted by flooding and rainfall of similar energy to the experiments reported here. Rainfall intensities of 40 and some 70 mm h⁻¹ were used. The data sets were too incomplete for proper inclusion in this thesis, but useful indications were nevertheless available from this work. Marked similarities between Kapunda and Trangie soils were observed in respect to:

- 1) steady state infiltration as a function of fine materials for both air dry and pre-wetted aggregates;
- 2) vertical stain as a function of method of wetting and rainfall properties;

3) the development of strength as a function of method of wetting and rainfall properties.

These preliminary comparisons support the notion that these two soils will behave in a similar way under most circumstances.

Gusli *et al.* (1994a and b) have established the relative behaviour of Trangie red-brown earth to that of a range of south eastern Australian soils. This work showed that a range of responses to flood wetting was present, indicating that soil behaviour to wetting depended on both intrinsic soil properties and management history. Accordingly, it is unlikely that the empirical results from the study reported here will be directly transferable to all soils without accounting for these factors. Further evidence indicating that some soil differences can be anticipated was reported by Hignett (1991). He showed that a kinetic energy of $12 \text{ J m}^{-2} \text{ mm}^{-1}$ was necessary for seal formation during rainfall on a range of South Australian soils. The equivalent kinetic energy for Kapunda was $6.2 \text{ J m}^{-2} \text{ mm}^{-1}$. However, the similarity between Trangie and Kapunda soils suggests that the Kapunda model will be applicable to at least some weakly structured red-brown earths without further adaptation.

7.6 Practical implications

The effect of rainfall kinetic energy flux density (determined by both kinetic energy and intensity) and antecedent water content on the surface condition of soil after rainfall has important implications for soil management. Practices that can influence kinetic energy and antecedent water content are, for example, mulching and sprinkler irrigation.

Covering the soil surface with mulch or by retaining stubble can reduce the impact energy of raindrops on the surface aggregates. Although mulching is likely to reduce rainfall kinetic energy, it will also reduce evaporation and keep the soil moist for longer periods. This might create conditions appropriate for the development of hardsetting in unstable soils such as Kapunda red-brown earth, especially if the rainfall intensity is high. If the intensity is low ($<40 \text{ mm h}^{-1}$), however, the soil should remain friable. Because rainfall intensity at Kapunda is generally below 40 mm h^{-1} (Canterford, 1987), surface cover will be effective in maintaining a friable soil condition. However, a short period of intense rain would be sufficient to cause aggregate disruption below the mulch layer, ultimately leading to hardsetting. Hardsetting of disturbed soil has been observed at Kapunda during the winter months which persists into the drier summer months (Hignett, 1989).

According to the isohyet map for South Australia (Canterford, 1987), rainfall of 16 mm h^{-1} for 1 hour duration has a recurrence interval of 2 years at Kapunda. From the intensity - kinetic energy relationship of Rosewell (1986), this rainfall intensity has a kinetic energy of $22 \text{ J m}^{-2} \text{ mm}^{-1}$, which is much higher than the estimated threshold value of kinetic energy ($>6.2 \text{ J m}^{-2} \text{ mm}^{-1}$) for seal formation on Kapunda soil. Clearly, when left bare, freshly tilled Kapunda red-brown earth would, under this rainfall, most likely form a surface seal and develop a crust on drying. Field observations support this assertion.

It is obvious that at the present level of aggregate stability, maintaining good structure in Kapunda soil is difficult. Management systems with emphasis on stubble retention are essential for improving aggregate stability and protecting the soil surface. The surface cover should reduce the kinetic energy to below the critical value of 6.2 J

$\text{m}^{-2} \text{mm}^{-1}$. The effect of mulch on slowing the rate of wetting needs to be investigated. Its effectiveness would probably depend on the rainfall pattern. Application of a thick layer of mulch might not prevent hardsetting if the rainfall is intense and prolonged. Under these conditions the rate of wetting at the subsurface soil might cause deeply distributed aggregate disruption, leading to hardsetting on drying.

Irrigation of Kapunda red-brown earth demands low intensity sprinkler irrigation systems ($\ll 25 \text{ mm h}^{-1}$). Low intensity sprinkler irrigation systems have the potential to maintain good soil structure (Keller, 1970; Thompson and James, 1985; Mohammed and Kohl, 1987).

7.7 Suggestions for future research

Owing to the complexity of hardsetting under rainfall, the use of computer modelling to describe the process would seem to be appropriate. Through modelling it should be possible to relate rainfall factors and soil conditions to surface aggregate breakdown, infiltration into sub-surface layers and how it relates to sub-surface aggregate collapse and strength development (Figure 7.1). For this purpose, the empirical relationships established in this study can be set in a conceptual framework through appropriate modelling as has been done by Bristow *et al.* (1994) for surface sealing. The limitation at present is the applicability of results for Kapunda red-brown earth to other soils. As previously mentioned, this is largely unknown at present.

To redress this deficiency, a study similar to that reported in this thesis, using various soil types which have different particle-size distributions, mineralogy, organic matter contents and management histories is needed. Differences in these factors should

reflect differences in aggregate stability and therefore resistance to breakdown by rainfall. Results from a wider range of soil types should strengthen our understanding of the process of hardsetting by rainfall and allow development of appropriate models for predicting how different soils might behave under different conditions.

This study was done without considering the role that plants play in moderating the energetics of wetting. The study needs to be extended to include effects of surface cover by crop residues and the influence of roots on soil structural stability. Roots and fungal hyphae are essential for improved soil aggregation and aggregate stability (Tisdall and Oades, 1979). They are likely to influence the stability of aggregates against sealing and deep disruption by rainfall. A better understanding of the interaction between the root system, soil matric suction and rainfall kinetic energy and intensity will improve our knowledge of the process of hardsetting by rainfall.

7.8 References

- Alder, W. F. (1979). The Mechanics of Liquid Impact. *In: Carolyn M. Preece (ed.). Treatise on Materials Science and Technology. Volume 16: Erosion.* Academic Press, New York, p. 127-183.
- Al-Durrah, M.M. and J.M. Bradford (1981). New methods of studying soil detachment due to waterdrop impact. *Soil Science Society of America Journal* 45: 949-953.
- Bedaiwy, M. N. and D. E. Rolston (1993). Soil surface densification under simulated high intensity rainfall. *Soil Technology* 6: 365-376.
- Bristow, K. L., A. Cass, K. R. J. Smettem, and P. J. Ross (1994). Modelling effects of surface sealing on water entry and re-distribution. Proceedings of the International Symposium on 'Sealing, Crusting, Hardsetting Soils: Productivity and Conservation' 7-11 February 1992, University of Queensland, Brisbane, Australia. (*in press*).
- Brunton, J. H. and M. C. Rochester (1979). Erosion of solid surfaces by the impact of liquid drops. *In: Carolyn M. Preece (ed.). Treatise on Materials Science and Technology. Volume 16: Erosion.* Academic Press, New York, p. 185-248.
- Canterford, R. P. (1987). Australian Rainfall and Runoff. A guide to flood estimation. Vol. 2. The Institution of Engineers Australia, Barton, p. 57-62.

- Chan, K. Y. and C. E. Mullins (1994). Slaking characteristics of some Australian and British soils. *European Journal of Soil Science* 45: 273-283.
- Collis-George, N. and R. S. B. Green (1979). The effect of aggregate size on infiltration behaviour of a slaking soil and its relevance to ponded irrigation. *Australian Journal of Soil Research* 17: 65-73.
- Emerson, W. W. (1977). Physical properties and structure. In: J. S. Russell and E. L. Greacen (eds.). *Soil Factors in Crop Production in a Semi-Arid Environment*. Queensland University Press. p. 78-104.
- Emerson, W. W. and G. M. F. Grundy (1954). The effect of rate of wetting on water uptake and cohesion of soil crumbs. *Journal of Agricultural Science* 44: 249-253.
- Farres, P. (1978). The role of time and aggregate size in the crusting process. *Earth Surface Processes* 3: 243-254.
- Francis, P. B. and R. M. Cruse (1983). Soil water matric potential effects on aggregate stability. *Soil Science Society of America Journal* 47: 578-581.
- Gusli, S., A. Cass, D. A. MacLeod, and P. S. Blackwell (1994a). Structural collapse and strength of some Australian soils in relation to hardsetting: I. Structural collapse on wetting and draining. *European Journal of Soil Science* 45: 15-21.
- Gusli, S., A. Cass, D. A. MacLeod, and P. S. Blackwell (1994b). Structural collapse and strength of some Australian soils in relation to hardsetting: II. Tensile strength of collapsed aggregates. *European Journal of Soil Science* 45: 23-29.
- Hignett, C. T. (1989). Physical measurements on a red-brown earth at Kapunda. CSIRO Div. of Soils. Div. Rep. 107.
- Hignett, C. T. (1991). Relating soil structure to runoff quality and quantity. *International Hydrology & Water Resources Symposium*, Perth 2-4 October, 1991. Institute of Engineers, Australia. Publication 91/22, p. 301-305.
- Keller, J. (1970). Sprinkle intensity and soil tilth. *Transactions of the American Society of Agricultural Engineers* 13: 118-125.
- Le Bissonnais, Y., A. Bruand and M. Jamagne (1989). Laboratory experimental study of soil crusting: relation between aggregate breakdown mechanisms and crust structure. *Catena* 16: 377-392.
- Mohammed, D. and R. A. Kohl (1987). Infiltration response to kinetic energy. *Transactions of American Society of Agricultural Engineers* 30: 108-111.
- Moss, A.J. (1991). Rain impact soil crust: I. Formation on a granite-derived soil. *Australian Journal of Soil Research* 29: 271-289.
- Panabokke, C. R. and J. P. Quirk (1957). Effect of initial water content on stability of soil aggregates in water. *Soil Science* 83: 185-195.
- Quirk, J. P. and C. R. Panabokke (1962). Incipient failure of soil aggregates. *Journal of Soil Science* 13: 60-70.
- Rosewell, C. J. (1986). Rainfall kinetic energy in Eastern Australia. *J. of Climate and Applied Meteorology* 25: 1695-1701.

5.3.2 Rainfall kinetic energy flux density and penetration resistance

Both kinetic energy of rainfall (Al-Durrah and Bradford, 1981; Bradford and Huang, 1991) and intensity (Holder and Brown, 1974; Morrison *et al.*, 1985) influence the surface crust strength of soil. Combining these two properties of rain to give rainfall kinetic energy flux density (the product of kinetic energy and intensity) provided a clearer representation of the effect of rainfall on subsequent surface strength development.

Surface penetration resistance increased linearly with increasing q . The linear regression accounted for 80 % of the variance in penetration resistance of aggregate beds equilibrated at a matric suction of 0.57 m, and 91 % in the case of soils equilibrated at 5 m (Figures 5.3a and b). When the aggregate bed was at 5.0 m matric suction (Figure 5.3b), wetting without rainfall energy led to a surface soil penetration resistance of 1.38 MPa. For every $\text{J m}^{-2} \text{h}^{-1}$ of rainfall kinetic energy flux density that the soil was exposed to, penetration resistance increased by 0.46 kPa. At a lower suction, 0.57 m (Figure 5.3a), crust penetration resistance was lower, and the effect of kinetic energy flux density was more muted ($0.08 \text{ kPa m}^2 \text{ h}^{-1} \text{ J}^{-1}$).

Antecedent water content of beds subjected to rain did not significantly influence the slope of the relationship between penetration resistance and rainfall kinetic energy flux density. This is consistent with the similarity of the penetration resistance characteristics for air-dry and pre-wetted aggregates after rainfall (Figures 5.2b and c).

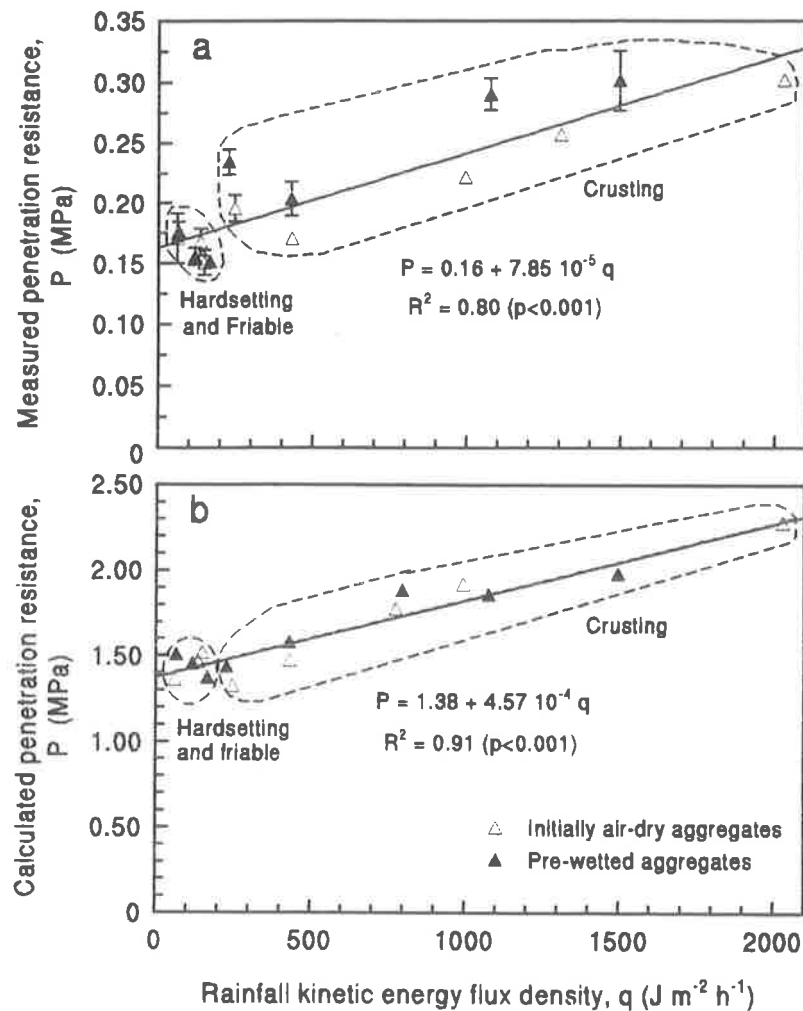


Figure 5.3. Effect of rainfall kinetic energy flux density (q) and antecedent water content on maximum penetration resistance at the surface 0 to 5 mm depth at matric suctions of (a) $\psi_m = 0.57$ m and (b) $\psi_m = 5$ m of water. Open triangles represent initially air-dry aggregates and closed triangles represent pre-wetted (0.30 m suction) aggregates. Error bars are $2 \times$ standard error of the means ($n = 8$). Penetration resistance at $\psi_m = 0.57$ was measured; that at $\psi_m = 5$ m was calculated using Equation (5.2). Boundaries drawn are around groups of data which are (i) crusting or (ii) friable or hardsetting.

5.3.3 Fine aggregates and penetration resistance

One way to assess the effect of rainfall kinetic energy flux density on aggregate structure is to measure how rainfall affects the production of fine aggregates at the soil surface

(Glanville and Smith, 1988; Loch, 1994). The present data showed that the strength of the surface soil on drying increased linearly with the amount of fine materials, less than 0.125 mm diameter (A_{125}), generated at the surface by rainfall (Figures 5.4a and b).

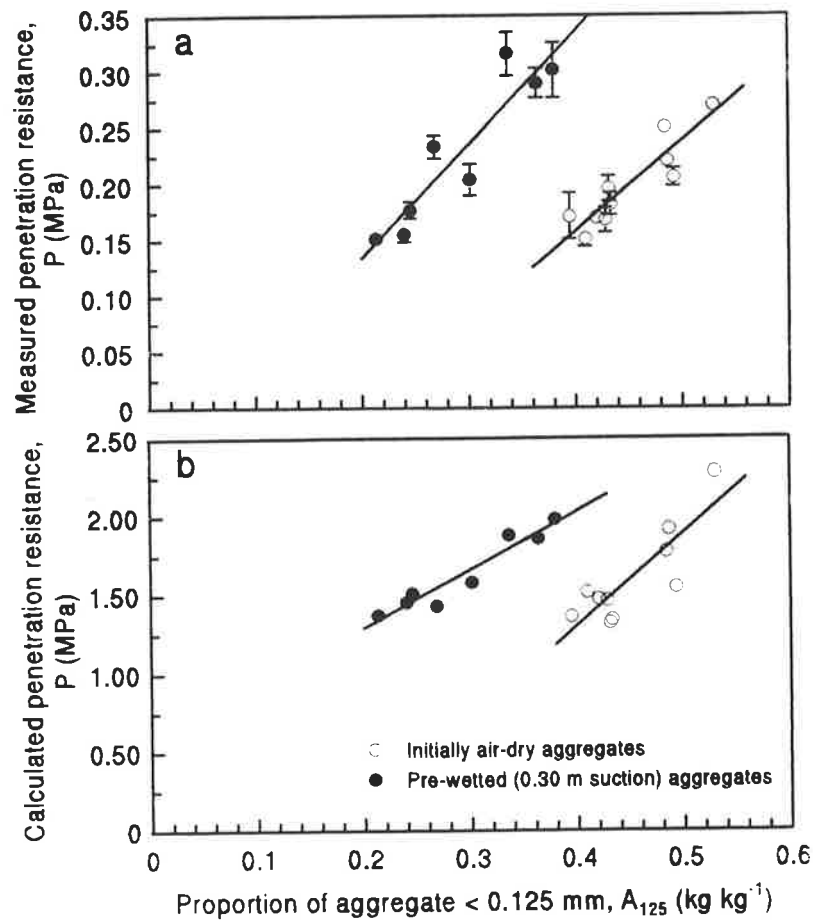


Figure 5.4. Effect of the proportion of materials less than 0.125 mm diameter (A_{125}) generated at the soil surface (0 to 5 mm) by rainfall on the surface penetration resistance (P) at matric suctions of (a) 0.57 m (P was measured), and (b) 5 m of water (P was calculated from Equation 5.2).

It is noticeable that pre-wetted aggregate beds required a smaller proportion of fine materials to give the same surface strength as initially air-dry aggregate beds. The differences between the two antecedent water contents was maintained on drying from

0.57 to 5 m of water matric suction. The proportion of materials less than 0.125 mm at the surface of the bed was shown to be a function of kinetic energy flux density (Figure 4.3.2). However, the extent of q affecting A_{125} was dependent on antecedent water content. At a given value of q , higher values of A_{125} were obtained in initially air-dry than in pre-wetted aggregate beds.

On the other hand, penetration resistance of surface soil (P) was also a linear function of q , independent of antecedent water content (Figure 5.3). This suggests that A_{125} only partially explains P , and that the influence of A_{125} on P should only be assessed at similar antecedent water contents. Pre-wetted aggregate beds appeared to pack more efficiently under rainfall than did initially air-dry beds (Section 4.3.3), as it allowed soil matric suction during wetting to decline to around zero which caused slumping (Figure 7.2, Chapter 7). Because rainfall caused larger collapse of pre-wetted than air-dry beds, despite the fact that in the latter a greater proportion of fine materials was generated at the surface, rearrangement and packing of disrupted aggregates are an important part of the collapse of aggregates which induces hardsetting. Packing of disintegrated aggregates, which influenced the strength of the surface crust, is explained only partially by A_{125} . The other major factor is the mode of packing of the disrupted materials, which determines pore-size distribution. This factor is not accounted for in measurement of A_{125} .

5.3.4 Infiltration rate and penetration resistance

Figure 5.5 shows that surface penetration resistance decreased as infiltration rate at 30 minutes (i_{30}) increased. Lower infiltration rate implies greater packing and hence higher

surface soil penetration resistance developed on drying. The relationship between penetration resistance (P) and infiltration rate after 30 minutes of rainfall (i_{30}) fitted an inverse function:

$$P = a' + b'/i_{30} \quad (5.6)$$

where a' and b' are regression coefficients, and i_{30} is always >0 . Values of a' and b' were 0.14 and 1.57 for a matric suction of 0.57 m, and 1.16 and 8.64 for a matric suction of 5.0 m of water. A relationship between infiltration rate and surface soil penetration resistance may be expected, because both are influenced by pore-size distribution. Carter (1990) and Gusli *et al.* (1994b) found that soil shear strength and penetration resistance were negatively related to the volume of pores greater than 50 μm diameter. Pores with diameters of 50 to 100 μm are classified as transmission pores (Greenland, 1977), which influence infiltration rate.

Figure 5.5 shows that antecedent water content did not influence the relationship between P and i_{30} , as was the case when P was related to A_{125} (Figure 5.4). Antecedent water content influences the proportion of pores in the aggregate beds which are able to resist the disruptive force of raindrop impact and therefore determine the value of i_{30} and P. Infiltration rate reflects pore-size distribution better than A_{125} and thus the relationship between i_{30} and P is not affected by antecedent water content. Pore-size distribution is fundamentally related to strength development (Carter, 1990; Gusli *et al.*, 1994b).

Figure 5.5, however, shows that the relationship between soil strength and infiltration rate was better at a matric suction of 5 m of water than at 0.57 m. The coefficients of determination for these two matric suctions were 0.64 ($p < 0.001$) compared to 0.22 ($p < 0.05$), respectively. The reason for this is that at a low matric

suction (0.57 m), differences in pore-size distribution are not readily detectable by strength measurements. This is consistent with vertical strain data shown in Figures 6.2 and 6.3 (Section 6.3.1).

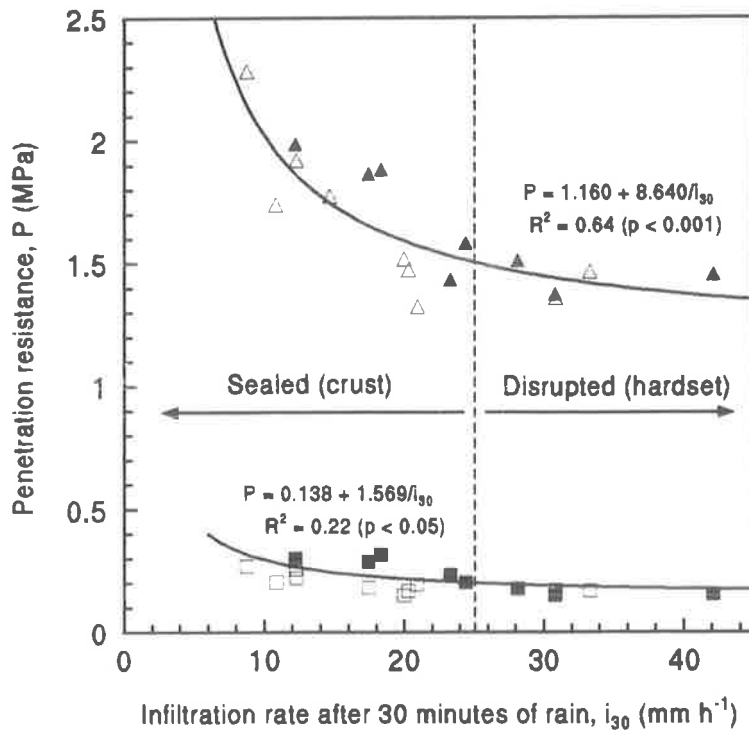


Figure 5.5. Penetration resistance (P) of aggregate beds at matric suctions (ψ_m) of 0.57 m (squares) and 5.0 m of water (triangles) after being subjected to rainfall, as a function of infiltration rate 30 minutes after commencement of rainfall, i_{30} . Open and closed symbols represent initially dry and pre-wetted (0.30 m suction) aggregates, respectively. The dashed line corresponds to i_{30} equal to 25 mm h^{-1} (associated with kinetic energy of $\geq 6.2 \text{ J m}^{-2} \text{ mm}^{-1}$), considered to be critical infiltration rate distinguishing sealed (crusted) from disrupted (hardset) surface soil. Error bars ($2 \times$ standard error) for measurements at ψ_m of 0.57 m are too small to be shown; P values for ψ_m of 5 m were calculated from Equation 5.2.

The different surface soil conditions (crusted or hardset) generated by rainfall did not alter the relationship between P and i_{30} . The hardset surface soil did not seal during rainfall and had high i_{30} ($>25 \text{ mm h}^{-1}$) and hence low P ($<1.5 \text{ MPa}$). In contrast, the

crusted surface soil, which developed from rainfall with kinetic energy greater than $6.2 \text{ J m}^{-2} \text{ mm}^{-1}$ (Chapter 6), had low i_{30} ($<25 \text{ mm h}^{-1}$) and high P ($>1.5 \text{ MPa}$). Therefore, the data for a crusted surface lay in the upper region of the regression line, while the data for hardset surface lay in the lower region.

5.4 Conclusions

- 1) Rapid flood wetting of aggregate beds, without rainfall, caused extensive surface aggregate disruption, and the rapid development of high strength on drying. Flood wetting of pre-wetted aggregates was particularly disruptive, causing severe hardsetting with surface soil strength developing even more rapidly than in the case of flood wetting of air-dry aggregates. Suction wetting, however, preserved the friability at the surface of the aggregate bed.
- 2) Penetration resistance characteristics of the surface soil obtained from flood wetting and rainfall wetting were similar, but were steeper than those from suction wetting. Penetration resistance for flood or rainfall wetted beds increased rapidly with drying, but not for suction wetted beds.
- 3) Rainfall formed a crust or caused the entire bed to set hard, depending on rainfall kinetic energy and intensity, and antecedent water content. However, whether the bed was crusted, hardset, or friable, the strength of the surface following rainfall and drying can be explained in terms of rainfall kinetic energy flux density. Penetration resistance of the surface (recorded at 4 to 5 mm depth) was a linear function of kinetic energy flux density (over a range of 0 to $2000 \text{ J m}^{-2} \text{ h}^{-1}$), independent of antecedent water content or whether the soil crusted or set hard. Penetration

resistance increased by about 0.46 kPa for each $\text{J m}^{-2} \text{h}^{-1}$ increase in kinetic energy flux density.

- 4) Strength of the surface soil on drying for a specific antecedent water content was a linear function of the proportion of materials smaller than 0.125 mm at the surface.
- 5) There was a significant relationship between infiltration rate after 30 minutes of rainfall (approximately equal to steady state infiltration rate) and surface penetration resistance. The relationship was independent of antecedent water content and surface soil condition (crusted, hardset or friable) on drying.

5.5 References

- Agassi, M., J. Morin, and I. Shainberg (1985). Effect of raindrop impact energy and water salinity on infiltration rates of sodic soils. *Soil Science Society of America Journal* 49: 186-190.
- Al-Durrah, M. M. and J. M. Bradford (1981). New methods of studying soil detachment due to waterdrop impact. *Soil Science Society of America Journal* 45: 949-953.
- Bohl, H. and Ch. H. Roth (1993). A simple method to assess the susceptibility of soils to form surface seals under field conditions. *Catena* 20: 247-256.
- Bradford, J. M. and C. Huang (1991). The morphology of surface crusts. In: *M.E. Sumner and B.A. Stewart (eds.). Soil Crusting. Chemical and Physical Processes. Advances in Soil Science. Lewis Publ., Boca Raton, pp.: 55-71.*
- Bristow, K. L., A. Cass, K. R. J. Smettem, and P. J. Ross (1994). Modelling effects of surface sealing on water entry and re-distribution. Proceedings of the International Symposium on 'Sealing, Crusting, Hardsetting Soils: Productivity and Conservation' 7-11 February 1992, University of Queensland, Brisbane, Australia. (*in press*).
- Carter (1990). Relationship of strength properties to bulk density and macroporosity in cultivated loamy sand to loam soils. *Soil & Tillage Research* 15: 257-268.
- Duley, F. L. (1939). Surface factors affecting the rate of intake of water by soils. *Soil Science Society of America Proceedings* 4: 60-64.
- Glanville, S. F and G. D. Smith (1988). Aggregate breakdown in clay soils under simulated rain and effects on infiltration. *Australian Journal of Soil Research* 26: 111-120.
- Greenland, D. J. (1977). Soil damage by intensive arable cultivation: temporary or permanent? *Phil. Trans. R. Soc. Lond. B.* 281: 193.

- Gusli, S., A. Cass, D. A. MacLeod, and P. S. Blackwell (1994a). Structural collapse and strength of some Australian soils in relation to hardsetting: I. Structural collapse on wetting and draining. *European Journal of Soil Science* 45: 15-21.
- Gusli, S., A. Cass, D. A. MacLeod, and P. S. Blackwell (1994b). Structural collapse and strength of some Australian soils in relation to hardsetting: II. Tensile strength of collapsed aggregates. *European Journal of Soil Science* 45: 23-29.
- Hillel, D. and W. R. Gardner (1969). Steady infiltration into crust topped profiles. *Soil Science* 108: 137-142.
- Holder, C. B. and K. W. Brown (1974). Evaluation of simulated seedling emergence through rainfall induced soil crusts. *Soil Science Society of America Proceedings* 38: 705-710.
- Loch, R. J. (1994). A method for measuring aggregate water stability of dryland soils with relevance to surface seal development. *Australian Journal of Soil Research* 32: 687-700.
- Morrison, M. W., L. Prunty, and J. F. Giles (1985). Characterizing strength of soil crusts formed by simulated rainfall. *Soil Science Society of America Journal* 49: 427-431.
- Mualet, Y., S. Assouline, and H. Rohdenburg (1990). Rainfall induced soil seal. (A) A critical review of observations and models. *Catena* 17: 185-203.
- Mullins, C. E., A. Cass, D. A. MacLeod, D. J. M. Hall and P. S. Blackwell (1992). Strength development during drying of cultivated, flood-irrigated hardsetting soil. II. Trangie soil, and comparison with theoretical predictions. *Soil and Tillage Research* 25: 129-147.
- Romkens, M. J. M., S. N. Prasad, and J.-Y. Parlange (1990). Surface seal development in relation to rainstorm intensity. In: R. B. Bryan (ed.) *Soil Erosion. Experiments and Models*. Catena Supplement 17: 1-11.
- Shainberg, I. and M. Singer (1988). Drop impact energy - soil exchangeable sodium percentage interactions in seal formation. *Soil Science Society of America Journal* 52: 1449-1452.
- Weaich, K., A. Cass, and K. L. Bristow (1992). Use of a penetration resistance characteristic to predict soil strength development during drying. *Soil and Tillage Research* 25: 149-166.

Chapter 6

Effect of rainfall kinetic energy and antecedent water content on emergence resistance through the soil surface

6.1 Introduction

Hardsetting is distinguished from crusting in that hardsetting develops from a deep (> 50 mm) layer of disrupted aggregates, while crusting develops from a thin (<10 mm) surface seal (Bristow *et al.*, 1994). Hardsetting has been shown to develop from friable, unstable aggregates wetted by flooding (Mullins *et al.*, 1992; Weaich *et al.*, 1992; Gusli *et al.*, 1994a, b). Crusts develop on soil subjected to raindrop impact (Agassi *et al.*, 1985; Shainberg and Singer, 1988). However, numerous casual field observations suggest that either hardsetting or crusting may develop on the same soil under rainfall, depending on soil conditions and management.

The literature on crusting clearly points to the presence of a thin disrupted layer at the soil surface, which becomes hard on drying. Below the crust, at a depth below 10 mm, aggregates are softer and more friable (Duley, 1939; Tackett and Pearson, 1965; Eigel and Moore, 1983). Hardsetting, in contrast, is associated with much deeper disruption of aggregates (Mullins *et al.*, 1992; Weaich, *et al.*, 1992). Crusting and hardsetting should, therefore, have a contrasting depth distribution of aggregate breakdown (Bristow *et al.*, 1994). How the depth of aggregate disruption by rainfall varies with antecedent water content (Le Bessonnais *et al.*, 1989) and the extent to which aggregates below the surface are wetted (Farres, 1978; Bedaiwy and Rolston,

1993) are known. However, quantitative knowledge concerning the mechanisms by which these factors determine the depth distribution of aggregate breakdown and subsequent strength development, in relation to crusting and hardsetting is lacking.

Soil matric suction during wetting has a strong influence on aggregate stability. In comparison to air-dry soil, pre-wetting aggregates to about field capacity matric suction (around 0.5 to 1 m of water) increased aggregate resistance to the disruptive force of wetting (Panabokke and Quirk, 1957). However, as matric suction was decreased further to zero or near zero, the stability of aggregates declined (Al-Durrah and Bradford, 1981; Francis and Cruse, 1983). Soil matric suction during wetting is influenced by the initial water content, rate of water influx (a function of water application rate and surface sealing), and soil drainage rate relative to water influx. Soil matric suction during wetting should therefore influence the thickness of a disrupted layer, and thus whether hardsetting or crusting develops.

Le Bissonnais *et al.* (1989) found that pre-moistening aggregates before rainfall slowed seal formation, but caused development of a thicker disrupted layer than if the aggregates were initially dry. Timm *et al.* (1971) observed a 'crust' as thick as 75 mm in the field, developed on the ridge of a furrow irrigated tilled soil following intense rainfall and drying. Aggregates on the ridge would have been wetted under suction. Consequently, it is likely that these suction-wetted aggregates could have been disrupted to 75 mm when subjected to rainfall. The 'crust' Timm observed was probably a hardset layer which developed from a deeply disrupted layer.

However, the distinctions between the mechanisms of hardsetting (developed from deeply disrupted layers) and crusting (developed from thin seals) in relation to methods of wetting, rainfall factors and soil antecedent water content is not clear. In

particular, how the above factors influence strength distribution down the soil profile is not known.

Arndt (1965), Holder and Brown (1974) and Morrison *et al.* (1985) made soil beds and measured “emergence resistance” (see List of terminology and abbreviation) by upward penetration of a rigid probe. The beds they made were thick, *i.e.* 153 mm (Holder and Brown, 1974). However, the emergence resistance was measured only at 25 mm from the surface, too shallow to allow expression of differences relating to crusting or hardsetting. If the measurements are made on deeper layers, this method can be effective in differentiating strength profiles of crusted and hardset soils. Measurement of penetration resistance from below mimics resistance to seedling emergence more closely than downward penetration from the surface.

The aims of the experiments described in this chapter are:

- 1) to measure the development of soil strength and its depth distribution in aggregate beds in response to different modes of wetting, rainfall kinetic energy and intensity, and antecedent soil water content;
- 2) to relate strength and its depth distribution to known strength characteristics of friable, hardset and crusted soils;
- 3) to investigate the effect of soil drainage condition on the development of soil strength resulting from rainfall wetting and drying;

6.2 Materials and methods

6.2.1 Soil properties and preparation and wetting of aggregate beds

A red-brown earth (fine, mixed, thermic, Calcic Rhodoxeralf) (Soil Survey Staff, 1988) from Kapunda, South Australia was used. The properties and behaviour of the soil in the field and management history are given in Section 3.2.1. Aggregate beds were prepared as described in Section 3.2.2, and either wetted by rainfall, or by flooding or suction without rainfall.

6.2.2 Measurements

6.2.2.1 Emergence resistance

Emergence resistance was measured using a blunt needle (1.6 mm tip diameter), driven vertically upwards by an electric motor at a speed of 1.4 mm s^{-1} , from the base until the surface soil ruptured, indicated by the sharp decline in emergence resistance (Holder and Brown, 1974). The force on the tip of the needle was recorded electronically every 0.5 mm of upward travel. Aggregate beds were clamped firmly above the needle and 3 to 4 penetrations were made vertically upwards through the base of each bed. The penetrations were about 20 mm apart, satisfying the spatial separation recommended by Dexter (1987) and Becher (1994b). The mean and standard error of emergence resistance were calculated at each depth.

Because the needle used was blunt (flat tip), the total emergence force (F_t) recorded during the upward movement consisted of the force required to penetrate the

soil (F_s) and the force due to soil - metal friction (F_f), measured during the withdrawal of the needle (Groenevelt *et al.*, 1985; Fritton, 1990; Becher, 1994a):

$$F_t = F_s + F_f \quad (6.1)$$

The emergence resistance (P_E) at any given depth (z) was calculated as

$$P_{E(z)} = F_{s(z)} / [\pi (d/2)^2] \quad (6.2)$$

where d is the needle diameter. Substituting F_s from Equation (6.1), Equation (6.2) becomes

$$P_{E(z)} = [F_{t(z)} - F_{f(z)}] / [\pi (d/2)^2]. \quad (6.3)$$

An emergence resistance characteristic (Mullins *et al.*, 1992; Weaich *et al.*, 1992) was established by relating emergence resistance (P_E) data to degree of saturation (S) by regression analysis. The relationship is best described by a power function

$$P_E = a S^{-b} \quad (6.4)$$

where a and b are coefficients of regression. The regression was performed for each method of wetting and antecedent water content for 0 to 10, 10 to 20, and 20 to 30 mm depths.

6.2.2.2 Bulk density and degree of saturation

After drying the bulk density of the soil bed was measured at different depths, as described in Section 4.2.4.5. The degree of saturation of each depth segment was calculated from mass water content measured at the surface (0 to 5 mm depth) and bulk density of individual depth segments (Equation 5.3). Sub-surface depths were assumed to have the same mass water content as the surface depth after overnight equilibration in a sealed, temperature-insulated container, despite gradients in bulk density. Keller

soil mass water content did not change with increasing bulk density Mg m^{-3} . To verify this assumption, several aggregate beds which had gradients were sectioned and mass water content measured. Mass change within the range of bulk densities of up to 1.7 Mg m^{-3} , and the range of 1.7 to 2.0 Mg m^{-3} (Figure 6.1).

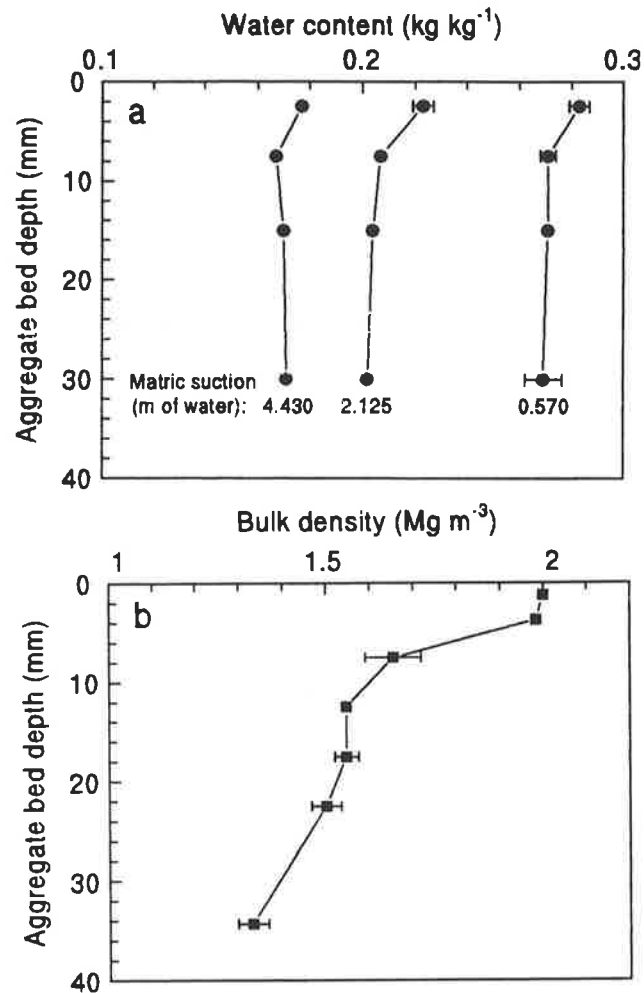


Figure 6.1. Profiles of: (a) mass water content measured at various matric suctions, and (b) the associated bulk density values. Error bars are $2 \times$ the standard error of the mean ($n = 3$). No error bars imply $2 \times$ SE was smaller than the symbol.

6.2.2.3 Visible pores

Change of surface roughness (microrelief) has been used as a measure of aggregate breakdown induced by rainfall after tillage (Burwell and Larson, 1969; Freebairn and

Gupta, 1990). Video imaging was used to estimate surface roughness (an estimate of porosity) of vertical sections of beds following different methods of wetting. Vertical sections of aggregate beds were obtained by carefully breaking the aggregate beds across their diameter. When the surface of the vertical section was lightly lit from all sides, pores showed up as shadowed areas. A video image comprising a regular grid of 256×512 points was obtained from a soil surface of about $40 \text{ mm} \times 50 \text{ mm}$. For crusted beds, observations were made only on the crusted layer, while for hardset and friable beds observation were made on the whole depth. The darkness of the image points were sampled as a 16 level grey scale (0 = black, 15 = white) and were classified into those above or below an empirically determined threshold level. The threshold was set to the level which displayed the best contrast between all the treatments. From calibration data (using a set visible soil pores of known diameter) the threshold level set was able to detect pores with approximate diameter greater than 0.25 mm. The fraction of points darker than that level was taken to be a measure of exposed pore area on the surface, and was assumed to be inversely related to aggregate disruption within the area of vertical section exposed. The lower the ratio of the pore area to the total area, the greater was aggregate disruption assumed to be. The data obtained were well correlated ($R^2 > 0.93$, significant at $p < 0.05$) with total porosity and air-filled porosity at a matric suction of 0.57 m of water.

6.3 Results and discussion

6.3.1 Emergence resistance

Figure 6.2 shows the effect of the treatments on the emergence resistance of aggregate beds at a matric suction of 0.57 m of water. In this relatively wet state, the emergence resistance each wetting method was fairly uniform throughout the depth of the bed (Figure 6.2a). This condition is typical of hardset soil strength profile.

Figure 6.2a shows that at a matric suction of 0.57 m of water, there was little consistently significant difference between the emergence resistance of initially air-dry aggregate beds that were wetted by flooding, by suction (0.30 m), or by suction then flooding. It should be noted that the aggregate packing (as indicated by vertical strain after rainfall) produced by these methods of wetting was different (Section 4.3.1). This indicates that at low matric suction (0.57 m), different degrees of packing arising from different wetting treatments, as indicated by values of vertical strain, did not translate into differences in emergence resistance.

Wetting of air-dry and suction-wetted aggregates by high energy rainfall of $19.9 \text{ J m}^{-2} \text{ mm}^{-1}$ resulted in higher emergence resistance at the surface (0 to 10 mm) than in the soil below (Figure 6.2b and c). A similar, though less pronounced, pattern was observed in suction wetted aggregate beds at rainfall kinetic energy of $6.2 \text{ J m}^{-2} \text{ mm}^{-1}$ (Figure 6.2c). However, below 10 mm, emergence resistance of the flood wetted beds as well as those that were first suction wetted then flooded was significantly higher than for beds subjected to rainfall. The lowest emergence resistance below 10 mm is shown by rainfall wetting of air-dry aggregates (Figure 6.2b).

It is seen that flooding of air-dry or previously suction-wetted aggregate beds, and low energy rainfall on suction-wetted beds tended to produce hardsetting, with

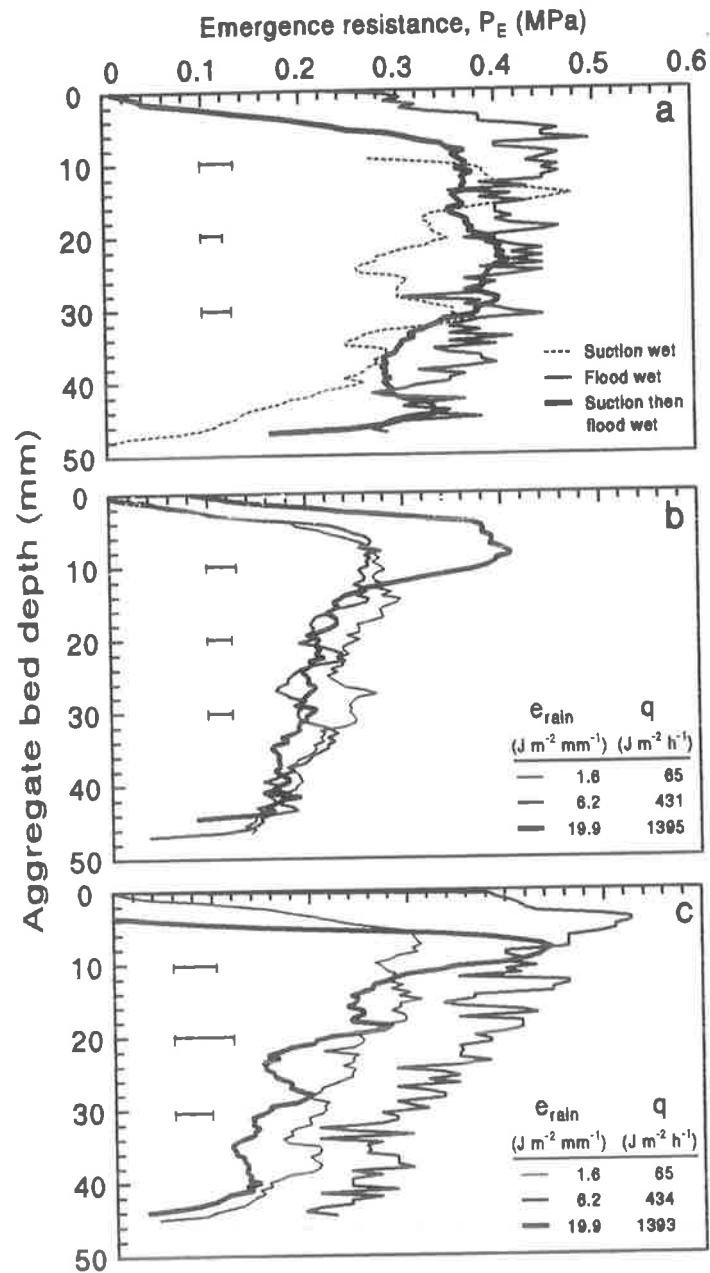


Figure 6.2. Emergence resistance of aggregate beds at a matric suction of 0.57 m of water after subjecting the beds to different methods of wetting at various antecedent water contents: (a) Wetting, without rainfall, of air-dry aggregates by a suction of 0.30 m of water; flooding; and suction (0.30 m) then flooding; (b and c) wetting by rainfall of various kinetic energies (e_{rain}) and intensities and therefore kinetic energy flux densities (q) on (b) air-dry aggregates and (c) suction (0.30 m) wetted aggregates. Error bars are $2 \times$ pooled standard error for 10, 20 and 30 mm depths.

uniform, high emergence resistance throughout the depth of the bed (Figures 6.2a and b). High energy rainfall ($19.9 \text{ J m}^{-2} \text{ mm}^{-1}$) on pre-wetted and air-dry aggregate beds produced strength profiles that conform to crusted conditions (Figure 6.2b and c). When applied to suction wetted beds, rainfall of $6.2 \text{ J m}^{-2} \text{ mm}^{-1}$ resulted in strength profiles that suggested both crusting and hardsetting. Rainfall of $1.6 \text{ J m}^{-2} \text{ mm}^{-1}$ produced hardsetting only (Figure 6.2c). On air-dry beds, rainfall of 1.6 and $6.2 \text{ J m}^{-2} \text{ mm}^{-1}$ produced a homogenous strength profile, but slightly weaker than that produced by rainfall of the same energies on pre-wetted beds.

At a matric suction of 0.57 m of water, the profile of emergence resistance for the suction-wetted aggregates was at some depths lower but generally similar to the profiles for the flood wetted beds (Figure 6.2a). Despite this similarity, the suction-wetted beds were friable, with aggregates not closely packed, whereas the flooded beds were hardset. However, as the soil dried to a matric suction of 5 m, the strength profiles of the friable and hardset beds were distinctly different (Figure 6.3a). Emergence resistance values increased in the order: suction wetting of air-dry aggregates < flood wetting of air-dry aggregates < flood wetting of pre-wetted aggregates.

The order of strength values matches the order of vertical strain (Section 4.3.3). The friable, suction wetted beds had vertical strains of less than 0.05 and emergence resistance less than 1 MPa at a matric suction of 5 m of water throughout the depth of the beds. In contrast, the hardsetting, flood-wetted aggregate beds were closely packed (vertical strain >0.11) through the entire bed profile, strong (emergence resistance >1.9 MPa at a matric suction of 5 m).

The strength profile of air-dry aggregate beds wetted by rainfall lay between that of suction and flood wetted aggregate beds, except for beds wetted by high energy

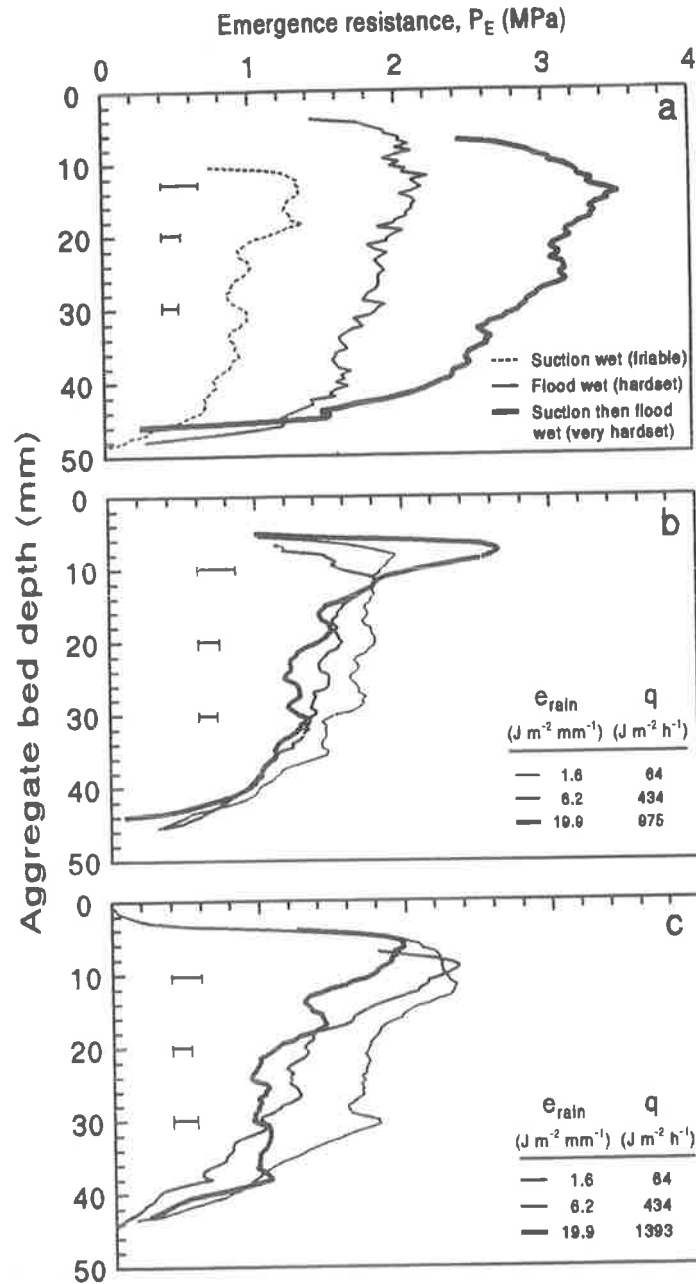


Figure 6.3. Emergence resistance of aggregate beds, at a matric suction of 5 m of water, after subjecting the beds to different methods of wetting at various antecedent water contents: (a) Wetting, without rainfall, of air-dry aggregates by a suction of 0.30 m of water; flooding; and suction (0.30 m) then flooding; (b and c) wetting by rainfall of various kinetic energies (e_{rain}) and intensities and therefore kinetic energy flux densities (q) on (b) air-dry aggregates and (c) suction (0.30 m) wetted aggregates. Error bars are $2 \times$ pooled standard error for 10, 20 and 30 mm depths.

rainfall (Figures 6.3a and b). Air-dry aggregate beds subjected to rainfall of high kinetic energy ($19.9 \text{ J m}^{-2} \text{ mm}^{-1}$) and high kinetic energy flux density ($975 \text{ J m}^{-2} \text{ h}^{-1}$) caused extensive aggregate disruption in the top 10 mm, producing a surface crust with a high emergence resistance. Rain with low kinetic energy ($1.6 \text{ J m}^{-2} \text{ mm}^{-1}$) and kinetic energy flux density ($64 \text{ J m}^{-2} \text{ h}^{-1}$) caused less aggregate disruption at the surface and emergence resistance values that were fairly uniform down the bed. The strength profile was similar to that obtained from flood wetting of air-dry aggregates (compare Figures 6.3a and b).

Similar results were observed for rainfall on pre-wetted aggregate beds (Figure 6.3c). However, high kinetic energy and kinetic energy flux density rainfall did not produce a surface crust as strong as that resulting from similar rainfall on air-dry aggregates; the strength profile was, nevertheless, typical of crusted soil. The weaker surface crust formed from rainfall on pre-wetted aggregates compared to rainfall on air-dry aggregates was consistent with the greater amount of materials smaller than 0.125 mm produced at 0 to 5 mm depth (Chapter 4).

Figures 6.2 and 6.3 show that pre-wetting of the Kapunda soil at 0.30 m of water suction preserved the friable aggregate structure of the original beds, which on drying had an emergence resistance less than 1 MPa at a matric suction of 5 m of water. Flood wetting of air-dry or pre-wetted aggregates caused severe aggregate disruption resulting in the development of typically hardset conditions with mean emergence resistance greater than 1.9 MPa at 5 m suction. Strength was fairly uniform down the profile (Figure 6.3a).

High energy rainfall ($19.9 \text{ J m}^{-2} \text{ mm}^{-1}$) on air-dry or pre-moistened aggregates produced a crust on drying with emergence resistance greater than 2 MPa at 0 to 10 mm

depth. Below the crust the soil remained friable with emergence resistance decreasing towards 1 MPa (Figures 6.3b and c). The large proportion of fine materials produced by high kinetic energy rainfall (Figure 4.5) caused infiltration rate to decrease during rainfall (Figures 3.4 and 4.4). This means that aggregates below the seal were wetted slowly, producing strength profiles which resembled those obtained from suction-wetted aggregates.

In the case of low energy rainfall ($1.6 \text{ J m}^{-2} \text{ mm}^{-1}$), a seal did not develop, water infiltrated more rapidly and aggregates below the surface were severely disrupted. The strength profile that developed on drying was similar to that for flood-wetted aggregates, with the soil being hardset rather than friable. Emergence resistance was generally higher for the pre-wetted than air-dry aggregates, which corresponds to the greater rate of infiltration for the former.

6.3.2 Emergence resistance characteristic

The relationship between degree of saturation of aggregate beds and emergence resistance (the emergence resistance characteristic) for various wetting treatments is shown in Figures 6.4 to 6.7. The strength of aggregate beds, arising from different methods of wetting, was depth dependent (Figures 6.2 to 6.7). Therefore, the emergence resistance characteristics of the beds were developed for depths of 0 to 10, 10 to 20 and 20 to 40 mm. The strength of suction wetted, flooded and suction wetted then flooded beds was uniform down the bed at all water contents. Consequently, only data for the 0 to 10 mm depths is shown in Figure 6.4. Data for other depths are shown as a contrast to rainfall data in Figures 6.6 and 6.7.

Figure 6.4 shows the emergence resistance characteristic for suction and flood wetting for the 0 to 10 mm depth. Similar characteristics were obtained for all depths. Suction wetted aggregate beds were weakest at all water contents. Drying the beds caused only a small increase in emergence resistance, from about 0.4 MPa at $S = 0.5$ to 2 MPa at $S = 0.06$. Flood wetting of air-dry aggregates caused greater aggregate disruption and a large increase of emergence resistance on drying. Flood wetting of pre-wetted aggregates caused the greatest amount of aggregate disruption and the strongest matrix on drying at all depths. Flood wetting of both air-dry and pre-wetted aggregate beds showed strength characteristics typical of hardsetting soil (Mullins *et al.*, 1990) throughout the depth of the aggregate beds.

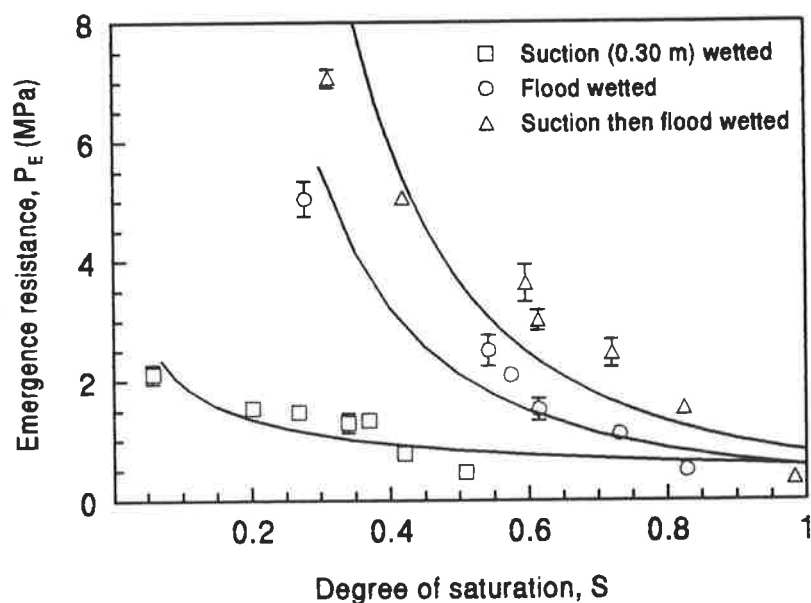


Figure 6.4. Emergence resistance characteristics for different methods of wetting at 0 to 10 mm depth. Error bars are $2 \times$ standard error of the means ($n = 8$).

Aggregate beds wetted by rainfall had a surface (0 to 10 mm) emergence characteristic which was similar to that resulting from flood wetting of air-dry aggregate beds (Figure 6.5). Neither antecedent water content of the beds, nor raindrop energy

appeared to have a marked effect on the emergence characteristic. However, when Equation 6.5 was fitted to these data, significant differences in the b values (Equation 6.4) were obtained for different rainfall kinetic energy flux density values (Table 6.1). The lower emergence resistance for rainfall wetting compared to flooding when the degree of saturation is less than 0.35 was due to a greater tendency for rainfall wetted aggregate beds to crack during the passage of the needle than flood wetted beds. (See also the results on emergence resistance, Section 5.3.1.2).

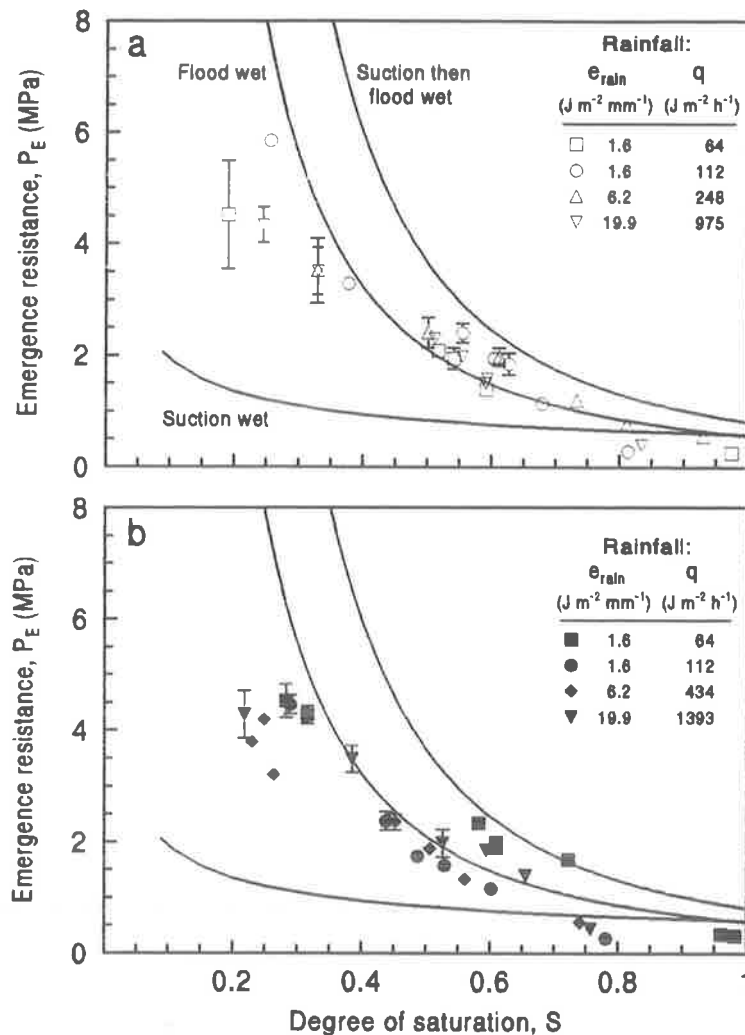


Figure 6.5. Emergence resistance characteristics of aggregate beds following rainfall of various kinetic energies (e_{rain}) and kinetic energy flux densities (q) on (a) initially air-dry and (b) pre-wetted (0.30 m suction) aggregate beds at 0 to 10 mm depth. Emergence resistance characteristics of suction (0.30 m), flood and suction then flood wetted beds (Figure 6.4) are superimposed on the data of rain treated beds for comparison. Error bars are $2 \times$ standard error of the means ($n = 8$).

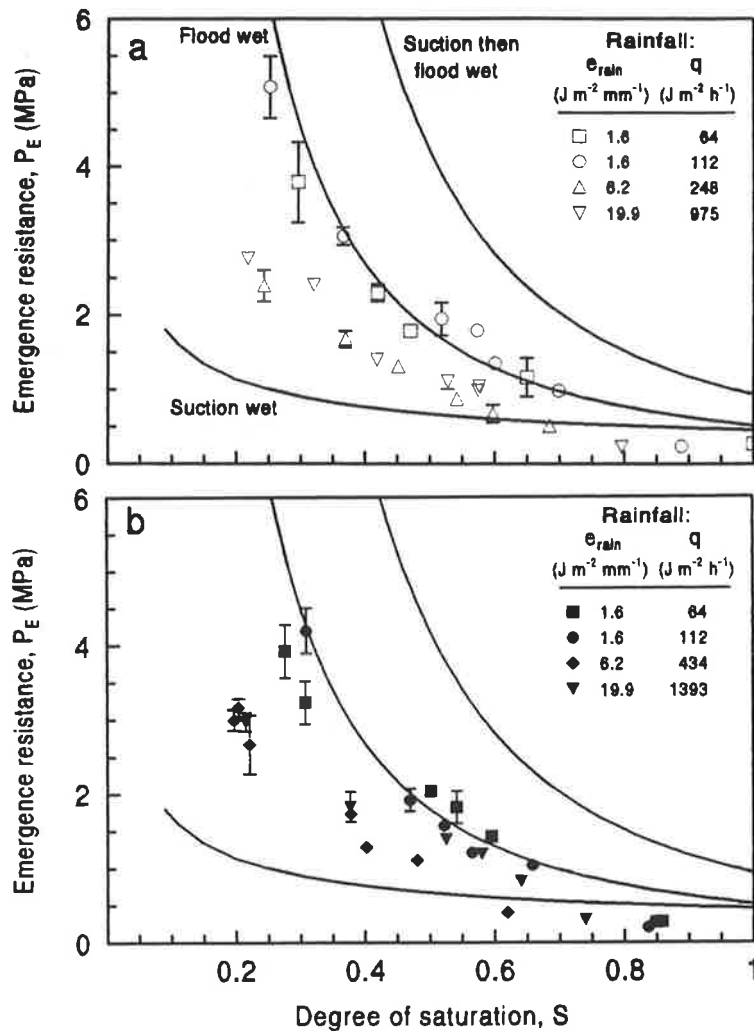


Figure 6.6. Emergence resistance characteristics of aggregate beds following rainfall of various kinetic energies (e_{rain}) and kinetic energy flux densities (q) on (a) initially air-dry and (b) pre-wetted (0.30 m suction) aggregate beds at 10 to 20 mm depth. Emergence resistance characteristics (10 to 20 mm) of suction (0.30 m), flood and suction then flood wetted beds are superimposed on the data of rain treated beds for comparison. Error bars are $2 \times$ standard error of the means ($n = 8$).

At the 10 to 20 mm depth, rainfall with kinetic energy of $1.6 J m^{-2} mm^{-1}$ and kinetic energy flux density of 64 to $112 J m^{-2} h^{-1}$ on air-dry aggregates gave emergence resistance characteristics similar to that for flood wetting of air-dry (Figure 6.6a), *i.e.* the

beds were hardset. At a rainfall kinetic energy of $6.2 \text{ J m}^{-2} \text{ mm}^{-1}$ or greater (kinetic energy flux density $> 248 \text{ J m}^{-2} \text{ h}^{-1}$), the aggregate beds at this depth were weaker, with the emergence resistance characteristic tending to approach that of the suction wetted aggregates, *i.e.* friable beds. Similar strength characteristics were observed for aggregate beds pre-wetted at 0.30 m suction prior to rainfall (Figure 6.6b).

At the 20 to 40 mm depth, the emergence resistance characteristics of pre-wetted aggregate beds and air-dry beds were similar for high kinetic energy ($>6.2 \text{ J m}^{-2} \text{ mm}^{-1}$) rainfall (Figures 6.7a and b). Low kinetic energy rainfall ($1.6 \text{ J m}^{-2} \text{ mm}^{-1}$) resulted in a stronger matrix at 20 to 40 mm, especially when the low kinetic energy rainfall was applied to pre-wetted beds. The shape of this characteristic resembled that of flood wetted beds (Figure 6.7b). These results indicate that low kinetic energy rainfall tended to produce hardsetting, while high kinetic energy rainfall produced crusting.

The effect of method of wetting and antecedent water content on the emergence resistance characteristic may be evaluated by the difference in value of the *b* exponent of Equation 6.4 as shown in Table 6.1. The smaller the *b* values (more negative), the more rapidly did emergence resistance develop on drying. Comparison of values of *b* for the surface (0 to 10 mm) with the layers below (10 to 20 and 20 to 40 mm) reflects differences in strength at these depths. Hardset beds had relatively constant and small *b* values throughout the entire depth of the bed. Crusted beds had smaller *b* values at the surface and larger at the deeper depths.

Data in Table 6.1 shows that both method of wetting and antecedent water content influenced the emergence resistance characteristic. Without rainfall, suction (0.30 m of water) wetting produced the largest (less negative) *b* values, *i.e.* weakest matrix structure. The *b* values were relatively constant (-0.526 to -0.576) at different depths in

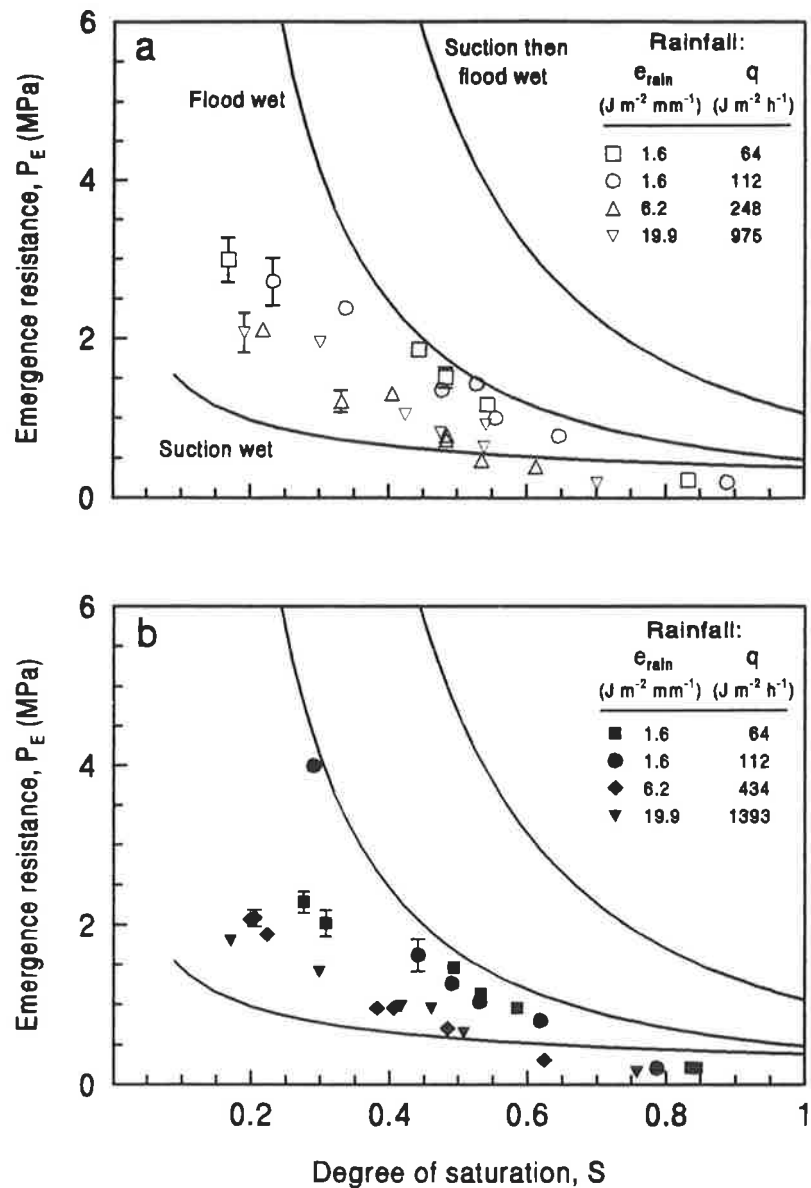


Figure 6.7. Emergence resistance characteristics of aggregate beds following rainfall of various kinetic energies (e_{rain}) and kinetic energy flux densities (q) on (a) initially air-dry and (b) pre-wetted (0.30 m suction) aggregate beds at 20 to 40 mm depth. Emergence resistance characteristics (20 to 40 mm) of suction (0.30 m), flood and suction then flood wetted beds are superimposed on the data of rain treated beds for comparison. Error bars are $2 \times$ standard error of the means ($n = 8$).

the soil bed. For flood wetting of air-dry aggregate beds, b values were lower (-1.788 to -1.905), and tended to increase slightly with depth. Flood wetting of pre-wetted (0.30 m suction) aggregate beds gave yet lower b values (-2.137 to -2.185), and again increased slightly with depth. The data indicate that, without rainfall, flood wetting of pre-wetted aggregate beds caused more rapid strength development than flood wetting of air-dry aggregate beds. Suction wetting caused little increase of emergence resistance on drying. Thus, without rainfall, flood wetting of pre-wetted aggregates caused the greatest aggregate disruption, followed by flood wetting, and suction wetting of air-dry aggregates (see data of vertical strain in Section 4.3.1).

Table 6.1 shows that wetting by rainfall at low kinetic energy ($1.6 \text{ J m}^{-2} \text{ mm}^{-1}$) gave more negative b values, reflecting a stronger matrix as the soil dried, than high kinetic energy rainfall ($>6 \text{ J m}^{-2} \text{ mm}^{-1}$). This difference between the two kinetic energies existed at all depths in the aggregate beds, but was more pronounced at depth than at the surface. Increasing rainfall kinetic energy flux density from 64 to $112 \text{ J m}^{-2} \text{ h}^{-1}$ at low raindrop energy ($1.6 \text{ J m}^{-2} \text{ mm}^{-1}$) led to a decreased value of b (stronger matrix), which was similar to the b value for flood wetting without rain.

Table 6.1. Effect of method of wetting on the coefficients (a and b) of the regression equation $P_E = a S^{-b}$, where P_E = emergence resistance and S = degree of saturation. Antecedent water content of dry and wet refer to air-dry and pre-wetted aggregates (0.30 m suction), respectively. R^2 is coefficient of determination. All relationships are significant at $p < 0.05$ to $p < 0.01$ (number of observations = 8).

Depth (mm)	Antecedent water content	Wetting method		a (MPa)	b	R^2	
		Without rainfall	With rainfall:				
			e_{rain} ($J m^{-2} mm^{-1}$)				q ($J m^{-2} h^{-1}$)
0 - 10	Dry	Suction		0.582	-0.526	0.596	
		Flood		0.565	-1.905	0.844	
		Flood		0.811	-2.185	0.782	
	Dry		1.6	64	0.493	-1.568	0.745
			1.6	112	0.471	-2.069	0.730
			6.2	248	0.611	-1.780	0.899
			19.9	975	0.544	-1.697	0.799
	Wet		1.6	64	0.493	-2.022	0.827
			1.6	112	0.235	-2.630	0.887
			6.2	434	0.546	-1.436	0.868
			19.9	1393	0.614	-1.492	0.710
	10 - 20	Dry	Suction		0.452	-0.575	0.601
Flood				0.518	-1.798	0.881	
Flood				0.938	-2.168	0.723	
Dry			1.6	64	0.344	-2.121	0.953
			1.6	112	0.375	-2.124	0.844
			6.2	248	0.338	-1.485	0.944
			19.9	975	0.307	-1.671	0.798
Wet			1.6	64	0.286	-2.272	0.861
			1.6	112	0.213	-2.804	0.878
			6.2	434	0.293	-1.517	0.896
			19.9	1393	0.382	-1.494	0.755
20 - 40		Dry	Suction		0.387	-0.576	0.567
	Flood			0.480	-1.788	0.879	
	Flood			1.061	-2.137	0.650	
	Dry		1.6	64	0.373	-1.390	0.686
			1.6	112	0.296	-1.813	0.815
			6.2	248	0.215	-1.599	0.880
			19.9	975	0.225	-1.582	0.743
	Wet		1.6	64	0.210	-2.102	0.851
			1.6	112	0.154	-2.810	0.935
			6.2	434	0.203	-1.502	0.943
			19.9	1393	0.198	-1.488	0.752

6.3.3 Effect of restricted drainage

High kinetic energy ($19 \text{ J m}^{-2} \text{ mm}^{-1}$) and intensity (70 mm h^{-1}) rainfall on pre-wetted aggregates, under conditions where drainage from the aggregate bed was restricted (Section 4.2.3), resulted in greater strength development of the aggregate bed on drying compared to well drained conditions (Figure 6.8). In poorly drained beds, a surface (0 to 10 mm) crust, with emergence resistance $>3 \text{ MPa}$ at matric suction of 5 m of water, was present and below this depth the bed was hardset (emergence resistance $>2 \text{ MPa}$ at 5 m suction). These strength values were appreciably greater than those obtained from well drained beds, where emergence resistance was 2 MPa at the surface and 1 MPa below 20 mm.

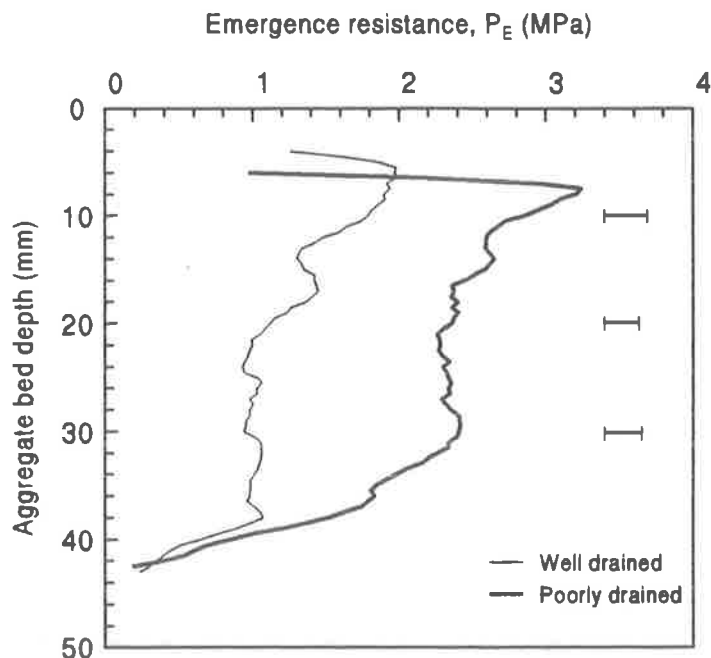


Figure 6.8. Effect of restricted drainage during rainfall on pre-wetted (0.30 m suction) aggregate beds on emergence resistance, measured at a matric suction of 5 m of water, after subjecting the beds to rainfall with kinetic energy of $19.9 \text{ J m}^{-2} \text{ mm}^{-1}$, and intensity of 70 mm h^{-1} . Error bars are $2 \times$ pooled standard error for 10, 20 and 30 mm depths.

Restriction of drainage caused considerably more aggregate disruption than when the beds were freely drained (Section 4.3.3). Drainage rate influences soil matric suction during wetting, an important factor affecting aggregate breakdown by wetting (Keller, 1970b; Ghavami *et al.*, 1974; Al-Durrah and Bradford, 1981; Francis and Cruse, 1983). Beds that had restricted drainage experienced considerably more aggregate disruption than the beds which had free drainage and developed greater strength on drying. The implications for field soils with poor drainage are clear. The effect of drainage on subsequent strength development has implications for studies using rainfall simulation on soil targets that do not have basal drainage. Results from such experiments may not be applicable to field conditions where free drainage exists.

6.3.4 Visible pores

Plate 6.1 shows the contrast of structural conditions between friable, crusted and hardset aggregate beds resulting from various methods of wetting and subsequent drying. Note the difference in disruption between the surface and the layer below the surface of crusted and hardset aggregate beds. The friable aggregate beds were weak when dry, so that they easily broke down during handling.

The difference in packing and strength between different methods of wetting shown in Plate 6.1 agrees well with the estimates of visible pores (>0.25 mm diameter) observed on the cross section of beds by video imaging (Table 6.2). Suction wetting preserved more pores of this size class than flood or rainfall wetting. Flood wetting of air-dry aggregates appears to have destroyed a large fraction of these pores, with only half of the amount being observed in suction-wetted beds. Flood wetting of pre-wetted

aggregate beds resulted in the lowest proportion of these pores. Rainfall of high kinetic energy and intensity, which produced a surface seal, destroyed a similar proportion of visible pores flood wetting of pre-wetted aggregates.

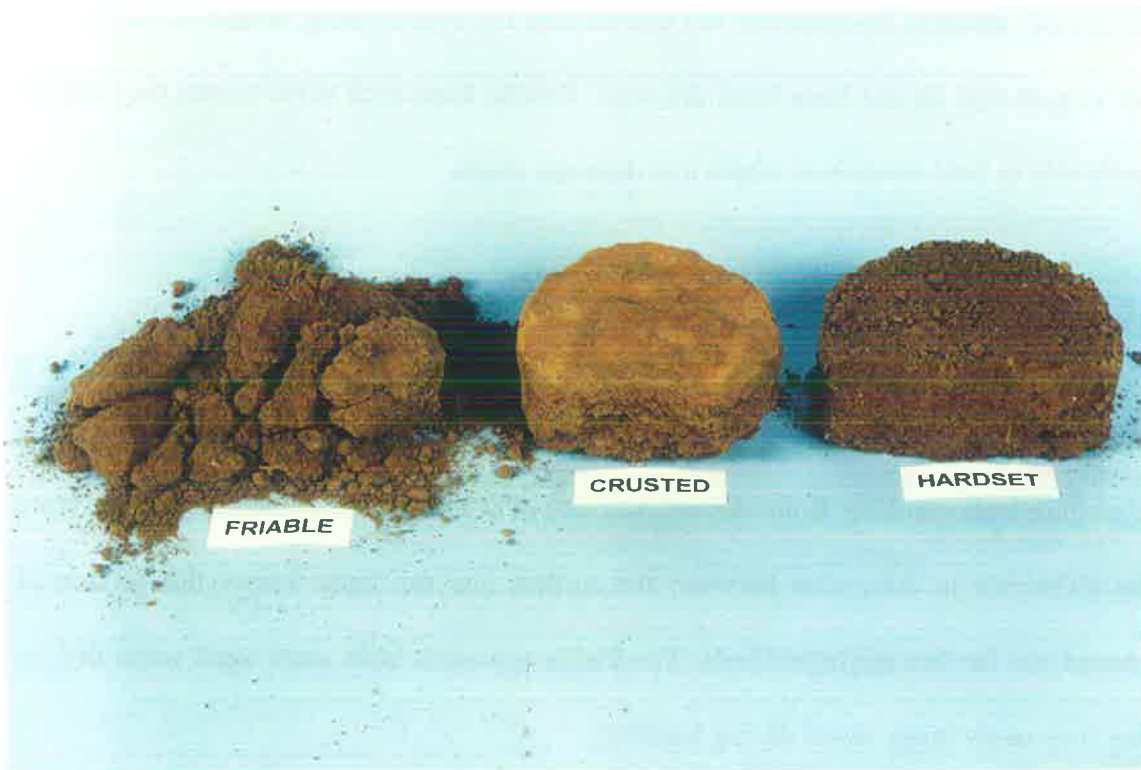


Plate 6.1. Surface features of Kapunda soil produced by different methods of wetting and different antecedent soil water contents: *friable* (resulted from suction wetting air-dry aggregates at 0.30 m of water suction); *crusted* (high rainfall kinetic energy and intensity, $19.9 \text{ J m}^{-2} \text{ mm}^{-1}$ and 70 mm h^{-1} , on air-dry aggregates); and *hardset* (flood wetting of air-dry aggregates).

Table 6.2. Effect of method of wetting on the proportion of pores > 0.25 mm, as measured by digital image processing of the vertical cross section of aggregate beds.*

Method of wetting	Structural condition	Relative pores > 0.25 mm	
		Mean	Standard error
Suction wetting	Friable	0.042	0.0034
Rainfall of 19.9 J m ⁻² mm ⁻¹ , 70 mm h ⁻¹ on air-dry aggregates	Crusted (0 to 10 mm)	0.014	0.0020
Flood wetting of air-dry aggregates	Hardset	0.020	0.0009
Flood wetting of suction (0.30 m) wetted aggregates	Hardset	0.011	0.0012

* Computer code for the digital image analysis was written by C. T. Hignett, CSIRO Div. of Soils, Adelaide, S.A., Australia

6.4 Conclusions

1. Suction wetting of friable air-dry aggregates, either by capillary rise or as a result of the development of a sealed layer above the aggregate bed, maintained the integrity of aggregates, reducing aggregate disruption and producing weak (friable) beds on drying (emergence resistance < 1 MPa at a matric suction of 5 m of water).

2. Wetting of air-dry or pre-wetted aggregates by flooding or by low kinetic energy rainfall but with high enough intensity so that water influx was high, tended to cause disruption throughout the aggregate bed, producing typically hardset profiles. Emergence resistance was > 1.9 MPa throughout the bed at a matric suction of 5 m of water. However, disruption by rainfall was deeper for the pre-wetted than for the air-dry aggregates.
3. High kinetic energy rainfall on air-dry or pre-moistened aggregates caused aggregate disruption at the surface, forming a surface seal which reduced influx of water, maintaining a higher soil water suction and reduced aggregate disruption below the seal. On drying, this produced a strong surface crust (emergence resistance > 2 MPa at a matric suction of 5 m), with weaker aggregates below the crust (≤ 1 MPa at matric suction of 5 m).
4. Rainfall on pre-moistened aggregates tended to form surface crusts at rainfall kinetic energies much lower ($6.2 \text{ J m}^{-2} \text{ mm}^{-1}$) than the kinetic energy that caused crusting on air-dry aggregates ($19.9 \text{ J m}^{-2} \text{ mm}^{-1}$).
5. Rainfall on aggregate beds with poor drainage produced a stronger matrix than similar rainfall on well drained beds. Poor drainage exacerbated hardsetting by rainfall.

6.5 References

- Agassi, M., J. Morin, and I. Shainberg (1985). Effect of raindrop impact energy and water salinity on infiltration rates of sodic soils. *Soil Science Society of America Journal* 49: 186-190.
- Al-Durrah, M. M. and J. M. Bradford (1981). New methods of studying soil detachment due to waterdrop impact. *Soil Science Society of America Journal* 45: 949-953.

- Arndt, W. (1965). The nature of the mechanical impedance to seedlings by soil surface seals. *Australian Journal of Soil Research* 3: 45-54.
- Becher, H. H. (1994a). Evaluating the resistance to penetration within the surface layer of soil aggregates. *Soil Technology* 7: 105-111.
- Becher, H. H. (1994b). Soil compaction around a small penetrating cylindrical body and its consequences. *Soil Technology* 7: 83-91.
- Bedaiwy, M. N. and D. E. Rolston (1993). Soil surface densification under simulated high intensity rainfall. *Soil Technology* 6: 365-376.
- Bristow, K. L., A. Cass, K. R. J. Smettem, and P. J. Ross (1994). Modelling effects of surface sealing on water entry and re-distribution. Proceedings of the International Symposium on 'Sealing, Crusting, Hardsetting Soils: Productivity and Conservation' 7-11 February 1994, University of Queensland, Brisbane, Australia (*in press*).
- Burwell, R. E. and W. E. Larson (1969). Infiltration as influenced by tillage-induced random roughness and pore space. *Soil Science Society of America Proceedings* 33: 449-452.
- Dexter, A. R. (1987). Compression of soil around roots. *Plant and Soil* 97: 401-406.
- Duley, F. L. (1939). Surface factors affecting the rate of intake of water by soils. *Soil Science Society of America Proceedings* 4: 60-64.
- Eigel, J. D. and I. D. Moore (1983). Effect of rainfall energy on infiltration into bare soil. Proc. of the National Conf. on Advances in Infiltration, Dec. 12-13, 1983, Chicago, Illinois, ASAE, p. 188-200.
- Farres, P. (1978). The role of time and aggregate size in the crusting process. *Earth Surface Processes* 3: 243-254.
- Francis, P. B. and R. M. Cruse (1983). Soil water matric potential effects on aggregate stability. *Soil Science Society of America Journal* 47: 578-581.
- Freebairn, D. M. and S. C. Gupta (1990). Microrelief, rainfall and cover effects on infiltration. *Soil and Tillage Research* 16: 307-327.
- Fritton, D. D. (1990). A standard for interpreting soil penetrometer measurements. *Soil Science* 150: 542-551.
- Ghavami, M., J. Keller, and I. S. Dunn (1974). Predicting soil density following irrigation. *Transactions of the American Society of Agricultural Engineers* 17: 166-171.
- Groenevelt, P. H., B. D. Kay, and C. D. Grant (1984). Physical assessment of a soil with respect to rooting potential. *Geoderma* 34: 101-114.
- Gusli, S., A. Cass, D. A. MacLeod, and P. S. Blackwell (1994a). Structural collapse and strength of some Australian soils in relation to hardsetting: I. Structural collapse on wetting and draining. *European Journal of Soil Science* 45: 15-21.
- Gusli, S., A. Cass, D. A. MacLeod, and P. S. Blackwell (1994b). Structural collapse and strength of some Australian soils in relation to hardsetting: II. Tensile strength of collapsed aggregates. *European Journal of Soil Science* 45: 23-29.

- Holder, C. B. and K. W. Brown (1974). Evaluation of simulated seedling emergence through rainfall induced soil crusts. *Soil Science Society of America Proceedings* 38: 705-710.
- Keller, J. (1970a). Control of soil moisture during sprinkler irrigation. *Transaction of the American Society of Agricultural Engineers* 13: 885-890.
- Keller, J. (1970b). Sprinkler intensity and soil tilth. *Transactions of the American Society of Agricultural Engineers* 13: 118-125.
- Le Bissonnais, Y., A. Bruand and M. Jamagne (1989). Laboratory experimental study of soil crusting: relation between aggregate breakdown mechanisms and crust structure. *Catena* 16: 377-392.
- Morrison, M. W., L. Prunty, and J. F. Giles (1985). Characterizing strength of soil crusts formed by simulated rainfall. *Soil Science Society of America Journal* 49: 427-431.
- Mullins, C. E., D. A. MacLeod, K. H. Northcote, J. M. Tisdall, and I. M. Young (1990). Hardsetting soils: behaviour, occurrence, and management. *Advances in Soil Science* 11: 37-108.
- Mullins, C. E., A. Cass, D. A. MacLeod, D. J. M. Hall and P. S. Blackwell (1992). Strength development during drying of cultivated, flood-irrigated hardsetting soil. II. Trangie soil, and comparison with theoretical predictions. *Soil and Tillage Research* 25: 129-147.
- Panabokke, C. R. and J. P. Quirk (1957). Effect of initial water content on stability of soil aggregates in water. *Soil Science* 83: 185-195.
- Shainberg, I. and M. Singer (1988). Drop impact energy - soil exchangeable sodium percentage interactions in seal formation. *Soil Science Society of America Journal* 52: 1449-1452.
- Tackett, J. L. and R. W. Pearson (1965). Some characteristics of soil crusts formed by simulated rainfall. *Soil Science* 99: 407-413.
- Timm, H., J. C. Bishop, J. W. Perdue, D. W. Grimes, R. E. Voss, and D. N. Wright (1971). Soil crusting effects on potato plant emergence and growth. *California Agriculture* 25 (8): 5-7.
- Weaich, K., A. Cass, and K. L. Bristow (1992). Use of a penetration resistance characteristic to predict soil strength development during drying. *Soil and Tillage Research* 25: 149-166.

Chapter 7

General discussion: Factors that determine crusting or hardsetting in Kapunda red-brown earth

7.1 Introduction

Figure 7.1 summarises the soil and rainfall factors and the sequence of processes that are thought to determine the surface condition of a soil after rainfall or irrigation. The extent of aggregate disruption during rainfall and the subsequent formation of a crust or hardset layer was found to be dependent on kinetic energy flux density of rainfall (a function of rainfall kinetic energy and intensity), soil antecedent water content, and internal drainage rate of the soil during rainfall.

The changes in surface soil structure induced by rainfall involved a number of stages (Figure 7.1), beginning with aggregate breakdown. The finer fragments generated by aggregate disruption increased the hydraulic resistance at the surface, restricting the rate of water entry into soil. In turn, reduced influx of water through the surface modified the matric suction of water in deeper layers of the soil. Disruption, packing and vertical straining of aggregates below the surface was decreased if the matric suction is high and *vice versa*. The structural condition of the aggregates then influenced the development of strength during drying. Because the changes were sequential, the extent of structural change in the first stage (aggregate breakdown and development of hydraulic resistance) determined the successive stages which ultimately determined whether an aggregate bed developed a friable, hardset or crusted surface condition.

RAIN FACTORS

SOIL PROCESSES

SOIL FACTORS

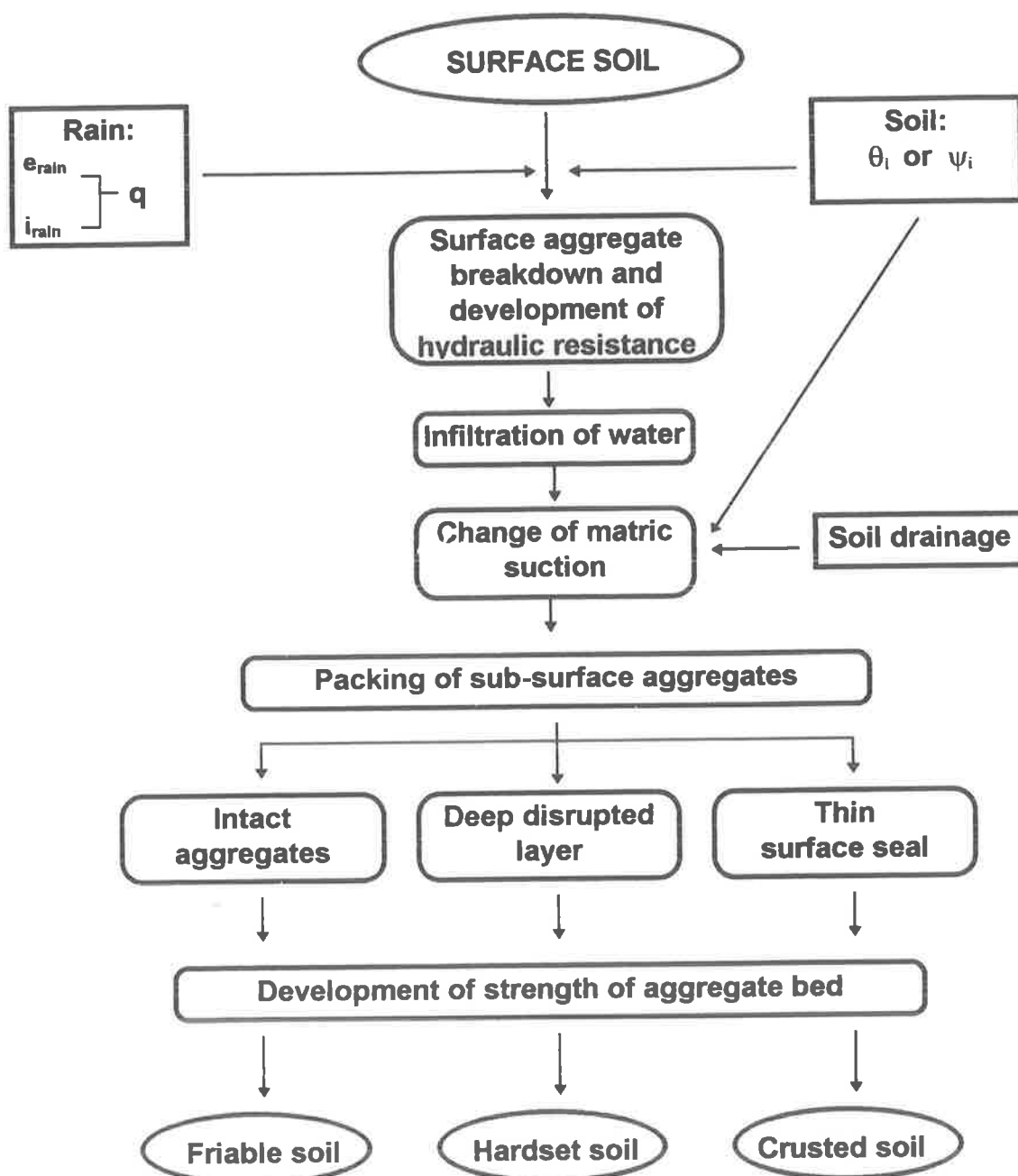


Figure 7.1. Factors and processes which determined the surface condition of Kapunda red-brown earth after rainfall. Symbols e_{rain} , i_{rain} , and q are rainfall kinetic energy, intensity, and kinetic energy flux density, respectively, θ_i is antecedent soil water content and ψ_i is antecedent soil matric suction.

The present results show that there were three distinct stages in the process of hardsetting due to rain falling on a bed of Kapunda friable aggregates: (1) some disruption and rearrangement of aggregates at the surface which lead to some reduction in surface hydraulic conductivity, yet allowed water to enter the soil at a relatively fast rate at a low matric suction; (2) disruption and packing of aggregates at depth below the surface; and (3) development of strength on drying that was more deeply distributed in the soil than a typical crust. Surface sealing occurred when aggregate disruption at the surface was more extensive and a large hydraulic resistance developed so that water entry was slow and occurred at a high matric suction.. Disruption and packing of aggregates below the seal was minimal and on drying a thin surface crust formed but aggregates below the crust remained friable .

7.2 Development of hydraulic resistance

The kinetic energy and intensity of rainfall and antecedent water content of the soil determine the extent of aggregate disruption and the magnitude of hydraulic resistance of the surface, *i.e.* whether a seal is formed or not (Figure 7.1). The development of hydraulic resistance during rainfall may be gauged by the progressive increase in the proportion of materials (aggregates or particles) smaller than 0.125 mm at the surface (Chapter 4). The higher the proportion of fine materials, the greater the hydraulic resistance and hence the smaller the infiltration rate and the higher the matric suction of the inflowing water. Soil matric suction during wetting is an important factor governing aggregate breakdown and packing (Panabokke and Quirk, 1957; Al-Durrah and Bradford, 1981; Francis and Cruse, 1983; Gusli *et al.*, 1994a).

Soil internal drainage rate also influenced matric suction during wetting, as it controlled the balance between inflow and outflow of water, and therefore the net rate of wetting and change of matric suction during rainfall. If rain water influx was higher than internal drainage rate, the soil become saturated, aggregates were weakened and easily deformed by the overburden weight, by pressure waves of raindrop impact (Alder, 1979; Moss, 1991), or possibly by the mechanical action of flowing water (Collis-George and Green, 1979) during rainfall. A fast rate of water influx combined with slow internal drainage rate produced optimum conditions for sub-surface aggregate disruption (Chapter 4).

7.3 Packing of disrupted aggregates

During rainfall, aggregate breakdown and packing of the fragments occurred at the surface as a result of wetting and the direct impact of raindrops. The extent of breakdown and size of fragments produced determined the magnitude of hydraulic resistance which controlled the rate of water entry through the soil surface (Figure 7.1). Disruption of aggregates below the surface (> 10 mm depth) is only possible if a surface seal does not form (Farres, 1978; West, *et al.*, 1992; Bedaiwy and Rolston, 1993). Rainfall intensity indirectly influenced packing of sub-surface (deeper than 10 mm) aggregates and, in the absence of a surface seal, dictated whether Kapunda soil developed a thin or deep disrupted layer or remained friable.

The higher the kinetic energy or kinetic energy flux density, the greater was the proportion of fine materials that were produced at the expense of large aggregates, and the greater the hydraulic resistance or degree of sealing. Extensive surface aggregate

breakdown during rainfall with high kinetic energy ($>6.2 \text{ J m}^{-2} \text{ mm}^{-1}$), resulted in a high proportion of fine material ($< 0.125 \text{ mm}$) at the surface, which allowed rapid development of a surface seal, which subsequently reduced wetting of aggregates below the surface. The disrupted layer was, therefore, thin and was limited to the immediate surface only. However, if kinetic energy was low ($1.6 \text{ J m}^{-2} \text{ mm}^{-1}$), less fine material was generated by aggregate breakdown, hydraulic resistance remained low and the possibility of rapid water penetration to depth existed. Consequently, if rainfall intensity was high ($> 40 \text{ mm h}^{-1}$) aggregate disruption below the surface occurred and the entire aggregate bed set hard on drying. If rainfall intensity was low, aggregate disruption was less and the aggregate bed remained friable.

One way to assess packing of disrupted aggregates is to measure vertical strain (Gusli *et al.*, 1994a). Vertical strain expresses the change of aggregate bed height after wetting and drying relative to the height before wetting. It is, therefore, a reflection of the overall change of structural condition within a given reference thickness of aggregate bed. Because the aggregate beds (50 mm deep) extended beyond the depth of the surface layer directly affected by raindrop energy ($<10 \text{ mm}$), the change of vertical strain as a result of rainfall gave a measure of the disruption of aggregates below the surface.

Vertical strain of aggregate beds following rainfall and drying was found to be directly related to water infiltration rate (Chapter 4). The higher the infiltration rate, the greater was the vertical strain. The relationship between vertical strain and infiltration rate varied, however, according to kinetic energy. The higher the kinetic energy, the greater the aggregate packing and the greater the vertical strain. This indicates that there was an interaction between effects of rate of wetting and the mechanical effects of raindrop energy.

Antecedent water content did not change the relationship between vertical strain and infiltration rate for Kapunda red-brown earth, but it controlled the extent of aggregate packing resulting from a given kinetic energy through its effect on infiltration rate. Pre-wetting of aggregates reduced the generation of fine materials by raindrop impact and hence increased infiltration rate and packing of aggregates below the surface (Chapter 4).

The higher infiltration rate for pre-wetted aggregates caused consistently greater vertical strain for any given rainfall kinetic energy. As explained in Section 7.2, the drop in matric suction during rainfall was associated with the greater packing observed in pre-wetted beds. A similar result was obtained for flood wetting treatments: flood wetting of pre-wetted beds caused greater collapse than flood wetting of air-dry beds (Chapter 4).

Figure 7.2 postulates a mechanism explaining why flood wetting of pre-wetted aggregates showed greater packing than flood wetting air-dry aggregates. Wetting air-dry aggregates to about zero matric suction (by flooding or by a high infiltration rate of rain water) caused slaking of aggregates (Figure 7.2 A). The precursors for slaking are differential stresses due to swelling and the pressure of entrapped air during rapid wetting (Emerson and Grundy, 1954; Emerson, 1977). Because of these stresses, the aggregates will tend to break down along any planes of weakness that exist in the aggregates. The size of slaked fragments is variable, but generally greater than 0.5 mm (Chan and Mullins, 1994). This indicates that forces induced by swelling and entrapped air are exerted at a high hierarchical level, between the coarser fragments that constitute the aggregates. Once the stresses are released by aggregate comminution, further aggregate breakdown to produce finer fragments or release primary particles does not seem to occur.

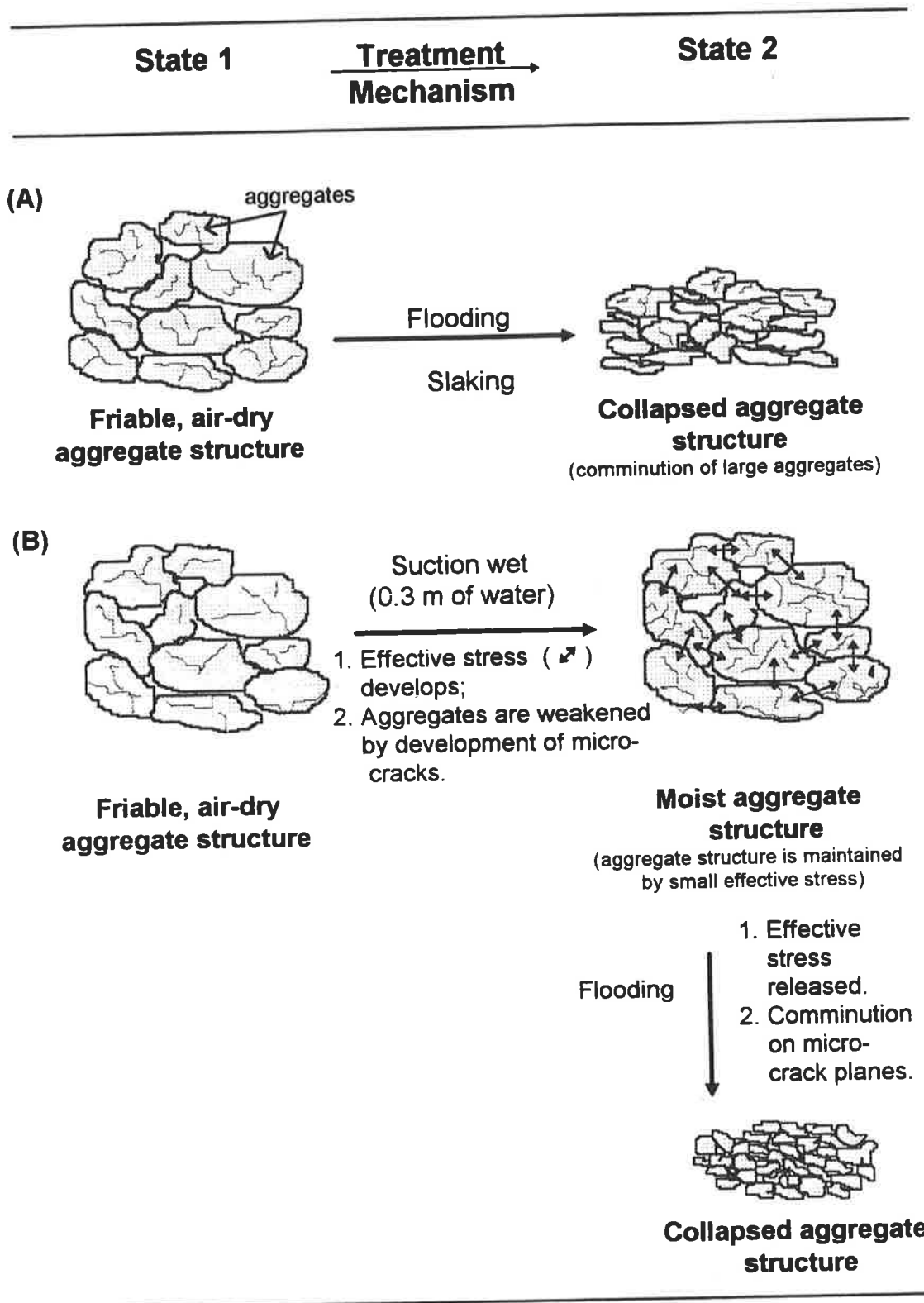


Figure 7.2. Aggregate deformation by wetting of friable aggregates (State 1) to produce collapsed aggregate structure (States 2). (A) flood wetting of air-dry aggregates causing disruption due to slaking (differential swelling and the pressure of trapped air); (B) suction wetting of air dry aggregates then flood wetting of the moist aggregates causing disruption due to the release of effective stress.

Pre-wetted aggregates of Kapunda soil did not slake, as expected from the work of Panabokke and Quirk (1957), Le Bissonnais *et al.* (1989) and Chan and Mullins (1994). Wetting air dry aggregates under a matric suction avoids the build up of stresses due to differential swelling and the pressure of entrapped air associated with flood wetting. The matric suction creates an effective stress which acts to hold aggregates and fragments of aggregates together during the wetting process (Figure 7.2 B). However, suction wetted aggregates are weakened due to the development of an extensive system of micro-cracks (Quirk and Panabokke, 1962). When wetted further by flooding at zero matric suction, the suction wetted Kapunda aggregates were disrupted by loss of effective stress. Because of the system of fine micro-cracks created by suction wetting, the fragments released were probably finer than those measured from flooding of air-dry aggregates (Section 4.3.2) and deformation and packing was more extensive than flood wetting of air-dry aggregates.

Depending on rainfall kinetic energy and intensity and antecedent soil water content, three different aggregate structures were produced at the surface of Kapunda soil (Figure 7.1). Low rainfall kinetic energy and intensity ($1.6 \text{ J m}^{-2} \text{ mm}^{-1}$ and 40 mm h^{-1} , respectively) did not disrupt aggregates, packing was minimal and the beds remained friable on drying. When rainfall kinetic energy was high ($>6.2 \text{ J m}^{-2} \text{ mm}^{-1}$), a surface seal formed, infiltration rate was reduced to less than 25 mm h^{-1} and deep aggregate disruption was prevented. The thickness of the surface seal tended to decrease with increasing intensity. A seal was readily formed on air-dry aggregates, but the seal was deeper for pre-wetted beds.

Rainfall of low kinetic energy ($1.6 \text{ J m}^{-2} \text{ mm}^{-1}$) but high intensity (70 mm h^{-1}) caused a deep ($\sim 50 \text{ mm}$) homogenous, disrupted layer to form. The depth of the

disrupted layer was greater for pre-wetted beds than for air-dry beds. The resulting aggregate packing was similar to that observed from flood wetting of air-dry aggregates (Chapter 4). The overall effect of wetting by rainfall of low kinetic energy and high (70 mm h^{-1}) intensity, especially on pre-wetted beds, was hardsetting on drying. Increasing intensity to 100 mm h^{-1} , for any kinetic energy level, tended to produce a thinner disrupted layer which formed a crust on drying.

7.4 Strength development

The primary difference between friable, on the one hand, and crusted or hardset soil on the other hand, is the magnitude of strength development on drying (*i.e.* the shape of the strength characteristic). The strength of a soil with friable structure does not increase markedly on drying while that of crusts and hardset layers does. The primary difference between crusted and hardset soil is the way strength is distributed with depth at any water content. Crusted soil has a high strength at the surface, which decreases with depths beyond about 10 mm. Hardset soil has uniformly high strength to greater depths which correspond to the depth to which water penetrated during wetting. Each of these strength features have been produced in Kapunda soil by varying antecedent soil water content, method of wetting and the energy and intensity of rain falling on the surface.

Strength development of soil during drying is determined by the extent of disruption and packing (vertical strain) during wetting and subsequently during drying (Gusli et al., 1994b). The greater the disruption and packing, the higher the strength. This study confirmed this finding and extended it to rainfall wetting. In the case of flood and suction wetting, soil strength remained fairly constant throughout the depth of the

aggregate bed because these modes of wetting produced fairly uniform aggregate wetting and consequently aggregate disruption. In the case of suction wetting, beds did not develop marked strength on drying because aggregates were not disrupted by the suction wetting. Flood wetted beds, on the other hand, did develop strength rapidly on drying because aggregate disruption was more extensive.

In the case of wetting by rainfall, distribution of strength with depth varied according to rainfall conditions and antecedent water content. This was because rainfall did not necessarily produce uniform wetting down the depth of the aggregate beds. Beds subjected to high energy rainfall ($>6.2 \text{ J m}^{-2} \text{ mm}^{-1}$) suffered rapid and extensive aggregate breakdown at the surface, forming a surface seal which moderated aggregate disruption below the surface. On drying they developed a thin crust ($< 10 \text{ mm}$), which had a high strength ($>2 \text{ MPa}$ at a matric suction of 5 m). Below the surface, aggregates remained friable and had low strength ($<1 \text{ MPa}$ at 5 m of water). Aggregate beds subjected to low energy ($<6.2 \text{ J m}^{-2} \text{ mm}^{-1}$) and high intensity ($>40 \text{ mm h}^{-1}$) rainfall had a high rate of water entry during rainfall and aggregate disruption at depth was more extensive and homogenous throughout a greater depth. These beds set hard on drying (strength was greater than 1.9 MPa at a matric suction of 5 m), resembling flood wetted beds in all respects.

The antecedent water content of the soil was an important factor in determining surface structural condition during wetting. Flood wetting of pre-wetted aggregate beds caused the most aggregate disruption and development of the highest strength. Rainfall on pre-wetted aggregate beds tended to form strong surface crusts at rainfall kinetic energies much lower ($6.2 \text{ J m}^{-2} \text{ mm}^{-1}$) than the kinetic energy that caused strong crusts to develop on air-dry aggregates ($19.9 \text{ J m}^{-2} \text{ mm}^{-1}$).

Rainfall on aggregate beds with restricted basal drainage caused more aggregate disruption than on well drained beds and this resulted in development of much greater strength on drying. Generally, poor drainage tended to exacerbate hardsetting by rainfall.

7.5 Relationship to other soils

Only one soil was used in this study, the Kapunda red-brown earth, although the original intention had been to investigate a range of soils. However, restrictions of time and the need to investigate fully the response of at least one soil to a range of rainfall conditions, wetting, initial water content and drainage precluded much work on the other soils.

Kapunda soil was chosen for this purpose because of field observations showing that the soil fluctuated between hardsetting, crusting or a friable condition, depending on management and environmental conditions. It therefore provided an ideal opportunity for establishing the methodology and basic principles of the study.

A red-brown earth from Trangie in New South Wales was one of the other soils sampled for inclusion in the research project reported in this thesis. Several experiments were done involving air-dry and pre-wetted aggregates wetted by flooding and rainfall of similar energy to the experiments reported here. Rainfall intensities of 40 and some 70 mm h⁻¹ were used. The data sets were too incomplete for proper inclusion in this thesis, but useful indications were nevertheless available from this work. Marked similarities between Kapunda and Trangie soils were observed in respect to:

- 1) steady state infiltration as a function of fine materials for both air dry and pre-wetted aggregates;
- 2) vertical stain as a function of method of wetting and rainfall properties;

3) the development of strength as a function of method of wetting and rainfall properties.

These preliminary comparisons support the notion that these two soils will behave in a similar way under most circumstances.

Gusli *et al.* (1994a and b) have established the relative behaviour of Trangie red-brown earth to that of a range of south eastern Australian soils. This work showed that a range of responses to flood wetting was present, indicating that soil behaviour to wetting depended on both intrinsic soil properties and management history. Accordingly, it is unlikely that the empirical results from the study reported here will be directly transferable to all soils without accounting for these factors. Further evidence indicating that some soil differences can be anticipated was reported by Hignett (1991). He showed that a kinetic energy of $12 \text{ J m}^{-2} \text{ mm}^{-1}$ was necessary for seal formation during rainfall on a range of South Australian soils. The equivalent kinetic energy for Kapunda was $6.2 \text{ J m}^{-2} \text{ mm}^{-1}$. However, the similarity between Trangie and Kapunda soils suggests that the Kapunda model will be applicable to at least some weakly structured red-brown earths without further adaptation.

7.6 Practical implications

The effect of rainfall kinetic energy flux density (determined by both kinetic energy and intensity) and antecedent water content on the surface condition of soil after rainfall has important implications for soil management. Practices that can influence kinetic energy and antecedent water content are, for example, mulching and sprinkler irrigation.

Covering the soil surface with mulch or by retaining stubble can reduce the impact energy of raindrops on the surface aggregates. Although mulching is likely to reduce rainfall kinetic energy, it will also reduce evaporation and keep the soil moist for longer periods. This might create conditions appropriate for the development of hardsetting in unstable soils such as Kapunda red-brown earth, especially if the rainfall intensity is high. If the intensity is low ($<40 \text{ mm h}^{-1}$), however, the soil should remain friable. Because rainfall intensity at Kapunda is generally below 40 mm h^{-1} (Canterford, 1987), surface cover will be effective in maintaining a friable soil condition. However, a short period of intense rain would be sufficient to cause aggregate disruption below the mulch layer, ultimately leading to hardsetting. Hardsetting of disturbed soil has been observed at Kapunda during the winter months which persists into the drier summer months (Hignett, 1989).

According to the isohyet map for South Australia (Canterford, 1987), rainfall of 16 mm h^{-1} for 1 hour duration has a recurrence interval of 2 years at Kapunda. From the intensity - kinetic energy relationship of Rosewell (1986), this rainfall intensity has a kinetic energy of $22 \text{ J m}^{-2} \text{ mm}^{-1}$, which is much higher than the estimated threshold value of kinetic energy ($>6.2 \text{ J m}^{-2} \text{ mm}^{-1}$) for seal formation on Kapunda soil. Clearly, when left bare, freshly tilled Kapunda red-brown earth would, under this rainfall, most likely form a surface seal and develop a crust on drying. Field observations support this assertion.

It is obvious that at the present level of aggregate stability, maintaining good structure in Kapunda soil is difficult. Management systems with emphasis on stubble retention are essential for improving aggregate stability and protecting the soil surface. The surface cover should reduce the kinetic energy to below the critical value of 6.2 J

$\text{m}^{-2} \text{mm}^{-1}$. The effect of mulch on slowing the rate of wetting needs to be investigated. Its effectiveness would probably depend on the rainfall pattern. Application of a thick layer of mulch might not prevent hardsetting if the rainfall is intense and prolonged. Under these conditions the rate of wetting at the subsurface soil might cause deeply distributed aggregate disruption, leading to hardsetting on drying.

Irrigation of Kapunda red-brown earth demands low intensity sprinkler irrigation systems ($\ll 25 \text{ mm h}^{-1}$). Low intensity sprinkler irrigation systems have the potential to maintain good soil structure (Keller, 1970; Thompson and James, 1985; Mohammed and Kohl, 1987).

7.7 Suggestions for future research

Owing to the complexity of hardsetting under rainfall, the use of computer modelling to describe the process would seem to be appropriate. Through modelling it should be possible to relate rainfall factors and soil conditions to surface aggregate breakdown, infiltration into sub-surface layers and how it relates to sub-surface aggregate collapse and strength development (Figure 7.1). For this purpose, the empirical relationships established in this study can be set in a conceptual framework through appropriate modelling as has been done by Bristow *et al.* (1994) for surface sealing. The limitation at present is the applicability of results for Kapunda red-brown earth to other soils. As previously mentioned, this is largely unknown at present.

To redress this deficiency, a study similar to that reported in this thesis, using various soil types which have different particle-size distributions, mineralogy, organic matter contents and management histories is needed. Differences in these factors should

reflect differences in aggregate stability and therefore resistance to breakdown by rainfall. Results from a wider range of soil types should strengthen our understanding of the process of hardsetting by rainfall and allow development of appropriate models for predicting how different soils might behave under different conditions.

This study was done without considering the role that plants play in moderating the energetics of wetting. The study needs to be extended to include effects of surface cover by crop residues and the influence of roots on soil structural stability. Roots and fungal hyphae are essential for improved soil aggregation and aggregate stability (Tisdall and Oades, 1979). They are likely to influence the stability of aggregates against sealing and deep disruption by rainfall. A better understanding of the interaction between the root system, soil matric suction and rainfall kinetic energy and intensity will improve our knowledge of the process of hardsetting by rainfall.

7.8 References

- Alder, W. F. (1979). The Mechanics of Liquid Impact. *In: Carolyn M. Preece (ed.). Treatise on Materials Science and Technology. Volume 16: Erosion.* Academic Press, New York, p. 127-183.
- Al-Durrah, M.M. and J.M. Bradford (1981). New methods of studying soil detachment due to waterdrop impact. *Soil Science Society of America Journal* 45: 949-953.
- Bedaiwy, M. N. and D. E. Rolston (1993). Soil surface densification under simulated high intensity rainfall. *Soil Technology* 6: 365-376.
- Bristow, K. L., A. Cass, K. R. J. Smettem, and P. J. Ross (1994). Modelling effects of surface sealing on water entry and re-distribution. Proceedings of the International Symposium on 'Sealing, Crusting, Hardsetting Soils: Productivity and Conservation' 7-11 February 1992, University of Queensland, Brisbane, Australia. (*in press*).
- Brunton, J. H. and M. C. Rochester (1979). Erosion of solid surfaces by the impact of liquid drops. *In: Carolyn M. Preece (ed.). Treatise on Materials Science and Technology. Volume 16: Erosion.* Academic Press, New York, p. 185-248.
- Canterford, R. P. (1987). Australian Rainfall and Runoff. A guide to flood estimation. Vol. 2. The Institution of Engineers Australia, Barton, p. 57-62.

- Chan, K. Y. and C. E. Mullins (1994). Slaking characteristics of some Australian and British soils. *European Journal of Soil Science* 45: 273-283.
- Collis-George, N. and R. S. B. Green (1979). The effect of aggregate size on infiltration behaviour of a slaking soil and its relevance to ponded irrigation. *Australian Journal of Soil Research* 17: 65-73.
- Emerson, W. W. (1977). Physical properties and structure. In: J. S. Russell and E. L. Greacen (eds.). *Soil Factors in Crop Production in a Semi-Arid Environment*. Queensland University Press. p. 78-104.
- Emerson, W. W. and G. M. F. Grundy (1954). The effect of rate of wetting on water uptake and cohesion of soil crumbs. *Journal of Agricultural Science* 44: 249-253.
- Farres, P. (1978). The role of time and aggregate size in the crusting process. *Earth Surface Processes* 3: 243-254.
- Francis, P. B. and R. M. Cruse (1983). Soil water matric potential effects on aggregate stability. *Soil Science Society of America Journal* 47: 578-581.
- Gusli, S., A. Cass, D. A. MacLeod, and P. S. Blackwell (1994a). Structural collapse and strength of some Australian soils in relation to hardsetting: I. Structural collapse on wetting and draining. *European Journal of Soil Science* 45: 15-21.
- Gusli, S., A. Cass, D. A. MacLeod, and P. S. Blackwell (1994b). Structural collapse and strength of some Australian soils in relation to hardsetting: II. Tensile strength of collapsed aggregates. *European Journal of Soil Science* 45: 23-29.
- Hignett, C. T. (1989). Physical measurements on a red-brown earth at Kapunda. CSIRO Div. of Soils. Div. Rep. 107.
- Hignett, C. T. (1991). Relating soil structure to runoff quality and quantity. *International Hydrology & Water Resources Symposium*, Perth 2-4 October, 1991. Institute of Engineers, Australia. Publication 91/22, p. 301-305.
- Keller, J. (1970). Sprinkle intensity and soil tilth. *Transactions of the American Society of Agricultural Engineers* 13: 118-125.
- Le Bissonnais, Y., A. Bruand and M. Jamagne (1989). Laboratory experimental study of soil crusting: relation between aggregate breakdown mechanisms and crust structure. *Catena* 16: 377-392.
- Mohammed, D. and R. A. Kohl (1987). Infiltration response to kinetic energy. *Transactions of American Society of Agricultural Engineers* 30: 108-111.
- Moss, A.J. (1991). Rain impact soil crust: I. Formation on a granite-derived soil. *Australian Journal of Soil Research* 29: 271-289.
- Panabokke, C. R. and J. P. Quirk (1957). Effect of initial water content on stability of soil aggregates in water. *Soil Science* 83: 185-195.
- Quirk, J. P. and C. R. Panabokke (1962). Incipient failure of soil aggregates. *Journal of Soil Science* 13: 60-70.
- Rosewell, C. J. (1986). Rainfall kinetic energy in Eastern Australia. *J. of Climate and Applied Meteorology* 25: 1695-1701.

- Thompson, A.L. and L.G. James (1985). Water droplet impact and its effect on infiltration. *Transactions of American Society of Agricultural Engineers* 28: 1506-1510, 1520.
- Tisdall, J. M. and J. M. Oades (1979). Stabilization of soil aggregates by the root systems of ryegrass. *Australian Journal of Soil Research* 17: 429-441.
- West, L.T., S.C. Chiang, and L.D. Norton (1992). The morphology of surface crusts. In: *M.E. Sumner and B.A. Stewart (eds.). Soil Crusting. Chemical and Physical Processes*. Advances in Soil Science. Lewis Publ., Boca Raton, pp.: 73-92.

